Radiobiological Optimization of Lung and Prostate Radiotherapy Treatments
- A Macroscopic Approach

Thesis submitted in accordance with the requirements of the University of Liverpool for the degree of Doctor in Philosophy by

Dhvanil Karia

February 2018

Student ID: 200927220
University of Liverpool (2012-2018)

ABSTRACT

"Radiobiological Optimization of Lung and Prostate Radiotherapy Treatments - A Macroscopic Approach" - D Karia

Radiobiological modelling is applied to different treatment individualization & optimization strategies and the resulting improvements in treatment outcomes quantified for lung and prostate cancer treatments; this is compared to current approaches based on delivering identical dose in fixed (size and number of) fractions to a given tumour type.

In the first investigation, dose-based escalation (level 0) is compared to Iso-toxic (i.e. Iso-NTCP) fixed fraction number prescriptions (level 1) and Iso-toxic prescription dose & fraction number optimization (level 2). NTCP, dose-scaling factor and number of fractions are the parameters used to optimize TCP; multiple dose-limiting OAR endpoints are accounted for in the above analysis. It is shown that Iso-toxic (at 8.6% NTCP) dose fractionation optimization improves the average TCP of the lung cohort by ~19% compared to standard dose fractionation (55 Gy in 20 fractions yielding 8.6% average NTCP). Similarly, for prostate cancer treatment, it is demonstrated that level-2 optimization is superior to standard treatment (60 Gy in 20 fractions): a population TCP increase of 12.6% (α/β=10 Gy) and 9.7% (α/β=1.5 Gy) is observed at 10% Iso-toxic NTCP. The entire analysis is performed with the software 'RadOpt' which was written as part of this PhD work and is described in detail in chapter three. 'RadOpt' will be made available for other researchers to perform similar cohort comparison analyses (to compare changes in parameters, regimens, etcetera as demonstrated in this thesis).

In chapter 4, the effect of patient-specific radiosensitivity information on treatment optimization & strategy selection is explored. For lung-tumour treatments it is shown that if patients are stratified into 3 or 5 subgroups of tumour radiosensitivity, the average TCP of the cohort would increase by about ~7.5% at 15 fractions (for most patients) after implementing level-2 optimization, compared to the current scenario where patient-specific radiosensitivity information is not available. For the prostate cancer cohort, level-2 TCP is improved marginally by ~1-2% at a reduced NTCP (1.7% lower NTCP compared to optimization where such information is unavailable). Further, it is reported that patients at the extreme ends of normally distributed tumour radiosensitivity would benefit significantly from changes in treatment strategies if patient-specific tumour radiosensitivity information is accounted for in treatment optimization.

In chapter 5, superiority of radiobiological-parameter-driven VMAT inverse treatment plans (in terms of TCP, NTCP and standard dose volume metrics) compared to dose-volume parameter based VMAT treatment plans for 4 patients (2 with lung & 2 with prostate cancer) is demonstrated. The analysis also shows that heterogeneous dose-distribution-based planning can yield improved TCP and dose sparing of OARs compared to standard planning approach that aims for a fixed and homogeneous tumour dose deposition. Further, it is observed that employing radiobiological model-based objectives/constraints reduces the risk of cold spots in the tumour and improves planning efficiency as additional 'dummy structures' for sparing an OAR (e.g. rectum) would not be required.

Chapter 6 introduces a novel method of iso-NTCP conversion of normal-tissue dose volume metrics (V_{xx}) from one regimen to the other. The analysis is carried out for two (each) lung and prostate treatment endpoints. We introduce two methods to perform this analysis (graphical & mathematical). The graphical method allows a clinician to find the equivalent V_{xx} for the new regimen such that the NTCPs of the OAR for the two regimens are equal.

Acknowledgement

This quest of answers was actually a journey of questions where I learnt the most intriguing lessons of life and lessons about myself. Reflecting upon the last few years, I write this as a different man, a student, a scientist, a son and a proud husband.

The most prominent contributors to this scientific endeavour were Prof. Alan E. Nahum and Dr Colin Baker. Both of these individuals not only contributed to my scientific development but also to my personality development. Both Alan and Colin, being on different sides of the spectrum in terms of thought processes, critical thinking and personality; helped me learn, the most interesting things about 'how to go about doing science and about life'. I cannot describe in words how thankful I am to both of them for guiding me to reach this far. I am thankful to Alan for the amazing extended conversations spanning a variety of topics and the philosophies about a lot of big and small things in life. I am thankful to Colin for the thought provoking lunchtime conversations and for shaping me to think out-of-the-box and critically. I would specifically like to acknowledge Colin for strongly supporting me battle university bureaucracy that helped me get my current job. I would like to specifically acknowledge Alan & Colin's mammoth effort towards the end of the write up period for the short notice corrections on the thesis. It goes without saying that I would not be writing these words without the support of both Alan & Colin.

Further, I would like to thank Kjell Eriksson for availing the RayStation Treatment Planning System to me and also for reviewing chapter 5 of the thesis. I expend my gratitude to Henrik Magnusson & the technical team at RaySearch Laboratories®, Sweden for maintaining the system and for their technical support. I would like to thank Dr Julien Uzan for his support in the earlier part of my PhD for his scientific advice on programming, BioSuite, Radiobiology and the profound knowledge of 'the never perfect coffee'. I would like to thank Danny (my colleague / scouse teacher / friend), George Georgiou, Alison Scott, Eva Onjukka and Rhydian Caines for their friendship and company during my time at Clatterbridge Cancer Centre. Lastly, I

would like to thank all the beneficiaries of Clatterbridge Cancer Charity that financially sponsored this project.

On a personal front, reaching at this stage of being able to submit my thesis in one piece was certainly an interesting journey. A path, I certainly did not travel alone. On this front, the most prolific support was given to me by Ms Chahna Mashru (…now Mrs Chahna Karia), who was always there ready for the next turn irrespective of the troughs and peaks that seemed to lay ahead. She supported us physically, mentally, financially and scientifically in this journey making her the ultimate life-partner. I will be in her debt forever for everything she has done to support me in this quest. Her most important contribution was in the form of working with me overnights, keeping me company and sane all the time. Further, she also helped me proofread the thesis and pushed me hard to achieve perfection in finishing the thesis.

Other than Chahna, a lot of credit goes to Amit Shah & Dr. Niti Shah for taking good care of mom and dad & other family matters that I could not attend. I would like to thank Shilraj Jadeja & Dr Vimple Bhalani for being there as a solid support and for always making me feel 'at home' away from home. I would like to thank Pinki & Arpit for their support to us as friends and for making us fall in love with Scotland. I would like to heartily acknowledge Nisarg, Shikhar, Abhiram and Utsav for their personal contribution to my life, bearing with my craziness and the interesting experiences we shared during the last many years. Further, there were many other individuals who contributed to this journey of mine in some way or the other and I would like to thank them too.

Lastly, I would like to acknowledge the support of my parents; who have made me what I am with their faith in me, their personal sacrifices for me & their life teachings. I would like to dedicate this work to my grandfather, Babulal Karia & my parents, Bharat & Geeta Karia.

Thank you all

Dhvanil

Table of Contents

Chapter 1 Introduction

Cancer by definition in the Oxford dictionary is “A disease caused by an uncontrolled division of abnormal cells in a part of the body”. The naming of different types of cancer involves using tissue type, location (lung, bone, blood, etc.) of the cancerous growth (commonly) and/or associated cell types involved in giving rise to the tumour (Non-small cell, melanoma, etc.). As per the latest report of the Office of National Statistics (UK), breast, lung, prostate and colorectal cancers formed about 53% of the total registered cases of cancers in 2013 (Office of National Statistics, 2015). The focus of attention here is on lung cancer and prostate cancer which are currently highly prevalent accounting for 13.7% (Prostate cancer) and 12.52% (Lung cancer) of the total registered cases of cancer (292,680 cases total) in the UK in 2013. The literature review covers different cancer types (of relevance to this work) in more detail along with the development of radiobiological models used to predict the response of patients with these cancer types to radiotherapy treatments. Now certain features of radiotherapy that will illuminate the core research questions addressed in this work are discussed.

Cancer is treated by surgery, chemotherapy and radiotherapy. Each of these treatment modalities has benefitted from rapid technological advances in recent decades. Radiotherapy has moved from using planar field X-rays (William & Wood, 1900) to treating tumours with megavoltage photon based Volumetric Modulated Arc Therapy (VMAT) and three-dimensional (3D) proton / carbon ion therapy (Grutters *et al.*, 2010; Komatsu *et al.*, 2011; Ramaekers *et al.*, 2013; Teoh *et al.*, 2011). This monograph is about generating evidence that will pave the way for current clinical cancer radiation treatments to move from today’s fixed (tumour) dose/fractionation regimens towards radiobiologically guided patient-specific regimens. The established practice is heavily focused on ensuring that complication rates in normal organs are acceptably low for a set radiation dose to the tumour.

1.1 Radiotherapy

The term 'Radiotherapy' includes unsealed source therapy (radioisotope or 'molecular' radiotherapy), sealed-source radiation therapy (brachytherapy), and external-beam radiotherapy (EBRT). All these forms of radiation therapy aim to impart a predetermined dose of ionizing radiation to the diseased part of the body to kill tumour cells. Sealed and unsealed sources of radiation include various chemical formulations of radium, iridium, iodine, etc. Early EBRT, also known as Röntgen therapy, involved directing kilovoltage X-rays towards a tumour to damage malignant tissue with poor or no control over the size and field of exposure. Despite this lack of geometrical precision (relative to current practice), there was sufficient reason to advocate the use of radiation to treat different types of cancer depending on the size and the extent of disease (Hirsch & Holzknecht, 1926; Pfahlery *et al.*, 1931).

1.1.1 Developments in EBRT

A successful cancer treatment means achieving local control of the tumour (this is assumed to equate to the eradication/killing of every clonogenic tumour cell) whilst avoiding serious damage to normal tissue cells. However, considerable harm can be done to surrounding normal (non-cancerous) organs. Early radiotherapy was performed by directing X-rays onto a rectangular area marked on the patient. The implications of this were quite severe as a high dose of radiation was imparted to the healthy parts of the patient's body and also to the radiographers, which was gradually realised as the late effects of radiation exposure came to light (Lambert, 2001; Stirling & Gee, 2002).

The idea of dividing the total dose into smaller amounts (*fractionation*) was introduced in order to reduce normal-tissue complications for a given effect on the tumour (Chapman & Nahum, 2015; Lambert, 2001). 3-D treatment planning was later introduced with the development of three-dimensional conformal radiotherapy (3D-CRT). This not only involved deposition of radiation dose in the tumour by beams from various directions but also planning of the distribution of

the dose to organs at risk (OARs) according to a 3-D representation of the patient anatomy generated using computed tomography (CT). However, imparting a radical dose[1] to the tumour can result in high dose deposition in the surrounding normal tissues with the risk of severe side effects (complications). With the evolution of treatment delivery technologies, the therapeutic ratio[2] has improved, i.e. lower toxicity levels for the same or improved tumour control.

1.1.2 Conformal Radiotherapy

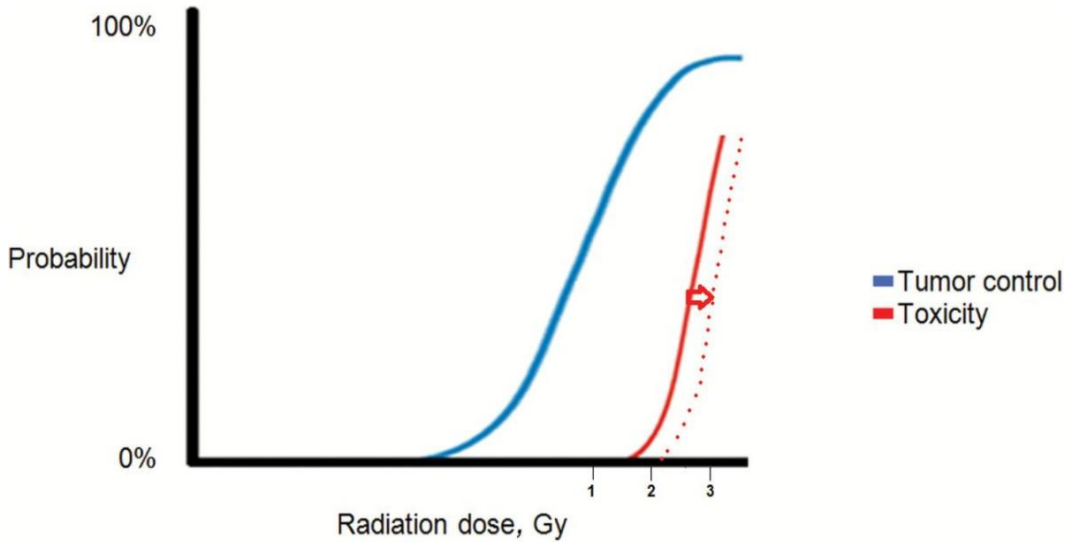

Figure 1-1 The concept of therapeutic ratio is explained in this figure. Number 1,2, and 3 denote three different prescription doses at which percentage probability of tumour control (blue) and percentage probability of normal organ toxicity (red solid) can be observed in the graph. The tumour control for prescription dose 1 is nearly 40% with a very low probability of toxicity. For prescription dose number 2, the tumour control is 80% and toxicity at 5%. For prescription dose 3, the tumour control is nearly 95% but the toxicity is 50% probable. Thus, in comparing treatment with prescription 1,2 or 3 it can be observed that prescription number 2 yields highest efficacy versus lowest possible toxicity (i.e. with highest therapeutic ratio compared to other treatment options) - Zindler *et al.* (2016)

The concept of 3D-CRT entails conforming (or 'shaping') the radiation dose to the 3D tumour volume, thereby reducing the dose outside the tumour as much as possible. This is done using computer-controlled geometric field shaping as opposed to the rectangular-field radiotherapy employed earlier. The advantage of 3D-CRT is

[1] 'Radical dose' generally indicates a dose of a magnitude sufficient to eliminate the tumour in a substantial proportion of patients.

[2] *"Therapeutic ratio is defined as the advantage in efficacy over the disadvantage in toxicity" (Joiner & van der Kogel, 2009) or as defined in Zindler et al. (2016), "The therapeutic ratio denotes the relationship between the probability of tumour control and the likelihood of normal tissue damage. An improved therapeutic ratio represents a more favorable trade-off between tumour control and toxicity".*

that the amount of radiation imparted to normal organs is reduced for a given dose to the target volume. Further developments in radiotherapy delivery have involved the introduction of intensity-modulated radiotherapy (IMRT) from the early 90s and, in the last decade, Image-guided radiotherapy (IGRT).

1.1.3 IMRT, VMAT and IGRT

IMRT uses modulation of beam intensity and beam shape (using multileaf collimator). This is undertaken either continuously (dynamic / sliding window IMRT technique) or in step and shoot (static IMRT) mode delivered from different angles relative to the delivery target with the beam turned off between each delivery angle. The beam shape is constricted such that the OARs in the path of the beam (directed towards the target) are avoided as much as possible from a given delivery angle. IMRT enables development of concave and inhomogeneous dose distributions that selectively spare Organs-at-Risk (OARs) whilst depositing the required radiation dose in the tumour.

Current IMRT planning systems use the beam's eye view technique to design irregularly shaped radiation-dose fields that conform to the target volume in 3D. These fields are then delivered by means of the multileaf-collimator (MLC) controlled beam shapes (Gerstner *et al.*, 1999). IMRT represents an improvement in conforming high dose to the tumour volume by modulating the intensity of each beam in a plane perpendicular to the beam direction (Bhide & Nutting, 2010).

There is credible evidence that IMRT is better at sparing organs at risk compared to the MLC-shaped beams of 3D conformal therapy. For head and neck tumours, IMRT has been beneficial in the sparing of optical nerves, digestive-tract mucosa, salivary glands, cochlea, brain and spinal cord (Chao *et al.*, 2001; Feng *et al.*, 2007; Nutting et al., 2011). Reduction of doses to the above organs has resulted in significant improvements in patients' quality of life post-radiotherapy. This improved normal-organ sparing also presents clinicians with the opportunity to increase tumour dose, thereby increasing the chances of achieving local control.

Improved local control and reduction in OAR toxicities have been reported for prostate cancer treatments via the use of IMRT and other advanced radiotherapy techniques. Prostate tumour treatment dose is limited due to genito-urinary and gastrointestinal toxicities. There is considerable evidence that the use of IMRT has resulted in acceptable bladder and rectal toxicities even for hypofractionated escalated doses (Kupelian *et al.*, 2005; Kupelian *et al.*, 2002; Zelefsky *et al.*, 2001, Dearnaley *et al.*, 2016; Livsey *et al.*, 2003; Wolff *et al.*, 2015).

A disadvantage of IMRT is increased delivery time which can result in patient discomfort, lower overall patient throughput and most importantly an increase in the possibility of patient movement. Further, compared to conventional conformal radiotherapy, IMRT plans require more monitor units (MUs) which results in increased radiation dose to the whole patient body. The solution to the above disadvantages is the arc-based (rotational) therapies that deliver radiation through continuous rotation of the gantry allowing treatment over the full 360° arc around the patient (Teoh *et al.*, 2011). The two primary forms of arc therapies are volumetric arc therapy and Tomotherapy. Tomotherapy is a hybrid of a linear accelerator (linac) and a CT scanner, delivering radiation from a continuously moving narrow slit while the patient is translated along an axis perpendicular to the slit direction. Tomotherapy can be delivered axially, serial (slice by slice) or helically (as a continuous spiral). VMAT, on the other hand, is delivered by varying three parameters related to the delivery system which are beam dose rate, gantry rotation speed and beam shape (via movement of MLC leaves). Conventional linear accelerators can be configured to have VMAT capabilities which is a distinct advantage compared to Tomotherapy as investment in a new piece of equipment is not required. Compared to standard fixed-field IMRT, arc therapies are delivered faster which is very useful clinically. The most recognized arc therapy systems are Elekta VMAT (Elekta), RapicArc (Varian) and SmartArc (Philips).

Image Guided Radiotherapy (IGRT) is characterised as "*Increasing the accuracy by repeated imaging of target and/or healthy tissues before the therapeutic action and matching the image with the therapy*" (van Herk, 2007).

The purpose of IGRT is to use advanced imaging methods to aid better delineation of tumours and OARs resulting in a potential reduction in margins and uncertainties in treatment planning. This results in more precise target dose deposition and improved sparing of OARs. During a course of radiotherapy, 3D imaging in the form of cone-beam CT is repeated multiple times to assess changes in tumour location, size and shape. Pre-treatment-fraction observation of these changes allows the treatment delivery to be modified to improve delivery of dose to the target and reduce the dose to the OARs. One other important use of IGRT is to accommodate organ motion (through pre-treatment 4D CT) especially in the case of lung, liver and prostate glands. IGRT also uses PET, SPECT and MRI marker based imaging techniques to guide precise target delineation (Arabloo *et al.*, 2016).

Today, it is well established that technological improvements in radiotherapy beam delivery and tumour & OAR delineation have delivered significant reductions in organ dose. However, the potential to individualize increase in tumour dose remains largely unexploited. Limiting the side effects of radiotherapy is essential but maximizing tumour control probability is of paramount importance as that is the primary objective of radiotherapy treatment.

1.2 Important Radiotherapy Concepts

Some of the important concepts of radiotherapy that are explicitly used throughout the thesis are now introduced.

1.2.1 Radiotherapy Treatment Planning

The present work involves analysing radiotherapy treatment data for cohorts of patients treated using radiotherapy. With advances in computer technology, radiotherapy has moved to computerised treatment planning in three dimensions. Thus, to ensure radiation treatment planning is consistent across centres, the International Commission on Radiological Units and Measurements (ICRU), established in 1925, coined the terms planning target volume (PTV), gross tumour volume (GTV) and clinical target volume in report 50 (ICRU, 1993a), report 62 (ICRU,

1999) and report 83 (ICRU, 2010). The upper and lower dose limits to the above volumes relative to the prescribed dose are also defined. GTV refers to the tumour that can be seen, palpated or imaged. GTV delineation aims to identify the demonstrable extent of the tumour and its location (See Figure 1-2). The GTV should also include any involved lymph nodes or noticeable spread into adjacent tissues. Surrounding the GTV is the CTV which is GTV plus a margin that will cover the microscopic spread of disease. The addition of a margin to the GTV to create the CTV is a matter of clinical assessment through biopsy or judgement based on experience which should take into account microscopic infiltrations of disease outside the GTV (Burnet, 2004). The local infiltration of a given tumour delineated by CTV is very variable. Some of the anatomical structures like bone cortex, muscular fascia and ligaments act as barriers and limit microscopic tumour infiltration. CTV delineation ideally accounts for such clinical information. However, the CTV covers the volume suspected of harbouring clonogenic tumour cells and thus should be treated with the prescribed dose as survival of even a single clonogenic cell can result in tumour relapse (i.e. treatment failure).

Figure 1-2 GTV, CTV and PTV as per ICRU report 50.

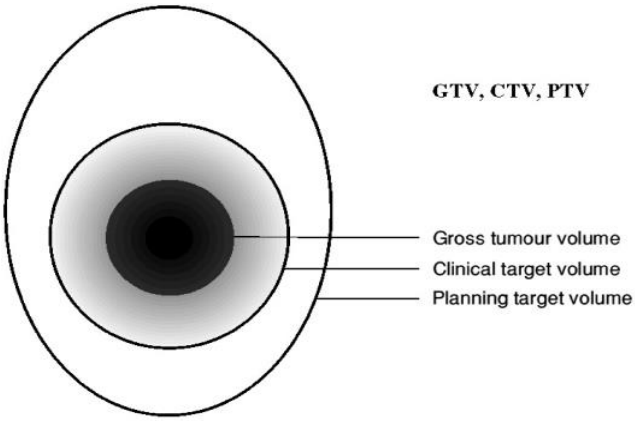

As per Report 62 & 83 (ICRU, 1999;2010), the PTV should account for internal variations such as changes in the position, size and shape of CTV due to movement of anatomical reference points or the tumour and external variations such as beam and patient positioning errors. The PTV encompasses the CTV in order that the prescribed dose is delivered to the whole of the CTV ensuring there is no under dosage to any part of the CTV.

1.2.2 Organs at Risk (OR / OAR)

The organs that surround a tumour or are in close proximity to the tumour, thereby receiving a high dose of radiation are known as Organs at Risk (OAR / OR) (ICRU, 1999).

The current work analyses lung and prostate radiotherapy treatment data. As far as clinical complications are concerned, both these tumour sites have OARs whose physiological function can be compromised as part of radiotherapy related side effects. In the case of lung tumours, the OARs are healthy lung (ipsilateral and contralateral), heart, oesophagus, and spinal cord (Jiang *et al.*, 2011). The radiotherapy related side effects to different OARs are usually reported using the radiation oncology group foundation's reporting schema (RTOG, 2015) or the Common Terminology Criteria for Adverse Events schema [CTCAE v5.0] (National Institute of Health, 2010). Further, RTOG and EORTC developed the LENT-SOMA scoring system to further standardize global toxicity scoring of clinical adverse events (i.e. OAR toxicity). These scoring systems allow quantification of the severity of an adverse event by means of a grade. The grade of an adverse event refers to a defined level of severity of the adverse event in relation to a patient's health. RTOG has defined toxicity grades from 1 to 5 for 15 tissues. Such scoring methods benefit clinicians as it allows justification for allocation and prioritization of resources required to manage a given patient's condition based on the severity of the event.

For healthy lungs, radiation pneumonitis[3] of grade 2 or above was the primary endpoint considered in this research work (RTOG,2015). Symptoms included moderate symptomatic fibrosis or pneumonitis, low-grade fever and/or patchy radiographic appearances. For the heart, pericarditis is the complication (i.e. Moderate angina on effort, Mild pericarditis, Normal heart size, Persistent abnormal T wave and ST changes – refers to an echocardiogram's QRS complex, Low ORS); for oesophagus, grade 2 oesophageal complication (i.e. patient unable to take solid food normally or swallowing semi-solid food only) and grade 2 spinal cord

[3] As per CTCAE v4 Pneumonitis of lung is defined as a disorder characterized by inflammation focally or diffusely affecting the lung parenchyma. Coughing is a typical symptom.

injury (i.e. Severe L'Hermitte's syndrome alias radiation myelopathy) were considered in the current analysis. In the case of prostate tumours, rectal bleeding, incontinence and bladder complications were considered (RTOG,2015).

1.2.3 Fractionation

In the early 1980's, it was established that early and late normal tissue reactions varied with change in dose per fraction of radiation treatment. This led to further study of radiobiology of normal tissues and the effect of changing fraction sizes on normal tissue responses (Joiner & van der Kogel, 2009). The term fractionation means the division of the total prescribed dose into smaller doses generally given once per day. Fractionation helps normal tissues recover from sub-lethal damage. Usually, the fractions are equal in size (dose), spread evenly over a given treatment period.

In the 1920s, Regaud & Baclesse introduced the idea of dividing the total prescription dose into several small parts rather than one single dose (Hunter, 2006). They were successful in improving uncomplicated laryngeal cancer control rates using low dose-rate protracted radiotherapy. They performed this over 2-3 hour daily fractions and a total treatment time of 4-6 weeks; this was medically superior to what had been done before but was not viable economically and resource-wise. This led to an increased interest in treatment regimens which were shorter in duration and practically deliverable (Hunter, 2006). Schwarz, Pape, Holzknecht and others by 1937 used fractionated high-dose-rate-per -fraction schemes imparting 0.63 Gy three times a day with four-hour gaps to treat cancer of the larynx (Hunter, 2006)[4]. Different centres in different parts of the world in the early part of the twentieth century started treating cancer (of the larynx at the least) with varying schemes of fractionation.

As of today, fractionation can be divided into the following categories: Hypo-fractionation, Conventional fractionation, Hyper-fractionation, Accelerated

[4] Hunter (2006) refers to - Schwarz G. Entwicklung, Prinzipien und biologische Grundlagen der Röntgentherapeutischen Bestrahlungstechnik. Strahlentherapie 1937, 58:523–544

fractionation and Protracted fractionation. The definitions of these fractionation types are taken from Dale & Jones (2007).

Conventional fractionation refers to 1.8 - 2 Gy per day each weekday. Hypo-fractionation schedules are of fraction size greater than 2 Gy/fraction, and hyper-fractionation refers to fractions less than 2 Gy (1-1.2 Gy per fraction - The Royal College of Radiologists, 2016). Accelerated fractionation means imparting more than 10 Gy per week total dose, and protracted fractionation refers to total doses of less than 10 Gy per week as per Dale & Jones (2007)[5].

The point being made here is that fractionation regimens are a compromise between many fractions or too few fractions to balance the sparing of normal tissues versus minimizing tumour repopulation. One may justifiably ask why one should prefer empirically derived fractionation schedules when radiobiological modelling based analysis can yield a more rationalized patient-specific fractionation schedule. Also, it is important to remember that fraction size is not the only parameter to optimize; dose-rate within a fraction, total dose, tumour volume and overall treatment time have a complex inter-relationship that govern the success of treatment for a given patient. More details about fractionation and its effects on the radiobiology of tumours and normal tissues are discussed in later sections of this chapter.

[5] Refer to: Chapter 4 Radiotherapy Fractionation, Page 52, Table 4.1

1.2.4 Dose-Volume Histograms

Treatment planning software generates a significant quantity of data on the dose deposited in the tumour and the contoured OARs. This information is commonly represented visually as Iso-dose lines over sagittal, transverse or coronal planes of a CT scan. Analysis of this information across three dimensions is challenging. Drzymala *et al.* in 1991 proposed compressing a 3-D dose distribution into a 2-D format known as a dose-volume histogram (DVH). Creating DVHs of a 3D dose distribution compresses a lot of information on the dose received by the delineated target volumes and healthy organs in the treatment plan. This makes plan evaluation and inter-plan comparison process much less complex.

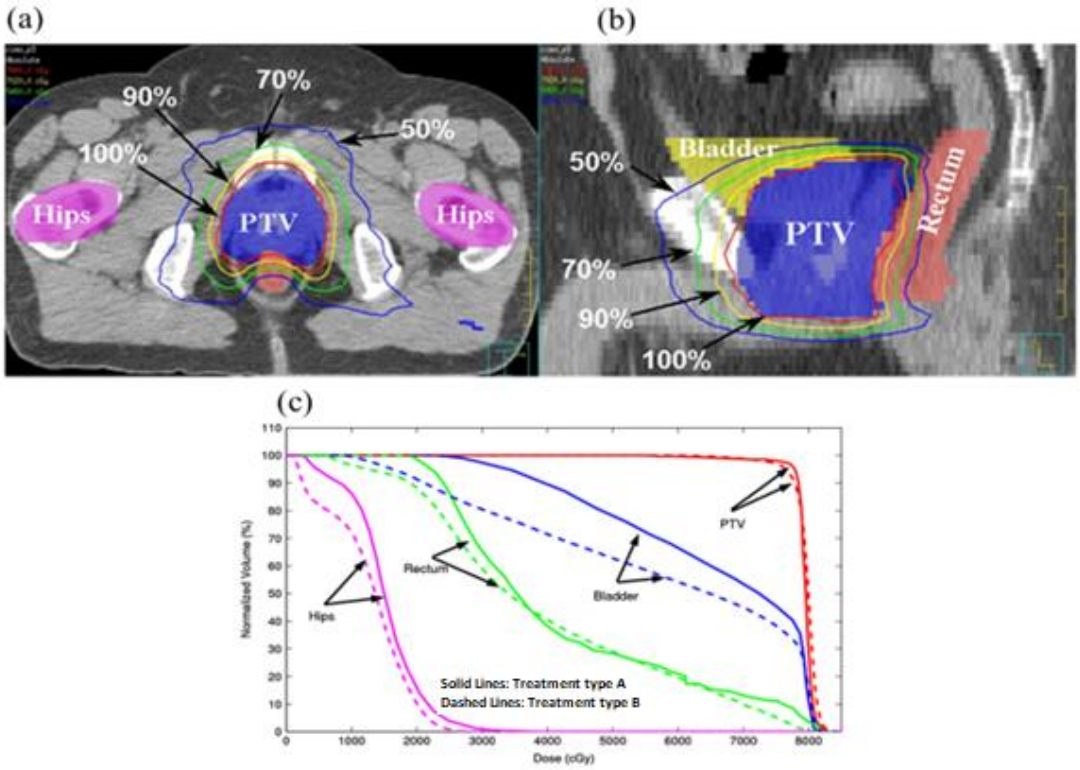

Figure 1-3 Images from a prostate radiotherapy treatment plan showing Iso-dose lines in the transverse (a) and sagittal (b) planes and the DVHs (c) of various OARs delineated along with that of the PTV – Chapter 5, Nenoi (2015).

A dose-volume histogram (DVH) is a histogram that relates radiation dose to the irradiated tissue volume in a given radiotherapy treatment plan. A DVH can be differential or cumulative in type. A histogram of the absolute (or percentage) dose received by a given structure versus the absolute (or percentage) volume of the structure receiving dose in a dose bin is called a *differential* DVH. The histogram can

also be *cumulative* which for a given dose (interval) can show the total volume receiving that given dose or greater. An example is of cumulative DVH is provided in figure 1-3(c).

Figure 1-3 above shows the Iso-doses of a treatment plan in a) Transverse Plane b) Sagittal Plane and in c) the cumulative DVHs of all the delineated Target volumes and OARs of a prostate patient. It is quite evident that the analysis of the dose distribution becomes relatively easy on comparing figure a), b) and c). A set of DVHs can be used for preliminary plan analysis and/or to rank different plans. The DVHs are also used as inputs to radiobiological models to calculate tumour control probability (TCP) and normal tissue complication probability (NTCP). TCP and NTCP models together with DVHs are a means to assess treatment plans quantitatively. These are discussed in detail in the next chapter. The limitation of using DVHs is that the spatial information associated with the voxels is irreversibly lost. Cheng & Das, (1999) tried to overcome this pitfall by proposing a zDVH that would be a supplement to the standard DVH but providing dose volume information (differential) with respect to a CT slice number. The standard DVH is still commonly employed for plan scoring and dose reporting possibly due to its simplicity.

As per (ICRU, 1993b), the dose planned for various organs and the tumour is to be reported using the below mentioned definitions of dose and volumes receiving radiation in Gray (Gy). The definition of various dose-volume metrics for tumour and normal tissue that can be derived using a DVH are given below. The current dose-volume limits for different OARs are described later when discussing clinical scenarios for lung and prostate tumour treatments. D_{mean}, D_{max}, D_{min}, D_{ref}, and V_{ref} are some of the metrics often reported.

Minimum Dose (D_{min}): The minimum dose received by a specific percentage (mostly it would be 95% or 99%) volume of a given structure. This is a useful metric in terms of target dose as minimum dose could be used to set a definite curative dose for a given tumour PTV.

Maximum Dose (D_{max}): The maximum dose received by a specific percentage volume (mostly it would be 1% organ/tissue volume) of a given structure. This metric is used to limit dose to critical organs that have a serial architecture (discussed in section 1.5). This excludes very small hotspots as defined in the (ICRU, 1993b) guidance report.

V_{Dref}: It is the volume of the structure receiving greater than or equal to the 'reference' dose.

D_{Vref}: This is defined as the minimum dose received by a 'reference' percentage volume of a given structure.

Report 83 (ICRU, 2010) superseded previous reports and defined three levels of recommendations for dose prescribing and reporting. Level 1 recommendations entail minimum standards for prescribing and reporting in radiotherapy sufficient for simple treatments and standards below which clinical radiotherapy should not be performed. Level 2 recommendations are for prescribing and reporting for state of the art techniques using computational dosimetry and 3D imaging. As per level 2 recommendations, it is expected that all volumes of interests (GTV, CTV, PTV, OAR and planning organ-at-risk) are defined over a 3D-CT or MRI image set, and that absorbed doses (heterogeneity corrected) are available along with DVHs of all the volumes. Level 3 recommendations are optional and research orientated, which involve reporting radiobiological concepts like TCP, NTCP or EUD.

1.3 Radiobiology

Radiobiology is the study of effects of ionizing radiation on cells and living organisms. Radiobiological modelling combines the physics of radiation and the biology of living cells under one umbrella. The most basic unit of a living organism is a cell. The cell is formed of different biological materials. The most important part of any cell is the nucleus that houses the genetic material which governs the response of a cell to any stimuli. A cell is bound by a thin membrane housing organic and inorganic materials in its cytoplasm (i.e. materials like water, minerals,

liposomes, lysosomes, etc. - Podgorsak, 2005). Cells can be classified into two categories:

1) Somatic cells: These are cells that can undergo mitotic division. A further classification of a somatic cell is a stem cell, transit cell and mature cell and the difference between these is explained in table 1-1. Of these, stem cells are most important as they are the cells that have the most potential to differentiate into a particular type of cell to form a given tissue.

Mitotic division of a cell leads to the formation of two daughter cells that have the same genetic material as the parent cell. Somatic cells are diploid with 46 chromosomes in a human cell.

Criteria	Stem cells	Transit cells	Maturing cells
(a) Differentiation marker	no	onset	yes
(b) Capable of proliferation	yes	yes	no
(c) Capable of self-maintenance	yes ($p_{sm} \geqslant 0.5$ possible)	no (but $0.5 > p_{sm} \geqslant 0$ possible)	no ($p_{sm} = 0$)
(d) Capable of many progeny cells	yes	limited	no
(e) Capable of regenerating tissues after injury	yes (long term)	temporarily	no
(f) Flexibility in options	(b)–(e)	(b), (d)	no

p_{sm}, self-maintenance probability.

Table 1-1 The difference between stem cells, transit cells and mature cells is explained in the image - Potten (1997).

2) Germ cells: The type of division that germ cells undergo is called meiosis which happens in two stages. Stage one is meiosis one where diploid parent cell is divided to form haploid daughter cells. In meiosis stage II, the haploid daughter cells; one from the male parent and one from the female each fuse to form a diploid daughter cell. In meiosis, the daughter cells have a mixture of genetic material derived from both parent cells through chromosomal crossover generating genetic diversity (Ohkura, 2015). Two cells from each parent combine to result into four daughter cells with genetic material from both male and female parents which further undergo mitotic cell division to form a group of cells. A group of cells of a given type forms a tissue that has certain characteristics / function and a group of tissues form an organ that performs a specific physiological function in the living organism (Podgorsak, 2005).

1.4 Normal-Tissue Radiobiology

When cells are exposed to radiation, the radiation passes through the cell, and a certain amount of energy is deposited in the cell. The cells may incur damage by acting as 'resistance', i.e. absorbers of energy in the path of radiation. The interaction of the radiation with the molecules in the cell produces excitation and ionization.

1.4.1 Cellular level radiation damage classification

There are two categories of damage to cells due to interaction with radiation:

1.4.1.1 Direct Damage

The ionization that directly interacts with the DNA and causes genetic cell damage is termed as direct damage. This type of cell damage is discussed in greater detail when the Linear-Quadratic model of cell killing is discussed in the literature review section 2.1.1.

1.4.1.2 Indirect Damage

The ionization of molecules in the cell produces free radicals that cause physical and/or chemical damage to other parts of the cell including the nucleus and the DNA within it. The majority of cell content is H_2O and ionization of water molecules produces reactive H^+ and OH^- free radicals. These cause the chemical bonds in other cell structures including the DNA to break thereby inducing internal damage that results in physiological changes in the cell. The indirect damage is a mixture of chemical and biological damage that can be enhanced or reduced by chemical sensitizers or radiation protectors (Chapman, J.D. & Nahum, 2015[6]; Dale & Jones, 2007[7]; Mayles, Nahum, & Rosenwald, 2007[8]).

[6] Refer Chapter 6, Page 66, Section 6.3
[7] Refer to Chapter 2 section 2.2
[8] Refer to Chapter 7 Section 7.5

1.4.2 Tissue-level radiation damage classification

On a macroscopic level, the consequences of radiation damage can be classified according to the type of damage, the timescale of realization of damage, and the intensity of damage.

1.4.2.1 Types of damage

A) Potentially Lethal Damage: Damage that is repaired by mechanisms within the cell.

B) Sub-lethal Damage: Repairable damage with more serious effects than potentially lethal damage. It takes about 4 to 24 hours for sub-lethal damage to be repaired provided that additional radiation damage is not incurred. Further, sub-lethal damage if not fully repaired may lead to lethal damage (Podgorsak, 2005). There are criteria to further grade the level of sub-lethal damage in OARs (i.e. RTOG criteria for normal-tissue complication).

C) Lethal damage: Irreparable damage is the type of damage that mostly leads to cell death. This type of radiation damage is irreversible. The aim of radiotherapy is to deliver lethal damage, i.e. cell death to 100% of the tumour clonogens without serious damage to normal tissues. After radiation exposure, cell death can occur by one of the many complex mechanisms as shown in figure 1-4. In the cells of a hematopoietic system, apoptosis (programmed cell death) is the predominant mode of cell death after irradiation. Apoptosis is characterised by chromatic fragmentation, followed by cell shrinkage and then blebbing (Charras, 2008) of cell membranes.

Senescence results in permanent cell-cycle arrest eventually leading to natural cell death whereas, secondary necrosis and necroptosis lead to plasma-membrane disintegration followed by mitotic catastrophe. Mitotic catastrophe is a condition that results in the formation of huge cells with hyper-amplified centromeres and multiple nuclei that live for a few days before transitioning into senescence or

apoptosis. Details on each of these pathways of cell death are given in Joiner & van der Kogel (2009) and Orth *et al.* (2014).

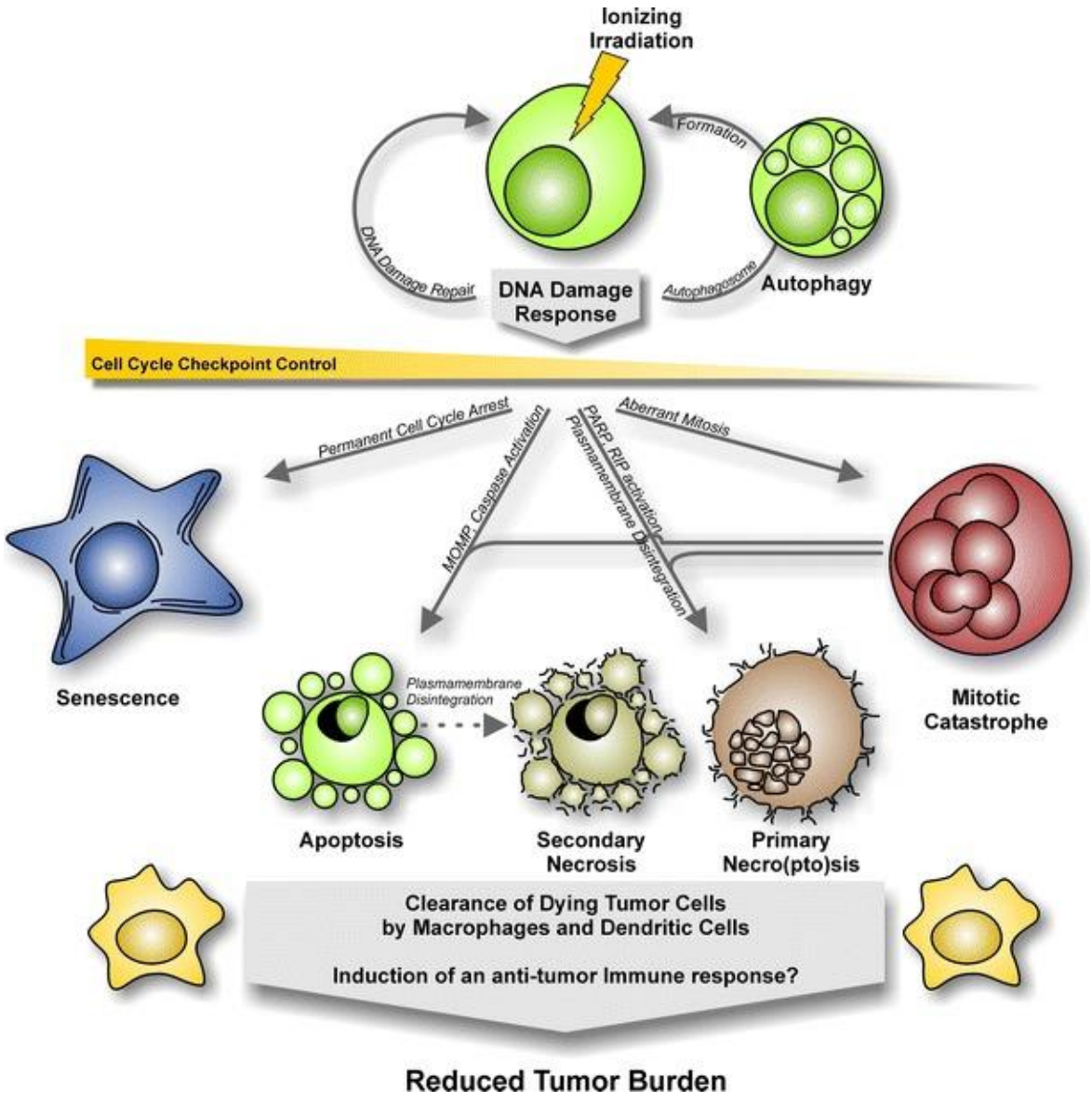

Figure 1-4 Different pathways of cell death after lethal radiation exposure - Orth *et al.* (2014)

1.4.2.2 Timescale

Radiation damage to the organism (e.g. to a human being) is generally not immediately apparent as would be the case with burns or cuts. The timescale for radiation damage to manifest itself depends on the intensity of radiation exposure, total exposure time and characteristic radiation sensitivity of the tissue. The physical realization of radiation damage can be divided into early and late tissue response.

A) Early effects

Early effects of radiation damage occur within 3 months of radiation treatment / exposure. The tissues most susceptible to early acute effects are renewal tissue like basal layers of skin (mucosa), stem cells in the small intestinal crypts and bone marrow. Complications that are likely to manifest themselves as early effects of radiation exposure are oedema, haemorrhage, inflammation and denudation of epithelial and haemopoietic tissue. (Mayles *et al.*, 2007[9]; Podgorsak, 2005[10]).

B) Late effects

With respect to normal tissue and clinical radiation treatment, late effects of radiation damage are chronic in nature. Late effects could be a result of depletion of stem cells, radiation damage to stromal elements of the tissue or because of repetitive radiation damage in overlying tissue. Late responses affect organ physiology in the long term. Fibrosis, ulceration, atrophy, obstruction or stenosis are some of the examples of symptoms associated with late chronic radiation damage (Chapman & Nahum, 2015[11]; Mayles *et al.*, 2007[12]; Podgorsak, 2005[13]).

C) Extended germinal effects

Radiation damage can either be fully repaired, lead to programmed cell death or result in genetic mutation. DNA damage due to free radical interaction with the chromosomes can sometimes lead to incomplete repair causing mutation and not cell apoptosis. This affects the germ cells of the organism. The effects of this kind of radiation damage are perpetuated and become evident in secondary, tertiary or later generations of the organism, many years after the original exposure (Podgorsak, 2005).

[9] Refer to chapter 8 section 8.4
[10] Refer to chapter 14 Section 14.6,14.7
[11] Refer to Chapter 9, section 9.1-9.2
[12] Refer to chapter 8 section 8.4
[13] Refer to chapter 14 Section 14.6,14.7

1.5 Organ Architecture

Different organs are made up of specific types of cells and tissues. The physiological function of a given tissue depends on the functional output of these cells and tissues. Organs are believed to react to radiation or drug toxicity in two specific ways. Before discussing this, it is important to introduce the concept of functional sub-units (FSUs). An FSU is a unit element of a given organ that contributes to the functional output of the organ and can be regenerated by a single surviving stem cell of the same tissue. Alveoli of the lung and B-cells of the liver are examples of FSUs that are responsible for the functionality of the respective organs. Withers *et al.* (1988) proposed the idea of serial and parallel organs and explained the difference in radiation response of different organs using the concept of FSUs. There are three categories of organs based on their architecture that govern the intensity of response to any type of damage to the organ.

The *parallel* architecture organs have FSUs working 'in parallel' just like several batteries connected in parallel to maintain a certain voltage (organ function) across the circuit (e.g. Lung, Liver). Total functional incapacitation is induced when a set percentage or majority of FSUs of the organ are damaged. The dosimetric factor associated with toxicity in parallel architecture organs is 'mean dose (D_{mean}) to the organ' (Källman *et al.*,1992).

Second are *serial* architecture organs, wherein the FSUs are linked serially as a chain that breaks if any of the links is severely damaged. A series electrical circuit is a good analogy here. These types of organs present with functional loss above a certain threshold of physical or biological damage (e.g. Spinal Cord, Oesophagus). For serial organs "maximum dose (D_{max}) to the OAR" is the dosimetric factor associated with toxicity. Källman *et al.* (1992) and Niemierko & Goitein (1993) developed NTCP models for inhomogeneous dose distributions using the serial and parallel organ architecture concepts as proposed by Withers *et al.* (1988).

For tumours, unless all the stem cells (FSUs) are eradicated, the tumour regrows which indicates that tumours effectively have parallel architecture. Complications for different organs occur at different dose levels. Studies have indicated that normal tissues can contain a combination of parallel and serial structures (which

form the third category of organs). The properties of cells important for understanding the way tumour- and normal tissue cells behave in response to radiation exposure are enumerated below. These properties are referred to as R's of Radiobiology.

1.6 The 5 R's of Radiobiology

- **Repair** – Cells have many ways of ascertaining their general well-being and this self-diagnostic process is almost continuous. The moment after a finite amount of radiation damage occurs in a living cell, the cell diagnostics pick up the anomaly of DNA strand breaks and initiate a very sophisticated repair mechanism. However, the time it takes for complete repair (mostly but not always) depends on the type of cell and extent of damage encountered.
- **Redistribution** – The radio-sensitivity of cells in different stages of the cell cycle varies. Some stages are more radio-resistant than others, and so cells in these stages of the cell cycle are more likely to survive a dose of radiation. However, radiation damage leads to two important cell-cycle phenomena where some cells get locked in the G2 phase of the cell cycle, and some are pushed into a radiosensitive phase of the cell cycle. This redistribution process contributes to radiation damage in subsequent fractions of therapy.
- **Reoxygenation** – Hypoxic cells are relatively resistant to radiation (Brown, 2007). The surviving hypoxic cells after a fraction of radiotherapy are likely to be re-oxygenated owing to angiogenesis and or a reduction in the number of oxygen-consuming cells. This increase in oxygenation makes them more radiosensitive. Thus, the damage to the same set of cells in subsequent fractions is likely to be higher as they are rendered radiosensitive. This is one more factor contributing to adaptation of fractionation in radiotherapy.
- **Repopulation** – Cells may move into the proliferative stage. Cell proliferation is advantageous for OARs and a disadvantage as far as radiotherapy treatment of tumours is concerned.
- **Radio-sensitivity** – For a given single dose of radiation, the damage incurred by different types of cells varies. This characteristic (known as radio-sensitivity) of cells of different types (tumour or OAR) plays a vital role in determining the

response of cells to a given dose of ionizing radiation (Mayles *et al.*, 2007[14]; Withers, 1975).

1.7 Tumour Radiobiology

Any given tissue undergoes a process of cell renewal in order to maintain its natural form (i.e. constant size and volume). The well differentiated and mature cells are replenished over time by differentiation of basic stem cells that have very high proliferation & differentiation capacity. Stem cells form the base of the hierarchy of cells that make up the epithelial and haemopoietic tissues of the body. Cancer tumour tissues also consist of these neoplastic stem cells at the base of their hierarchy that differentiate into malignant cells of carcinoma and undergo uncontrolled mitotic division (Reya *et al.*, 2001). The total mass of a tumour also includes cells that are non-proliferative but have the same characteristics as those of the malignant cells. The aim behind any curative cancer treatment is to eradicate the malignant stem cells that have the proliferative capacity. If a tumour relapses post radiation therapy, then at least one stem cell must have survived the radiation exposure.

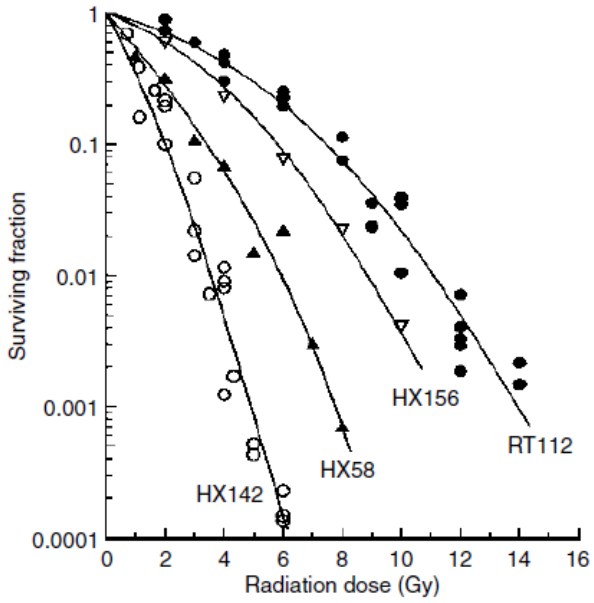

Figure 1-5 Cell survival curves for four representative human tumour cell lines irradiated at high dose rate. HX142 neuroblastoma; HX58 pancreatic; HX156 cervix; RT112 bladder carcinoma. From Steel (1991)

1.7.1 Clonogenic Cells

Clonogenic means capable of forming colonies. The term "clonogenic cell" refers to cancer stem cells (CSCs). CSCs are very difficult to identify in situ, and generally

[14] Refer to chapter 7 section 7.8

must be identified using in vitro cell-growth assays. The main aim of curative cancer treatment is to eliminate clonogenic cells. The survival of irradiated cancer cell lines is studied by radiobiologists using clonogenic assaying techniques (Mayles *et al.*, 2007[15]). The assays are controlled growth environments in which cancer cells are allowed to regrow post-irradiation. The growth environment is maintained at 37°C with aeration to promote normal cell growth. The cells that survive are counted once they have undergone several cycles of mitosis. The plot of surviving fraction of cells after correcting for plating efficiency (logarithmic scale) versus radiation dose (linear scale) known as *cell survival curves* are fitted with mathematical models to obtain radiosensitivity parameters for the cell type under study (IAEA, 2010). The disadvantages of this process are that it deals with a limited range of doses and that the mitotic viability of cells cannot be tested using the assays. Nevertheless, many such studies have been undertaken and many papers published that validate the use of parameters for modelling cell survival (Burman *et al.*, 1991; Chapman & Nahum, 2015; Chapman, 2003; Marks, Yorke, *et al.*, 2010).

Mitotic division leads to two daughter cells from one parent, and thus the number of tumour cells would be expected to grow exponentially, and the volume will increase as a logarithmic function of time. If the cells are continuously dividing, the tumour doubling time can be established. Modelling cell survival helps uncover characteristics of specific tumours (IAEA, 2010). An example of a cell survival plot for different cell lines is shown in Fig. 1-5 (from Steel, 1991).

1.8 Mathematical Modelling

The importance of a model lies in its ability to represent, define or explain a real-time phenomenon or a problem and mimic its behaviour to a certain level of accuracy. Testing a model on various independent known datasets is a good method of validating the applicability of the model. The right balance must be found between prediction accuracy and model complexity. Further, it is also

[15] Refer to chapter 7 section 7.2

important to note that a model with enough parameters can be a good fit to the data but may be incorrect in characterizing the data.

1.8.1 Types of models

Models can be built using two methods.

1) Building a logical system based on a theory – Mechanistic Approach
2) Fitting equations to observed data – Empirical Approach

Mechanistic models specifically consider the mechanisms involved in the process being modelled. The analogy of a group of cells forming a tissue and a group of tissues forming an organ is quite applicable here. The design starts with modelling of simple processes which together form a complex process. Simple processes are governed by basic theoretical knowledge. These processes are then combined mathematically to form a complex mechanistic model. Next, the model is to be validated with known outcome/response data and refined to improve predictive accuracy. The Marsden model that predicts tumour control probability is an example of a simple mechanistic model (refer section 2.3).

Empirical Models are built using data and may have no relation to the actual physical processes to which they are applied. In constructing an empirical model, an equation is fitted to the data observed or recorded. The goodness-of-fit metric associated with the model fitting process gives an indication of the accuracy of a model's prediction. An empirical model aims to quantitatively take account of the different results that are expected from the system's observed behaviour. However, the accuracy is heavily compromised if the quality of sample data used to build the model is not representative of the process being modelled. This is one of the biggest pitfalls of the empirical approach to modelling a process. The Lyman-Kutcher-Burman (LKB) model that predicts normal tissue complication probability is an example of an empirical model (refer section 2.4).

1.9 Thesis Outline

The primary aim of this research is the individualisation of radiotherapy treatment using radiobiological models to optimize treatment dose, no. of fractions and individual treatment plans. The available patient-specific clinical data are categorised below following West & Barnett (2011). All the possible patient-specific information below could be explored to design treatments on a patient-specific basis.

Category	**Patient Specific Information**
Tumour	Type, stage (tumour, node, metastases (TNM)), pathology, volume
Patient	Age, smoking history, alcohol use, ethnicity, weight, height, breast volume for breast patients (cup size), co-morbidity (for example, diabetes, collagen vascular disease, hypertension, inflammatory bowel disease)
Treatment	Total dose, number of fractions, dose per fraction, overall treatment time, use of chemotherapy, use of hormone therapy, use of surgery and postoperative complications, concurrent medications (for example, statins)
Physics	Total radiation dose, dose per fraction, overall treatment time, planned dose distributions to critical normal tissues
Toxicity	Pre-treatment data, toxicity data collection at the end of treatment, post 6 months and then yearly.

This work is concerned with radiotherapy and the use of radiobiological models of TCP and NTCP to optimize and individualize radiotherapy treatment response using patient-specific DVH datasets. The aim is to answer some of the below-listed questions from this research thesis.

- How can treatment optimization and individualisation be performed using the mathematical modelling process?
- What are the potential clinical benefits and or risks of applying treatment optimization based on radiobiological models?

This is undertaken by developing and applying a methodology to quantify the predicted improvement in clinical outcomes that is possible by individualizing radiotherapy treatments using mathematical radiobiological models.

So far radiotherapy and associated concepts have been introduced. Chapter two describes the radiobiological models employed in this work. A broad overview is given of the publications on different types of TCP and NTCP models. Treatment options for lung and prostate tumours are then described. After this, published papers that entail the clinical use of radiobiology are briefly discussed. Then, various dose-escalation and optimization strategies with or without the use of radiobiological modelling are presented. The literature associated with all the respective chapters is then presented section-wise. Lastly, inverse planning is discussed with respect to the use of radiobiological models; this is relevant to the research described in chapter five.

Chapter three presents the results of implementing three different radiotherapy treatment optimization and individualization methods on two different patient cohorts, one of prostate tumours and one of lung tumours. Nahum & Uzan (2012) gave an overview of radiobiological-model based dose optimization in radiotherapy treatment planning. They introduced different levels of dose optimization. These optimization concepts are implemented for the two above-mentioned tumour types using an in-house MATLAB-based software with results presented in the form of novel population strategy assessment plots (with TCP vs NTCP curves).

Chapter four explores how incorporating tumour radio-sensitivity information might impact treatment planning strategies. It is assumed that there is a method to stratify patients into different groups based on the radio-sensitivity of their tumours. A radiosensitivity assay or a biopsy could be one example or let us say the patient has been given medication that as a side-effect increases or decreases tumour radio-sensitivity as a part of combination therapy. Here, a technique that will help quantify the effect of this patient-specific radiosensitivity knowledge and show the potential benefit of using this knowledge via predictions of tumour control / normal tissue complication probability for a given cohort of patients is developed.

Chapter five describes the use of radiobiological models in the inverse treatment-planning phase. Chapter six describes the NTCP-based conversion of dose-based normal-tissue treatment planning constraints (V_{20}, V_{35},…, V_{xx}) for a given dose/fractionation scheme to a different dose/fractionation scheme. Currently, the prescribed dose is converted to alternate fractionation schemes using the Withers' Iso-effect formula (Withers *et al.*, 1983). This, however, does not help clinicians understand the relative effect of the change in prescription of the doses received by the normal tissues. A radiobiological model based Iso-toxic dose fractionation conversion scheme is thus developed to allow conversion of a given V_{xx} for a given dose fractionation scheme to an effective V_{xx} for a desired or proposed dose fractionation scheme. Further, details of the clinical usefulness of this technique are demonstrated for Lung and Prostate tumour cases.

Chapters three to six have a structure and each have an introduction, methodology, results, discussion and a conclusion section. Chapter 7 summarizes each of the chapters and reflects on the results of each of the chapters drawing conclusions from this research work.

Chapter 2 Overview of Radiobiological Modelling

2.1 Introduction

In this chapter, a detailed description of the mathematical models (used in this thesis) applied to radiobiology associated with tumours and normal tissues is provided. Current clinical practice in radiotherapy for lung and prostate tumour treatments is then described including a brief history of these treatments. The background literature relevant to the topics of subsequent chapters is then presented; this will emphasize the novelty of the presented approach compared to current practice (clinical or research) in the area.

2.1.1 The Linear Quadratic model for cell survival

Figure 1-5 in chapter 1 shows cell-survival data for a population of different cell-lines. These data are fitted with an expression containing a quadratic function of absorbed dose as the exponent. The so-called linear-quadratic (LQ) equation fitted to the data is:

$$\textbf{Surviving Fraction SF} = e^{-\alpha D-\beta D^2} \qquad \textbf{Eqn. 2-1}$$

where,
D is the radiation dose (Gy)
α is a parameter that describes the initial slope (Gy^{-1})
β describes the curvature of the survival curve on a semi-log plot

The α-component relates to the direct radiation damage ('one hit' and irreparable) to cells also referred to as single-hit killing. The β component refers to cell killing which requires two sub-lethal events and is mostly DNA damage consisting of single-strand breaks, double strand breaks and base chain breaks (Chadwick *et al.*, 1973; Chapman, 2014). The total dose, total treatment time and dose-rate have different effects on the tumour and the normal tissue reactions. These are described in the following sections of this chapter. Further, potentially important factors like clonogen repopulation and time-dependent sub-lethal damage repair have major implications on tumour control. As the overall treatment time increases, the tumour repopulates and the chances of tumour control diminish. Redistribution

and re-oxygenation work in favour of tumour control by increasing the sensitivity of a tumour to radiation damage. Looking at these from the normal-tissue point of view, a given dose of radiation is likely to produce α-inactivation dominant damage and fractionating enables more sub-lethal damage repair. The α/β ratio for a cell line is the dose at which the α-inactivation and β-inactivation are equal. The effect of different α/β ratios characterising the tissue response is shown in figure 2.1 by Mayles, Nahum, & Rosenwald (2007)[16,17].

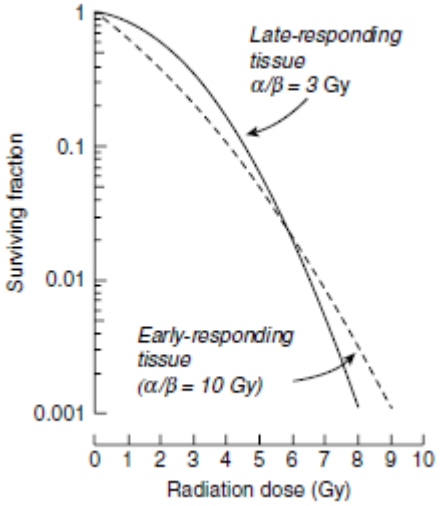

Figure 2-1 Cell survival curve of early (high α/β ratio) and late responding tissue (low α/β ratio). A lower α/β ratio produces a relatively bendy curve - Mayles, Nahum, & Rosenwald (2007).

The LQ expression can be written as

$$\mathbf{-\ln(SF)= \alpha D + \beta D^2} \qquad \textbf{Eqn. 2-2}$$

Considering the effect of fractionation, the total prescribed dose *D* can be expressed as *n* equal-sized fractions of dose *d*; thus, - log (surviving fraction), *E*, can be written as

$$\boldsymbol{E}\mathbf{= -\log_e(SF) = } \boldsymbol{n} * \boldsymbol{(\alpha d + \beta d^2)} \qquad \textbf{Eqn. 2-3}$$

Dividing both sides by α and recognising that *n* x *d* = *D,* yields

$$\frac{\boldsymbol{E}}{\boldsymbol{\alpha}} = \boldsymbol{D}\,\{\mathbf{1} + \frac{\boldsymbol{\beta}}{\boldsymbol{\alpha}}\boldsymbol{d}\,\} \qquad \textbf{Eqn. 2-4}$$

[16] See section 7.6 Chapter 7 Nahum & Mayles

[17] See section 9.3.2 Chapter 9 Nahum & Mayles

2.1.2 Biologically effective dose (BED)

The linear quadratic model was first proposed by Chadwick *et al.* (1973), but it was the article by Fowler (1989) incorporating the overall treatment time factor in the LQ-equation and introducing the concept of *BED* (biologically effective dose), that was responsible for the renaissance in the use of mathematical models in the radiobiology of radiotherapy.

Fowler (1989) coined $\frac{E}{\alpha}$ as the biologically effective dose (BED), which is radiation damage expressed as a function of total dose imparted. Thus, the total damage inflicted by a given prescription dose *D* in *n* fractions of size *d* is given by

$$\boldsymbol{Relative\ Effectiveness\ (RE) = \{1 + \frac{\beta}{\alpha} d\}}$$

where

$$\boldsymbol{BED = D\ x\ RE} \qquad \textbf{Eqn. 2-5}$$

Assuming now that there is a new fractionation regimen which yields the same biological damage, this new regimen will have the same *BED* as the reference regimen.

So, assume that the standard fractionation schedule has prescription dose D_{std} and the new prescription dose is D_{new} which produces an equal biological effect. Then it is required that

$$\boldsymbol{BED_{ref} = BED_{new}}$$

$$\boldsymbol{D_{ref}\{1+(\frac{\beta}{\alpha})d_{ref}\} = D_{new}\{1+(\frac{\beta}{\alpha})d_{new}\}} \qquad \textbf{Eqn. 2-6}$$

Rearranging eqn. 2-6 it is obtained,

$$\boldsymbol{\frac{D_{new}}{D_{ref}} = \frac{\{1+(\frac{\beta}{\alpha})d_{ref}\}}{\{1+(\frac{\beta}{\alpha})d_{new}\}}} \qquad \textbf{Eqn. 2-7}$$

This is the Iso-effect relationship initially developed and proposed by Withers *et al.* (1983). It is worth noting that delivering total dose D in many small fractions will allow clonogenic repopulation in a tumour (after approximately 3 weeks of radiotherapy in a lung tumour) which is not accounted for by the above formula.

This was accounted for by Fowler (1989) as he factored delay in tumour repopulation and the tumour doubling time into the BED equation as shown below:

$$\frac{E}{\alpha} = D\left\{1 + \frac{\beta}{\alpha}d\right\} - (log_e 2 * (T - T_k)/\alpha T_d) \qquad \text{Eqn. 2-8}$$

where *D = n x d*
n= no. of fraction d= fractional dose D= Total dose T=Total treatment time
T_k=Time to onset of repopulation T_d= Tumour doubling time

2.2 Radiobiological Modelling

In this section, the basics of radiation-effect modelling in tumours and normal tissues are covered. The advantages and assumptions made in different published models are also presented. The models used here are of empirical and mechanistic types characterizing radiation biology.

Chadwick and Leenhouts (1981) explain radiobiological modelling and associated caveats very efficiently as:

"Any model is an attempt to generalize a series of experimental observations and therefore aims to reduce and simplify the parameters which describe the experimental data. In radiation biology, a model should have a basic simplicity which permits it to include many different physical, chemical and biological processes which may influence the biological effect. Ideally, the model should be capable of extensions to the description of more than one biological endpoint. At the same time, the restrictions and limitations in the validity of the model should be well delineated so that the area within which the predictive potential of the model is applicable is well defined."

Dale & Jones (2007) mention that a successful biological model needs to be able to produce results that agree with both clinical & experimental data.

Radiobiological models are useful in radiation therapy for the following reasons[18]:

- To compare different treatment plans.
- To modify prescriptions to compensate for gaps in the treatment (Dale & Jones, 2007).

[18] This list is not exhaustive.

- To compare the biological effects of different treatment schedules (Fowler, 1989).
- To predict TCP and NTCP effects of different types of particles and energies (photon vs proton treatments) for a given cohort (Fowler, 2010).
- To design clinical trials with supporting evidence for a given hypothesis (Fowler, 2010).
- To individualize and improve treatment strategies (Hoffmann *et al.*, 2013; Nahum & Uzan, 2012).

2.2.1 Basic assumptions about the models used in this research work

- Cell survival after radiation exposure is binomial and follows Poisson statistics. This is applicable to the Marsden TCP model described in the next section.
- Intra-OAR / Intra-Tumour radiosensitivity is constant.
- Complete sub-lethal damage repair between fractions for a given OAR & tumour.

The assumptions listed above are non-exhaustive in relation to radiobiological models but are taken into consideration to maintain the simplicity of these models (not developed as part of this research work). There are many known effects (e.g. hypoxia) that have an overall effect on model predictions which could be modelled for a given tumour type, but the inclusion of this would complicate the model. The availability of model parameters that account for such effects is limited which dictates the use of available set of model parameters with given assumptions. Also, some of the assumptions are based on the results of radiobiological studies on cell-lines or animal tumour models. It is acknowledged that these assumptions contribute to the uncertainties associated with model predictions and necessitates qualification of model predictions against clinical response data.

2.3 The Marsden TCP model

Clinical dose-response curves are found to have an approximately sigmoid shape. There have been attempts to fit functions to this curve shape to construct a model of tumour response (Carlone *et al.*, 2006; Källman, Ågren, & Brahme, 1992; Walker & Suit, 1981) but it is not obvious how tumour-to-tumour variations in clonogenic cell density, dose distribution inhomogeneity, radiosensitivity and volume can be considered using a curve-fitting approach. Carlone *et al.*(2006) attempted to simplify the 8 parameter TCP equation into a 4-parameter based sigmoidal function built on D_{50} (Dose achieving 50% TCP), γ_{50} (Slope of the TCP dose response curve), heterogeneity in clonogen number and generalized radiosensitivity (fig. 2-2). They concluded that the dose response curves of TCP can be built based on D_{50} and γ_{50} but would yield limited information in explaining the radiobiology of tumour control and absolute values of radiobiological parameters will need other physical measurements. An alternative is the mechanistic approach that may be able to take into account the above variations. A mechanistic model was proposed by Nahum & Tait (1992) which was further developed by Webb & Nahum (1993) and is commonly known as the Marsden model (Nahum & Sanchez-Nieto, 2001; Sanchez-Nieto & Nahum, 1999; Webb & Nahum, 1993). The Marsden model is used for analysis in this work and is discussed in detail below.

$$\mathrm{TCP}_{\mathrm{pop}} = \frac{1}{(2\pi)^2 \sigma_\alpha \sigma_\beta \sigma_{\lambda'} \sigma_{\ln N_0}} \times \int_{-\infty}^{\infty}\int_{-\infty}^{\infty}\int_{-\infty}^{\infty}\int_{-\infty}^{\infty} \exp\left(-\frac{1}{2}\left[\frac{(\alpha-\bar{\alpha})^2}{\sigma_\alpha^2} + \frac{(\beta-\bar{\beta})^2}{\sigma_\beta^2} + \frac{(\lambda'-\overline{\lambda'})^2}{\sigma_{\lambda'}^2} + \frac{(\ln N_0 - \overline{\ln N_0})^2}{\sigma_{\ln N_0}^2}\right] - \exp[-(\alpha+\beta d-\lambda'/d)D + \ln N_0]\right) \times d\alpha d\beta d\lambda' d(\ln N_0),$$

where $\bar{\alpha}$ and $\bar{\beta}$ are the population mean values of the radiosensitivity parameters, $\overline{\lambda'}$ is the mean of the scaled growth rate constant, $\overline{\ln N_0}$ is the mean of the lognormal distribution of the number of cells, and σ_α, σ_β, $\sigma_{\lambda'}$, and $\sigma_{\ln N_0}$ are the corresponding standard deviations.

Figure 2-2 The eight parameter TCP model theorised by Carlone *et al.* (2006)

Following from equations 2-3 and 2-8,
Let R_{pop}= $(ln_2(T - T_k)/\boldsymbol{\alpha} T_d)$ be the repopulation term in the surviving fraction equation 2.8

$$\boldsymbol{E = e^{-\alpha D\left\{1+\frac{\beta}{\alpha}d\right\}+R_{pop}}} \qquad \textbf{Eqn. 2-9}$$

Let us assume that the number of (tumour clonogenic) cells before irradiation is N_o and the number that survives after total dose *D* in *n* equal fractions of dose *d* is *N* ; the surviving fraction will be given by

$$\boldsymbol{\frac{N}{No} = e^{-\alpha D\left\{1+\frac{\beta}{\alpha}d\right\}+R_{pop}}} \qquad \textbf{Eqn. 2-10}$$

For any tumour to be 'controlled', all the clonogens (aka stem cells) must be eradicated. Applying Poisson statistics, the probability of the number of surviving cells being zero if the average number of cells surviving is *N,* is given by

$$\textbf{P (N,0) = } \boldsymbol{e^{-N}} \qquad \textbf{Eqn. 2-11}$$

Thus, the probability of controlling the tumour (TCP) is given by,

$$\textbf{TCP = } \boldsymbol{e^{(-N_0(e^{(-\alpha D\left\{1+\left(\frac{\beta}{\alpha}\right)d\right\}+R_{pop})))}}} \qquad \textbf{Eqn. 2-12}$$

This is the basic form of the model; it does not yet incorporate dose inhomogeneity, inter-patient radiosensitivity variation or clonogenic cell density.

N_0 being the initial clonogen number is equated to density of clonogenic cells (ρ) multiplied by volume (*V*) of the GTV giving,

$$\textbf{TCP = } \boldsymbol{e^{(-\rho V(e^{(-\alpha D\{1+(\frac{\beta}{\alpha})d\}+R_{pop})))}}} \qquad \textbf{Eqn. 2-13}$$

The radiosensitivity of tumour clonogens in the patient population (or a representative sample) is assumed to follow a Gaussian (or 'normal') distribution with a mean ($\bar{\alpha}$) and a standard deviation (σ_α). The TCP value is an average of $TCP_{\alpha=1....i}$ with radiosensitivity (α_i) over a population:

$$\textbf{TCP}_{\textbf{pop}} \textbf{ = (g}_1\textbf{TCP}_{\alpha 1} \textbf{ + g}_2\textbf{TCP}_{\alpha 2} \textbf{ + g}_3\textbf{TCP}_{\alpha 3}\textbf{.....g}_n\textbf{TCP}_{\alpha n}\textbf{)} \qquad \textbf{Eqn. 2-14}$$

where the weighting factors g_i are calculated from the above-described Gaussian distribution such that $\Sigma g_i = 1$.

Considering that the normally distributed patient population has a given number (g) of patients with radiosensitivity α_i, then

$$g_i \propto [e^{(-(\alpha_i - \bar{\alpha})^2/2\sigma_\alpha{}^2)}] \qquad \text{Eqn. 2-15}$$

The β sensitivity could also be represented as an independent gaussian distribution. However, Chapman (2003) suggests that α-inactivation is the dominant effect causing cell inactivation for a clinical dose fraction >3 Gy, thereby variation in β is assumed to be causing no effect except for very large fractions. In practice ,the ratio α/β is kept constant. As per Chapman (2014) and Nahum *et al.* (2015) the quadratic component of the LQ based double hit cell killing will become significant at a higher dose. At high dose/fractions, the total dose required to achieve the equivalent biological effect as produced by a conventional or a low dose/fraction (say 2 Gy/fraction) regimen will be thus lower. This is demonstrated in figure 2-3 for tissues of varying α/β. The effect of hypofractionation is larger in tissues with lower α/β compared to tissues with higher α/β.

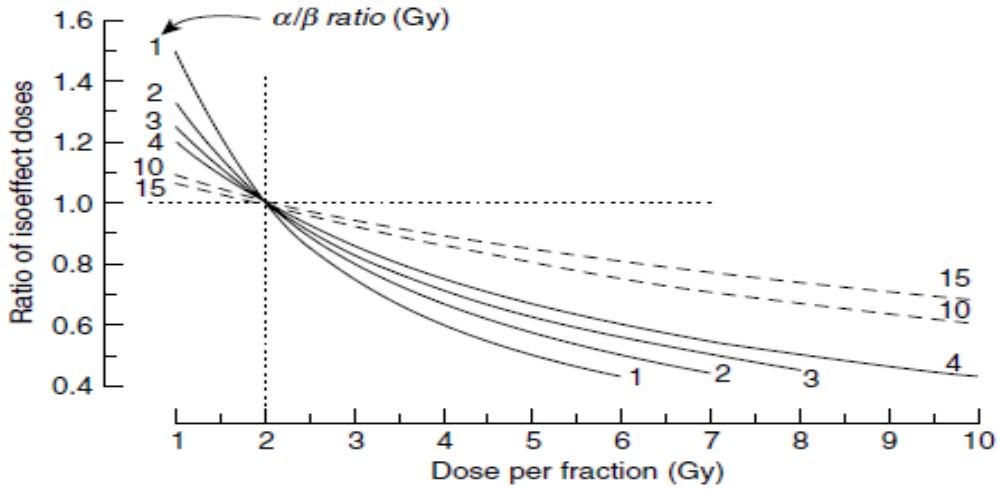

Figure 2-3 The figure shows the effect of fractionation for achieving a given iso-effect for tissues with different α/β values – Chapter 7, Mayles, Nahum & Rosenwald (2007)

The Dose-Volume-Histogram (DVH) computed by a treatment planning system is a 2-dimensional (2D) histogram (frequency distribution) of volume vs dose in a given delineated organ. Up to this point, the expression for TCP has assumed that the

dose is constant (or uniform) across the entire tumour (target) volume. However, using DVHs as the input to the TCP model, the inhomogeneity in the dose distribution can be taken into account.

The DVH has dose bins and corresponding volumes that receive a dose in that bin. A TCP calculation for each dose bin (Bin Control Probability - BCP) considering the corresponding volume associated with the bin and taking a normalized value of the results should give the tumour control probability for the patient.

$$\mathbf{TCP = \prod (BCP_i)} \qquad \textbf{Eqn. 2-16}$$

The final formulation of TCP calculation that includes accounting for repopulation effect, inhomogeneity in dose distribution, and radiosensitivity variation across the population is given by the equation below from (Mayles *et al.*, 2007[19]):

$$TCP = \frac{1}{\sigma_\alpha \sqrt{(2\pi)}} \int_0^\infty \left(\prod_i e^{\left[-\rho_{cl} V_i * e^{\left\{ -\left(\alpha D_i \left(1 + \frac{\beta}{\alpha} d_i \right) - (ln_2 (T - T_k)/\alpha T_d) \right) \right\}} \right]} \right) * e^{\left[-(\alpha - \bar{\alpha})^2 / 2{\sigma_\alpha}^2 \right]} d\alpha$$

Eqn. 2-17

2.3.1 Other Tumour Control Probability Models

Zaider & Minerbo (2000) developed a TCP model based on the stochastic process of birth & death of a cell. Their model accounted for exponential tumour proliferation and regrowth between fractions. Their model was extended by Dawson & Hillen (2006) to incorporate cell cycle dynamics. Cells in the G_0-phase of mitosis are radio-resistant compared to the same cell in G_1, G_2, S or M-phase. Thus, Dawson & Hillen (2006) split the cell proliferation into two compartments (active and quiescent) accounting for repopulation in a more specific manner. This method of incorporating the biological process governing cells' response to radiation exposure is quite complex (Dawson & Hillen, 2006; Zaider & Minerbo, 2000). O'Rourke *et al.* (2009) give a very good account of the application of different TCP models to radiotherapy critically assessing the benefits and pitfalls of the different models.

[19] See section 36.2.14 Chapter 36, Mayles, Nahum & Rosenwald (2007)

2.4 Lyman-Kutcher-Burman (LKB) NTCP Model

The LKB and *Relative Seriality* NTCP models (Lyman, 1985; Källman *et al.*,1992) are the most frequently employed models for predicting radiotherapy complications. The LKB model is represented by an error function and estimates complication probability considering the volume of the tissue and the dose. The best-fit parameters for each complication are derived using published outcome data. The model is based on three parameters: TD_{50}, the (uniform) dose for which the chances of a given complication are 50% (assuming that this dose covers 100% of the normal tissue volume, sometimes written as $TD_{50}(1)$), n is the 'volume effect' parameter and m is related to the slope of the NTCP vs dose curve ('volume effect' is explained at the end of the current section).

The equations for the model are given below,

$$\boldsymbol{NTCP = \frac{1}{\sqrt{(2\pi)}} \int_{-\infty}^{t} e^{-\frac{t^2}{2}} dt} \qquad \textbf{Eqn. 2-18}$$

$$\boldsymbol{t = \frac{D_{eff} - TD_{50(\frac{V}{V_{ref}})}}{m * TD_{50(\frac{V}{V_{ref}})}}} \qquad \textbf{Eqn. 2-19}$$

$$\boldsymbol{TD_{50}(1) = TD_{50(\frac{V}{V_{ref}})} * (\frac{V}{V_{ref}})^{n}} \qquad \textbf{Eqn. 2-20}$$

The above equations assume a homogenous dose distribution. The DVH must be corrected for fractionation which is described in the next section. To account for in-homogenous dose distribution, the effective volume method proposed by Kutcher *et al.* (1989) is implemented. The correction method converts the non-uniform DVH into a uniform one with an effective volume (V_{eff}) that will result in the same biological effect as the non-uniform DVH in a given tissue (Niemierko, 1997).

$$\boldsymbol{V_{eff} = \sum_{i=1}^{k} \Delta V_i * \left[\frac{D_i}{D_{max}}\right]^{1/n}} \qquad \textbf{Eqn. 2-21}$$

i=1 to k represents the number of the bin in the differential DVH. **From Mayles, Nahum & Rosenwald (2007)[20]**

[20] See section 36.3.2.2 Chapter 36, Mayles, Nahum & Rosenwald (2007)

It is possible to use any effective volume or dose from a family of equivalent uniform DVHs defined by the power-law relationship. Thus, an effective dose D_{eff} (also known as EUD) applied to the whole organ (V_T) is used which gives the same NTCP.

$$\boldsymbol{D_{eff} = \sum_i \left[D_i^{\frac{1}{n}} * \frac{V_i}{V_T} \right]^n} \qquad \textbf{Eqn. 2-22}$$

Pericarditis/pericardial effusion: Dose–volume predictors and NTCP parameters

Authors, Year, Reference	Diagnosis, No. of patients, Years of treatment	OAR	Fractionation schedule, dose data	Predictive parameters	NTCP parameters
Carmel and Kaplan* 1976 (3)	Hodgkin's 377 Patients 1964–1972	Pericardium		$D_{pericardium} > 30$ Gy 50% pericarditis, 36% requiring treatment	
Cosset *et al.* 1991 (65)	Hodgkin's 499 Patients 1971–1984		35–43 Gy/ 2.5–3.3 Gy/fraction pre-3D dose data	$D_{Mediastinum} \geq 41$ Gy d/ fraction ≥ 3 Gy (marginal significance)	
Burman *et al.* 1991 (66)	Historical data				LKB† *TD50* = 48 Gy *m* = 0.10 *n* = 0.35
Martel *et al.* 1998 (26)	Esophagus 57 Patients 1985–1991	Pericardium	37.5–49 Gy/ 1.5–3.5 Gy / fraction 3D data	$D_{mean} > 27.1$ Gy‡ $D_{max} > 47$ Gy‡ d/ fraction 3.5 Gy	LKB (95% CI) *TD50* = 50.6 Gy (–9; 23.1) *m* = 0.13 (–0.07; 0.13) *n* = 0.64 (–0.58; 3)
Wei *et al.* 2008 (27)	Esophagus 101 Patients 2000–2003	Pericardium	45–50.4 Gy 1.8–2.0 Gy/fraction 3D data	D_{mean}pericardium > 26.1 Gy $V_{30} < 46\%$	

Abbreviations: CI = confidence interval; LKB = Lyman-Kutcher-Burman (model); OAR = organs at risk; NTCP = normal tissue complication probabilities.

* Patients were grouped according to the estimated pericardium doses. Incidence of pericarditis was distributed as follows: 14/198 (7%): ≤6 Gy; 5/42 (12%): 6–15 Gy;23/123 (19%): 15–30 Gy; 7/14 (50%): >30 Gy. For pericarditis requiring treatment the corresponding distribution was: 3/198 (1.5%), 4/42 (9.5%), 8/123 (6.5%), and 5/14 (36%).

† In the LKB model (47, 66) the parameters meaning is *TD50:* dose to the whole organ which will lead to complication in 50% of the population; *m* is related to the steepness of the dose–response curve, *n* represents the volume effect (large volume effect for *n* close to unity; small volume effect for *n* close to zero).

‡ Corrected to 2 Gy per fraction, $\alpha/\beta = 2.5$ Gy.

Figure 2-4 shows the recommended predictive dosimetric and NTCP model parameters reported by various studies.

This transformation is based on the assumption that the whole organ has a homogeneous response to radiation and obeys the power-law relation. Also, small values of *n* will mean that volumes at lower doses will contribute less to the effective volume making the effective dose more or less equal to the maximum dose. If *n*=1, the effective dose will be equal to the mean dose.

When *n* is close to 1, the normal tissue behaves like a 'parallel' organ with mean dose governing the complication probability (i.e. lung, liver); when *n* is really small

(<=0.1), the organ behaves as a 'serial' organ with the maximum dose determining the complication probability (e.g. spinal cord).

The LKB NTCP model has been used extensively in the analysis of radiotherapy outcome data and model parameters for various organs have been reported regularly in the literature (Emami *et al.*, 1991; Marks, Yorke, *et al.*, 2010; Seppenwoolde *et al.*, 2003). A copy of the table of parameters published for pericarditis complication NTCP model and dosimetric predictive parameters is given in Figure 2-4 from Gagliardi *et al.* (2010).

2.4.1 Relative Seriality NTCP model

Proposed by Källman *et al.* (1992), this NTCP model is a quasi-mechanistic model that takes account of normal-tissue architecture. The model involves the concept of functional subunits (FSUs) that contribute to the overall function of the organ. The serial or parallel arrangement of the FSUs define the response of the organ which is described by parameter *'s* - relative seriality' in the equation below. The model also accounts for *non-uniform* dose distribution and is completely defined by parameters TD_{50}, s, and γ.

$$\boldsymbol{P(D_{tot}) = 2^{-e^{[e\gamma(1-\frac{D_{tot}}{TD_{50}})]}}} \qquad \textbf{Eqn. 2-23}$$

$P(D_{tot})$ = probability of no cell surviving
γ= normalised dose response gradient
TD_{50}= Dose causing 50% response rate

$$\boldsymbol{NTCP = \left[1 - \prod_{i=1}^{M}[1 - P(D_i)^s]^{\Delta V_i}\right]^{1/s}} \qquad \textbf{Eqn. 2-24}$$

where ΔV_i is the fractional volume at doses D_i from the bins of a differential DVH

2.5 Fraction size effect correction in NTCP models

The LKB NTCP model described above takes into account inhomogeneous dose distributions and the 'organ architecture' (via the volume parameter). However, it does not explicitly correct for fraction size. In other words, differences in fraction size, for a given total dose (distribution) will have no effect on NTCP prediction (using Eqn. 2-18 to 2-20) which is obviously incorrect. The parameters predicted for

the quasi-empirical LKB model are mostly based on data of treatments with 1.8-2 Gy (tumour) fraction sizes.

Thus, Fowler in (2001) proposed using the linear quadratic formulae to correct the DVH for fractionation effect. The dose bins in the DVHs are corrected to be 2-Gy equivalent. These fractionation-corrected DVHs are then used to evaluate NTCP. The formula for correcting the dose bins is given below. Fig 2-5 shows the effect of using the linear-quadratic fraction-size correction where the overestimation of volumes below 2 Gy fraction size (~60Gy) and under-estimation above this size is corrected.

$$EQD_2 = D_{tot,j}\left[\frac{\frac{\alpha}{\beta}+d_j}{\frac{\alpha}{\beta}+2}\right] \qquad \textbf{Eqn. 2-25}$$

where $D_{tot,j}$ **= DVH Bin dose**
d_j**=the fraction size of the proposed regimen**
α/β= Normal Tissue α/β ratio[21]

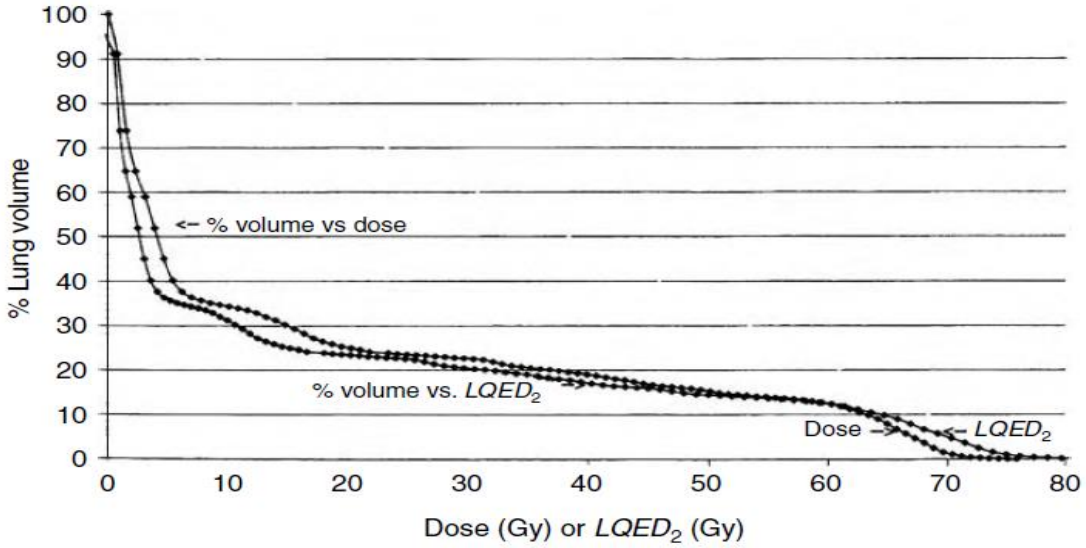

Figure 2-5 EQD_2 conversion of a conformal plan based cumulative DVH of the lung to 2 Gy per fraction equivalent DVH (α/β=3.3 Gy, 60 Gy prescription dose). All volumes at doses below the total dose at which the fraction size is 2 Gy (~60 Gy in this case) are shifted to lower LQED2 doses, and all volumes above this (prescription) dose are shifted to higher EQD_2 doses - Mayles, Nahum & Rosenwald (2007).

The effect of this correction on the NTCP calculations has been described in Mayles *et al.* (2007) by a simple exercise. For a given DVH of rectum OAR of a patient prescribed with 74 Gy prescription dose, the NTCP is calculated after varying

[21] See section 36.3.4 Chapter 36 Nahum & Mayles

fraction from 1.6Gy to 5.9Gy keeping the total OAR dose Iso-effective. As the dose is Iso-effective, the change in NTCP should ideally be zero or negligible.

However, without any DVH dose correction, the NTCP varies from 15.7% and 0.1%.; which is incorrect. Using the LQED based DVH dose correction as shown in equation 2-25, NTCP variation is minimized (7.3% to 8%) for the range of Iso-effective dose calculated for different fraction sizes. The effect of such correction on a DVH is shown in figure 2-5

2.6 Clinical Radiotherapy Practice

2.6.1 Radiotherapy for Lung Tumour Treatment

Currently, radiotherapy remains the only option of treatment for inoperable advance stage NSCLC. The 5-year survival is less than 10% with local relapse being the major cause of mortality (Cox *et al.*, 1991; CTCA, 2015; Perez *et al.*, 1987; Saunders *et al.*, 1997, 1999).

At the time of writing, two radiotherapy regimens were in common use for treating NSCLC across different centres in the UK (1,2 below):

As per NICE guidelines *"Patients with stages IIIA or IIIB NSCLC who are eligible for radical radiotherapy and who cannot tolerate or do not wish to have chemoradiotherapy should be offered the CHART regimen. If CHART is not available, conventionally fractionated radiotherapy to a dose of 64–66 Gy in 32–33 fractions over 6 1/2 weeks or 55 Gy in 20 fractions over 4 weeks should be offered."* (NICE Guideline Lung cancer: diagnosis and management, 2011).

The SOCCAR trial (Maguire *et al.*, 2014) assessed tolerability of concurrent & sequential chemotherapy with radiotherapy (55 Gy in 20#) in stage III inoperable NSCLC patients and concluded that accelerated hypofractionated radiotherapy was a feasible (2 year OS 46% sequential arm & 50% concurrent arm) and well-tolerated approach (grade 3 oesophagitis - 8.5-8.8% in both the arms) that should be

compared with standard 2 Gy/fraction NSCLC radiotherapy treatment (Kaster *et al.*, 2015; Schuster-Uitterhoeve *et al.*, 1990; Williams *et al.*, 2006)

The CHART Trial delivered continuous, hyper-fractionated, accelerated radiotherapy; a 54Gy radiation dose was delivered in 36 fractions over a period of only 12 days, thus 3 fractions a day with 6 hours between fractions. The CHART regimen showed a 22% reduction in mortality, improving the 2-year survival from 20% to 29% compared to conventional radiotherapy (60 Gy in 30 fractions) in the randomised trial for NSCLC radiotherapy treatments (Saunders *et al.*, 1997, 1999).

RTOG 9410 was a randomised phase III multi-centre trial comparing concurrent chemotherapy (cisplatin-based treatment) plus radiotherapy with radiotherapy alone. The radiotherapy treatment was 1.8-2 Gy/fraction in arm 1,2 and 1.2 Gy twice daily fractions in arm 3. After a mean follow up time of 11 years, it was reported that concurrent chemo-radio-therapy improved 5-year survival rates compared to radiotherapy alone or to sequential chemo-radiotherapy and also reported that late toxicities were similar in all arms (Curran *et al.*, 2011; Fournel, 2011). RTOG 0617 trial compared 60Gy in 30 fractions concurrent chemotherapy (paclitaxel and carboplatin) treatment with 74Gy in 37 fractions concurrent. The escalated dose arm had poorer overall survival compared to the standard arm.

2.6.2 Radiotherapy for Prostate Tumour Treatment

The broad categories of treatment regimens are hyperfractionated, conventional and hypofractionated radiotherapy. The most recent publication by Dearnaley & Hall (2017) shows that there is good evidence based on recently concluded trials' (like CHHiP, HYPRO) results that α/β for the prostate tumour is less than 3 Gy. The software built for chapter 3 allows comparative analysis of different types of regimen for a given cohort considering different values of α/β for the prostate tumour.

1) Conventional regimens

74 Gy in 37 fractions is a regimen mostly adopted in the UK to treat prostate cancer until recently (NICE, 2014). There have been a number of clinical trials that looked into benefits of dose escalation. The trials from MD Anderson, USA; the Royal Marsden, London and a Dutch institute compared conventional 2 Gy per fraction treatments of escalated dose regimens (70-78 Gy in 35-39 fractions) with standard regimens (Dearnaley *et al.*, 2005; Peeters *et al.*, 2005; Pollack *et al.*, 2002; Zietman *et al.*, 2005). Late rectal and bowel complications increased following the dose escalation with minimal improvement in overall failure-free survival over 3-6 years. Long term results of the RT01 trial show that escalated dose group had better 10-year biochemical progression free survival (55% in 74Gy 34# group) versus the control arm (43% in 64Gy in 32 fractions) as per Dearnaley *et al.*,(2014).

2) Hypofractionated regimens

Hypofractionated versus conventional radiotherapy of prostate cancer has been trialled; the results are summarised below. One of the trials used 55 Gy in 20 fractions (Yeoh *et al.* 2003), and the other used 52.5 Gy in 20 fractions (Lukka *et al.*, 2005) versus 64Gy and 66Gy total dose regimens (delivered as 2 Gy/fraction). Lukka (2005) study reported lower 5-year freedom from biochemical failure with hypofractionation. However, the Yeoh (2003) study reported a higher biochemical relapse-free survival at 4 years for the hypofractionated group concluding that hypofractionated radiotherapy for prostate was equally effective and well tolerated compared to conventional regimens. Recently, the CHIPP & PROFIT trials completed recruitment of over 4000 patients comparing 2 Gy per fraction regimens (Total dose 74-78 Gy) with 3 Gy per fraction regimens (total dose 57-60 Gy). Dearnaley & Hall (2017) report non-inferiority of the 60Gy in 20 fraction regimen over the conventional 74Gy in 37 fraction regimen. They also recommend establishing 60 Gy in 20 fractions as the new standard of care regimen as this would reduce the overall treatment time for patients and aid resource utilization. The Christie hospital in Manchester has reported a biochemical-free survival (bNED) at 5

years of 65% (T1), 62% (T2) and 38% (T3/4)[22] compared to other protracted treatment schemes (Livsey *et al.,* 2003). Another trial looking at hypofractionated regimens was reported by Norkus *et al.* (2013) where they compared 76 Gy in 38 fractions to 63 Gy in 20 fractions. The reports indicated that hypofractionated treatment was well tolerated and the overall toxicity of gastrointestinal and gastrourinary types were the same (Dearnaley & Hall, 2017).

3) Hyperfractionated regimens

Very few studies have reported using hyperfractionation in prostate radiotherapy treatments (67-83Gy dose in 1.2-1.5 b.i.d [23] schedules). The conclusion drawn from those studies suggests that compared to conventional regimens, hyperfractionation regimens reduce late genitourinary complications with no major improvement in GI toxicity (Forman *et al.*, 1996; Valdagni *et al.*, 2005). Forman *et al.* (1996) conducted a study comparing conventional 2 Gy fractionation (78 Gy prescription dose and n=24) with a (Iso-effective adjusted dose) hyperfractionated regimen (82.8 Gy prescription 1.15 b.i.d and n=25) for a cohort of total 49 advanced stage prostate cancer patients. They concluded that hyperfractionation allowed for safe dose escalation and histologic control was markedly improved in hyperfractionation over a follow up period of 20 months. Valdagni *et al.* (2005) compared standard 74 Gy in 37 fraction regimen (n=209) to radiobiologically adjusted Iso-effective hyperfractionated regimen (1.2 Gy b.i.d for 162 patients prescribed a median EQD_2 dose of 73.9 Gy) in a prostate cancer treatment study. The biochemical recurrence-free survival (bRFS) for hyperfractionated regimen was reported to be no less effective than the standard regimen. Also, based on a median follow up of 29.4 months the authors concluded that α/β for the prostate tumour was close to 10 Gy and their results were not consistent with the low value of α/β reported by other groups. Currently, there is rather strong evidence from analysis of CHHiP and PROFIT Trial results indicating that α/β for the prostate tumour is low (1.3 Gy based on PROFIT Trial results and 1.8 Gy from CHHIP trial results -- (Dearnaley & Hall,

[22] T1-4 corresponds to TNM disease staging for prostate tumour as defined by American Society for Therapeutic Radiology and Oncology (http://www.cancer.org/cancer/prostatecancer/detailedguide/prostate-cancer-staging)
[23] b.i.d - "bis in diem" – Twice a day

2017) and that hypofractionation is therapeutically equally effective compared to a conventional 2 Gy regimen.

2.6.3 Use of radiobiological modelling in Clinical Practice

Radiobiological metrics like BED, EUD, TCP, NTCP and P^+ (Probability of complication free survival) have played a minor role in clinical practice for many years. Applications of radiobiological models in radiotherapy are summarised below.

One of these is to convert between dose fractionation schemes keeping the biological effect on tumours and normal tissues constant (Jones & Dale, 2000). Radiobiological modelling is also used to (via the use of the BED concept) correct prescription doses for gaps in treatments or schedule alteration due to unforeseen circumstances (RCR, 2008).

Radiobiological model-based metrics have also been used to compare treatment modalities or strategies for a given tumour type. Comparison of 3D CRT and IMRT (using NTCP metric) has been reported by many groups demonstrating the superior OAR sparing capability offered by IMRT (De La Fuente Herman *et al.*, 2010; Deb & Fielding, 2009; Luxton 2004) based on a comparison of radiobiological and dosimetric metrics. De La Fuente Herman *et al.* (2010) compare 10 Head & Neck Glioblastoma 3D CRT plans to IMRT plans using LQ based TCP model by Niemierko & Goitein (1993) and the LKB NTCP model-based on parameters published by Burman *et al.* (1991). They demonstrate that the variability in TCP for both the treatment methods was nominal and that the average NTCP for the IMRT plans was lower by 7% in the escalated dose cohort. Deb & Fielding (2009) use the Kallman TCP model to calculate TCP, the relative seriality model to calculate NTCP and the P+ metric to show that the IMRT plans are superior to 3D CRT plans for a single prostate patient CT structure set. They used the radiobiological evaluation module of Pinnacle (v7.6) software to undertake the analysis. The parameters used for radiobiological models were obtained from the Pinnacle treatment planning system database and were assumed to be based on published data by the same authors. The analysis is based

on data from one single patient and lacks any form of validation of model parameters. Koontz *et al.* (2009) reported no difference in gains in NTCP when comparing 3D CRT plans versus IMRT plans developed for 15 post-prostatectomy radiation treatment patients. Although dose sparing was observed for both rectum and bladder, the difference in NTCP values was very small (Koontz *et al.*, 2009).

Chatterjee *et al.* (2011) compared helical tomotherapy, forward planned IMRT and two-phase conformal treatment plans for 5 head & neck squamous cell cancer patients using a combination of dosimetric and radiobiological metrics (TCP & NTCP using BIOPlan software by Sanchez-Nieto & Nahum, 2000). They present qualitative and quantitative evidence supporting the superiority of helical tomography compared to forward planned IMRT. There have been other instances where radiobiological metrics have been used to compare forward versus inverse IMRT (Ferreira *et al.*, 2010), Low dose rate brachytherapy versus High dose rate brachytherapy (King, 2002) or effects of using different energies for a treatment (6 MV compared to 15 MV (Hussein *et al.*, 2012). All these studies are retrospective and demonstrate the usability of radiobiological models for the purpose of comparative analysis.

None of the studies have undertaken validation of model parameters but use model- based metrics in addition to dose-based metrics in their analyses. A combinational approach in the absence of resources to validate model parameters is not ideal but viable. The pitfall associated with comparative analysis using radiobiological metrics is that due to the high degree of uncertainty, exaggeration of results is possible. As an example, if one is calculating the TCP at two different doses say 78 Gy and 60 Gy for conventional 2 Gy fraction treatment plan for a given patient. It is likely that TCP of the plans will be higher/lower than the true TCPs resulting in the perceived difference to be more/less than expected between the plans. However, as long as the base assumptions about the model hold true (in relation to the tumour/OAR), the model is likely to provide the correct understanding of the trend when comparing different dose/fractionation schemes.

Another important use of radiobiological modelling as reported in the literature is to quantify setup errors and effects of organ movement management methods. Roland *et al.* (2009) use the LQ based TCP model described in Mavroidis *et al.* (2001) and relative seriality NTCP model to analyse the effect of undertaking 4D CT based treatment planning versus 3D CT based treatment planning. Their study based on 6 patient datasets concludes that 4D CT based planning does not provide additional benefit compared to 3D CT (static or gated) based treatment planning. The observed difference in the P+ metric was in the range of 1-3% with a large standard deviation. These radiobiological metric-based results were also in alignment with the dosimetric analysis of the plans reported by them and in line with other similar studies they quoted.

Siochi *et al*., (2015) quantified the effects of tumour motion in terms of reduction in TCP. Their analysis over 5 NSCLC patient datasets showed that motion greater than 5 mm resulted in TCP reduction of 1.7% up to 11.9%. They calculated TCP for all the plans using the Poisson TCP model and Logistic TCP model using 5 different parameters sets for each TCP model. The difference in TCP values as calculated by both the models for different sets of parameters (Fitted over 1 and 2-year local progression-free survival data by Martel *et al.*, 1999; Wilner *et al.*, 2002; Guckenberger *et al.*,2009) was maximum 2% in 23 of 25 reported values. This shows good compliance between the two models. Partridge *et al.* (2009) have used the logistic TCP model to quantify the therapeutic gains of implementing active breathing control for an NSCLC cohort (n=28). Their method does not require an increase in normal lung dose to improve tumour dose and they also demonstrate the possibility of Iso-NTCP dose escalation (quantified using mean lung dose and TCP metrics). Many other post treatment data analysis studies have been reported that use radiobiological metrics (TCP/NTCP/P+/EUD) to quantify the possible clinical gain of a proposed clinical methodology / update to treatment technique (Lee *et al.*, 2015; Mavroidis, 2013; Miller *et al.*, 2009; Wang, 2010).

Further use of radiobiological models has been to perform dose escalation and treatment strategy analysis. Fenwick *et al.*, (2009) compared different NSCLC dose

escalation approaches prevalent in the UK using radiobiological models and concluded that the 30-month progression free survival could be improved by up to 20% at safely deliverable escalated dose schedules. Nahum & Uzan (2012) introduced biological optimization that uses TCP & NTCP models in different ways to optimize a given treatment plan. The approaches they introduced start with retrospective optimization of clinical data and are later applied to pre-treatment phases. Also, they only account for a single principal OAR complication during the analysis whereas in reality there are likely to be more than one dose limiting OAR. There have been a handful of approaches where radiobiological models are used as a part of pre-treatment analysis. One of these approaches was shown by Syndikus *et al.* (2011) where they used radiobiological modelling based inverse treatment planning to form prostate RT plans to boost dose to the tumour keeping conditions Iso-toxic for the normal tissue. Further, the use of radiobiological model-based analysis has been reported by Ko *et al.* (2011) where the linear quadratic model has been used to assess the validity of the hypofractionation approach in treating prostate cancer. Geng *et al.* (2017) have recently developed a mathematical model that predicts the local response of tumour for combined chemo-radiotherapy of advanced NSCLC patients. They use the exponential Gompertz model to account for tumour growth along with the LQ model for radiation-based cell kill and log-cell kill model to account for chemotherapy-based cell kill. They validated their predictions for sequential, concurrent and radiotherapy only NSCLC clinical response data of RTOG 8808 and RTOG 9410 trials. The model predicts the data on which they are based very well, however, the performance of the model for hypo/hyper fractionated regimens is pending. Also, the data is fit to a limited set of outcome data which is not ideal.

Above instances demonstrated the use of radiobiological models using retrospective data. A small number of commercial treatment planning systems now include radiobiological-model-based planning and / or plan assessment tools. These include systems by RaySearch®, Monaco® V1.0 (CMS/Elekta, Maryland Heights, MO), Research Pinnacle® V8.0h (Philips Medical Systems, Andover, MA), and Eclipse V10.0 Allen Li *et al.* (2012). The effectiveness of such an approach has been

advocated by Syndikus *et al.* (2011) who employed radiobiological models as cost functions in inverse treatment planning. The results of the pilot study were recently reported by Onjukka *et al.* (2017) where they concluded that radiobiological optimization based hypofractionated dose-painting escalated radiotherapy (over 28 prostate patients) results in plans with higher average PTV dose and the observed toxicity over median 38 months results in low gastrointestinal and gastro-urinal toxicities (i.e. an acceptable safety profile). However, it is to be noted that the authors strictly recommend the use of online image guidance using fiducial markers to manage inter-fraction tumour motion and the use of MRI to target intra-prostatic boost region accurately. The same approach has been proposed by other users in the field previously (Semenenko *et al.*, 2008; Tai *et al.*, 2008; Zaider *et al.*, 2005).

Model-based metrics have been used in many ways as described in the previous paragraphs, however, these are only good if the parameters used to calculate such metrics are correct and validated. There has been a lot of literature published that gives an account of model parameters to be used for analysis purposes (Gagliardi *et al.*, 2010; Gulliford *et al.*, 2012; Marks *et al.*, 2010; Michalski *et al.*, 2010). The validity of the available model parameters and uncertainty associated with them is certainly up for debate, but it is aimed to address these in the discussion section of relevant chapters. One of the most comprehensively reviewed publications for this purpose is the Quantec 2010 (Jackson *et al.*, 2010) review supplement that gives recommendations on the use of dosimetric constraints and NTCP model parameters for different OARs. Caution has been advocated in the literature about reliance on radiobiological models and the uncertainties associated with absolute model predictions (Marks *et al.*, 2010; Wang, 2010).

In recent years, radiobiological information is frequently used in designing clinical trials which form a relatively safe and established method of assessing/validating radiobiological assumptions about biological responses of a given cohort. The lack of robust model parameters and assumptions behind the underlying biological processes (where there are many unknowns) that govern the biological response contribute majorly to lack of confidence in the predictive power of models. The

reluctance in the clinical use of absolute predictions by radiobiological models is thus expected. The designing of the CHHiP trial based on the assumption that α/β for prostate tumour is lower than 3 Gy and its recently published results is a very good example of the above approach (Dearnaley & Hall, 2017). In the subsequent chapters, the use of radiobiological models to optimize radiotherapy treatments over a cohort of prostate and lung patients is explored. The relevant literature in relation to each of the chapters is presented in the upcoming sections.

2.7 Individualization and Optimization of Prescription Dose & Fractionation

The conformity of dose to the respective tumour and OARs has improved significantly but the way dose is prescribed has remained the same: a "one size fits all" approach. Section 2.6 reviews current clinical protocols that have been developed so far for the radiotherapy of non-small cell lung cancer and prostate cancer. As per the literature studies in the paper by Yaromina *et al.* (2012), many different factors lead to differences in the treatment response of a given patient. These factors, which have been studied extensively in the literature, include tumour re-oxygenation capacity, tumour hypoxia, tumour repopulation rate, radiosensitivity (an extensively studied parameter for major cancer types) of tumours & normal tissues and the number & density of stem cells in a tumour. Possible methods to individualize a treatment plan are enumerated below

- The first step is the individualization of patients' treatment plans; as accomplished in a study by van Baardwijk *et al.* (2012).
- A second possibility is the use of biological information on patient-specific tissue (OAR/tumour) characteristics (like radiosensitivity) through cellular assays (biopsy) and hormone tests (indicating disease state) that are known to influence a patient's response to a given treatment (West *et al.*, 2014).
- The third is incorporating patient-specific, non-invasive diagnostic functional information (Hypoxia / Angiogenesis) from PET / MRI scans that show regions of different physiological activity that could be targeted to improve local disease control (Alonzi, 2015).

- Fourth is using radiobiological models, assimilating the currently available information on the normal tissue & tumour characteristics (i.e. volume, density, best estimates of α/β and organ architecture) and individualising / boosting tumour prescription dose. This can be based on evidence from retrospective radiobiological analysis of treatment plans to individualize treatments (Onjukka *et al.*, 2017).

It is likely that a combination of the above mentioned methods can be used to individualize treatment plans (e.g. identification of hypoxic region using advanced imaging method - PET-boost trial - ClinicalTrials.gov Identifier: NCT01024829) and boosting the dose to the hypoxic region using an online adaptive or radiobiologically advanced treatment plan (Christodoulou *et al.*, 2014).

2.7.1 Biomarker based individualization approaches to optimize treatment

The group of patients with tumour (or normal tissue) radiosensitivity far from the population mean may suffer the extreme effect of over / under dosage of radiation for a given dose of radiation. Various attempts to identify and utilize biomarkers to individualize treatments are presented below.

Individualization of treatments has been advocated in a few publications with one of the early entries by Slevin *et al.* (1999) where they suggest individualization of radiotherapy prescriptions in head & neck tumours on the basis of histological grade as well as cell kinetics/loss/response indices. Mariano Ruiz de Almodóvar *et al.* (2002) reported the use of a DNA damage assay on lymphocytes to classify breast cancer patients on the basis of normal tissue radiosensitivity. They concluded that this DNA damage assay had a fair-poor discriminating capacity to classify patients that have a higher risk of acute reactions to breast radiotherapy.

Nordsmark *et al.* (2007) studied five hypoxia specific markers (carboxyanhydrase 9 (CA9) by immunohistochemistry, hypoxia inducible factor 1α (HIF-1α), pre-treatment plasma osteopontin – ELISA test, pO2 needle electrode based tumour oxygenation and tumour osteopontin (OPN) levels) for 76 patients over a five-year follow up period and reported that "*High plasma osteopontin, high HIF-1α and high*

proportion of tumour pO2 ⩽ 2.5 mm Hg (HP2.5) related significantly with poorer loco-regional control, whereas CA9 and tumour OPN failed to predict local control". Yaromina *et al.* (2012) in their review article summarised that in-vitro osteopontin levels in head & neck patients appeared to be negatively correlated with oxygen partial pressure (PO_2) levels of the tumour[24]. Further, they also referred to evidence indicating biopsy-based testing of pimonidazole as a biomarker for hypoxia. Additionally, they shed light on genetic markers such as Epidermal Growth Factor Receptor (EGFR), γH2AX protein and poly(ADP-ribose)-polymerase-1 (PARP-1) protein that have been shown to correlate with cell growth, single DNA strand breaks and double DNA strand breaks. They also reported on studies investigating biomarkers to identify cancer stem cells (CSCs) responsible for tumour regrowth.

Based on the above, it is clear that there are multiple methods that can provide information about patient specific biology to help individualize treatments. The results reported in relation to the above methods are mostly from underpowered studies, observational or retrospective data from large trial subgroups. Biomarker based individualization although promising in smaller studies requires primary data from randomized, statistically powered and validated large studies. This will allow unbiased estimation of the efficacy of such methods and help in standardization of these methods; for adoption in clinical practice.

2.7.2 Non- Biomarker based treatment individualization approaches

Alonzi (2015) and Lambin *et al.* (2010) have provided a detailed account on individualization that can be introduced alongside radiotherapy using imaging markers like FDG, ^{61}Cu-ATSM, FAZA & FMISO through PET modality, T2 Weighted to dynamic contrast enhanced techniques in MRI and a combinational approach using PET-MRI modality. The patient specific information gathered through above imaging methods can be used to selectively increase or decrease prescribed dose to the tumours and / or change the treatment method altogether to improve outcome using radiotherapy.

[24] Yaromina *et al.* (2012) refer to Le *et al.* (2003)

Mackay & Hendry (1999) published a simulation-based study looking at potential benefits of individualizing radiotherapy treatments using patient specific radiosensitivity derived from surviving fraction at 2 Gy (SF_2) data of fibroblasts. The information was incorporated into TCP and NTCP models to see if dose escalation could be achieved for the breast cancer patients keeping toxicity to less than 5% (in terms of NTCP). They concluded that a tripartite division of population could provide good benefit of treatment individualization and this approach is likely to be robust against assay result uncertainties.

Yaromina *et al.* (2012) have given a critical review of the use of the F^{18}-FDG tracer as a marker to be used for dose escalation in radiotherapy. Some groups believe that areas of a tumour with no / less F^{18}-FDG tracer uptake show hypoxic / necrotic regions and some groups report similar areas of tumours as rather aggressive, leading to disease relapse.

Lievens *et al.* (2011) and Warren *et al.* (2014) performed a treatment planning study demonstrating evidence in favour of individualized prescription dose escalation. The retrospective planning studies reported that using IMRT, dose escalation & individualization was achievable keeping within recommended OAR tolerances. Warren *et al.* (2014) reported that mean escalations of dose by around 19% (3D-CRT) and 25% (IMRT) respectively were possible whilst maintaining recommended OAR dose tolerance constraints in Stage II-III NSCLC patient cohort of 20 patients. Lievens *et al.* (2011) showed that dose escalation could be performed on an individual basis and prescription dose escalated by 15-21% for NSCLC patients keeping in recommended dose tolerance limit for OAR complications. Marshall *et al.* (2016) performed a similar treatment planning comparison study in the NSCLC cohort of 24 patients utilizing PET imaging to escalate dose to tumours. They showed that PET imaging could be used to boost tumour dose without violating OAR dose tolerance limits. C^{11}- and F^{18}- PET probes like choline and fluciclovine are now FDA approved for use in medical imaging of prostate cancer. Clinical trials assessing possible improvement in prostate radiotherapy plans after inclusion of

choline/ fluciclovine based PET imaging data have been recently reported and some are still underway (Calais *et al.*, 2018).

Further, van Baardwijk *et al.* (2008, 2010, 2011, 2012) of the Maastro group have implemented the concept of individualized radiotherapy clinically. In 2008, they reported a feasibility study with 28 NSCLC patients all of whom were prescribed radiation dose individually using a hyper-fractionated accelerated routine with twice daily fractions of 1.8 Gy. The main OAR constraints were set around keeping mean lung dose, doses to the spinal cord, main brachial plexus and main bronchi under clinically recommended dose tolerance limits. They reported the mean total tumour dose as 63 Gy (range - 46.8-79.2) with a median survival of 19.6 months and 1-year overall survival of 57.1%. The toxicities observed in the patients were reported to be acceptable. The success of the feasibility study led to a Phase II trial on the same lines where 166 patients (Stage I-III NSCLC) were included in the trial with sequential chemo-radiotherapy or radiotherapy alone. The results were reported in 2010 for Stage I-III patient and in 2011 for Stage III alone cohorts by van Baardwijk *et al.* (2010, 2011). As per the 2010 paper, the mean prescribed dose was 64.8+/-11.4 Gy with the 1-year overall survival of 68% and 2-year overall survival of 45% with acceptable acute and late toxicities. The 2012 paper by the same group reported the results of the phase II concurrent chemo-radiotherapy trial (137 patients) based on individualized accelerated radiotherapy as in other trials mentioned above. Even in patients with large tumours and multimodal disease, the results were better compared to previous trials (reported in 2008, 2010 & 2011) with an improved 2-year overall survival of 52.4% and similar acceptable acute and late toxicities. All the treatments were delivered using conformal radiotherapy.

This initiated a series of IMRT based feasibility trials in the UK on an Iso-toxicity approach. ISOTOXIC IMRT (ClinicalTrials.gov Identifier: NCT01836692 – ISOTOXIC IMRT: A Feasibility Study) is an Iso-toxic hyperfractionated accelerated radiotherapy trial where radiotherapy will be delivered in sets of 2 fractions a day (Haslett *et al.*, 2016). I-START is an Iso-toxic hypofractionated radiotherapy study where the

number of fractions to be delivered to the patients is fixed (20) but tumour dose is escalated up to known limits of OAR doses.

IDEAL-CRT (Iso-toxic, concurrent chemo-radiotherapy; Clinical Trial Identifier: ISRCTN12155469) is an individualized prescription dose escalation trial with fixed 30-fraction treatments with concurrent chemotherapy. Landau *et al.* (2016) reported on the observed survival and toxicity in the IDEAL-CRT trial. For oesophageal toxicity, 68 Gy was declared to be the maximum tolerated dose. The overall toxicity (radiation pneumonitis and oesophageal toxicity) observed in the IDEAL-CRT trial was comparable to that observed in other concurrent CRT studies (e.g. RTOG 0617, MAASTRO Study). Intensification of treatment dose in a defined range was shown to be feasible with acceptable survival rates (based on a median follow-up of 35 months, median overall survival was 36.9 months, 2-year overall survival and progression-free survival was 68.0% and 48.5%).

Sanchez-Nieto & Nahum (2000) put forward treatment individualization as one of the uses of radiobiological models, introducing the BIOPLAN software tool for treatment-outcome prediction in radiotherapy. Further, Fenwick *et al.*, (2009) performed a radiobiological model based retrospective study of NSCLC data (reporting on oesophagitis, lung fibrosis, pneumonitis, spinal cord and the 30-month progression-free survival) for different dose escalation approaches. They report

"*Worthwhile (approximately 20%) gains in 30-month local progression-free survival should be achievable at safely deliverable levels of dose escalation. The analysis suggests that longer schedules may be more beneficial than shorter ones, but this finding is governed by the relative rates of tumour and oesophageal accelerated proliferation, which are quite imprecisely known".*

Nahum & Uzan (2012) introduced four levels of prescription dose individualization that could be undertaken using radiobiological models to improve radiotherapy response.

1) The first method consists of escalating dose for a patient at a fixed NTCP and constant fraction number for a given treatment.
2) The second level looks for fraction number that maximises TCP at a set Iso-toxic limit.
3) Level 3 incorporates radiobiological models as cost functions for inverse treatment planning.
4) Level 4 takes into account patient-specific biological markers to improve prescription dose estimate using TCP / NTCP models to individualize treatment plans.

They considered the toxicity of a single OAR when optimizing the doses for a given tumour (i.e. radiation pneumonitis for lung cancer treatment). In reality, Oesophagitis, Pericarditis and or spinal cord myelopathy can become dose limiting OARs in lung tumour dose escalation which limits the applicability of the results of Nahum & Uzan (2012) in clinical practice.

In chapter 3, a dose escalation methodology that accounts for multiple OARs / toxicity endpoints when escalating dose to the tumour for a large cohort is introduced. Syndikus *et al.* (2011) report a study (BioProp) that uses radiobiological model-based inverse treatment planning to increase TCP in 6 patient plans. Azzeroni *et al.* (2013) provide evidence in support of biological optimization with regards to boosting dose to intra-prostatic lesions. In the paper, they evaluate the feasibility of boosting doses to dominant intra-prostatic lesions (DILs) using TCP and NTCP. They reported large variation in TCP values for the DILs because of variation in TCP model parameters. The result of such parameter variation is likely to affect dose optimization, and biologically based treatment plans should thus be evaluated carefully. van Baardwijk *et al.* (2010) report results of a single arm study where the prescription doses were escalated on an individual basis in cases of NSCLC stage I to III (166 patients) under normal-tissue tolerance limits. They concluded that *"individualized prescribed radical radiotherapy based on normal tissue constraints with sequential chemoradiation shows survival rates that come close to results of concurrent chemoradiation schedules, with acceptable acute and late toxicity. A prospective randomized study is warranted to further investigate its efficacy."*

Zindler *et al.* (2016) report another retrospective analysis for prescription dose individualization in Stereotactic Ablative Radiotherapy (SABR) treatments. They propose dose escalation to tumours at the highest levels until set OAR dose tolerance limits are not exceeded. Zhang *et al.* (2010) demonstrate the use of individualization to escalate prescription dose in intensity modulated proton therapy compared to standard photon based IMRT in a retrospective study of 20 patients. Their analysis also reports that an increase in prescription dose is possible keeping normal tissue doses under standard published tolerance limits.

All these above approaches support the work in chapter 3 where a software system that allows comparison of radiotherapy treatment strategies and optimizations over a large cohort is showcased. This system is used to show the effect of changes in regimens, optimization strategies and model parameters on lung and prostate cohorts as a whole through TCP-NTCP graphs.

2.8 Radiosensitivity based treatment optimization

The susceptibility of a given tissue to radiation exposure is called radiosensitivity. It is quantified in terms of α, β and surviving fractions (e.g. SF_2 is surviving fractions at a 2 Gy in-vitro dose on a cell line) for the LQ model. It has been shown that radiosensitivity correlates with the outcome at least for head & neck and cervical cancers (West *et al.*, 1997). Studies by Menegakis *et al.* (2009) and Olive & Banáth (2004) show that assessment of γ-histone H2AX (A DNA damage marker) immuno-histo-chemically would shed some light onto intrinsic radiosensitivity of a tumour. A few prominent methods used to quantify tissue radiosensitivity are listed in the upcoming sections.

First and the most common (even referred to as the gold standard) is the method of clonogenic assays. In this method, cells are extracted from a tumour and divided into two samples where one of the samples is irradiated and the other is not (control sample). Both the samples are placed in an identical growth environment allowing them to form sizeable colonies over a predefined growth period. The number of colonies in both the samples are now counted and corrected for plating

efficiency to establish cell surviving fraction. Undertaking the same exercise over different irradiation doses allows formation of a cell survival curve which can be modelled using the LQ equation by fitting α and β parameters (Joiner & van der Kogel, 2009)[25].This method takes a long time to give results and therefore alternative assay techniques have been proposed which are faster for measuring radiosensitivity. These include DNA damage assays, apoptosis and micronucleus assays (West & Barnett, 2011).

DNA damage assays (e.g. alkaline comet assay) measure single or double DNA strand breaks induced post irradiation. The comet assay requires few cells and allows processing of results within hours of sample collection. Although sensitivity of DNA damage assays has been found questionable in the past, the phosphorylated histone H2AX assay as a surrogate marker for double-strand breaks has been found very promising (Dunne et al., 2003).

Micronucleus assays measure micronuclei that are formed by a chromosome break or when the chromosome is lagging in the anaphase post radiation damage. The use of cytoplasmic division inhibitor upon formation of micronuclei arrests the cell division process allowing identification of binucleated cells that are counted. This forms a very sensitive method of assessing the sensitivity of cells to radiation damage. (Vral *et al.*, 2011).

Apoptosis is a radiation-induced cytotoxic response in a cell that is expressed very quickly after radiation damage to a cell. Cytotoxicity can be evaluated rapidly using flow cytometry. This added with the sensitivity of the method and ease of sample collection (i.e. blood) make apoptosis assays very attractive for measuring radiosensitivity (Azria *et al*., 2008; Crompton & Ozsahin, 1997) compared to the clonogenic assay method.

Compared to clonogenic assays all of the above methods of assessing radiosensitivity are significantly quick due to their mechanism of action, sample collection and or sample processing techniques. Some pitfalls of the clonogenic

[25] Refer Chapter 4 Section 4.2 for more details on clonogenic assay technique

assay methodology for assessing radiosensitivity (intrinsic or clinical) are discussed below.

First is the time it takes for the cell-survival data to be determined. Secondly, the conversion of in-vitro results to patient tumour/OAR radiosensitivity is not ideal as the in-vivo growth environment of the tissue is different to in-vitro conditions. Thirdly, studies reporting on this do so with variations in methodology which can make radiosensitivity estimates non-reproducible (i.e. standardization of assay technique is important). Also, not many validation studies are reported that detail the quality of published work on a given tumour type. Assay techniques are not available in the clinic for various reasons that include the complexity of processes, clinical implementation issues, and the availability of samples as the process is invasive.

As far as non-invasive methods of assessing radiosensitivity-related tissue characteristics are concerned, advances in diagnostic imaging technology specifically PET & MRI have played a major role that allows assessment of hypoxia and angiogenesis in a tumour. It is common knowledge that hypoxia leads to radio-resistance and poor radiotherapy response in patients (Krause *et al.*, 2006). In their paper, Krause *et al.* (2006) discuss the role of PET/CT in IMRT regarding hypoxic region dose boosting (also referred to as "dose painting"). Dubois *et al.* (2011) have shown in in-vivo studies that [^{18}F]HX4 is a very promising hypoxia marker for PET imaging. However, incorporating this kind of imaging information into standardized clinical practice will require a large body of clinical evidence (to demonstrate the efficacy of the method).

There is a lot of literature on using genetic markers to individualize treatments and thereby improve treatment outcomes (Barnett *et al.*, 2015; Coco Martin *et al.*, 1999; Liu *et al.*, 2015; Wang *et al.*, 2006; West *et al.*, 2014; West & Barnett, 2011; Williams *et al.*, 2008). There have been instances where mixed reviews about a correlating factor to toxicity have been published (Girinsky *et al.*, 1994; Stausbøl-Grøn & Overgaard, 1999). Either way, the point is that a single genetic marker or a biomarker that conclusively predicts the radiosensitivity of a given cell sample from

a patient has not been reported to date. However, evidence has been accumulating in the direction of assimilating more than one type of genetic marker to stratify patients into specific categories of radiosensitivity (Barnett *et al.*, 2012; Hall *et al.*, 2014). 'Radiogenomics' as it is known looks into genetic variation associated with response to radiotherapy and attempts to uncover groups of genetic markers that can predict individual response to treatments (Kerns *et al.*, 2014; Rosenstein, 2011). The biomarker grouping that can predict specific radio-response is achieved by conducting large genome-wide association studies (GWAS). The final aim of the whole exercise would be to formulate a clinically feasible predictive profiling test enabling the individualization of patient treatments. Such evidence correlating genetic variation and radiotherapy toxicity is presented by Barnett *et al.* (2014) and Kerns *et al.* (2014, 2016).

Tumour dose, cell density and tumour volume are important variables that help predict tumour control probability. However, only assumptions or best estimates are available for the tumour's intrinsic radiosensitivity, hypoxic tumour cell mass and rate of tumour cell proliferation. The best estimates are from published studies based on *in vitro* experiments which come with uncertainties of their own (Fertil & Malaise, 1985; Słonina & Gasińska, 1997).

In a report on human radiosensitivity (Public Health England, 2013), radiosensitivity is defined on different levels ranging from whole organism radiosensitivity to organ radiosensitivity to cellular level radiosensitivity. The report comprehensively explains radiosensitivity for tumours and normal tissues. It also looks at different factors that are believed to affect normal tissue (clinical) radiosensitivity. In summary, it states that sex, body mass index, alcohol consumption or diet may or may not influence clinical radiosensitivity but increase in age, genetic variation, diabetes, smoking and collagen vascular disease are very likely to increase clinical radiosensitivity.

In chapter 4 of this thesis, a hypothetical study to assess the effect of using patient specific radiosensitivity information on radiotherapy treatment individualization & optimization is undertaken. This involves segregating patients into three groups

based on tumour radiosensitivity and applying different optimization methodologies to optimize treatments. The results are presented as a large table of analysis comparing the clinical scenario of

1) Optimization of treatment plans **'without'** versus **'with'** stratification of patients based on patient specific tumour radiosensitivity information

2) If patients could be stratified into subgroups based on radiosensitivity information what difference is observed in the optimization if the stratification was used '**before**' vs **'after'** treatment planning

2.9 Inverse-Treatment planning - New Approaches

Inverse treatment planning is defined as a computerised iterative process of optimising dose fluence from every beam direction to develop a dose distribution (i.e. treatment plan) that conforms to a given set of objectives and constraints. The aim of the iterative inverse plan algorithm is to find a solution that has the lowest cost function value (the quantified difference between expected ideal dose distribution and the dose distribution of a given iteration). This is discussed in more detail in Chapter 5, section 5.1 of this thesis.

From the radiotherapy treatment planner's point of view, the goal is to form a dose distribution keeping OAR doses within 'tolerance' limits whilst forming a plan that would deliver the prescribed radiation dose to the PTV. From the inverse planning software point of view, the aim is to find beam-intensity profiles (and beam directions) that satisfy the objectives & constraints set by the planner. A clinically unacceptable plan is likely to result if the objectives and constraints are not defined precisely. There have been different approaches to achieve the 'ideal treatment plan' (i.e. class solution) that are discussed next.

Amongst the new and interesting clinical approaches to treatment planning are *Knowledge-Based* treatment planning® (KBRT), *Online adaptive* planning and *Radiobiological Model*-based treatment planning. KBRT is a novel way to create effective treatment plans using a database of clinically approved treatment plans. The premise behind knowledge-based treatment planning is to find an improved

starting point for the treatment plan optimizer allowing it to find a solution faster than the standard iterative solution finding process.

The KBRT system houses a database of patient structure sets and clinically approved treatment plans. When a new plan is to be created for a given patient, the CT structure set 'query set' of the patient is given as input to the KBRT system which looks into the database to find a closely matching patient structure set 'match set' using 'Mutual Information' metric (which is a metric for image matching, allowing a purely statistical comparison of image histograms between given image datasets). The 'mutual information' metric (MI) is generated by comparing two dimensional BEV images of two CT structure sets from one angle. The MI value generated for different angles of the 3D CT structure set are averaged to form a composite MI metric which is used as the final similarity score of a given comparison iteration (Chanyavanich, 2011).

The algorithm tries to find a 'match case' with the highest 'mutual information' within the patient plan library. Once a matching patient dataset is found, the system adapts the treatment plan associated with the matching patient dataset and optimizes it for the current patient structure set. The knowledge-based planning system then allows manual adjustments of objective/constraint to further improve the plan once an automated solution has been formed. The successful application of this methodology has been reported by many (Cao *et al.*, 2015; Chanyavanich *et al.*, 2011; Good *et al.*, 2013; Nwankwo *et al.*, 2015; South *et al.*, 2015). However, the caveat here to keep in mind is that the plans will be as good as the initial library and for situations where plans matching a given anatomy are not available, results may not be optimum.

Next, adaptive radiotherapy treatment planning is briefly discussed. Adaptive radiotherapy (ART) is a technique whereby the treatment plan is modified between fractions to adjust for inter-fraction variation in a tumour/organ position, size and shape (Ghilezan *et al.*, 2010). Different ART techniques are shown in figure 2-6 (Kibrom & Knight, 2015).

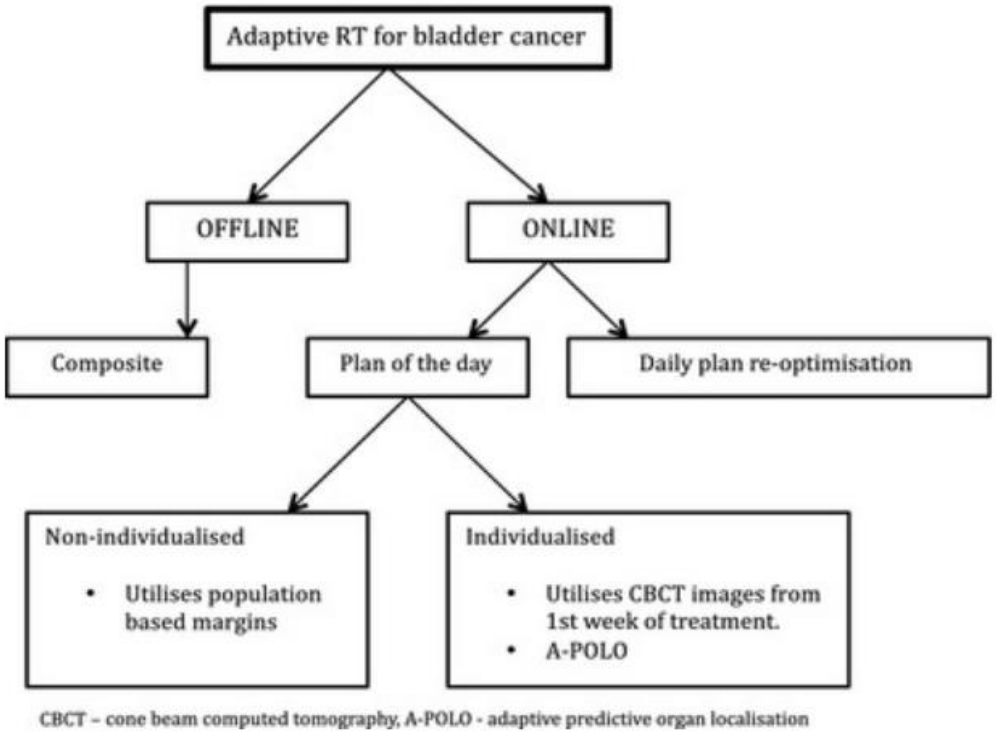

Figure 2-6 Various Adaptive Radiotherapy techniques and sub techniques are shown in the flow chart. From Kibrom & Knight (2015)

Adaptive radiotherapy can be divided into two categories 1) Offline (a.k.a composite method) ART technique and 2) Online ART technique. The offline ART method involves using CBCT images of the patient taken in the early weeks of treatment period to amend the treatment plan to match various organ's shape, size and position during a given (later) period of treatment. Although some of the reported studies show a reduction in PTV volume by up to 40% and reduced OAR irradiation, the offline method only accounts for systematic error between the planning and treatment phase and is not optimal when there are frequent (possibly daily) changes to patient anatomy (e.g. bladder size).

The Online ART method is categorised further into 'plan of the day' (PoD) ART technique and daily plan re-optimization technique. The PoD ART technique has been further classified into non-individualized and individualized categories. In the non-individualized PoD ART method, a library of plans is created for a given patient CT dataset. The PTV is created for each plan in the library by adding population-based isotropic or anisotropic margin around the CTV. At the time of treatment, a

CBCT image-set taken prior to the treatment is used to select the plan in the library that provides the best coverage of the target.

In the individualized PoD ART method, an individualized patient plan library is created for each patient using the initial planning CT and combination of CBCTs from the first week of treatment resulting in three plans with small, medium and large CTV. The plan providing the best coverage when compared to the CBCT prior to treatment is selected for the given fraction. Another type of individualized PoD ART method is the adaptive predictive organ localization (A-POLO) method. In this method, a library of plans is created by taking a set of CT scans of the patient with an empty bladder and then after consumption of water (at least two separate scans over an interval of roughly 20 mins) during the planning stage.

This allows the formation of plans that cover all the anatomical scenarios in relation to the bladder shape and size. Using the pre-fraction delivery CBCT, the plan providing the best coverage of the target is chosen from the library for delivery. It has been shown that online ART method is successful in reducing the size of the irradiated target volume and also spares OARs considerably compared to conventional radiotherapy technique. Daily plan re-optimization which is the latest reported Online ART technique could be very useful in improvising treatment response. Different methods of achieving this have been reported by Li *et al.* (2013) and Ahunbay *et al.* (2010) where the inter-fraction variation in patient anatomy are accounted for in the treatment 'plan on the day' (automatically and dynamically). The daily planning technique has been shown to be very useful at target volume reduction and sparing OAR dose but requires a large resource commitment (i.e. involvement of personnel participating in various aspects of clinical RT and increase in total time for treatment which reduces patient throughput) which may jeopardize its clinical feasibility.

Attempts to use radiobiological models to optimize radiotherapy treatment plans are presented next. Optimization of treatment plans using radiobiological models was first introduced by Raphael *et al.* (1992). They present the model-based radiotherapy optimization in its mathematical form and use a computer program-

based experiment to show the difference between constraint-based optimization plan and probabilistic model-based optimization plan. The study is very theoretically orientated providing a very clear and concise explanation of difference between constraint-based planning and model-based planning. The idea was taken further by Alber *et al.* (1999) who developed & demonstrated use of different types of models to form objectives/constraints and how these are likely to affect optimization compared to using dose volume-based metrics for optimization. They demonstrated the mathematical integration of radiobiological models into objective/constraint functions for inverse treatment-planning purposes. These papers thoroughly discussed ways of adding different types of models to the inverse optimization algorithm but there was a lack of clinical evidence of such planning methodology; which can be attributed to the era of publication where inverse treatment planning was in its infancy.

The apprehension in relation to lack of clinical data to validate model parameter based absolute TCP/NTCP metrics was raised against this methodology by Bortfeld *et al.* (1996). The superior dose sparing achieved through biologically based optimization (using EUD metric) was presented by a few authors which include (Das, 2009; Qi *et al.*, 2009; Semenenko *et al.*, 2008). EUD[26] is a useful metric that is simpler to calculate and accounts for tissue volume effect, but it does not account for radiosensitivity of the target tissue. In Chapter 5 using RayStation for inverse treatment plan individualization, the approach differs from the one presented by above authors as Iso-toxic plan optimization is undertaken (based on the Marsden TCP and Lyman-Kutcher-Burman NTCP models) with an aim to increase the dose in the tumour without increasing OAR toxicity.

[26] "EUD is defined as the equivalent uniform dose, which if distributed uniformly across the target volume, would lead to the same level of cell killing as the actual dose distribution of interest. Based on the EUD concept, a complex dose plan with 3D dose distribution can be reduced to a single EUD parameter, which relates to treatment outcome of a biologically equivalent dose delivered in 2-Gy fractions of EBRT" - Wang *et al.*, 2008

Schell *et al.* (2010) used LQ-model-based objective functions to optimize an inverse treatment plan for a head & neck patient dataset and a prostate cancer dataset as a case study to introduce "Radiobiological-effect-based treatment plan optimization". They implemented radiobiological-model-based cost functions in their in-house treatment planning software KonRad and compared conventional treatment plans to LQ-model-based inverse treatment plans. They emphasized the assumptions, advantages and pitfalls of using the LQ model-based objectives for the inverse planning process. However, they did not use NTCP model based constraints as dose limiting functions for the OARs.

Radiobiological-model-driven inverse treatment planning was demonstrated by Nahum & Uzan (2012) where they used the Marsden TCP as an objective function, and the LKB NTCP (for lung-GTV) as a constraint function to form an inverse treatment plan (3-field IMRT plan) of an NSCLC patient; the planning software was the in-house-modified Research Pinnacle system. They obtained an increased TCP for the "Bio-plan" compared to the conventional plan, with OAR constraints being the same for both plans. Details about the constraints/objectives used for other OARs were not given.

Conventionally, treatment planning approaches do not involve radiobiology; plans are based solely on (physical) dose-volume (D-V) objectives & constraints with the additional key assumption that a uniform/homogenous dose distribution in the target volume yields the best solution. In this work, it is demonstrated that the use of radiobiological-model-based objective / constraint functions can yield treatment plans with a higher therapeutic benefit than plans created from D-V objectives. The D-V metrics of the plans generated using both methods are also reported for comparison.

In chapter 5, conventional Dose-volume Based (DB) planning is compared to radiobiological objective & constraints based (RB) planning for lung and prostate cancer patients. The findings are reported in terms of the therapeutic gain as a function of TCP, NTCP and dose-volume-based parameters. TCP-NTCP graphs (cf. Chapter 3) and DVHs are used to illustrate the differences between overall

conventional dose-escalation strategy and the radiobiologically individualized inverse-planning strategy.

2.10 Iso-toxic Dose constraint conversion

Dose-based metrics like V_{20Gy}, V_{50Gy} (i.e. $V_{xx\ Gy}$) are widely used in clinical radiotherapy treatment plan assessment that is based on published clinical reports that correlate OAR toxicity risk to such metrics (Jackson *et al.*, 2010). Several publications on estimates of best-fit parameters for various NTCP models have been published and are extensively used by various research groups all over the world. Gulliford *et al.* (2012), Marks *et al.* (2010) & Werner-Wasik *et al.* (2010) give a comprehensive review of reported NTCP model parameters for different complications like radiation pneumonitis, rectal bleeding and oesophagitis.

Gulliford *et al.* (2012) concluded that there was considerable variation in derived model parameters for different endpoints related to rectum which suggests that it is likely that there is more than one pathophysiological process that governs the response of rectum to radiation exposure. Werner-Wasik *et al.* (2010) point out the variability associated with using single threshold dose volume constraints to predict esophagitis and also caveat the tentativeness of the models and recommend performing internal (centre specific) data based validation of model predictions before using them in clinical decision making. Currently, ICRU (2010) *requires* the reporting of $V_{xx\ Gy}$ and $D_{yy\ \%}$ (Level 2 mandatory requirement) parameters for treatment plans and *recommends* reporting of TCP, NTCP & EUD values (Level 3 Optional reporting). The QUANTEC (Jackson *et al.*, 2010) review papers provide recommendations for both dose-volume based constraints and NTCP model parameters for complication rates in different OARs.

2.10.1 Problem statement

A diagram depicting the IGRT workflow is shown in Figure 2.7 (Gupta & Narayan, 2012). Once the patient's tumour has been diagnosed and referred for radiotherapy, the patient visits the treatment centre for a CT scan. A CT scan is used for target and OAR delineation which is essential for planning purposes. The patient may also be referred for a PET / MRI scan that gives functional information about

the cancer and its spread in the part/whole of the body. At this point, the oncologist prescribes the dose regimen and the physicist, dosimetrist or therapy radiographer form a clinically acceptable 'geometric' treatment plan to impart the prescribed dose.

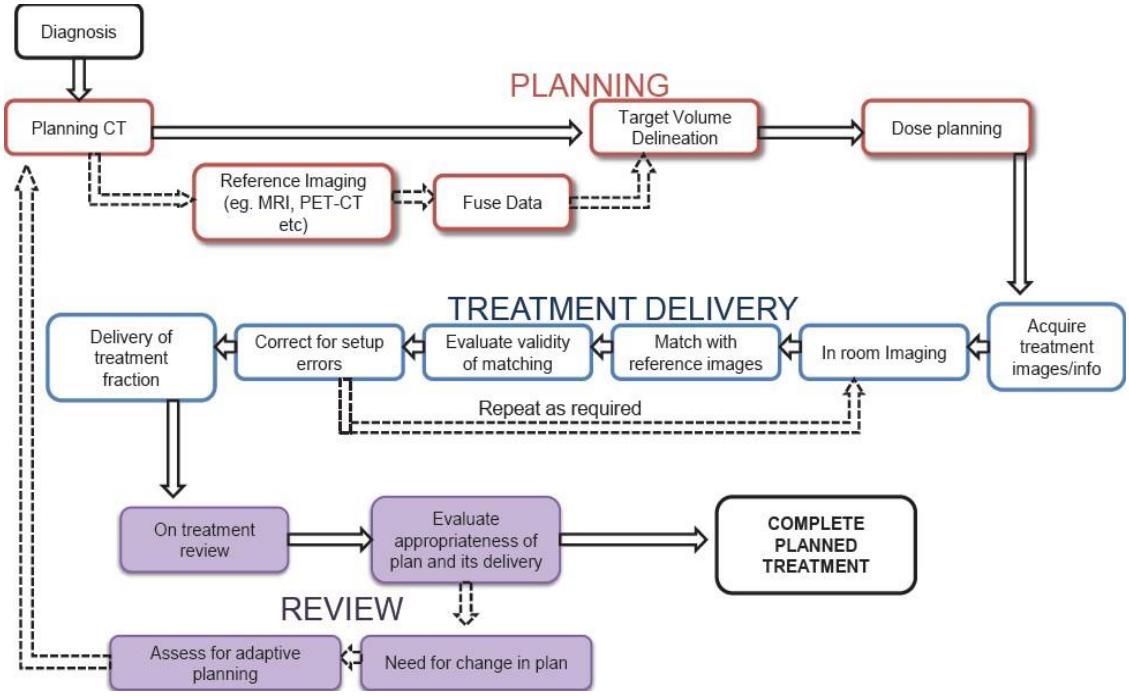

Figure 2-7 Workflow of a routine clinical IGRT radiotherapy treatment (redrawn from Gupta & Narayan, 2012)

Each centre would follow a protocol to deliver a given regimen. Depending on the extent of disease, the oncologist decides on the standard regimen, a research regimen (clinical trial) or a palliative regimen of radiotherapy. These regimens (aka protocols) consist of dose and fractionation details along with OAR dose limits or NTCP limits and target coverage requirements. The treatment planner may use a manual (aka 'forward') or an 'inverse' (automated) treatment planning technique to create the treatment plan. This plan is then independently verified by a physicist for correct radiation dose and dose distribution in the tumour and OARs. Once a plan passes through the plan quality check (QC), it is 'signed off' by the oncologist for implementation. The patient is then treated as per the schedule of fractions that will deliver the prescribed dose to the tumour.

The above describes an 'ideal world' scenario. There are a small number of situations where the scheduled treatment fraction cannot be given to the patient;

these may include machine breakdown, staff unavailability, public holidays, a serious problem with the patient's health and even transport problems (public or private). If a 'gap' in the treatment occurs, this may result in increased clonogen repopulation and therefore the treatment prescription may need to be changed to achieve an unchanged treatment outcome. Thus, take for example a 55 Gy in 20 fractions lung treatment protocol with a normal lung (OAR) radiation pneumonitis dose limit of V20< 30% (Marks, Bentzen, *et al.*, 2010). After a treatment gap, how does the clinician decide on the new regimen keeping the OAR dose/NTCP to the same limit? Or, simply put, how can a clinician obtain equivalent dose limits from one regimen to another? The BED formula is currently used to address the questions above which is described in the upcoming sections.

Another scenario where a similar question arises is when the treatment strategy is to be decided for a patient or even a cohort. For many years, 2 Gy/fraction was a standard treatment for lung cancer. Per the published literature, many centres have tried different protocols, some preferring hypofractionated, accelerated or hyper-fractionated treatments as shown by Méry *et al.* (2015) in their review of NSCLC treatments. So, if a centre following a given radiotherapy regimen wants to change to a different regimen, how do clinicians establish new OAR tolerance dose limits that will not exceed OAR tolerance dose limits of previously established protocols? A new approach based on NTCP modelling addressing the above questions is described in Chapter 6.

Few of the methods that have been established in the literature to compensate for treatment gaps and or dosimetric limit conversion are described in the next section. These methods are described in detail in RCR (2008) guidelines.

2.15.1.1 Accelerated Scheduling

When the treatment gap is not very big (<=3 days) it is easy to compensate for the missed fractions by treating the patient on a weekend to maintain the same total dose delivered in prescribed treatment time. Per this scheme, multiple fractions are delivered in a single day until the total dose is 'compensated for'. However, the

assumption here is that sub-lethal repair of normal tissues between fractions is complete, i.e. fractions are planned with a gap of at least 6 hours between them. A strong word of caution has been given for the safety of this method when the fraction sizes are greater than 2.2 Gy (Barrett, 2008; Thames, Peters, & Ang, 1989). This does not require any conversion of the dosimetric constraints as the prescription dose and fractionation do not change.

2.15.1.2 Biological effectiveness compensation

Further, a modelling approach can be used as shown by (Fowler, 1989) where BED term is used to compare dose regimens. The BED is a single metric for comparing dose/fraction equivalence between any two regimens (Dale & Jones, 2007).

2.15.1.3 Increasing Total Dose

The last resort to any treatment rescheduling is to increase the total treatment time to compensate for the loss of dose due to the gap(s). This raises the issue of repopulation. The precise time when the gap occurred is critical, as later treatment gaps tend to result in higher repopulation that must be accounted for if the treatment time is to be increased. Conventionally lung tumour treatment gap compensation would need a higher extra total dose to compensate for repopulation. In the case for prostate, repopulation conventionally is assumed to be negligible so the total dose can remain the same (assuming less than 58 days' total treatment time - repopulation is quoted to start after 58 days with 90% confidence - Gao *et al.,* 2010). The proposed method in the literature uses a $K(T-T_d)$ factor along with the BED equation to compensate for the radiation 'wasted' in counteracting the repopulation that occurs due to increase in total treatment time. The best estimated recommended value of the K-factor used in the BED formula is 0.9 Gy day^{-1} for head and neck cases (Dale *et al.*, 2002). The same publication also provides worked examples and enumerates all pros and cons of using different time gap compensation methods applicable to radiotherapy.

The next section describes the current method that is employed to convert tolerance dose limits of different OARs to find their equivalent for different treatment schedules.

2.10.2 Dosimetric Parameter Conversion

To convert V_{xx} of a given OAR in regimen A to an equivalent V_{xx} in regimen B, one of the simplest methods available is as follows. Convert the DVH dose bins of one DVH using the Withers' correction formula to the other regimen (Withers *et al.*, 1983). The V_{xx} value of both the schedules can be now compared on an Iso-BED basis.

The BED formulation is so far the most useful and a simple way to convert dose in one regimen to dose of another regimen or compensate for treatment gaps. The BED Iso-effect formula is heavily reliant on the α/β parameter that has errors of its own contributed by derivation of α and β from laboratory experiments on cell lines or data fitting over clinical studies. Further, the BED formula fails to account for the effect of total volume or organ architecture in the conversion of metrics. NTCP models address the above pitfalls and are utilized in the Iso-toxic conversion method that is developed.

In chapter 6, an NTCP-model based conversion platform is described; where LKB NTCP model (see the literature review section) is used to perform the conversion of V_{xx} constraint from one regimen to the other in Iso-toxic conditions. Here, the OAR DVHs are the input, along with conversion the metric in terms of V_{xx}, the current regimen (A) and the new regimen (B). The method uses Iso-toxic OAR complication probability as the bridge to link regimen A and regimen B.

Chapter 3 Dose Individualization & Optimization in Radiotherapy: A Radiobiological Modelling-based approach

3.1 Introduction

Current treatment strategies for lung & prostate tumours and the progress to date on establishing prescription doses and regimens for improving the overall population response to radiotherapy are discussed in chapter 2. It was emphasised that fixed dose and fractionation regimens are prescribed to all the patients eligible for curative radiotherapy. The current regimens for (non-small-cell) lung cancer treatment in the UK are 52.5-55 Gy in 20 fractions and 60 Gy in 30 fractions (Bezjak *et al.*, 2012; Haslett *et al.*,2014). For prostate, it is 74 Gy in 37 fractions or 60 Gy in 20 fractions (Dearnaley *et al.*, 2016).

However, in a patient cohort (or population) not all tumours have the same size/volume or the same radiosensitivity (West *et al.*, 1997). Concurrent chemotherapy has been shown to radiosensitize tumour cells. It has been observed that radiation treatments are more effective with concurrent chemotherapy (O'Rourke *et al.*, 2010; Rowell & O'Rourke, 2004). The radiosensitivity of tumour cells can only be determined via a biopsy followed by a clonogenic assay which takes several weeks because of which it cannot be taken into account in radiotherapy dose prescription. Cell-survival curves as a function of radiation dose have been published for many cell lines for various tumours. Using these data, the α and β parameters have been derived (Chapman and Nahum, 2015; Chapman, 2003). Tumour size can be estimated via various methods (Imaging methods like CT, MRI, etcetera) and this allows a crude estimate of total clonogen number to be made. Further, the location of a tumour with respect to normal tissues can be used to escalate dose to the tumour limiting the normal tissue complication rate. DVHs obtained from treatment plans are used to estimate TCP and NTCP for a given patient (DVHs described in Chapter 2). An Iso-toxic approach could be used to

individualize the dose to the tumour (thereby improving TCP). However, individualized radiotherapy dose prescription is not a standard clinical practice currently except in research radiotherapy treatment protocols (e.g. lung cancer RT treatments).

In the research described in this chapter, the potential effects of *individualizing* treatment prescription for each patient by varying the plan dose on an Iso-toxic (or Iso-NTCP) basis are demonstrated. Treatment individualization (in terms of prescription dose and no of fractions) is performed for all the patients (one at a time) in the cohort. The change in overall population response to individualized RT treatment is then reported (in terms of population-averaged TCP & NTCP).

3.1.1 Analysis Goals

The current analysis focuses on dose-fractionation optimization on an individual patient basis for lung and prostate tumour plans. The primary goal is, for different strategies of dose optimization, to compare the population-averaged TCP and NTCP in order to identify the strategy that would yield the most impactful improvement in clinical outcomes compared to the standard fixed dose and fractionation approach.

3.1.2 Patient Data Sets

Two cohorts of patients have been used for the dose-fractionation-optimization analysis. There are 59 lung tumour DVH datasets, for 3D-CRT and IMRT patients that were prescribed 52.5-55 Gy in 20 fractions. The datasets consist of DVHs for GTV, PTV, total paired lung (Lung- GTV), Spinal Cord, Oesophagus, and Heart. It is to be noted that some of the datasets did not contain DVHs of Oesophagus and Heart. The data made available was completely anonymized (per conditions of REC application reference: 14/NW/1345 IRAS project ID: 159143) and therefore the reasons for the exclusion of DVHs of Oesophagus and Heart in individual plans could not be investigated. One can assume that in these cases the organs were not in

Table 3-1 PTV Lung Tumour Volume (cc)	
Min	8.3
Max	344.3
Median	82.8
Mean	100.1

Table 3-2 PTV Prostate Tumour Volume (cc)	
Min	111.7
Max	241.2
Median	156.6
Mean	161.4

the treatment field and therefore were not in the 'at risk' category. For the prostate tumour cohort, 56 DVH datasets consisting of DVHs of PTV, prostate, rectum, bowel, urinary bladder and femoral heads are analysed. These patients were treated with 60 Gy (to the tumour volume) in 20 fractions. It is again to be noted that not all the datasets included all the above-mentioned DVHs for the reasons stated above. All datasets included DVHs of PTV, prostate, rectum and the urinary bladder.

3.2 Methodology

This section describes the current approach to radiotherapy treatment dose & fraction-size optimization presented as a population response to different strategies of individual dose customization. This prescription-dose-fractionation individualization is purely based on dose-volume data derived from treatment plans. Incorporating biomarker or diagnostic information into the analysis would most likely further improve the treatment plan to achieve a better therapeutic gain for patients. In the analysis that follows, the published dose-volume constraints and/or published NTCP model parameters are used to derive the individualized prescription doses. The results are expressed as population-averaged TCP (TCP_{pop}) as a function of NTCP ($NTCP_{pop}$).

For the lung tumour treatment plans, the tumour DVH is formed of the PTV DVH (i.e. derived from the dose distribution in the PTV) but with the volume of the GTV. As per ICRU report 83, GTV is the gross demonstrable extent of a tumour that consists of the primary tumour and any regional tumour nodes. Tumour control probability might therefore be expected to be a function of the DVH of the GTV. It is however important to account for geometric uncertainty in the location of the GTV due to organ motion and geometrical setup variations (consisting of patient positioning and beam alignment errors). Thus, PTV is defined in treatment plans and is planned to receive 95% to 107% of the prescribed dose to be treated. PTV volume is formed by adding margins to the CTV; and the CTV is formed by adding a margin to GTV to account for the suspected clonogen presence beyond the edges of the GTV (ICRU Report 83; Burnet,2004). However, for estimating the average number of tumour cells, the best approximation of the volume is the structure delineated as

the GTV. Hence in this work the predicted tumour control probability is based on the *dose distribution of the PTV* and the *volume of the GTV*.

The aim is to determine the maximum dose that can be delivered to the tumour without exceeding NTCP for the principal OAR. The optimization parameters for the DVH dataset in terms of radiobiological models are TCP, NTCP and fraction number. Other OAR toxicity is accounted for using organ-specific NTCP limits or dose-volume based parameters like V_{xx}, mean organ dose and maximum tolerance dose (only when NTCP model is unavailable for the OAR) to limit the escalation of the prescription dose (D_{pres}).

This entire analysis is performed using an in-house software with a GUI shown in Figure 3-4. The computation of TCP & NTCP was checked against the Biosuite (Uzan & Nahum, 2012) software package. The results of the quality control are shown in the results section. The absolute errors and uncertainty associated with the TCP and NTCP models are discussed in section 3.4.3.

MARSDEN TCP MODEL						
Tumour	**Lung**	**Lung2**	**Prostate1**	**Prostate2**	**Prostate3**	**Prostate4**
α (Gy^{-1})	**0.307**	**0.293**	**0.3**	**0.258**	**0.218**	**0.155**
α_σ	**0.037**	**0.051**	**0.114**	**0.099**	**0.082**	**0.058**
α/β (cGy)	**1000**	**1000**	**1000**	**500**	**300**	**150**
Clonogenic Density	**10^7**	**10^7**	**10^7**	**10^7**	**10^7**	**10^7**
Repopulation Constant	**3.7**	**3.7**	**-**	**-**	**-**	**-**
Delay to repopulation (days)	**21**	**21**				**-**
Reference	**Uzan (2012)**	**Baker *et al.* (2015)**	**Uzan (2012)**	**Uzan (2012)**	**Uzan (2012)**	**Uzan (2012)**

Table 3-3 The Marsden TCP model parameters used in this analysis are shown above.

LKB NTCP MODEL								
End Point	**Radiation Pneumonitis**	**Oesophagus Complication**	**Myelopathy**	**Heart**	**Rectal Bleeding**	**Faecal Incontinence**	**Bladder Complication**	
m	**0.45**	**0.44**	**-**	**0.64**	**0.13**	**0.42**	**-**	**-**
n	**1**	**0.32**	**-**	**0.13**	**0.09**	**1**	**-**	**-**
TD50 (cGy)	**3140**	**5100**	**-**		**7690**	**10570**	**-**	**-**
α/β OAR (cGy)	**300**	**1000**	**87**	**250**	**300**	**300**	**600**	**600**
Vxx	**V20**	**-**	**-**	**V30**	**V50**	**V50**	**V80**	**V65**
Vxx Limit	**30%**	**-**	**-**	**46%**	**50%**	**50%**	**15%**	**50%**
Dmean (cGy)	**-**	**3400**	**-**				**-**	
Dmax (cGy)	**-**	**-**	**5000**					
Reference	**Uzan (2012)**	**Chapet *et al.* (2005)**	**Kirkpatrick (2010)**	**Martel *et al.* (1998)**	**Michalski *et al.* (2010)**	**Peeters *et al.* (2006)**	**Viswanathan (2010)**	
	Marks *et al.* (2010)			**Wei (2008)**				

Table 3-4 LKB NTCP model parameters and dose-based constraints for different endpoints/complication; accounted for in this analysis are shown above.

The LKB NTCP model is used for calculating NTCP of OARs in this work. An EQD_2 correction (see chapter 2) is performed to convert the OAR dose distributions (in the form of DVHs) to equivalent 2 Gy-fraction (total) dose distributions as LKB NTCP model does not explicitly account for the effect of different fraction sizes. In contrast, the LQ-based mechanistic Marsden TCP Model has the fraction size as an explicit parameter in its formalism; therefore, no EQD_2 correction to the target-volume DVH is required. The NTCP calculations are performed using model parameters taken from the QUANTEC review (Jackson *et al.*, 2010) or later publications as shown in Table 3-3 and Table 3-4.

3.2.1 Program Algorithm

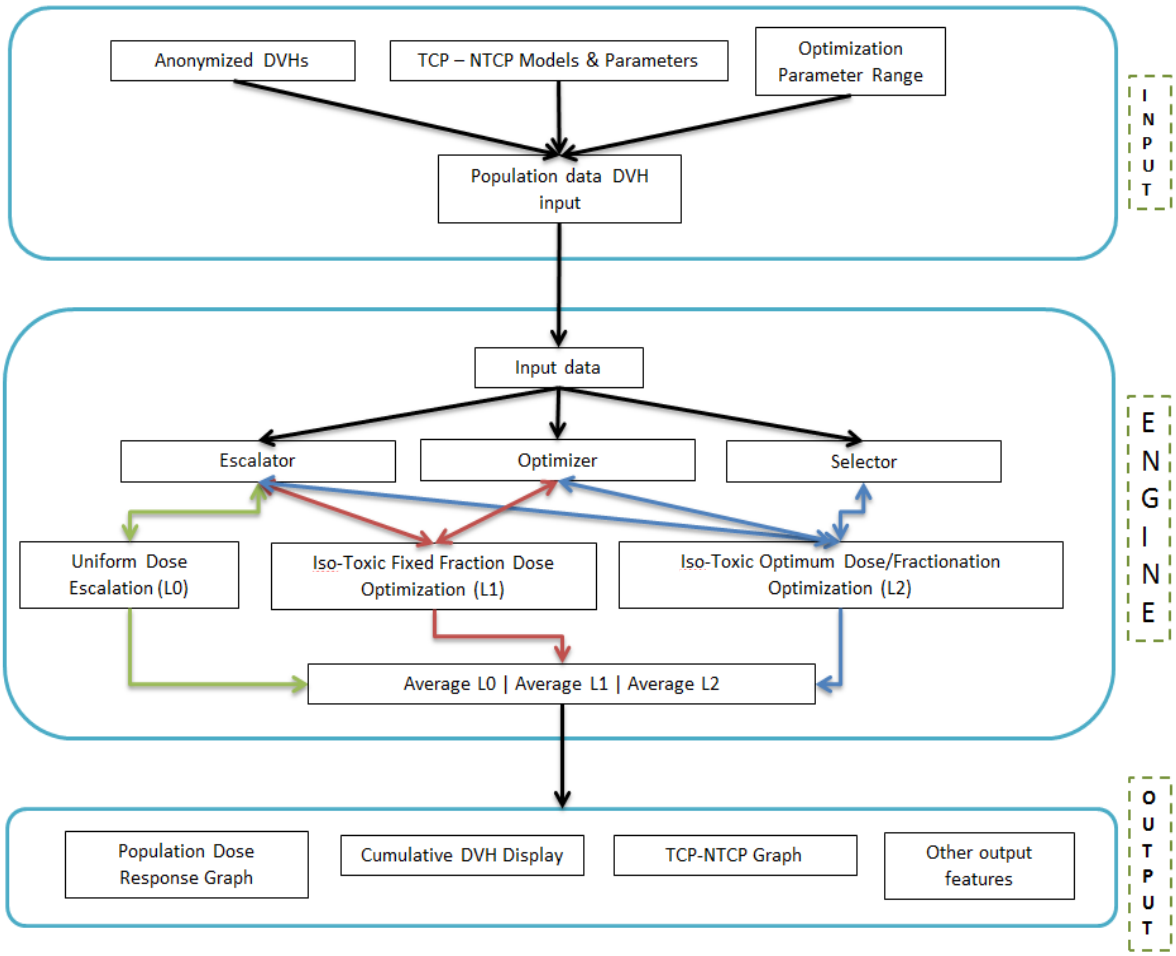

Figure 3-1 Flow diagram of the in-house graphical user interface based program "RadOpt".

The 'RadOpt' software is made up of three components: Input | Engine | Output. The 'input' section allows the user to specify modelling and optimization conditions as well as input data from different sources. The 'engine' part uses three software modules, namely the 'escalator', the 'optimizer' and the 'selector' to analyse the

data. The roles played by these modules are explained in the sections below. The output section allows data QC, displays results (strategy assessment plots) and outputs important metrics about the most recently completed optimization. The graphical user interface (GUI) is shown in Figure 3-4 (and its modules are explained in section 3.2.2-3.2.4). The software was developed in the MATLAB environment version R2015b licensed from MathWorks®. The code was gradually built in successive versions after testing and adding extra features, all of which are included in the version employed to generate the final results of this chapter.

3.2.2 The Escalator

This part of the program multiplies the doses in a DVH of a given patient by a factor (also referred to as 'dose scaling factor' (DSF)) in the range from 0.01 to 3. So, if the nominal prescription dose at a scaling factor of 1 is say 55Gy than this can be scaled from 0.55 Gy to 165 Gy for the purpose of dose escalation/dose reduction. The range of the dose scaling factor is selected such that all possible scenarios can be covered for the OAR and tumour DVHs. This is equivalent to dose scaling function available in treatment planning systems that allows modification of the treatment dose of a plan by means of a multiplication factor.

3.2.3 The Optimizer

The Optimizer scans the range of a given input variable and evaluates a cost function trying to minimize target cost. Thus, the optimizer will accept the dose range as the input variable to optimize the cost function ([$f(dose)_{current}$ - $f(dose)_{target}$], where $f(dose)$ can be NTCP or TCP). The optimization is denoted here by the phrase 'window scanning' and is similar to an interval halving search optimization method. The variable is bound at the lower limit (a) and upper limit (b). An analogy of this optimization is a sliding shutter window, where the window aperture represents the cost function, and the shutters act as boundaries (fig 3-2).

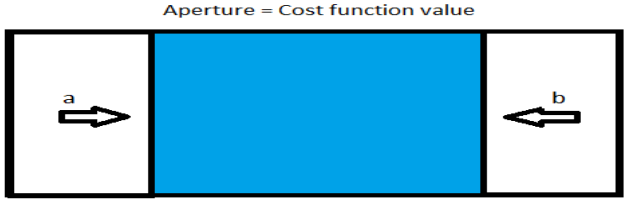

Figure 3-2 explains the optimizer function program in terms of an analogous sliding shutter window. The boundary conditions of the optimized variable 'x' are 'a' and 'b' and the blue aperture of the window is the cost function to be minimized for a given value of 'x'.

The algorithm takes the mean of the upper and lower bounds of the variable and computes the cost function. If the cost function is positive the upper bound is replaced by the mean value of the variable and if negative, the lower bound of the window is replaced by the mean value. Continuing this for about 25 iterations will reduce the cost function to within +/- 10^{-6} tolerance.

x= Variable to optimize, V= Target limit where V=f(x)

For a<x<b, m=(a+b/2)

$g(x) = V_{Xm} - V_{target}$

While |g(x)|>= 0.001 if g(x)<0, b=mean(a,b)

if g(x)>0, a=mean(a,b)

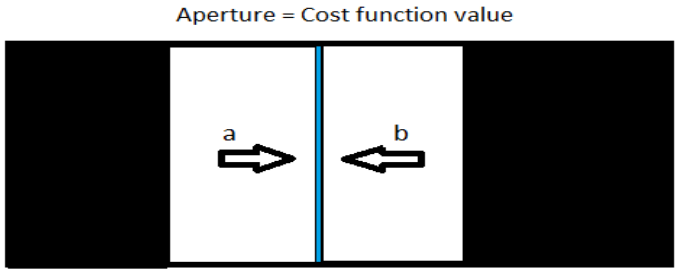

Figure 3-3 shows that at optimized 'x' the window aperture is smallest.

As the optimizer finds the optimum variable value for the associated cost function, the window aperture shrinks until no further improvement in the optimized value of the variable can be achieved. The important thing about the algorithm is that it can find an optimum value of the variable within 20 iterations and the precision/tolerance can be specified. Also, the programming is quite efficient for the algorithm. Performing a literature search after originally programming the optimizer with the above algorithm, it became apparent that this method was not original (Press *et al.*, 1992). This algorithm is efficient where the optimization search is limited to analysis resulting in a unique maximum. For optimizations resulting in multiple maxima, the window scanning approach is likely to yield sub-optimal results. The TCP and NTCP being exponentially increasing functions (due to the

increase in dose) will have a single maximum with respect to dose escalation and thus are suitable to be used with the window scanning optimization method.

3.2.4 The Selector

This module scans through a matrix of optimized values of different variables associated with the optimization process and selects the appropriate combination of values for each variable in the order of preference. Assume there is a table of three related variables where VarX has the highest importance (weight) followed by VarY, followed by VarZ.

Table 3-5 Example table

VarX C1	VarY C2	VarZ C3
65	7.3	12
56	3.2	13
79	6.1	14
88	5.4	19
88	8.1	20

C_i = Column i

The selector is required to select a combination of VarX, VarY and Var3 such that

VarX= max(C_1); then VarY = C_2($_{\text{row of max(C1)}}$) and VarZ= C_3($_{\text{row of max(C1)}}$) for a unique maximum value of VarX

If there are more than one maximum values of VarX= max(C_1), then;

VarY = minimum (C_2($_{\text{row of max(C1)}}$))

if VarY has more than one similar values then;

VarZ= minimum (C_3($_{\text{row of min(C2)}}$)).

The VarX corresponds to TCP, VarY corresponds to NTCP and VarZ corresponds to fraction number. The aim of the selector is to find a combination of these variables where TCP is maximum at minimum NTCP (below a given set Iso-toxic limit; say 10% in the example above so all the VarY NTCP limits are valid to be considered for

selection) and at minimum fraction number. The numbers in table 3-5 are randomly chosen merely to demonstrate the working of the selector module of the software.

Thus, the selector will choose the maximum of VarX with the minimum of VarY at the minimum of VarZ; if there is repetition in either VarX or VarY values. In the example table above the selector will choose

VarX=88 VarY=5.4 VarZ=19

3.2.5 *'RadOpt'* User Interface

Figure 3-4 The Graphical User Interface of the 'RadOpt' Software built in-house for this analysis. Plot 1 shows the comparison between different optimizations. Plot 2 shows individual patient DVH dose response curves – orange curves are TCP vs Dose with green demonstrating the population average and red curves are NTCP vs Dose with a dotted red curve showing population average. Plot 3 shows cumulative PTV DVH and principal OAR DVH of each patient for visual QC of input data. Plot 4 is a plot of Vxx vs NTCP to enable the clinician to assess the correlation between V20 and NTCP (in the current figure).

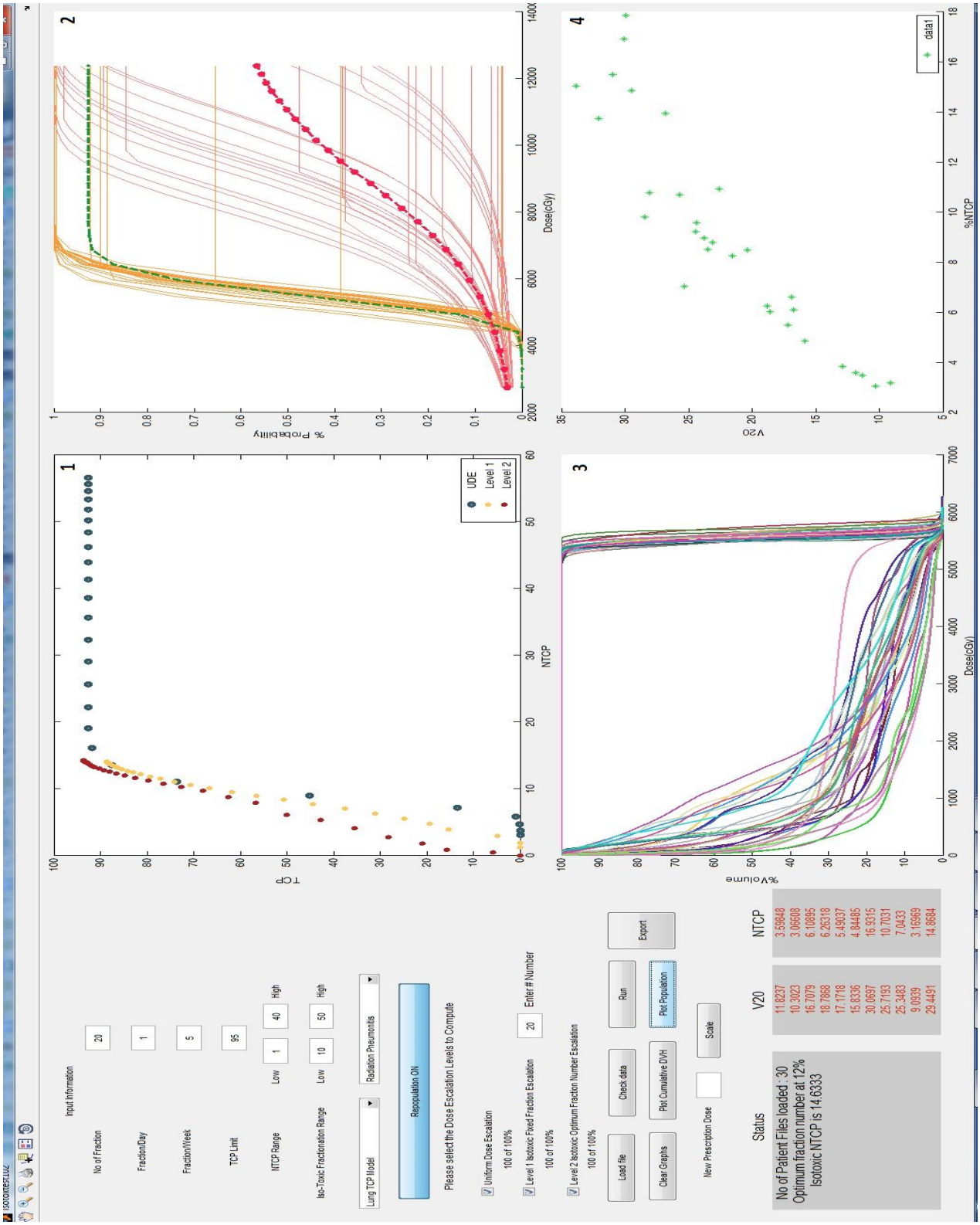

3.2.6 Interface Description

3.2.6.1 Regimen & Optimization Range Input

The user interface shown in Figure 3-4 has the input section on the left-hand side and the output display section on the right (covering most of the area of the 'GUI'). The software can simulate various radiotherapy regimens (accelerated & / or hypo/hyper-fractionation). The process starts with the input of the 'original' regimen in order to access the treatment DVHs. 'RadOpt' performs uniform dose escalation (Level 0), Iso-toxic prescription dose individualization (Level 1) and Iso-toxic optimum dose/fractionation individualization (Level 2). Level 1 and level 2 optimizations require NTCP values and the fractionation range in order to achieve patient-specific individual optimum treatment prescription. The optimizations mentioned above are described in section 3.2.10 of this chapter.

The dose-response curve of tumour and OARs are sigmoidal in shape and plateau beyond a given prescription dose as the slope of the respective curves become very small (as prescription dose increases). A limit on TCP for dose escalation at this point is placed (called TCP_{cap}). Continuing dose escalation beyond TCP_{cap} will increase NTCP to an unacceptable value without a significant increase in TCP. A value of 95% was thus chosen for TCP_{cap}. Figure 3-4 depicts this in quadrant 2 with the orange curves showing the dose-response curves for various tumour DVHs and the red curves showing the same for OAR DVHs.

3.2.6.2 Models and File Input

Specific models for TCP and NTCP calculations and the type of subsequent analysis must be selected for the respective tumour and primary OAR endpoints by the user. Following this, the user can choose to turn on/off the 'repopulation effect' in the TCP calculation. Next, the optimization to be performed on a given set of DVHs is to be selected using the checkboxes. Thus, the informational inputs required to steer the optimization correctly are set for the software. Clicking the 'load' button allows the user to input DVH files.

The program can process Eclipse and Pinnacle DVHs or VODCA Database DVH output files. The data used in this thesis was obtained from Pinnacle & Eclipse[27] DVH output files (Eclipse DVH Data – 29 Lung Patient dataset, 56 Prostate Patient datasets & Pinnacle DVH Data – 30 Lung Patient Dataset). The 'plot cumulative DVH' button converts all the loaded differential DVHs into the cumulative format and plots individual cumulative DVHs for visual quality checking in the section marked by '3' in figure 3.4. Using this feature, 'rogue', incorrectly loaded and/or non-curative treatment DVH datasets (i.e. palliative treatment DVHs) can be identified, and either corrected or removed.

3.2.6.3 Additional Features

There are additional functions built into the software that allows the user to export the results of the analysis, clear the output display area, plot individual patient TCP/NTCP against Dose data separately on a different graph, and manually scale the dose of a given DVH.

3.2.7 Quality Check

The 'check data' function checks if the no. of DVHs loaded for TCP and NTCP calculations match. If they do not match an error is generated. Further, when exporting DVHs from the VODCA[28] radiotherapy database, a separate file with patient IDs is also exported for Tumour DVHs and OAR DVHs. If VODCA datasets are processed, the program also matches the IDs of tumour and OAR DVH export files and flags up an error if a mismatch is found.

3.2.8 Output

The output has a text display and a graphical display of the outcomes of the chosen types of analysis. The text display gives information on the number of files loaded and the loading sequence number of rogue DVH datasets (if any are detected by means of sanity checking the value of rise in TCP after level '0' optimization. If the rise in TCP after dose escalation is 'nil' or negligible this indicates an error in the

[27] Pinnacle and Eclipse are treatment planning systems by 'Varian' and 'Elekta'.

[28] Visualization & Organization of Data for Cancer Analysis (***VODCA***) is the database used in this work to collect radiotherapy treatment data. Further information about it can be found at www.vodca.ch

data which is flagged by the system for review and excluded from TCP_{pop} & $NTCP_{pop}$ calculation). Further, on completion of level 2 optimization (described in section 3.2.10.3 of this chapter), the mean fraction number at 10% toxicity for the population yielding the highest TCP is displayed. The results are available for 1% to 50% NTCP, but 10% is the arbitrarily chosen value for the display of the results; this can be modified as required.

In figure 3-4, there are 4 display graphs that give different information. Graphs 2 & 3 (numbered in figure 3.4) are for visual quality-checking of the data. Graph 2 is a plot of all the cumulative DVHs loaded for the analysis. This helps the user identify any rogue or invalid DVH datasets. Graph 3 is a plot of TCP & NTCP versus dose (i.e. prescribed dose) in the scenario of fixed-fraction-number dose escalation. This helps the user ensure that the DVHs are from curative and not palliative treatments. Graph 4 plots the NTCP of all the DVHs of the principal 'dose-limiting' normal tissue versus V_{xx} (e.g. V_{20}<30% for radiation pneumonitis risk of healthy lung as per Marks *et al.*, 2010). This helps the user assess the correlation between NTCP model values derived from the normal-tissue DVHs under analysis and the selected V_{xx} metric[29]. Graph 1 is a plot of population-averaged TCP versus population-averaged NTCP for all selected optimization types. This graph enables the user to rank various treatment optimization strategies in terms of cohort-mean TCP at a given NTCP. All the analyses can be performed accounting for single/multiple dosimetric and/or NTCP-based OAR tolerance endpoints.

3.2.9 Dose tolerance limits

Reliable LKB model parameters for all OAR complications are not always available (e.g. Bladder complication). Some OARs (like the spinal cord) having serial architecture have maximum dose thresholds beyond which toxicity is clinically observed. This needs to be accounted for whilst performing dose individualization and optimization for a given patient. The Level 1 & Level 2 analysis program modules (see section 3.2.10.2 & 3.2.10.3) account for various dosimetric and NTCP model based endpoints and constraints (D_{max}, D_{mean}, V_{xx} & NTCP) and limit dose

[29] Chapter 6 of this thesis discusses in detail the co-relation between NTCP and V_{xx} and how this can be used to Iso-toxically convert V_{xx} for one regimen to another.

escalation to maintain an acceptable complication risk scenario for all OARs. Dose-based constraints for a given OAR are used in this analysis only when the NTCP model for the OAR is not available. Dose-volume parameters limiting the escalation of dose for various OARs for cancer treatment optimization are listed in Table 3-4 for both prostate and lung treatment OARs.

3.2.10 Optimizations and Individualization Techniques

The following subsections describe different optimization techniques applied to generate pseudo-clinical optimization results for lung and prostate treatment plan data.

3.2.10.1 Dose Escalation (Level 0)

This approach is not an optimization but instead a straightforward increase in (nominal prescription) dose, showing how TCP_{pop} (average of TCP of all patients at a given prescription dose) increases as a function of $NTCP_{pop}$ (average of NTCP of all patients at a given prescription dose) for the principal OAR/complication endpoint in lung and prostate cancer treatments. This curve is shown in Figure 3-4 (plot no 2) for all the patients of the lung cohort and also for the population TCP (green curve, plot 2, fig 3-4) and NTCP (red curve, plot 2, fig 3-4) at 20 fractions. Further, the same analysis is performed after adding other OAR constraints (like spinal cord complication or oesophagitis complication for lung treatment; faecal incontinence and bladder complication for prostate treatment) to see how this changes the TCP and NTCP (for the primary complication). The analysis is performed using both the NTCP model & standard dose-volume constraints for OARs.

3.2.10.2 Iso-toxic Fixed Fraction Dose Optimization (Level 1)

Level 1 Iso-toxic optimization applies the prescribed dose to the tumour at the (original) fixed fraction number corresponding to a given NTCP. The analysis is initially performed considering a single primary OAR DVH as well as the tumour DVH and subsequently extended to include other secondary OAR complications. The standard regimens used are 55 Gy in 20 fractions for (non-small-cell) lung tumour treatments and 60 Gy in 20 fractions for prostate treatments for Level 1 analysis. The analysis proceeds by supplying to the software the parameters of the standard treatment regimen (Number of fractions, Fractions/Day, Treatment days/week),

TCP model (Tumour clonogen density, α, σ_α, β, T_{pot}, T_d) and NTCP (n, m, TD_{50}) model parameters as per latest available peer-reviewed & or task-group recommended literature. There are two parts to the level 1 optimization module (shown in Figure 3-1) - the dose escalator and the optimizer (explained in section 3.2.2 and 3.2.3). First, the escalator is used to find the dose scaling factor (DSF) that yields the set (Iso-toxic) NTCP for the principal OAR. Using this DSF, the tumour DVH doses are rescaled and then it is checked whether the TCP maximum level (aka 'cap' or 'upper bound') is reached (e.g. 95%, 99.9 %, etc.). If the TCP_{cap} has been reached, the optimizer will search to find the dose-scaling factor that yields TCP within 0.01% of the upper bound level. Thus, a new DSF is determined that is lower than the IsoNTCP based DSF; this new DSF is used to rescale the OAR DVH dose resulting in the new, slightly reduced NTCP.

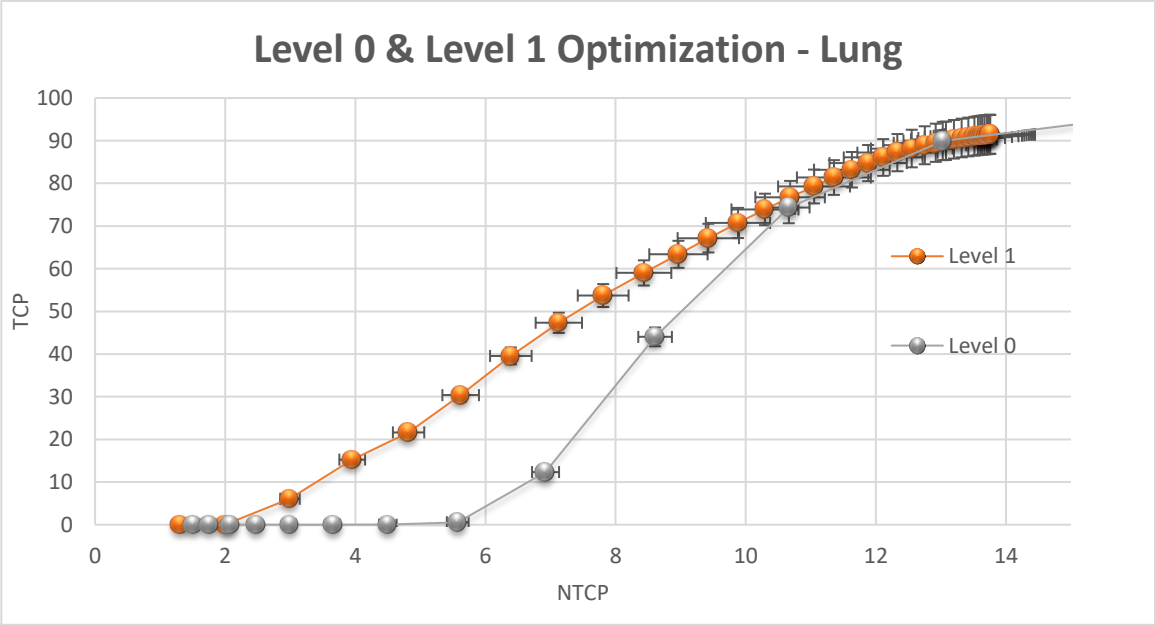

Figure 3-5 Level 0 and Level 1 optimization TCP_{pop}-$NTCP_{pop}$ plot for lung cancer cohort for a 20-fraction schedule. The Therapeutic Operating Curve (TOC) graph was first proposed by Hoffmann, Huizenga, & Kaanders (2013) where they plotted TCP against NTCP for a single patient to assess the therapeutic index. This concept is used here to plot the therapeutic response of a population of patients.

Next, the NTCP is increased by 1% (as defined in range input in section 3.2.6.1) and the exercise as described above is repeated to derive the doses corresponding to this new NTCP value. Once the exercise is completed for a given patient (for the defined range of NTCP of the primary OAR of a patient), other patients' DVH datasets are analysed in a similar fashion. The final result is a matrix of TCP, NTCP &

Level-1 Optimum D_{pres} ($L1D_{opt\ pres}$) for each patient. The TCP, NTCP and $L1D_{opt\ pres}$ of all the patients, when averaged, form the population TCP_{popL1}, $NTCP_{popL1}$ and $L1D_{opt\ pop}$. Further, the same exercise is performed with multiple organ tolerances limiting the escalation of prescription dose. Thus, the dose corresponding to a range of NTCP limits (i.e. 1%-10% for the primary endpoint) with set constraints of NTCP/ Dose-Volume parameter for other OARs is computed. The algorithm escalates the dose until the NTCP value is reached for a given iteration without violating the specified tolerance limits of other OARs. An example of such a TCP vs NTCP curve is shown in Figure 3-5.

3.2.10.3 Iso-toxic Dose/Fractionation Optimization (Level 2)

The level-2 algorithm chooses the optimum dose-fractionation schedule (as explained in the example in section 3.2.4) for a given patient DVH dataset at set tolerance limits (NTCP based & or DV constraint based). The level 2 algorithm requires input(s) similar to those for level 1 algorithm along with the additional input of the range of fraction numbers. For IMRT and 3D-CRT, the range of 1 to 40 fractions is considered reasonable. The algorithm for level 2 optimization has three important components. One is the dose escalator (section 3.2.2), second is the optimizer (section 3.2.3), and the third is the selector (section 3.2.4).

For each patient DVH dataset, the algorithm scales the nominal prescription dose for a fixed NTCP limit of the primary OARs at a given fraction number. If TCP_{cap} of 95% is reached, the optimizer reduces the dose scaling factor and also the NTCP until the TCP is within 0.01% of the TCP upper bound value, i.e. 95% TCP_{cap}. Summarizing, the 'scaler' algorithm searches for maximum DSF for which the tolerance limit of the principal OAR is not exceeded (or the selected Iso-toxic/NTCP limit is just reached). If at this point the TCP_{cap} is exceeded, the optimizer reduces the DSF and hence the NTCP until the TCP is within 0.01% of the TCP_{cap}. The improvement in the therapeutic gain (increased TCP at Iso-toxic NTCP) as a result of the optimization is shown in the results section (e.g. section 3.3.1 figure 3-12). The above procedure is performed at a fixed fraction number, starting at the lowest number in the input range, for one patient dataset at a time. The fraction number is then increased by one and the procedure is repeated until the entire range of

fraction numbers has been processed for a given patient DVH dataset, as shown in Figure 3-6. All OAR DVHs are corrected for fractionation using the EQD_2 correction as proposed by Fowler (2001) with every change of the number of fractions in a given cycle.

Thus, for each patient, a matrix of values of TCP, NTCP and fraction number is formed. This can be compared to performing level-1 optimization for each fraction number in turn and the results gathered together. After the results at all the fraction numbers in the provided range have been 'processed', the 'selector' module is activated to examine the generated matrix of values to select the highest TCP that was achieved across the range of fraction numbers (under 0.01% tolerance of the selected TCP and NTCP) for each patient; if this maximum TCP is equal to the 'cap' then several fraction numbers may fulfil this and the *minimum* fraction number is chosen. The calculations are performed such that the set NTCP limit or dosimetric constraint is never exceeded during optimization. Summarizing, the 'selector' selects the fraction number for each patient that gives the highest TCP at Iso-toxic/lower NTCP (not compromising TCP) for the lowest fraction number for the entire range of fraction numbers.

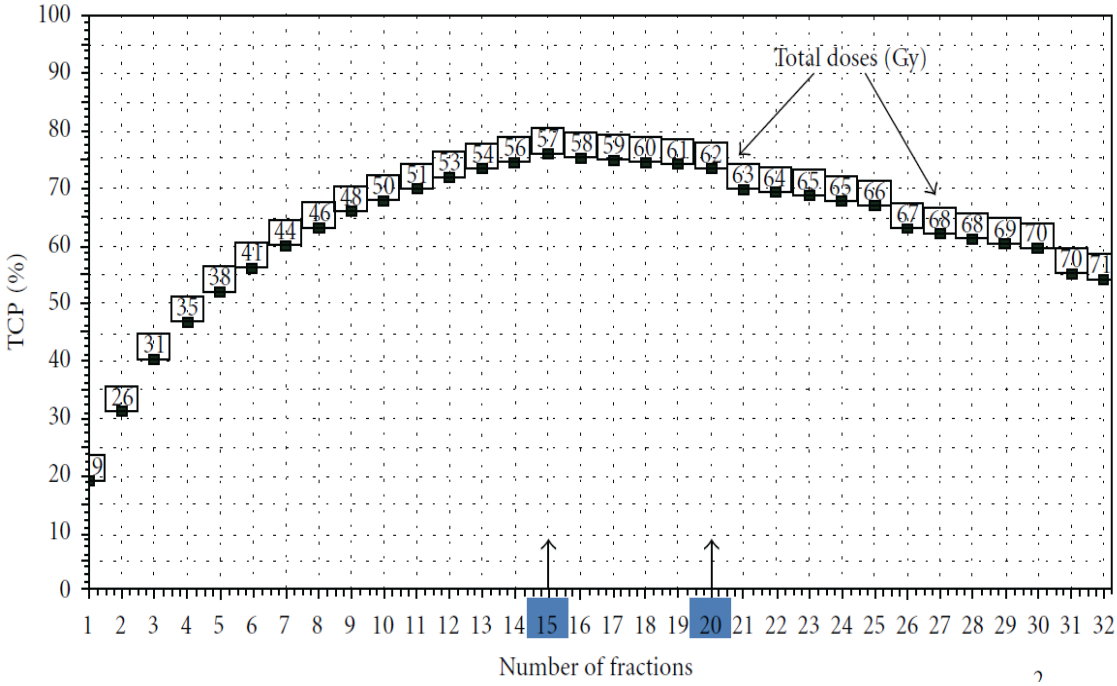

Figure 3-6 A level 2 optimization result for a single patient with lung cancer treatment is shown here from Nahum & Uzan (2012) NTCP was set to 10% in this example. In this research work, the 'selector' module is used to select the fraction number yielding the highest TCP (15 in this case) at a chosen NTCP. This process is repeated for all the patient DVH datasets to yield Iso-toxic individualised treatments for each dataset.

The primary OAR NTCP limit is now increased (by 1%) and the entire procedure is repeated. The result for each patient is a matrix of TCP, NTCP, Optimum Fraction number (OPT_{frac}) and Level 2 Optimum prescription dose ($L2D_{opt\ pres}$). These values, when averaged over the entire cohort, yield the population averaged TCP_{pop}, $NTCP_{pop}$, OPT_{frac}, and D_{pop} that can be compared with level-1 results for each Iso-NTCP limit. The results are reported for both Lung and Prostate Cancer cohorts in the next section.

3.3 Results

This section gives the results for various dose-fractionation optimization strategies discussed in the methodology section.

a) Quality check of TCP and NTCP calculation algorithm : Initially, a snapshot of the software user interface is shown that allows the user to visually check cumulative DVHs to ensure if all the loaded DVHs correspond to curative treatments and that there are no rogue datasets. A quality check of TCP and NTCP calculations of the system against the 'Biosuite' software module developed by (Uzan & Nahum, 2012) for 56 patients was performed with and without considering the repopulation effect. The results showed that the maximum absolute difference in TCP values calculated using 'RadOpt' are within +/-0.04% of the TCP calculation by Biosuite and the standard deviation is 0.02%. Similarly, the difference in NTCP values between 'Biosuite' and 'RadOpt' is +/-0.01% with a standard deviation of +/-0.01%.

b) Quality check of Iso-toxic Optimization Algorithm : The difference in fixed-fraction Iso-toxic optimization results between 'BioSuite' & 'RadOpt' algorithm was assessed next (fig 3-7). It is reported that the maximum error in the calculation of level 1 optimized TCP results at different fraction numbers is +/-0.25 with the mean %error of 0.01 and a standard deviation of 0.06. The error is nominal considering the variations in the rounding errors employed by the programming languages and the algorithm coding itself. The errors quoted here are strictly associated with

systematic calculation errors. Errors associated with TCP & NTCP calculations due to uncertainties in model parameters are addressed in the discussion section.

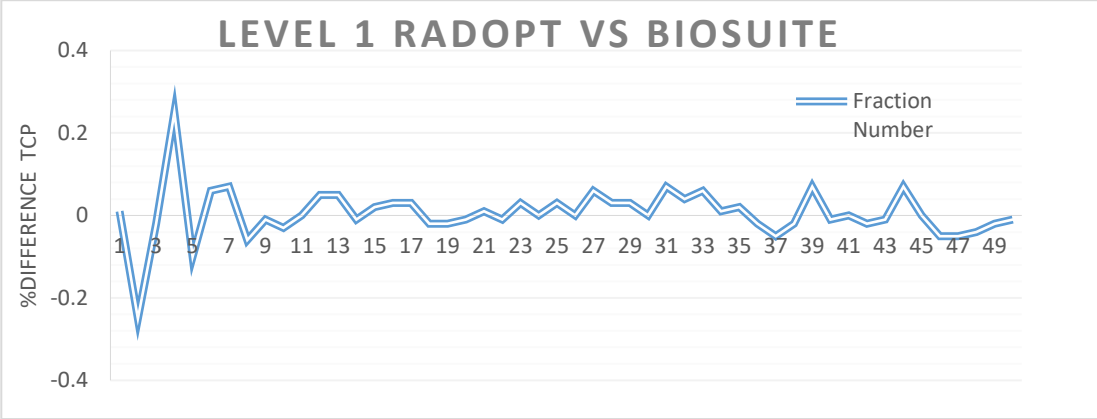

Figure 3-7 shows the % difference between level 1 TCP optimization calculation between RadOpt' and 'Biosuite' performed for a single patient dataset. The oscillations are higher at low fraction numbers where TCP values are very small, i.e. %differences are higher.

3.3.1 Dose-Fractionation Optimization of Lung Cancer Treatments

The DVHs of the lung cancer datasets for a visual quality check of the data are shown in Figure 3-8. It can be seen that D95 of the DVHs are spread around the 55Gy prescription dose region. Typically, a tumour DVH is highly concentrated around the D95 point in the plot. The data used here was provided in a completely anonymised form and thus there was no way to quality check the data except for a visual QC of the DVHs.

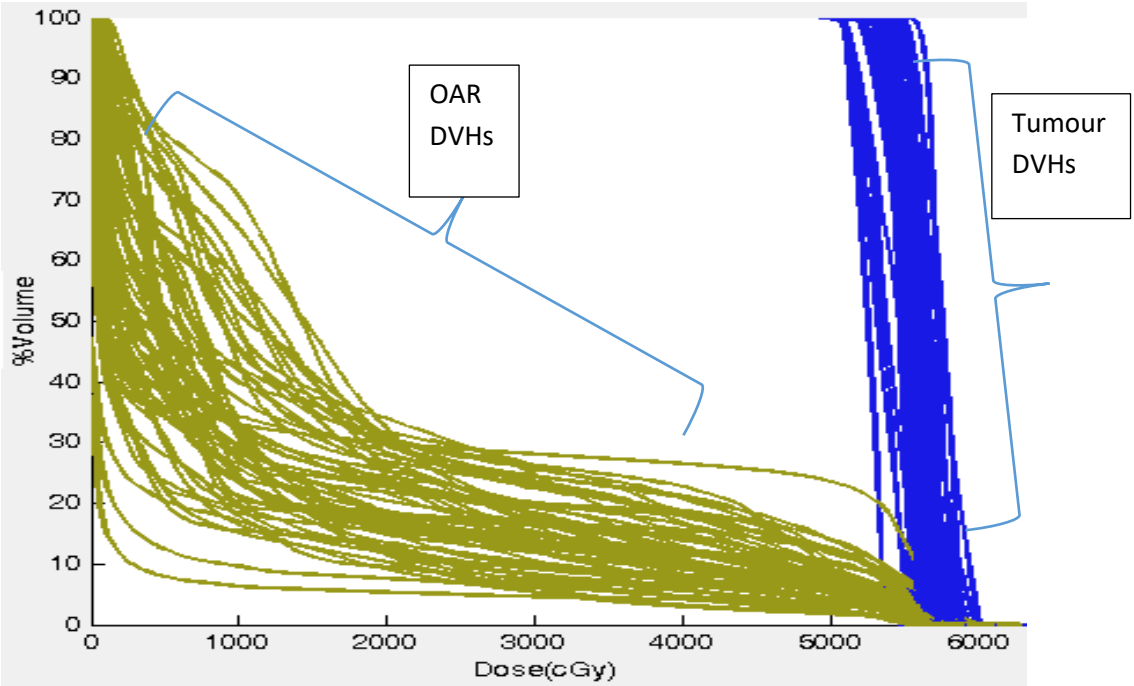

Figure 3-8 The cumulative DVHs of the tumour and the principal OAR (healthy lung) of the lung cohort are shown above.

In figure 3.9 the population-average curves formed by averaging individual TCP-Dose curves (orange) and NTCP-Dose curves (pink) are shown by dashed green and dash-dotted blue curves respectively.

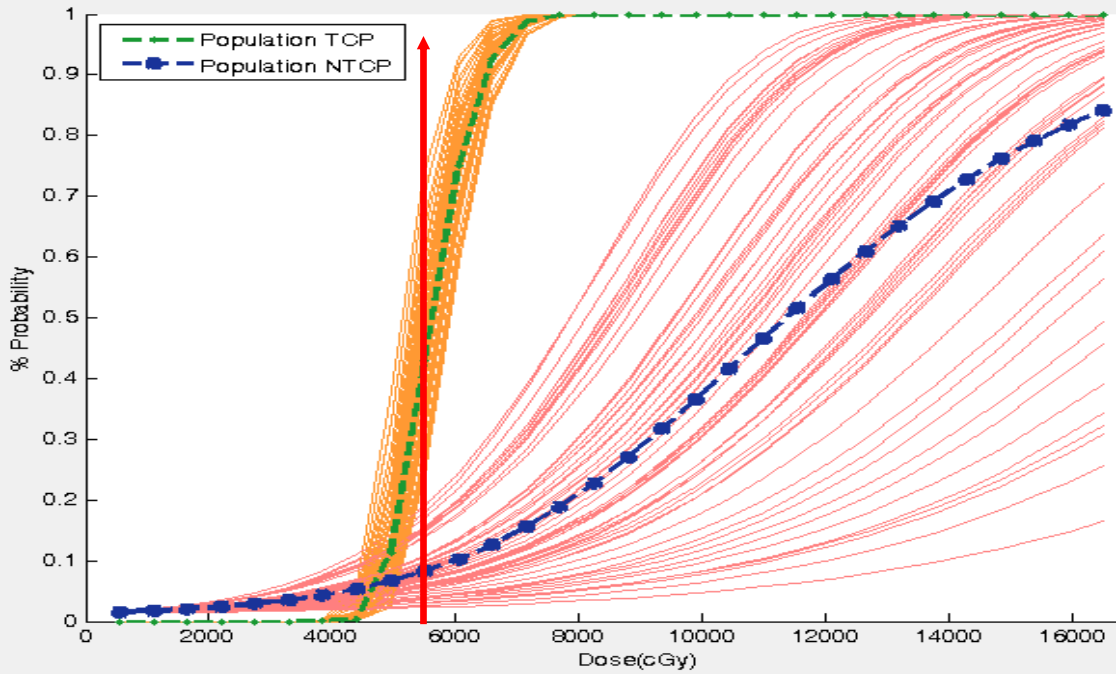

Figure 3-9 shows the dose response curves of all the patient tumour DVH TCP and principal OAR (healthy lung) NTCP with X-axis corresponding to prescription dose (obtained by multiplying scaling factor to the prescription dose of the original DVHs) in 20 fractions. The population average dose response curves are shown by the green (TCP_{pop}) and blue sigmoid curves($NTCP_{pop}$). This is a visual QC to ensure no rogue datasets are used in the analysis. 55Gy in 20 fractions corresponds to 45% average TCP and 8.6% average NTCP of the entire cohort as indicated by the bright red arrow.

The population dose-response graph shown in Figure 3-9 looks quite cluttered and does not provide a straightforward assessment of the population's behaviour to a given strategy of treatment. Thus, the TCP curves are averaged to create the $TCP_{population}$ dose-response curve (green curve) and similarly the $NTCP_{population}$ (blue curve) dose-response curve as shown in Figure 3-9. It is emphasized that the aim of this work is to assess the population response of different optimization & individualization strategies in terms of therapeutic gain for a large cohort of patients. In order to make this assessment simpler, the population average TCP versus NTCP for each proposed strategy of optimization is plotted. This creates the TCP-NTCP population strategy assessment graphs that are extensively used in this work.

The power of this graphical analysis is realized when comparing treatment strategies, parameter variations, and/or treatment techniques over multiple

cohorts. This graphical method of analysis enables a large amount of data to be compressed & summarized. Using this type of plot, the population response to different prescription dose-fractionation optimization techniques is compared in the upcoming section.

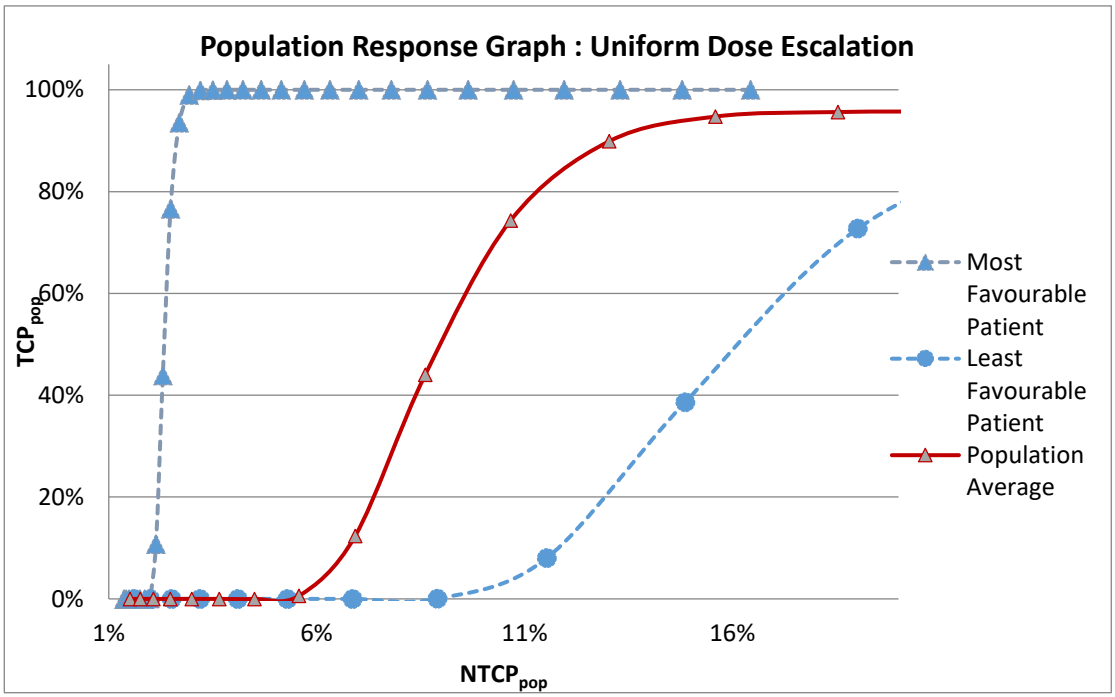

Figure 3-10 shows the population strategy assessment graph of a cohort of lung patients. The graph shows the spread of therapeutic responses over a cohort of patients. The red curve is representative of the central tendency of the cohort response in the area covered by the therapeutic response of most favourable and the least favourable patients.

Next, the population averaged TCP-NTCP graphs obtained after subjecting each of the patient datasets to level 0, level 1 and level 2 optimization is displayed. Firstly, the results of the analysis considering the tumour DVH and the primary OAR DVH that limits dose escalation is shown.

Figure 3-11 shows that for Lung-tumour patients, Iso-toxic prescription dose individualization (level 1) would yield improved therapeutic results compared to uniform dose escalation (level 0), at a constant total number of treatment fractions (20 here for lung cancer treatments). Further, if the number of fractions is optimised (as a variable), it is observed that population response in terms of average TCP and NTCP (level 2 vs level 1 vs level 0 in Figure 3-11) is further improved with better therapeutic results achieved at a lower total number of fractions. At NTCP of 10%, it can be seen that $TCP_{population}$ for level 0 is about 64.5% whereas level 1 (in 20 fractions) results in $TCP_{population}$ of 73.5%. For level 2

optimization, $TCP_{population}$ is about 75% at 10% NTCP at an average of 16 fractions. The optimized number of fractions vary from patient to patient.

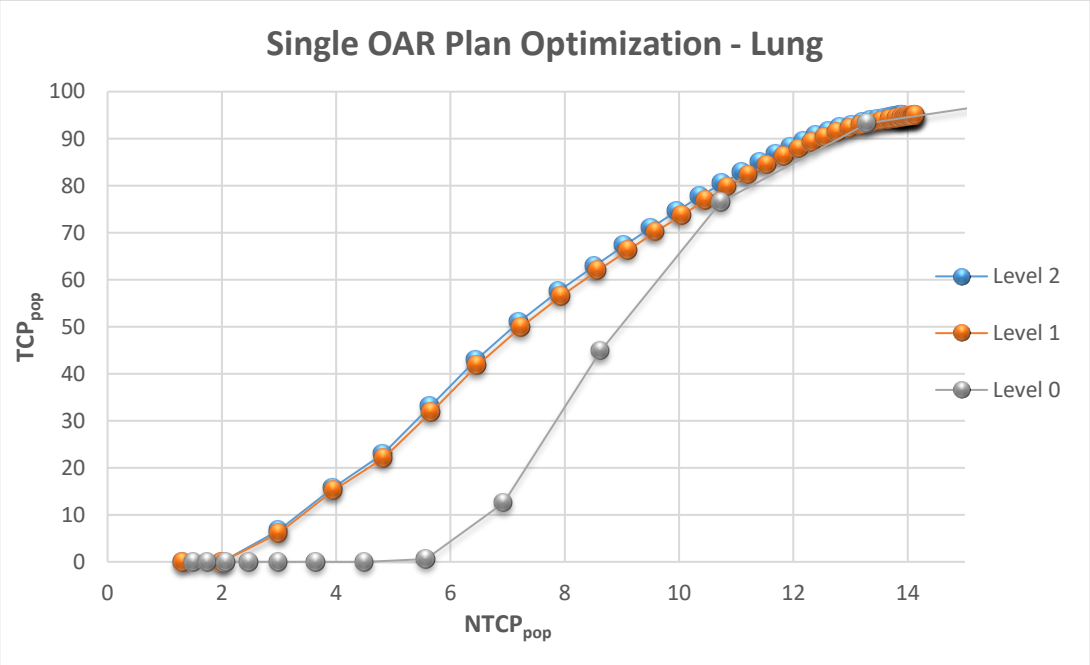

Figure 3-11 above shows the population average TCP-NTCP (TCP_{pop} & $NTCP_{pop}$) graph after applying different dose optimization methods on a cohort of lung patients considering the primary tumour and principal OAR complication (radiation pneumonitis).

The clinical 55Gy20# regimen corresponds to $NTCP_{pop}$=8.6% and TCP_{pop}=45%. The TCP_{pop} for level 1 (62%) and level 2(64%) optimization at 8.6% Iso-toxic NTCP yield significant TCP increases (17% at 20 fractions using level 1 optimization and 19% in at a mean of 15 fractions using level 2 optimization). However, considering just a single OAR as the basis for optimizing the prescription dose would be clinically unrealistic and possibly dangerous; it is essential to account for other possible complications.

For lung cancer radiotherapy, myelopathy of the spinal cord, pericarditis of the heart and oesophagitis of the oesophagus are the most reported complications after radiation pneumonitis and all of these potential complications must be addressed as a part of the treatment planning process (in terms of radiation dose) as per Marks *et al.* (2010). Thus, the recommendations of dose-tolerance limits of these OARs are taken from the QUANTEC review (Gagliardi *et al.*, 2010; Mayo *et al.*, 2010; Werner-Wasik *et al.* 2010) and included as dose-limiting constraints (as per Table 3-4) when optimizing the dose and fractionation for each patient. The dose is

escalated (resulting in an increase in TCP) until either the selected NTCP level of the principal OAR or a dosimetric constraint of the additional OAR is breached. The results have been calculated for each strategy for each patient and averaged to form the population response plot (Population TCP-NTCP curve) shown in Figure 3-12.

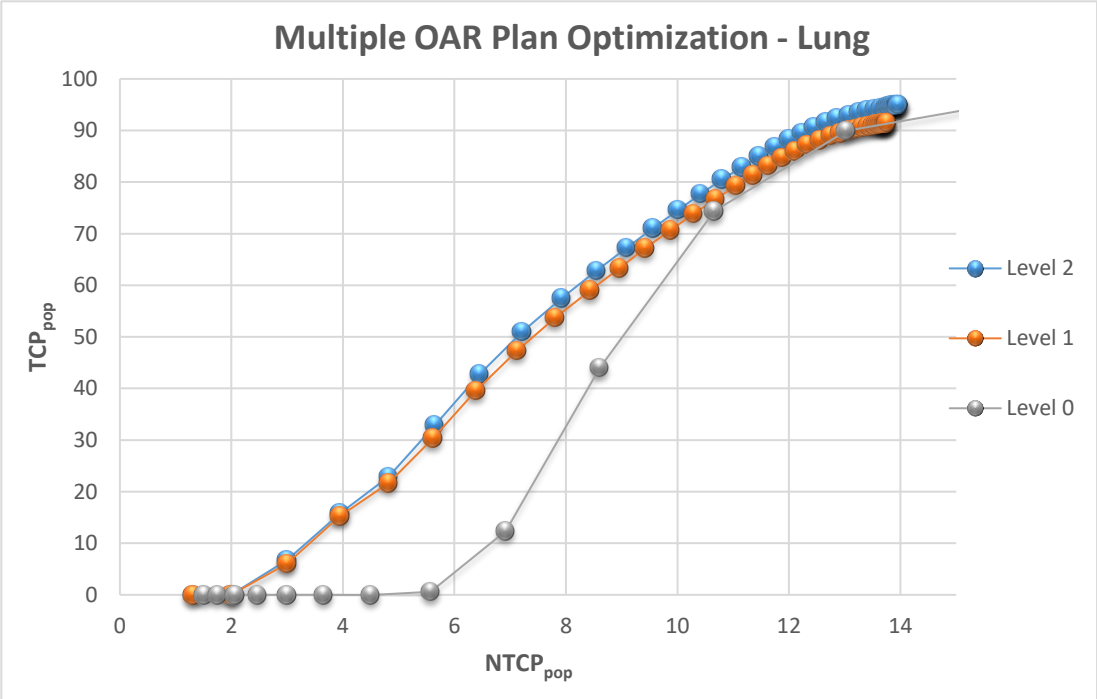

Figure 3-12 above shows the population-average TCP-NTCP graph after applying different dose optimization methods on a cohort of lung patients considering the primary tumour and multiple OAR complications such as radiation pneumonitis, myelopathy, pericarditis and oesophagitis.

$NTCP_{pop}$ is the average of NTCP of principal OARs at the optimized dose scaling achieved after considering other OAR constraints during the optimization. At $NTCP_{pop}$ of 8.6% ($NTCP_{pop}$ of the lung cohort at the standard 55Gy20# schedule), it is seen that $TCP_{population}$ for level 0 is about 44% whereas for level 1 (in 20 fractions) TCP_{pop} = 60%. For level 2 optimization, TCP_{pop} reaches about 63% at 8.6% NTCP for an average of 16 fractions. At the 8.6% Iso-NTCP limit, the TCP for multiple-OAR-constraint based optimization is lower for all three strategies by about 1-2% compared to single-OAR-constraint-based optimization.

Comparing the three different optimization strategies, it can be seen that inclusion of multiple OARs in the optimization limits dose escalation but still results in improved therapeutic response for level 2 optimization compared to level 1 and level 0 strategies for a cohort.

'RadOpt' software output for level 2 optimization provides TCP, NTCP, optimum fraction and prescription dose scaling factor for each DVH dataset. The graph in Figure 3-13 depicts the optimized fractions resulting in the population average curve of level 2 (Average $Fraction_{optimum}$ versus Iso-toxic $NTCP_{limit}$). It is observed that the number of fractions varies considerably, ranging from 5 to 34 for level-2 fraction-number individualization. However, for most patients, the optimum fraction number at Iso-toxic limit of 8% NTCP or above was in the 15-17 range. The reader is reminded that NTCP = 8.6% corresponds to the standard 55Gy20# regimen. The graph in Figure 3-14 (Prescription dose versus NTCP) shows the population mean prescription dose that results from level-2 individualization at optimum fraction number (see Figure 3-13). It is inferred that there is considerable variation in prescription dose that could individualize the treatment and improve the therapeutic ratio of TCP-NTCP at a lower fraction number compared to a fixed 20-fraction regimen. Figure 3-12 to 3-14 are linked by the Iso-toxic NTCP limit which forms the x-axis of the respective figures.

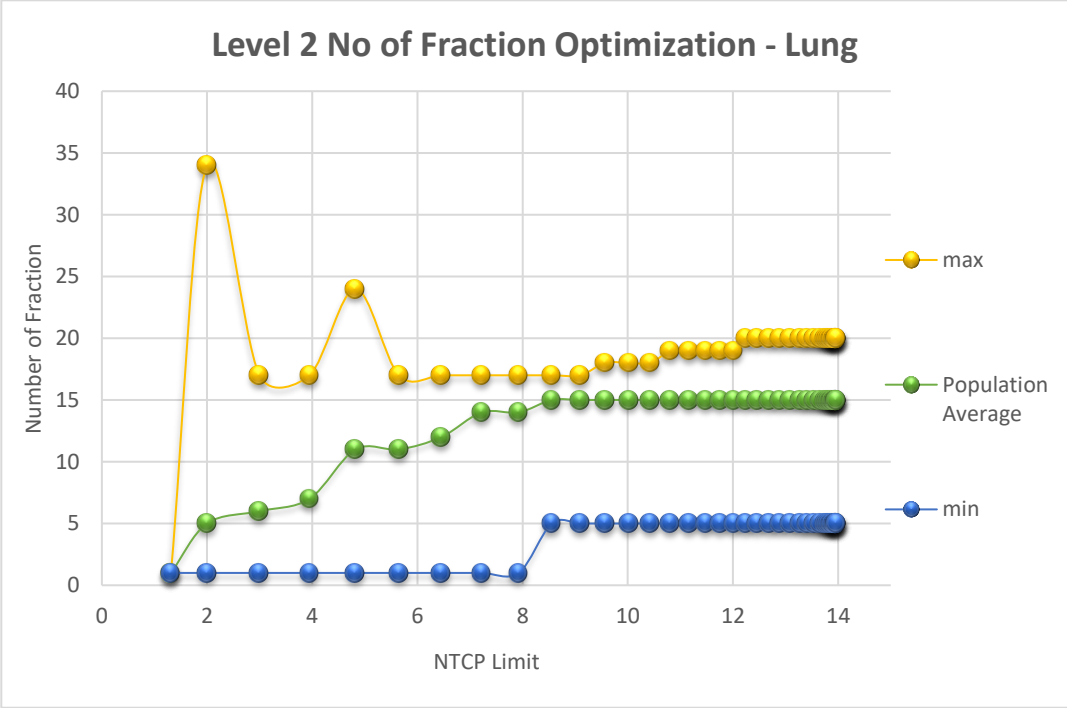

Figure 3-13 shows the graph of the range of Optimum Fraction number vs $NTCP_{pop}$ for level-2 optimization. The green line represents the average no. of fractions for which the level-2 optimizer yields highest TCP. The NTCP on the X-axis can be correlated to the X-axis of Figure 3-12. The yellow and blue data points represent the maximum and minimum fraction numbers at which patients in the cohort reached the highest TCP at the corresponding Iso-toxic $NTCP_{pop}$.

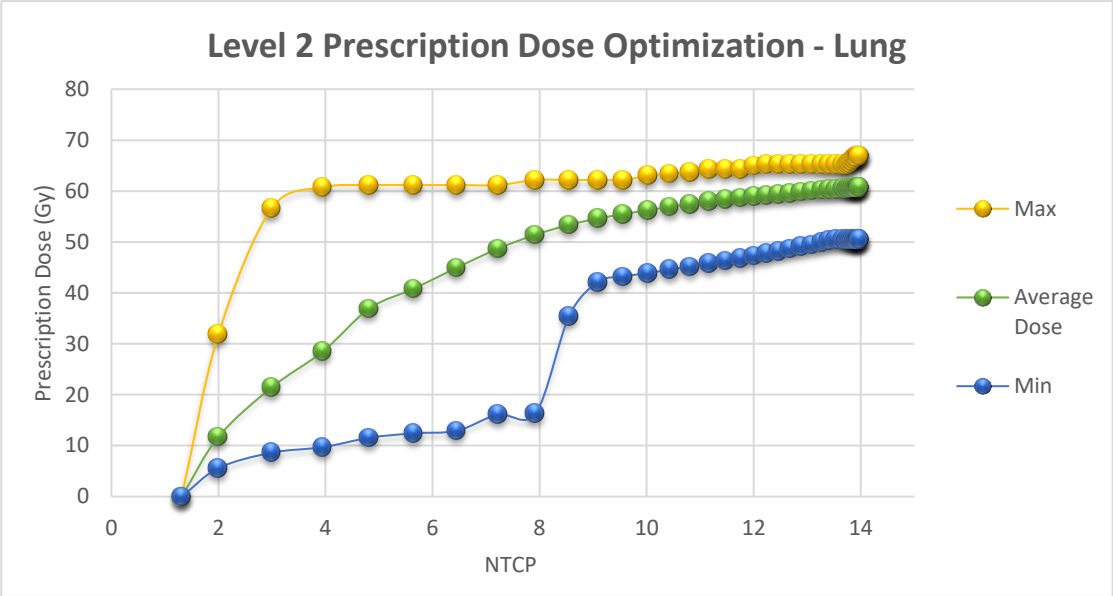

Figure 3-14 shows the range of Dpres as a function of NTCP as per the level-2 dose individualization results for the cohort of lung-tumour patients. The green line represents the average NTCP-specific prescription dose of the population. The blue and yellow lines show the minimum and maximum values of Dpres over the entire cohort.

3.3.1.1 Estimating population response to change in model parameter

During the course of this work, the Marsden TCP parameters for (non-small cell) lung tumours were revised using recent clinical published data; the new parameters are α_{new}=0.293 $^{-1}$Gy and σ_{α}=0.051 for NSCLC tumours (Baker *et al.*,2015).

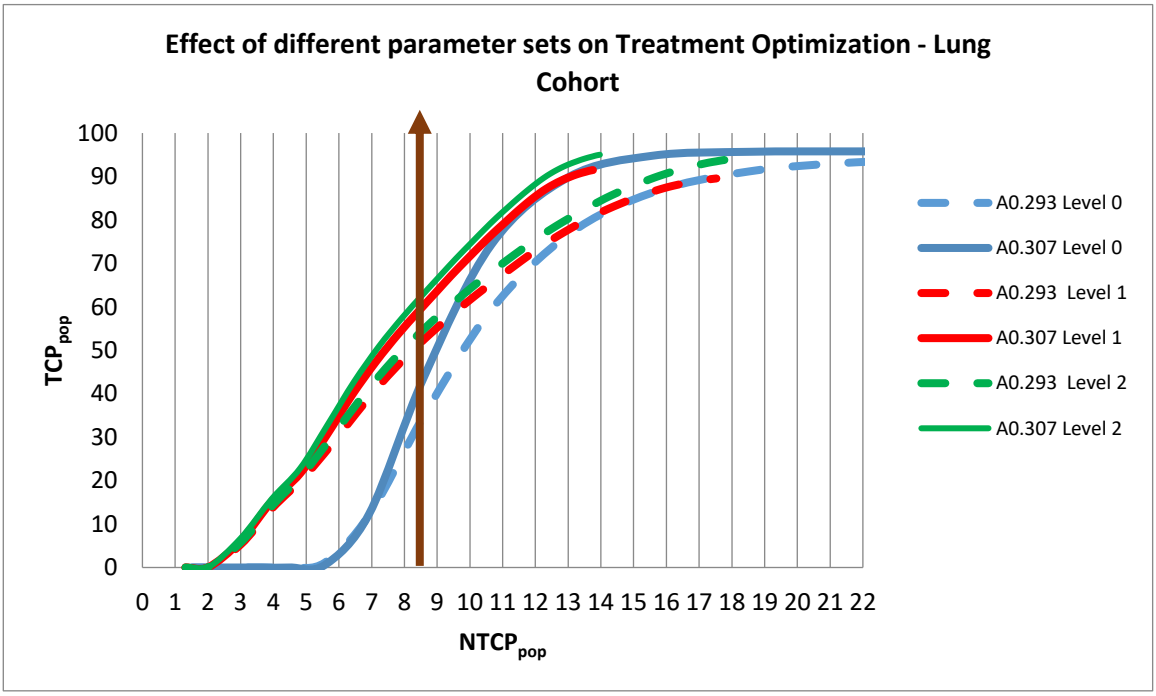

Figure 3-15 shows the effect of using α_{old}=0.307 $^{-1}$Gy, σ_{α}=0.037 Gy^{-1} versus the new estimate of α_{new}=0.293 Gy^{-1}, σ_{α}=0.051 Gy^{-1} for individualization and optimization of radiotherapy treatment for 3 strategies using 'RadOpt' software. The solid lines are constructed using the $(\alpha, \sigma_{\alpha})_{old}$ and broken lines using $(\alpha, \sigma_{\alpha})_{new}$. The brown line corresponds to NTCPpop=8.6% which relates to the 55Gy 20 fractions regimen.

For NSC lung tumours the parameters used in the Marsden TCP model to generate all the results reported up to this point were α=0.307 $^{-1}$Gy and σ_α=0.037 (also mentioned in Table 3-3). TCP based on the revised parameters have been computed in order to compare the results produced by the two sets of parameters.

It is observed that using $(\alpha, \sigma_\alpha)_{new}$ in the TCP model reduces the TCP_{pop} results for all forms of optimization. At 10% $NTCP_{pop}$, the TCP_{pop} values are about 10-12% lower for all the individualization methods (Level 0-2) compared to TCP_{pop} for Level 0-2 individualization calculated using the $(\alpha, \sigma_\alpha)_{old}$. The TCP_{pop} at NTCP=8.6% for the $(\alpha, \sigma_\alpha)_{new}$ parameter set is 35% compared to 44% for the $(\alpha, \sigma_\alpha)_{old}$ parameter set. In the two parameter sets, the change in α is minimal but the change in σ_α is significant and is responsible for the large change in TCP_{pop}. However, the relative improvement in TCP from level 0 to level 1 to level 2 is very similar for both the sets of parameters. This emphasizes the usefulness of the TCP-NTCP population strategy assessment graphs developed in this work.

3.3.2 Dose-Fractionation Optimization of Prostate Cancer Treatments

The cumulative DVHs of all prostate cancer patient datasets are plotted on a dose-volume graph shown below. The tumour DVHs shown in Figure 3-16 have D_{90} between 95% and 107% of the prescription dose, thus qualifying them to be valid plans.

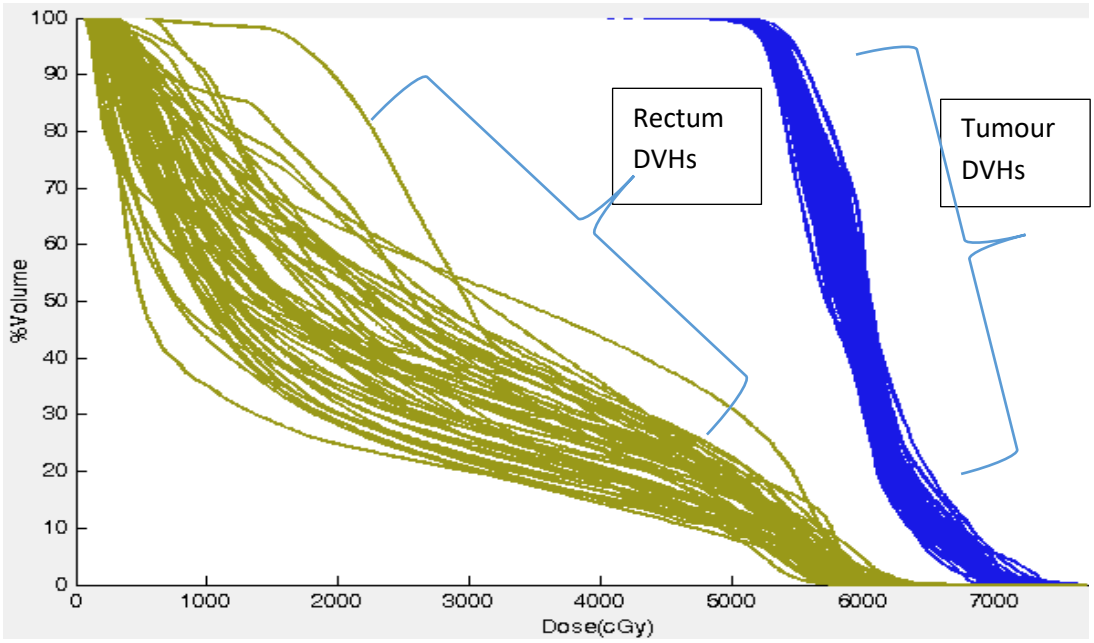

Figure 3-16 shows the cumulative DVHs of the prostate tumour and the principal OAR (rectum) of the prostate cohort.

Similarly, none of the principal OAR DVHs have $V_{40.8\ Gy}$>50% or $V_{60\ Gy}$>5% and thus conform to their respective clinical protocol tolerance standards (data derived from patients treated under the CHIPP protocol).

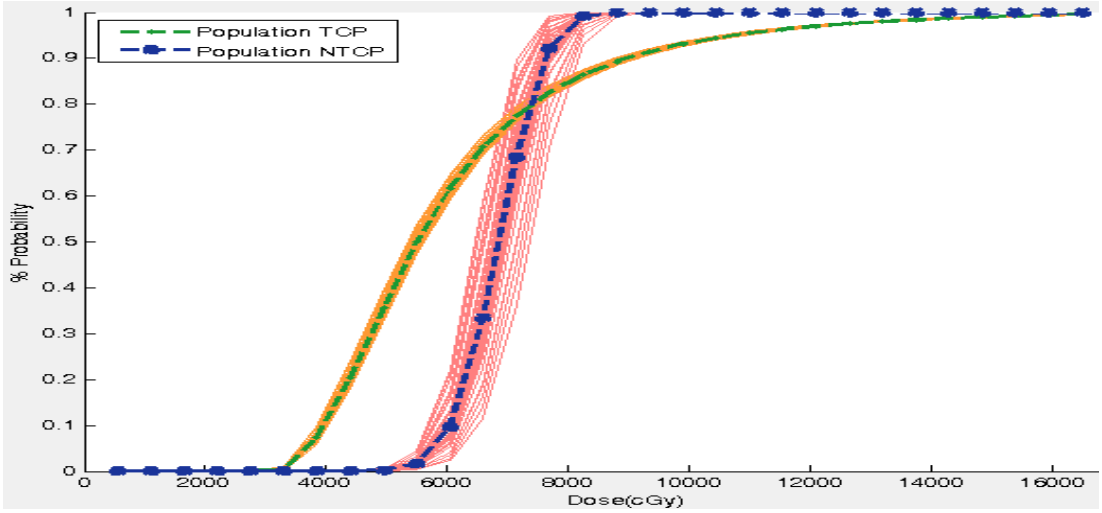

Figure 3-17 shows a dose response graph of constant fraction number (20) dose escalation for all the 56 prostate patients calculated using prostate1 (α/β=10 Gy) TCP parameter set in table 3-3 and LKB NTCP model parameter set from table 3-4). Green dashed line represents TCPpop dose response curve and the blue line represents NTCPpop dose response curve.

The uniform trends and absence of abnormalities in fig 3-17 suggest that the 'escalator' module of the program is working correctly. The orange curves show Dose vs TCP and the pink curves show Dose vs NTCP. The population average TCP (TCP_{pop}) curve is shown in green and the population average NTCP ($NTCP_{pop}$) is shown in blue. Tumour α/β=10 Gy is assumed here; later the difference in optimization for α/β=3 Gy and α/β=1.5 Gy is explored.

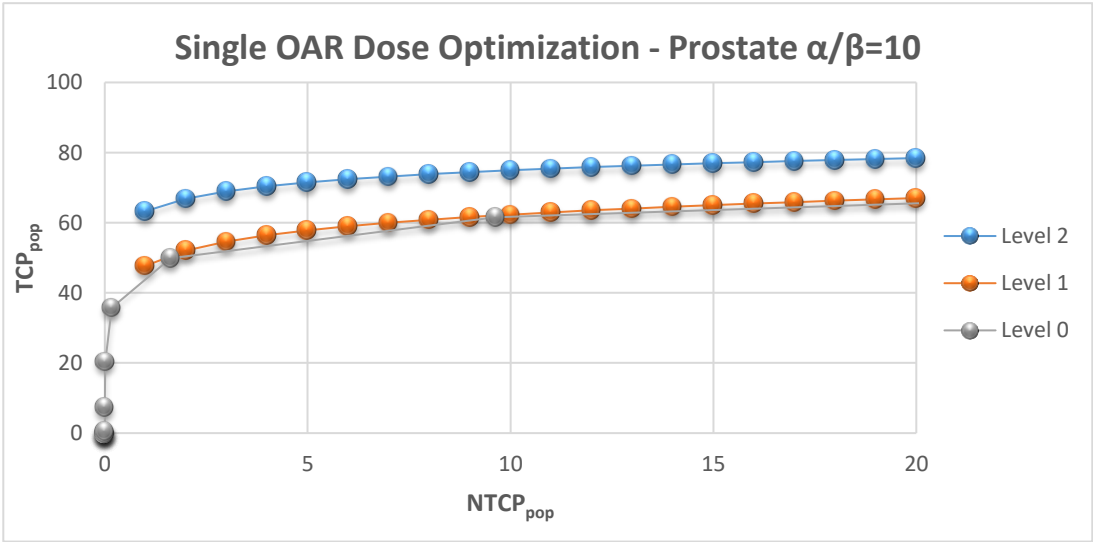

Figure 3-18 above shows the population average TCP-NTCP (TCP_{pop} & $NTCP_{pop}$) graph after applying different dose optimization methods on a cohort of prostate patients considering the primary tumour (α/β=10 Gy) and principal OAR complication (rectal bleeding).

This analysis takes rectal bleeding as the primary endpoint limiting the prostate tumour dose. The uniform dose escalation (level 0) and Iso-toxic fixed-fraction-number optimization (level 1) are performed considering 20-fraction treatments, and level 2 optimization optimizes over the range of 1-50 fractions. The result of the single OAR based optimization strategies are shown in fig 3-18.

To make the scenario truly clinically realistic, two other complications based on dose volume constraints rather than a full NTCP optimization are considered. The population-averaged TCP-NTCP curves for level (0-2) optimization taking into account faecal incontinence and bladder complication are shown in Figure 3-19. During each iteration of the program, the optimizer checks the tolerance of the additional OARs and stops dose escalation if the set constraints are breached for either of the OARs in terms of NTCP/dose-based constraints.

The additional OAR dose tolerance constraints (bladder complication and faecal incontinence) act to provide a limit to the permitted increase in dose and this limits the TCP gain. This is the same method as applied in lung cohort optimization accounting for multiple OAR dose constraints. It was observed that the inclusion of other OAR constraints (such as faecal incontinence and bladder complication) did not result in any notable change in the optimization results for the prostate cohort. This is likely to reflect the fact that the treatments were planned to minimize dose to the bladder volume. Also, these patient datasets came from a single centre where the prostate treatment planning protocol was probably applied in a uniform way across the entire cohort.

It can be observed that Iso-toxic optimal dose-fractionation (level 2) offers a higher therapeutic ratio (i.e. higher TCP at a given NTCP) compared to fixed-fraction Iso-toxic dose optimization (level 1) and uniform dose escalation (level 0). However, the level-2 result is achieved at a higher fraction number (50) than the standard 20-35 fraction range. This can be attributed to assuming zero prostate clonogen proliferation and the 'classical radiobiological' result of larger numbers of fractions minimizing the complication rate at a given TCP. In this particular case, α/β=10 Gy has been assumed for prostate tumour clonogens with α/β=3 Gy for rectal bleeding.

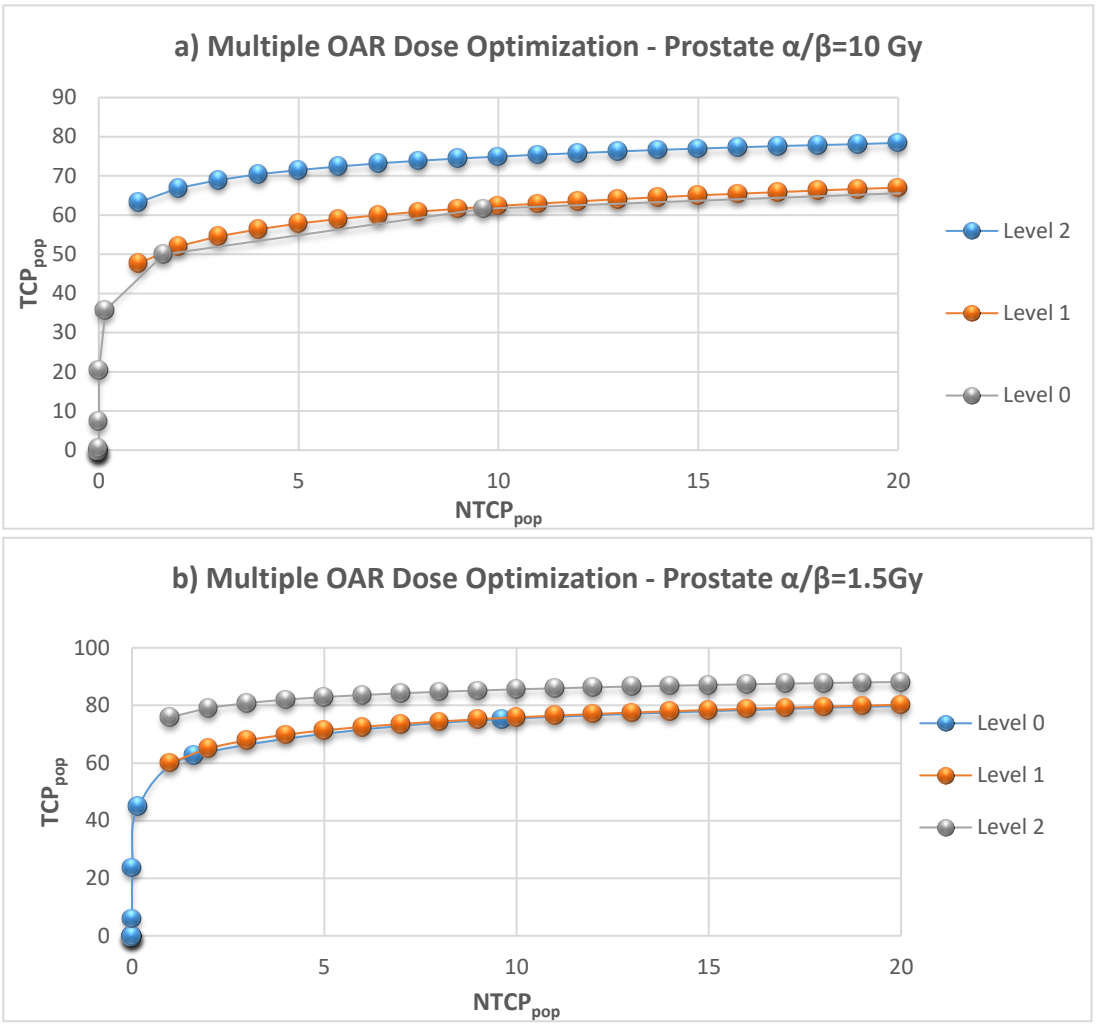

Figure 3-19 above shows the TCP_{pop}-$NTCP_{pop}$ graph after applying different dose optimization methods for a cohort of prostate patients considering the primary tumour and multiple OAR complications such as rectal bleeding, faecal incontinence and bladder complication. a) Results for α/β =10 Gy b) Results for α/β =1.5 Gy.

The prostate cohort optimization results for α/β =10 Gy show that at a 10% complication rate, level-2 optimization yields the highest TCP, being superior to the level 1 and level 0 strategies by approximately 12%. This difference is achieved at an average of 50 fractions. If the tumour clonogen α/β=1.5 Gy, based on findings reported by Dearnaley & Hall (2017), then large fractions would yield the highest TCP at really low fraction numbers for a given Iso-toxic limit (see fig 2-3 for explanation). The difference in the population TCP & NTCP observed for level 0 and level 1 optimization (α/β=1.5 Gy, fig. 3-19b) for the prostate cohort was also negligible (similar to the negligible difference between level-1 and level-0 optimization result for α/β=10 Gy). Although level 1 optimization results in marginally better TCP at Iso-toxic NTCP compared to level 0, the difference considering uncertainties in TCP & NTCP model parameters is not significant. Level 2

optimization, however, results in a significant improvement in the TCP compared to level 1 & level 0 strategies with 1 fraction yielding the highest TCP for all patients which is attributable to α/β=1.5 Gy. Single fraction or very low number of fractions regimen would mean that the fractions will be quite large (> 5Gy) and thus exceeding the applicable range of the L-Q cell kill model.

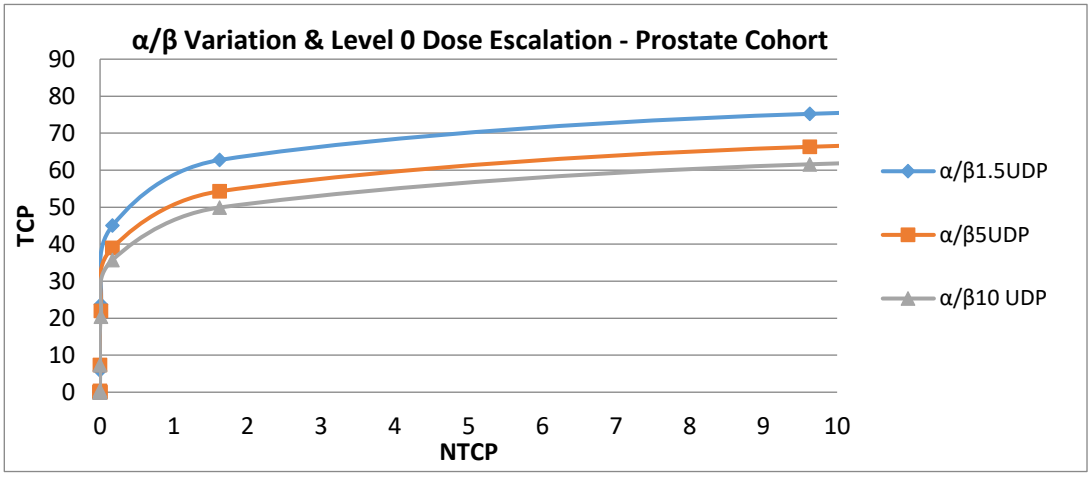

Figure 3-20 shows the changes in the population-average TCP at fixed NTCPpop for Level 0 dose escalation for three different Marsden TCP model parameter sets for prostate tumours (treated at 20 fractions). The blue lines correspond to α/β=1.5 Gy, red corresponds to α/β=5 Gy and green to α/β=10 Gy.

Uzan & Nahum (2012) published four sets of Marsden TCP model parameters for different assumed values of α/β (Table 3-3). Three of these have been used to perform optimization on the available patient datasets to observe the variation this produces on the results of the optimization strategies presented here. Figures 3-20 to 3-22 compare the effect of different model parameters on level 0, 1 and 2 optimizations applied to the cohort. The blue lines correspond to α/β=1.5 Gy, red corresponds to α/β=5 Gy and green to α/β=10 Gy.

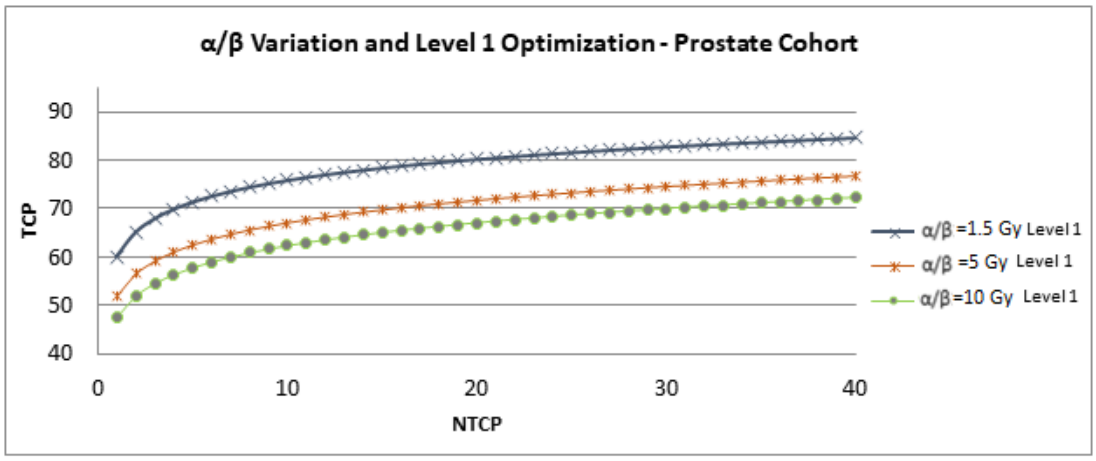

Figure 3-21 above shows the changes in the population-averaged TCP & NTCP for Level-1 optimization at a constant 20 fractions for three different Marsden TCP model parameter sets (corresponding to α/β=1.5 Gy, α/β=5 Gy and α/β=10 Gy) for the prostate tumour and multiple OAR complications. The blue line corresponds to α/β=1.5 Gy, red corresponds to α/β=5 Gy and green to α/β=10 Gy.

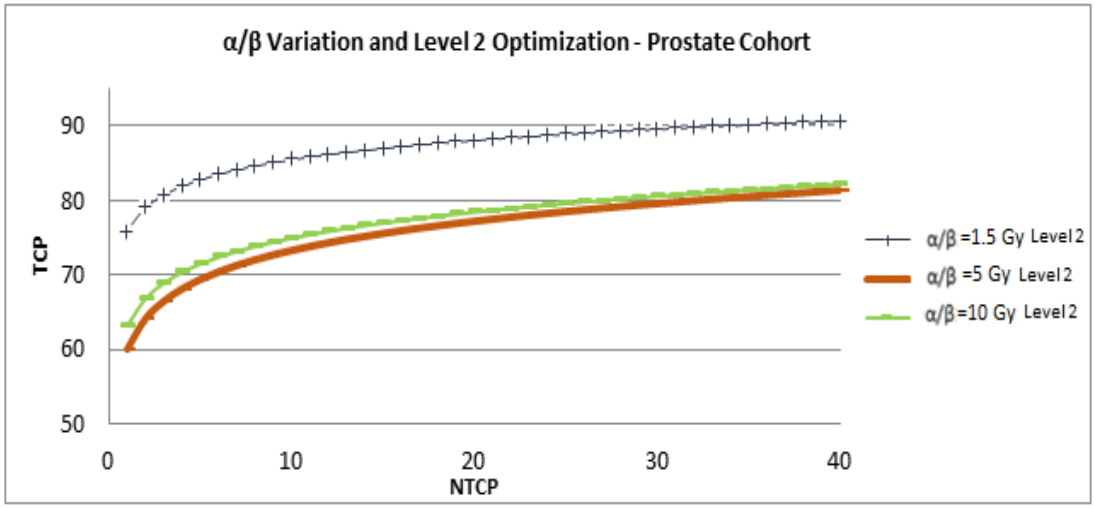

Figure 3-22 above shows the changes in the population-averaged TCP & NTCP for Level-2 optimization at optimized number of fractions for three different Marsden TCP model parameter sets for a prostate tumour and multiple OAR complications. The blue lines correspond to α/β=1.5 Gy, red corresponds to α/β=5 Gy and green to α/β=10 Gy.

Table 3.6 Assessing variation in TCP for prostate tumour for various Marsden model parameter sets at NTCPpop=10%

	α/β=1.5 Gy	α/β=5 Gy	α/β=10 Gy
Level 0 TCP	75.2	66.3	61.6
Level 1 TCP	75.8	67.0	62.3
Level 2 TCP	85.6	73.2	74.9

The use of different TCP-model parameters relating to different α/β values (1.5, 5 & 10 Gy) for prostate tumour (see table 3.6) clonogens shows that the percentage difference in level-0 estimates of TCP between $\alpha/\beta_{1.5\ Gy\ vs\ 10Gy}$ is 13.6% and $\alpha/\beta_{5\ Gy\ vs\ 10\ Gy}$ is 4.7% at 10% Iso-toxicity. Similarly, for level-1 optimization the percentage difference in TCP at 10% Iso-toxicity for $\alpha/\beta_{1.5\ Gy\ vs\ 10\ Gy}$ and $\alpha/\beta_{5\ Gy\ vs\ 10\ Gy}$ are 13.5% and 4.7% respectively. The corresponding results for level-2 optimization are 10.7% for $\alpha/\beta_{1.5\ Gy\ vs\ 10Gy}$ is and 1.7% for $\alpha/\beta_{5\ Gy\ vs\ 10\ Gy}$.

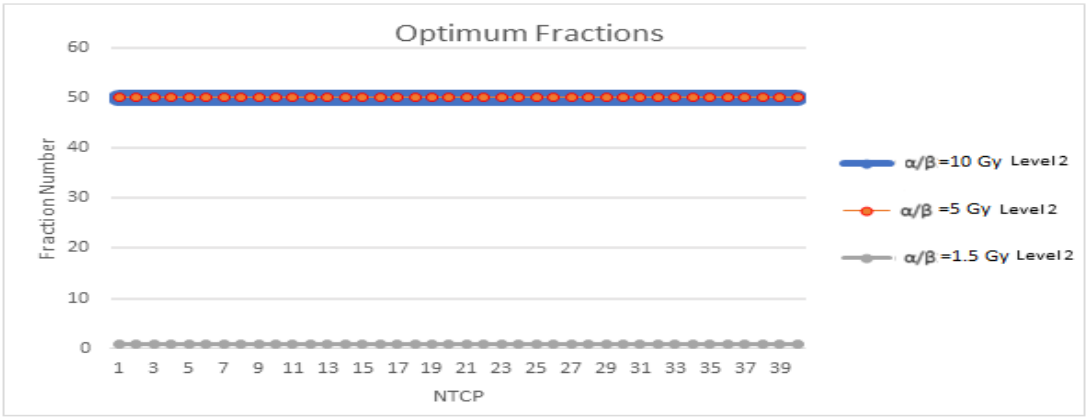

Figure 3-23 shows the optimum fraction numbers at which level 2 TCP-NTCP curves of figure 3-22 were obtained for different α/β values of prostate tumour. Also see Appendix B, figure A - Plot of TCP vs no. of fractions

Thus, it can be seen that changes in model parameters have a big influence on treatment individualization - the use of correct parameters for modelling cannot be over-emphasized. A low α/β=1.5 Gy ratio for tumour clonogens indicates that large fractions are best and a high α/β=10 Gy results in smaller fractions yielding the best therapeutic response as demonstrated by Figure 3-23. It is emphasized that repopulation for the prostate tumour has been set to zero.

3.4 Discussion

The aim of the current analysis is to demonstrate the improvement that radiobiological-model based individualization and optimization of radiotherapy treatments can bring for (non-small-cell) lung and prostate tumour patients (compared to the current fixed-regimen approach). TCP and NTCP models have been used for individualizing the prescription dose and the number of fractions in this chapter. The results compare the overall effect of optimization for the entire cohort of lung and prostate cancer DVH datasets.

The results section started with the presentation of the QC check between 'RadOpt' software and 'Biosuite' assessing consistency in calculating TCP and NTCP & Level 1 optimization. The largest percentage error in the calculation of TCP & NTCP when comparing the systems was <1% which is acceptably small.

Three types of optimizations were carried out on both lung and prostate patient DVH datasets. In level 0, the dose is escalated for each patient (and the entire cohort similarly) and the effect on TCP & NTCP is noted. Level 1 optimization calculates maximum achievable TCP based on NTCP based Iso-toxicity at fixed 20 fractions for both cohorts. Level 2 optimization escalates TCP at a given NTCP (Iso-toxicity) and further searches for the smallest number of fractions achieving the same TCP-NTCP optimization results. The order of preference in the optimization is to first achieve Iso-toxicity then optimize TCP (reduce NTCP if the TCP_{cap} is reached) and then optimize the number of fractions. The results are averaged over the entire cohort (after all patient plans are optimized) for all the strategies and displayed on the TCP-NTCP plot to make population strategy comparison easier.

3.4.1 Discussion: Lung Cohort Optimization

In the lung cohorts, it is seen in Figure 3-12 that the level-2 individualization and optimization strategy is superior to level 0 and level 1 strategies. The TCP_{pop} =44% and $NTCP_{pop}$=8.6% for the standard clinical 55 Gy 20 fraction regimen. Now looking at level 1 & 2 TCP-NTCP graphs shown in Figure 3-12, it is observed that level 1 optimization at 8.6% Iso-toxic limit yields 60% TCP_{pop} at 20 fractions and level 2 optimization yields a TCP_{pop} of 63% at 15 fractions (for most of the patients). Thus, compared to the current scenario, using radiobiological optimization the TCP_{pop} can be improved by about 16% using level 1 optimization and by about 19% applying level 2 optimization (for a reduced number of fractions). On an individual basis, it is observed that the nominal prescription dose can be individualized over a wide range at a given (Iso-toxic) NTCP value (Figure 3-14) for individual patients. Similarly, the optimum number of fractions can also be considerably different for each patient at a given Iso-toxic NTCP limit (Figure 3-13). Thus, it is shown that individualization and optimization of lung treatments based on radiobiological models can yield improved therapeutic responses in individual lung cancer patients.

Evidence in favour of radiobiology-based dose escalation is presented by Machtay *et al.* (2012) who use the BED formulation to analyse various planning studies and show that BED is associated with local regional control and survival rates for NSCLC patient cohorts. Further, Onishi *et al.* (2007) give a similar account of association between the BED and local regional control rates reported by various other studies treating Stage I NSCLC through Stereotactic Ablative Radiotherapy (SABR). Huang *et al.*(2015) demonstrate a correlation between BED and TCP in their radiobiological model-based analysis searching for the optimal fractionation scheme in Stereotactic Body Radiotherapy (SBRT) of NSCLC. Ohri *et al.* (2012) developed a TCP model that linked 2-year overall survival to tumour size and BED specifically applicable to NSCLC SBRT patient data.

Christodoulou *et al.* (2014) and Méry *et al.* (2015) give a very detailed account of the latest approaches to radiotherapy where Iso-toxic dose escalation in patients is also reported. Further clinical evidence in favour of Iso-toxic dose escalation comes from clinical trial results reported by the Maastro Group (van Baardwijk *et al.*, 2008,

2010, 2011, 2012); they reported improved clinical results from employing individualized radiotherapy prescription to patients based on recommended tolerance doses to OARs. The results demonstrate that significant therapeutic gain can be achieved for a cohort by implementing radiobiological model based dose individualization and optimization techniques. The software presented in this thesis is ideally suited to assess population treatment response trends which can aid clinical lung radiotherapy treatment development.

3.4.2 Discussion: Prostate Cohort Optimization

It was observed from figure 3-19 to figure 3-21 that level 1 Iso-toxic optimization for the prostate cohort did not yield significant improvement over level 0 dose escalation. This result was markedly different to lung cohort optimization of the same level. To investigate this further, data for individual patients was analysed and correlated to the tumour & OAR behaviour and to the observed response. Let's focus on level 0 & level 1 results relevant to prostate tumours (α/β=1.5 Gy) and rectum OARs (α/β=3 Gy with n=0.09, m=0.13 – LKB NTCP model parameter).

Level 0 DSF	Dose (Gy)	Level 0 TCP	TCP Std. deviation	Difference	Level 0 NTCP	NTCP Std. deviation	Difference
0.9	54	45.0%	1.8%		0.1	0.0%	
1	60	62.7%	1.5%	17.7	1.6%	1.0%	1.0
1.1	66	75.2%	1.1%	12.5	9.6%	4.0%	8.0

Table 3-7 Analysis of TCP_{pop} and $NTCP_{pop}$ for level 0 escalation to understand the small improvement in TCP as a result of level 1 optimization

Table 3.7 shows that when prescription dose increases from 60 Gy to 66 Gy for a fixed fraction number (20 here), the rise in TCP_{pop} is 12.5% against the rise in $NTCP_{pop}$ (1.6% to 9.6%) which is 8%. The difference in the slope of TCP versus dose and the slope of rectum NTCP versus dose is very small (rectum is a serial organ and the rise in $NTCP_{rectum}$ is dominated by D_{max} and not the D_{mean} of the OAR DVH). This also demonstrates that the room for optimization by means of increased fraction size is limited as offered by level 1 optimization (where DVH dose is escalated up to a set Iso-toxic NTCP- maximum 10%). Thus, Level 1 optimization, in this case, is unlikely to provide any notable benefit compared to level 0 optimization beyond the 60 Gy prescription dose.

Prostate tumours are very slow growing and thus the effect of repopulation is considered to be negligible. Uzan & Nahum (2012) published the Marsden TCP model parameters after performing a fitting exercise on the set of patient data from the MRC RT01 randomised controlled trial. The ambiguity with prostate tumour modelling arises from the lack of consensus between different research groups over the value of α/β. Bentzen & Ritter (2005) have written about the ambiguity in the derivation of α/β of prostate tumours using clinical data reported by 2 different research groups.

The trial PR5 by the national cancer institute of Canada estimate prostate tumour α/β as 1.12 Gy (-3.3,5.6) (Bentzen & Ritter,2005; Lukka et al., 2005) and a study by Valdagni *et al.* (2005) estimated the same quantity at 8.3 Gy (0.7,16). The debate about the correct α/β value for the prostate tumour continues but there is strong evidence supporting α/β=1.3-1.8 Gy (Dearnaley & Hall, 2017) without correcting for overall treatment time, and α/β=1.93 Gy (or α/β=4.14 Gy 'worst' case scenario) considering the effect of overall treatment time as per Vogelius & Bentzen (2013).

The current analysis shows the effect of changes in α/β of prostate tumours from a radiobiological viewpoint (assessed through treatment individualization results of a set of prostate patient data).

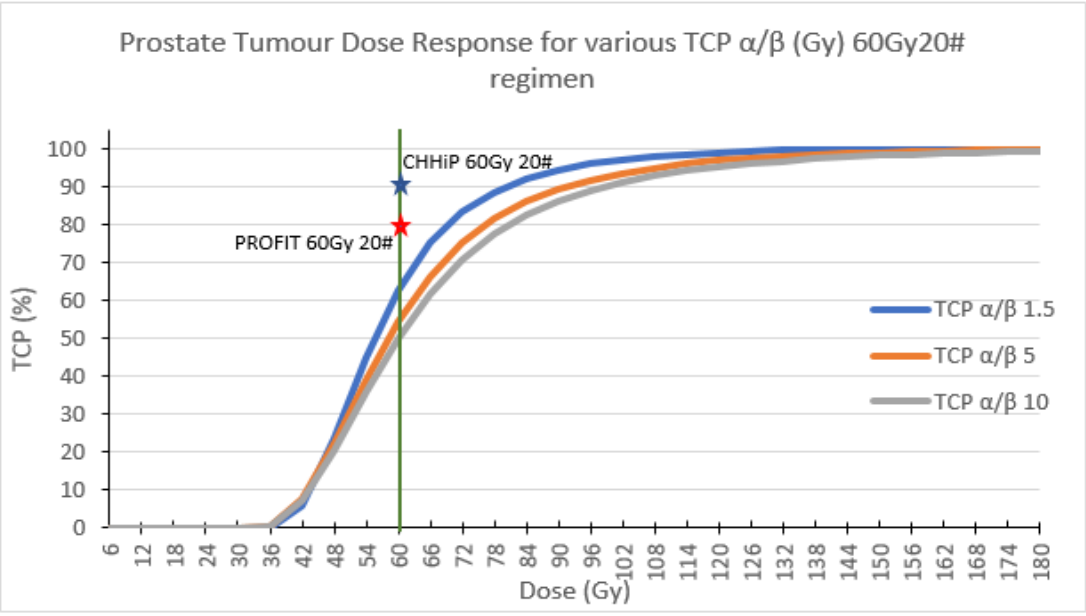

Figure 3-24 Comparison of Population TCP prediction for various α/β values compared to recent clinical trial results for 60Gy20# regimen

Comparison of population TCP of the current dataset using (α/β=1.5, 5 and 10 Gy for a 60-Gy 20 fraction regimen) with recently published clinical trial results (Dearnaley & Hall, 2017) suggests that without considering the time factor for proliferation, α/β is likely to be low (close to α/β=1.5). A TCP model fitting exercise for different values of α/β using the latest clinical results is likely to provide a better estimate of the absolute value of α/β for prostate tumours as shown in figure 3.24.

It is seen in figure 3.24 that average population TCP (using the current prostate tumour Marsden TCP model parameter set derived by fitting model to MRC RT01 trial outcome data) at 60 Gy prescription dose in 20 fractions is nearly 14-15% lower than the average tumour control rate result of the PROFIT trail and nearly 25% lower than that of the CHHiP trial result. It is to be noted that MRC RT01 was based on a 37 fractions schedule and the current analysis is for 20 fractions treatment which would mean that tumour repopulation is could to have been a contributory factor to this large difference in the predictions of TCP for prostate tumour. Based on the prostate tumour TCP model parameter set (α/β=1.5 Gy), it was observed that Iso-toxic dose escalation at large fraction sizes (low total no of fractions) is still advantageous compared to fixed fraction uniform dose escalation. The current outcome data from PROFIT, CHHiP and HYPRO trial also suggests a similar trend. As latest outcome data on prostate treatment is available, refinement of prostate TCP & NTCP model parameters is thus necessitated which will reduce error in absolute predictions by the models and thereby in RadOpt software module results. RadOpt allows alteration of model parameters so once the new parameter set is available, the strategy comparison analysis could be repeated seamlessly.

3.4.3 Uncertainty analysis

The absolute uncertainty on TCP or NTCP model predictions associated with the current results can be categorised into two types.

1) Uncertainty in the results due to systematic error

The optimization algorithm uses the dose scaling factor 'variable' to optimize TCP and NTCP for a given fraction number regimen. The optimization algorithm is set to minimize the cost function to the tolerance of 10^{-4}. Thus, the error in percentage on

any calculation is 0.01% for optimized TCP and NTCP calculation contributed by the optimization algorithm. This is the systematic error on the output from the optimization algorithm.

2) Uncertainty in results due to uncertainty associated with the used model parameters.

Different methods were investigated to try and address this source of uncertainty which contributes to error in the results derived by the RadOpt software module.

One of the ways to assess the error on the model prediction (i.e. TCP or NTCP) would be to calculate the root mean square error (RMSE) of the model fit to clinical data. The RMSE provides an estimate of the distance between the predictive model line fit and the data points used to fit the model. None of the publications from which the model parameters have been derived report the RMSE of the fitting curve (over clinical outcome or toxicity data) that would facilitate quantifiable assessment of the uncertainty on the assessed variables (i.e. TCP assessed from fitting outcome data or NTCP assessed by the fitting of toxicity data).

Uncertainty associated with any model fit is dependent on the input data quality and fitting algorithms employed. Data quality here relates to homogeneity in treatments (e.g. use of concurrent therapies), planning criteria, data collection & reporting methods; and homogeneity in the patient population (age group, disease classification stage, secondary co-morbidities, etc.). Model parameters are mostly reported with 68%-95% confidence intervals by individual research groups. In order to estimate realistic parameters & associated uncertainty in prediction, clinical data reported by various groups should be used for fitting as undertaken in the QUANTEC series of publications (Jackson *et al.*, 2010). With technical advances in treatment planning and delivery systems, the outcome data reported has shown improvement in toxicity control rates which requires updating of data fitted model parameters (e.g. Results of MRC RT01 compared to PROFIT Trial or CHHiP Trial) with updated 95% confidence interval limit for fitted parameters.

The uncertainty analysis undertaken on L-K-B NTCP model and Marsden TCP models used in this research work is reviewed in the next section. It is important to reiterate that TCP/NTCP model parameter fitting was not the aim of this research thesis. It is acknowledged that the absolute uncertainty in model calculations should be addressed, or at least the gap between model derived predictions and actual outcome data should be demonstrated. It is planned to address the latter by updating the graphical display of RadOpt software to allow plotting of reference clinical outcome data in parallel to the software output.

3.4.3.1 NTCP model related uncertainties

The L-K-B model parameters have been derived and reported in the literature by Marks *et al.*(2010), Gagliardi *et al.*(2010) and Gulliford *et al.* (2012). As the L-K-B model is empirical in nature, the model parameters are derived by fitting the model to reported data. The data fitting aims to achieve a fit that passes through all the data points included in the fitting process.

The LKB NTCP model is dependent on the fitting of three parameters (n, m and TD_{50}) that are non-linearly co-related with each other. This makes the process of estimating error on overall predictions of the model quite complicated. Luijk *et al.* (2003) presented four methods of confidence interval analysis using the covariance matrix method, likelihood landscape method, Monte Carlo simulation method and the Jackknife method (bootstrapping). Each of these methods was applied to parameters of the critical volume model (A. Niemierko & Goitein, 1993b). Luijk *et al.* (2003) concluded that employing likelihood landscape (LL method) as demonstrated by Schilstra & Meertens (2001) would be the best-suited method to establish confidence intervals on fitted "CV model" parameters (accounting for non-linear interdependences of various model parameters being fitted). LL method requires extensive computation whereas covariance matrix method was shown to fail when parameter correlations for a given model are non-linear (which is the case with the LKB model parameters).

Ideally, if the outcome data is available at one's own organisation, model parameter fitting should be carried out on this data using fitting techniques as demonstrated by Schilstra & Meertens (2001). Comparing the results of this exercise to the

published model parameters for a given model & OAR should allow error estimation in NTCP calculations. The outcome data for the patient datasets used in this thesis is unavailable, so the above error analysis cannot be carried out.

The LKB NTCP model parameters used in this thesis are reported with confidence interval limits (derived using maximum likelihood fitting) after fitting over various reported clinical results data [See Marks *et al.*(2010) for Radiation Pneumonitis in Lung radiotherapy NTCP model parameters & Michalski (2010) for Rectal Injury in Prostate radiotherapy NTCP model parameters]. Using the lower and higher confidence interval limits quoted in the literature to form an assessment of uncertainty in NTCP calculations for radiation pneumonitis and rectal bleeding complications is likely to be incorrect as the correlation between n, m and TD_{50} is non-linear.

Further, the average rectal bleeding (grade 2 or lower) NTCP (assuming rectum α/β= 3 Gy) for the current DVH datasets (56 patients – 2%) was compared to the CHHiP trial results for 60 Gy 20 fractions arm (CHHiP- 11.9%; Dearnaley *et al.*, 2016) and it was found that the population average NTCP was significantly lower than the results of the CHHiP trial. For, the 74 Gy 37 fractions regimen the cohort rectal bleeding NTCP was 3% and CHHiP trial reported (13.7%). The change in NTCP (from 60 Gy 20 fraction to 74 Gy 37 fraction) was ~1% in both model predictions versus trial results.

There is a clear underestimation of the population NTCP in this case, although the relative change in $NTCP_{population}$ is predicted correctly by 'RadOpt'. After comparing the NTCP prediction for each patient dataset on both 'BioSuite' and 'RadOpt', it is believed that either the cohort made available for this analysis was very small or consisting of largely favourable patients or that the NTCP parameters need re-fitting (which is very likely the case considering the recent availability of results from large clinical trials). A comparison of results between 'BioSuite' and 'RadOpt' only signifies consistency in application of the TCP & NTCP models across the two systems developed at our institute; with *BioSuite* having been adopted/distributed widely. The error contributed by the algorithms of 'RadOpt' software thus remains low. Further, RadOpt allows the user to alter the NTCP/TCP model parameters,

which will enable users to use more recently published parameters to calculate results. Model parameter refitting is out of the scope of this research work, but if access (DVH plus outcomes) to data from a recently concluded trial like CHHiP or PROFIT is gained, a complete refitting and error analysis of the model parameters could be carried out.

Grade II radiation pneumonitis risk ($NTCP_{pop}$) predicted by 'RadOpt' for the lung patient cohort is 8.6% for the 55 Gy 20 fraction regimen. Assuming the population of patients in the available database of 59 DVH datasets is representative, the calculated $NTCP_{pop}$ prediction is compared with published data by Lester *et al.* (2004), Clenton *et al.* (2005), Faria *et al.* (2006), Pemberton *et al.* (2009), Din *et al.* (2013) and Maguire *et al.* (2014) who reported clinical outcome data for hypofractionated accelerated NSCLC radiotherapy treatment. Faria *et al.* (2006) reported a radiation pneumonitis grade II risk of 6.2% (n=32), Clenton *et al.* (2005) reported this risk as 6.6% (n=90) and Pemberton *et al.* (2009) found the risk was 14% (n=140). Din *et al.* (2013) reported a combined grade I/II risk of radiation pneumonitis for the 55Gy 20 fraction regimen to be 15% (i.e. the grade II radiation pneumonitis risk is likely to be lower than 15%). Maguire *et al.* (2014) only reported the risk of radiation pneumonitis grade III but it was as high as 8.3% (n=128, 69 concurrent arm, 59 sequential arm) whereas Lester *et al.* (2004) had no grade III complication (n=97). Based on the above data, it is observed that grade II radiation pneumonitis predicted by RadOpt software (8.6%, n=59) is within the clinically reported range (6-15%, mean 9-10%) with a difference of ~2% from the mean.

3.4.3.2 TCP model related uncertainties

The Marsden model (which is a mechanistically derived model) is used for TCP calculations in the current research work. The parameters of the Lung tumour model used here were reported by Carver et al. (2015), Baker et al. (2015) and Nahum et al. (2011). Nahum et al. (2011) used outcome data reported by Bentzen, Saunders, & Dische (2002), Martel et al. (1999) and Clatterbridge Cancer Center data to estimate lung TCP model parameters quoted in table 3.1. Nahum *et al.* (2011) reported excellent fit to the data and also undertook uncertainty analysis by repeating the fitting exercise 50 times over TCP sampled from a normal distribution

of reported TCP values plus 5% standard deviation. The resulting data fits accrued an average standard deviation of 0.1% in α and σ_α and about 5% in T_k and T_d. The resultant effect in TCP calculations due to these errors in individual parameters would be minimal. It is emphasized that the co-relation between the parameters is non-linear and thus to assess the absolute error a log-likelihood analysis spanning extreme variations in the parameter is likely to provide a more robust assessment of the errors associated with TCP calculations. The SOCCAR trial results of 2-year overall survival (46%) for sequential radiotherapy (55Gy 20 fraction) is very well predicted by the software results for level 0 (TCP_{pop} - 44%) as shown in figure 3-13 (Maguire *et al.*, 2014). Lester *et al.* (2004) reported a 2-year survival of 44.4% in 135 lung cancer patients treated with accelerated hypofractionated 3D CRT in their study. However, the total dose varied from 50-55Gy delivered over 15-20 fraction, but 72% of the patients received 55Gy in 20 fraction treatment. Din *et al.* (2013) reported a 2-year survival of 50% in an NSCLC cohort of 609 patients treated with a 55Gy 20 fraction regimen across 4 different centres in the UK. Based on the above, it is inferred that the Lung TCP model prediction has an absolute difference of 2-3% in the population average TCP compared to the mean for the 55Gy 20 fraction outcome results.

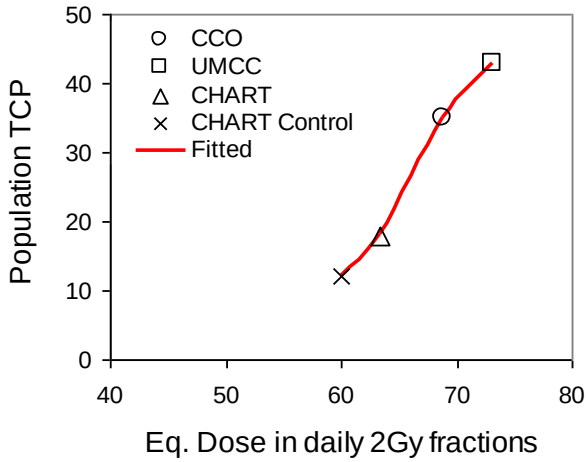

Figure 3-25 Comparison of reported tumour control for each dose/fractionation schedule (CCO – Nahum,2011; UMCC – Martel, 1999; CHART – Bentzen, 2000) with predicted control for fitted parameters; = 0.307 Gy^{-1}= 0.037 Gy^{-1},T_k = 20.9 days, T_d = 3.7 days. (With permission from Nahum *et al.*,2011)

Carver *et al.* (2015) employed the likelihood landscape methodology to establish correlation and uncertainty on fitted α and σ_α model parameters of the Marsden TCP model over the studies reported by Bradley *et al.* (2005) and Kong *et al.* (2005). Their findings suggest that robustness of the likelihood landscape method is high when estimating uncertainties over the fitted parameters if sufficient data are available for analysis. They also report that there is a significant correlation between the α and σ_α parameters, and uncertainties in fitted α and σ_α cause a

significant effect on Lung tumour TCP calculations. Using a similar uncertainty analysis method, Baker *et al.* (2015) published the latest Lung Marsden TCP model parameters that are used to generate the optimization results shown in figure 3-15.

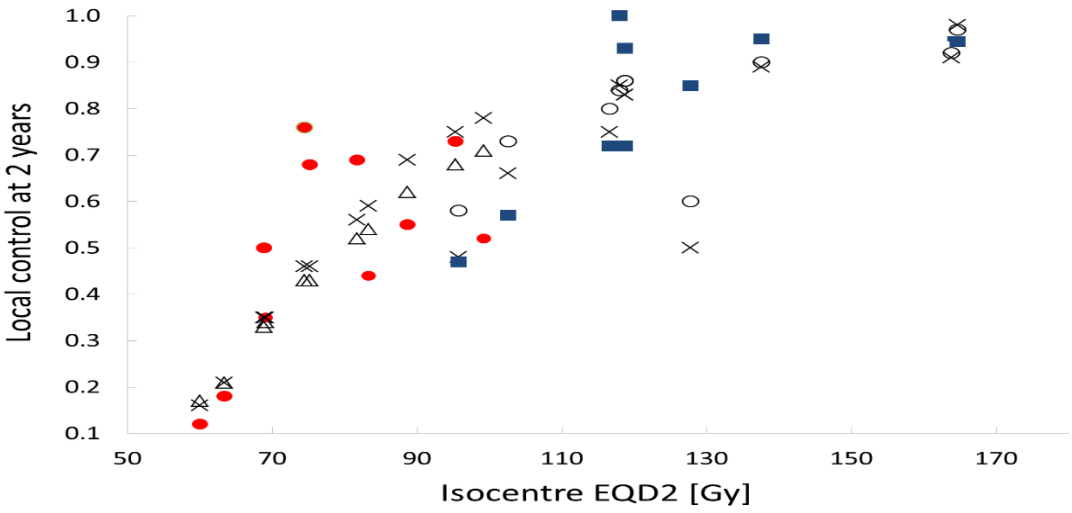

Figure 3-26 Comparison of TCP model prediction with reported local control at 2 years. Published 3D-CRT for mixed-stage disease (●), published stage I SABR (■), parameter fit to combined 3D-CRT and SABR data (X), 3D-CRT only model (△), SABR only model (○). Reproduced from Baker *et al.* (2015)

Their fitting showed an excellent fit of predicted model data to the clinical data (fig 3-26). However, an absolute fitting error was not reported which could be used to assess the propagated error in results derived through 'RadOpt' software. From a comparison of clinical outcome data and TCP calculation from 'RadOpt' software, it is concluded that the lung TCP model parameter set has an absolute error of 2-3% in its prediction and fits the outcome data from multiple sources well.

For the prostate TCP model error analysis, the average TCP of the prostate cohort DVH dataset was calculated using the TCP model parameters published by Uzan & Nahum (2012) using the α/β=1.5 Gy. This was undertaken considering the latest evidence from results of the reported trials in Dearnaley & Hall *et al.* (2017) that report prostate tumour α/β to be 1.8 Gy (CHHiP) whereas results of the PROFIT trial α/β suggest it is 1.3 Gy. Further, there is ambiguity concerning the use of a time factor which adds to the uncertainty of predictions by models as reported by Dearnaley & Hall (2017), Tree *et al.* (2013) and Vogelius & Bentzen (2013).

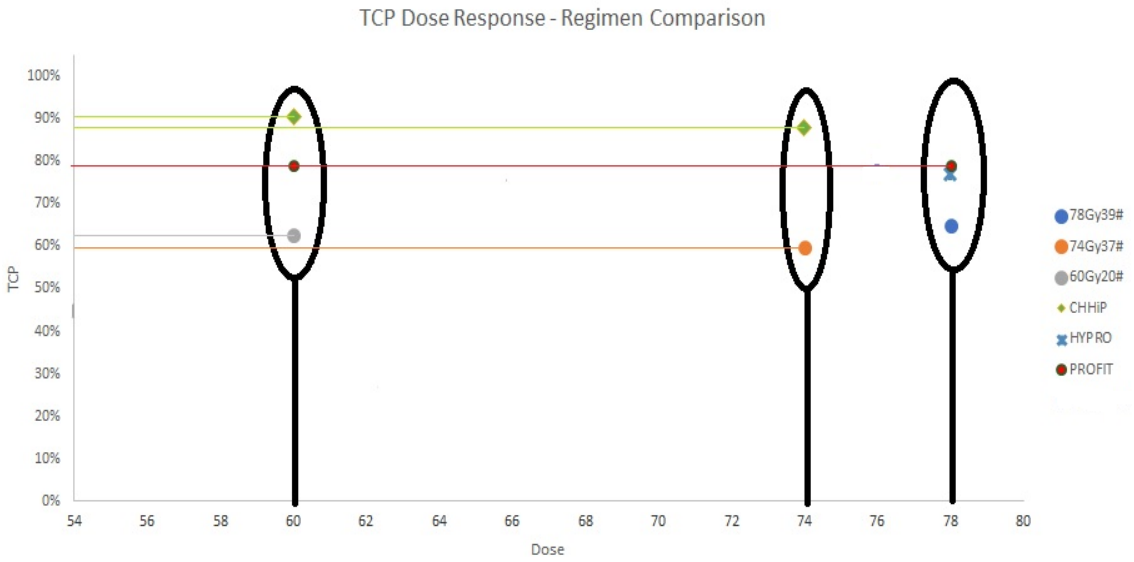

Figure 3-27 The 'RadOpt' based TCP_{pop} compared with the recently published Prostate radiotherapy clinical trial results. Black circles encompass specific arms of the reference studies. All the point grouped by the circle are same regimen (e.g. group 1 has 60Gy20# for results of CHHIP & PROFIT along with one point from RadOpt output).

As per 'RadOpt' calculations, the average prostate tumour TCP was 63% compared to the CHHiP report of 91% and the PROFIT trial report of 79% for 5-year biochemical (bfs) or clinical recurrence free survival for the 60-Gy 20-fraction regimen. For the 2 Gy/fraction regimens (74Gy 37 fraction CHHiP the 5-year bfs was 88% and for 78 Gy 39 fraction PROFIT regimen it was 79%. For the 2 Gy/fraction regimen, RadOpt average TCP prediction was 60% (74Gy 37 fraction) and 65% (78Gy 39 fraction). Thus, the relative change in TCP due to change in regimen is <5% which is in line with clinical results. However, the absolute TCP is underestimated for both the regimens (fig 3-27). The model parameters for calculating prostate tumour TCP thus need to be updated using the latest available trial results to form absolute error estimates.

3.4.3.3 Error on use of recommended dosimetric tolerance limits

Marks *et al.* (2010) in making recommendations of dose volume limits to restrict radiation pneumonitis (after radiotherapy) state that "*Recommending dose/volume limits is challenging because there are no clear and consistent ''thresholds'' for candidate metrics (i.e., the response function is often gradual), and the ''acceptable'' risk level varies with the clinic scenario. Radiotherapy fields for lung cancer may be appropriately large for target coverage; physicians and patients often need to accept the significant pulmonary risks. Furthermore, there are marked interpatient variations in pre-RT lung function that may impact symptom*

development, and tumour-related dysfunction may improve after RT. Despite these caveats, it is prudent to limit V20 to <30–35 %and MLD to <20–23 Gy (with conventional fractionation) if one wants to limit the risk of RP to <20% in definitively treated patients with non–small-cell lung cancer."

It may well be that V20 < 30-35% or MLD <20-23 Gy is the best radiation pneumonitis predictor, but the error around this clinically used limit is not given in the literature.

Similarly, for rectal incontinence (after prostate radiotherapy treatment) the dose-volume limits currently recommended & used for planning do not include any error associated with the dose or the % volume irradiated. As per Michaliski *et al.* (2010)

"The following dose–volume constraints are provided as a conservative starting point for 3D treatment planning: V50 < 50%, V60 < 35%, V65 < 25%, V70 < 20%, and V75 < 15%. However, they have yet to be validated as ***''relatively-safe''****.For typical DVHs, the NTCP models predict that following these constraints should limit Grade 2 or > late rectal toxicity to <15% and the probability of Grade 3 or > late rectal toxicity to <10% for prescriptions up to 79.2 Gy in standard 1.8- to 2-Gy fractions."*

As of now due to differences in treatment practice, data-collection methods and restrictions on access to collected data, it is not possible to quantify the error in predictions even for the dosimetric constraints currently recommended. Using TCP / NTCP models is a step towards quantification of this error. Ideally, if the complete treatment & follow up data of clinical trials (like CHIPP & PROFIT) was made available to a researcher, quantification of the error on TCP & NTCP model parameters would be facilitated.

3.4.3.4 Uncertainty Analysis Summary

In summary, the uncertainties associated with toxicity prediction of TCP and NTCP models used in this thesis have been investigated. The systematic uncertainty contributed by the algorithm in the calculation is reported to be of the order of 0.01%. The absolute difference in population average TCP calculated by the Marsden TCP model (Lung tumour parameter) for our data and outcome data used by Nahum *et al.* (2011) was about 2% indicating a low absolute error in model

prediction. The uncertainty propagated in the results due to inherent uncertainties in the model parameter could not be quantified further using methods described in detail by Luijk *et al.* (2003) due to the lack of outcome data. However, log-likelihood error analysis of the lung model parameters set published by Baker *et al.* (2015) and used for analysis in this chapter fitted well to clinical data with a small 95% confidence interval window for α= 0.293 (0.286 to 0.302) Gy^{-1} and σ_α = 0.051 (0.042 to 0.067) parameters. Further, assessment of the effect of the **absolute** error on model predictions for prostate tumour TCP is currently very high and necessitates refitting of parameters.

However, it is important to reiterate that the primary goal of this chapter was to establish a methodology & create a software to allow comparison of treatment strategies over a population in order to assess trends in population response due to changes in treatment strategies. The functionality to undertake Iso-toxic prescription dose optimization (level 1) and Iso-toxic dose-fractionation optimization (Level 2) is also built into the software. The therapeutic gain for a population is the key metric that is provided by 'RadOpt' software when comparing two strategies (be it changes in regimen, models or treatment optimization strategies).

3.5 Conclusion

In this chapter, an analysis of radiotherapy treatment data for lung and prostate tumour cohorts was performed to assess if individualization of radiotherapy prescription dose and fractionation can improve the overall population tumour control probability as a function of the population-averaged normal tissue complication rate. The TCP and NTCP calculations by the in-house software were 'quality checked' against BioSuite software (Uzan & Nahum, 2012) to ensure consistency and precision in the use of models. The architecture of the software algorithm built to perform the analysis was described and the assumptions made were discussed. Three different levels of dose optimization on both tumour cohorts were performed. Initially, only a single OAR toxicity constraint was considered for the optimization but this was subsequently extended to other OAR constraints in order to make the analysis as clinically realistic as possible. The analysis for both

cohorts was performed using various sets of 'best estimates' of model parameters; it was shown that individualization of prescription dose and fractionation (level 2) is beneficial for both lung and prostate cancer cohorts (α/β=10,3 and 1.5 Gy).

It is concluded that individualization of radiotherapy dose prescription has the potential to significantly improve radiotherapy outcomes; this is particularly the case for lung cancer radiotherapy for which current outcomes are poor. Furthermore, it has been found that for lung tumours the average number of fractions required to achieve the highest TCP is around 15 compared to current regimens of 20 or more fractions. This is a very favourable result from the point of view of resources and patient convenience; a reduced number of fractions mean fewer visits for the patient and consequently a greater patient throughput. The above finding from this study should be cautiously approached and validated by clinical data.

There is much controversy regarding the actual α/β value of the prostate tumour. The level 2 optimization results for α/β=1.5 Gy indicate that hypofractionation would be the best course of treatment. However, the best course of treatment needs to be ascertained using multiple factors like clinical outcome reports for various regimens, laboratory tumour cell survival analysis and radiobiological modelling analysis (considering the uncertainty in results due to the lack of robust model parameters). The point being made is that now a tool/software system is available by means of which analysis of large sets of cohorts can be done to assess the actual population behaviour, predict effects on the population response due to changes in regimens, parameters or even cohorts and present the data in an easily understandable format. This is believed to be an original contribution to the field of radiotherapy quite apart from the results of using this system to analyse different cohorts as presented here.

1) For future work, I would like to implement data fitting to model the relation of specific Vxx for a given OAR and related NTCP as shown in plot 4 of figure 3-4. That analysis is to be accompanied by a statistical report display which will provide information on errors associated with the fitting and the related

confidence interval. This will allow clinicians to estimate the relation between dosimetric constraints and OAR toxicity for a given set of cohort data.

2) Secondly, I would like to develop a flagging system to segregate results into a true positive, false positive decision matrix and develop a validation marker to associate results with clinically observed data. This is to be implemented by calculating the squared difference of TCP_{pop} & $NTCP_{pop}$ observed for a set of data processed using RadOpt software and reported clinical outcome data for the same regimen for the same indication. Accounting for errors associated with a model's absolute prediction, a 1 or 0 to TCP_{flag} variable and $NTCP_{flag}$ variable are to be assigned.

$$TCP_{score}=\sqrt{(|TCP_{pop} - TCP_{clinical}|^2 - TCP_{error}^2)}$$

$$NTCP_{score}=\sqrt{(|NTCP_{pop} - NTCP_{clinical}|^2 - NTCP_{error}^2)}$$

Decision Matrix		TCP flag	
		0	1
NTCPflag	0	True Negative	False Positive
	1	False Positive	True Positive

TCP_{flag}= 0 if TCP_{score} > Set threshold value*

=1 if TCPscore <= Set threshold value*

$NTCP_{flag}$= 0 if $NTCP_{score}$ > Set threshold value*

=1 if NTCPscore<= Set threshold value*

In the 2 X 2 matrix shown above, the values of calculated TCP_{flag} and $NTCP_{flag}$ are to be input which will provide an indication of the validity of the observed results compared to clinical data. The method critically depends on how the 'absolute error' on TCP and NTCP model predictions is quantified and the value of the threshold (* above) that assigns the 'flag' a zero or one which is under consideration as of now. This process will also require building a library of clinical outcome data for all clinically used regimens for a given tumour type.

Chapter 4 Radiotherapy Treatment Optimization based on Patient-Specific Tumour Radio- sensitivity Information

4.1 Introduction

Exploring different strategies for individualizing radiotherapy treatments using radiobiological models and then analysing the results is the key idea of this thesis. The focus of the previous chapter was on individualization of tumour prescription dose & fraction number (using dose-volume information) which provided evidence in support of the individualization techniques (or 'levels') proposed by Nahum & Uzan (2012). The TCP model employed in the previous chapter takes into account heterogeneity in tumour-clonogen radiosensitivity over a population through the parameter σ_α (Nahum & Sanchez-Nieto, 2001). It has been shown by Gerweck *et al.* (2006) and West *et al.* (1997) that tumour radiosensitivity is an important marker that helps determine therapy response. Chapman (2003, 2014) discusses in detail the mechanisms responsible for tumour cell killing: the radiosensitivity parameter α describes 'direct' or 'one-hit' unrepairable damage and the parameter β corresponds to the combination of sub-lethal damage events, separated in time, that result in cell death.

Another important set of variables that would aid tumour-response and/or normal-tissue tolerance/complication prediction are biomarkers (e.g. H2AX, [18F]HX4) [Dubois *et al.*, 2011; Olive & Banáth, 2004]. Correlations between biomarker expression and treatment response have been established in several studies. However, variability in results from different groups has been observed which suggests a need for technique standardization (Menegakis *et al.*, 2009; Olive & Banáth, 2004).

Thus, if patients could be stratified into smaller groups of radiosensitivity (determined from some yet to be discovered, fast and minimally invasive biomarker driven assay), it is hypothesized that model predictions would be more accurate, i.e.

more 'individualized'. It is assumed that there is a genetic profiling test / multivariate-factor analysis that can stratify patients into different sub-groups based on intrinsic tumour radiosensitivity.

The benefit of having this patient specific information in individualization of radiotherapy treatment is explored in this chapter. It is emphasised that the investigation described in what follows is based on *tumour* radiosensitivity rather than on *normal-tissue* radiosensitivity; ideally one would have knowledge of both. The Marsden TCP model is used for TCP calculation and the L-K-B model is used to calculate NTCP, that are explained in detail in chapter 2 (section 2.3, 2.4). Model parameters used in the TCP and NTCP models are shown in table 4-1 and table 4-2.

MARSDEN TCP MODEL						
Tumour	**Lung**	**Lung2**	**Prostate1**	**Prostate2**	**Prostate3**	**Prostate4**
α (Gy^{-1})	**0.307**	**0.293**	**0.3**	**0.258**	**0.218**	**0.155**
α_σ	**0.037**	**0.051**	**0.114**	**0.099**	**0.082**	**0.058**
α/β (cGy)	**1000**	**1000**	**1000**	**500**	**300**	**150**
Clonogenic Density	**10^7**	**10^7**	**10^7**	**10^7**	**10^7**	**10^7**
Repopulation Constant	**3.7**	**3.7**	**-**	**-**	**-**	**-**
Delay to repopulation (days)	**21**	**21**				**-**
Reference	**Uzan (2012)**	**Baker *et al.* (2015)**	**Uzan (2012)**	**Uzan (2012)**	**Uzan (2012)**	**Uzan (2012)**

Table 4-1 The Marsden TCP model parameters used in this analysis are shown above

LKB NTCP MODEL								
End Point	**Radiation Pneumonitis**	**Oesophagus Complication**	**Myelopathy**	**Heart**	**Rectal Bleeding**	**Faecal Incontinence**	**Bladder Complication**	
m	**0.45**	**0.44**	**-**	**0.64**	**0.13**	**0.42**	**-**	**-**
n	**1**	**0.32**	**-**	**0.13**	**0.09**	**1**	**-**	**-**
TD50 (cGy)	**3140**	**5100**	**-**		**7690**	**10570**	**-**	**-**
α/β OAR (cGy)	**300**	**1000**	**87**	**250**	**300**	**300**	**600**	**600**
Vxx	**V20**	**-**	**-**	**V30**	**V50**	**V50**	**V80**	**V65**
Vxx Limit	**30%**	**-**	**-**	**46%**	**50%**	**50%**	**15%**	**50%**
Dmean (cGy)	**-**	**3400**	**-**				**-**	
Dmax (cGy)	**-**	**-**	**5000**					
Reference	**Uzan (2012)**	**Chapet *et al.* (2005)**	**Kirkpatrick (2010)**	**Martel *et al.* (1998)**	**Michalski *et al.* (2010)**	**Peeters *et al.* (2006)**	**Viswanathan (2010)**	
	Marks *et al.* (2010)			**Wei (2008)**				

Table 4-2 LKB NTCP model parameters and dose-based constraints for different endpoints/complication; accounted for in this analysis are shown above.

4.2 Methodology

4.2.1 Radiosensitivity based Stratification of cohorts and TCP calculation

The Marsden TCP model accounts for patient radiosensitivity in terms of mean radiosensitivity α_x and standard deviation σ_α spread across a population as shown in Figure 4.1 below. The x-axis represents patient specific tumour radiosensitivity with standard deviation σ. If the patient's clonogens are highly radiosensitive or highly radio-resistant, the patient will belong to the tail end of the normal distribution beyond the $+2\sigma$, $+3\sigma$ or -2σ, -3σ dashed lines away from $\alpha_{mean} = \alpha_x$.

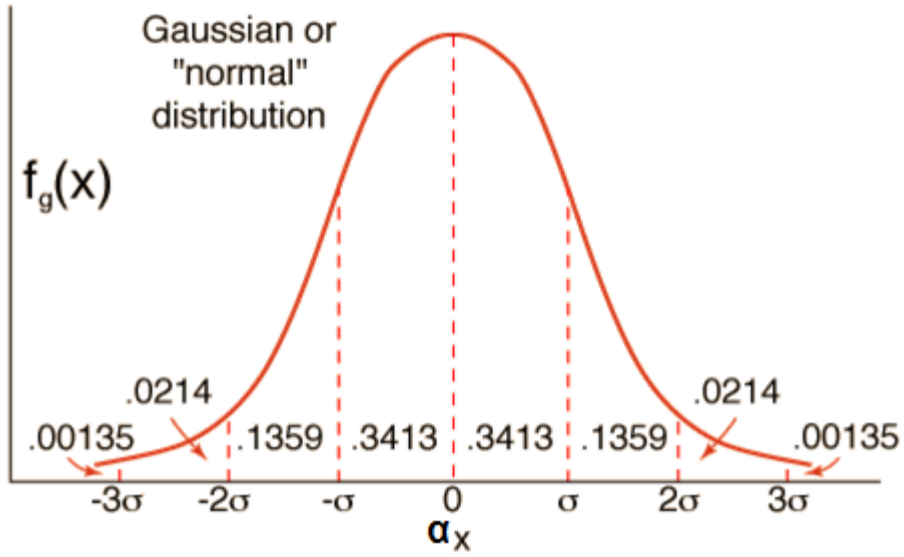

Figure 4-1 The normal distribution is shown in the figure marked by dotted lines indicating the area covered by mean+/-standard deviation. For the purpose of this research work, the variable assumed to be normally distributed is tumour radiosensitivity (x) with population mean α_x and its standard deviation given by σ_α.

The Marsden TCP model assumes that radiosensitivity of tumour clonogens for a specific patient is not known and that radiosensitivity in a given cohort is normally distributed, bounded by α_x-3σ to α_x+3σ as in figure 4-1. However, if the patient population can be stratified into sub-groups of low, medium and high radiosensitivity through a biopsy or genetic test, the patients' radiosensitivity will now belong to a specific subpopulation of the original cohort (green, yellow or blue zone indicated in figure 4-2 (tumour radiosensitivity of each patient tumour is indicated by the red circles).

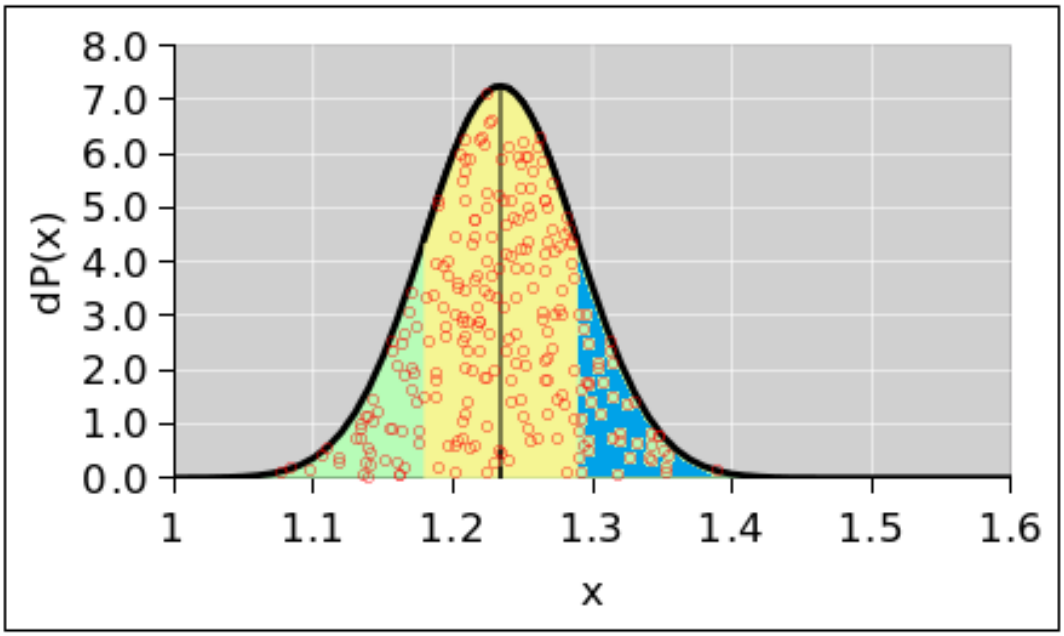

Figure 4-2 Normal distribution of patients' tumour radiosensitivity 'x' with α_x being mean radiosensitivity and σα being the standard deviation. The yellow area represents patients' radiosensitivity spread across α_x+/-σ_α and the green & blue regions are patients' radiosensitivity spread across α_x+/- σ_α to α_x+/-3 σ_α. The green and blue regions account for 31.6% (15.8% each) of the population, and the yellow region accounts for 68.4% of the population (Denker, 2012).

Two methods of accounting for the normally-distributed variation in tumour radiosensitivity in calculating the TCP for a given patient using the Marsden TCP model are described next.

1. In method 1, it is assumed that absolute patient tumour radiosensitivity is unknown and radiosensitivity is randomly chosen from a normally distributed pool and assigned to the patients' tumour. For each sample drawn signifying absolute radiosensitivity x_i, $TCP(x)_i$ is calculated using the Marsden model TCP equation (eqn.4-2 with $\alpha_x=x_i$ and $\sigma_x=0$). An average of $TCP(x)_i$ for i=1…n should result in a TCP estimate accounting for normally distributed radiosensitivity across a population provided that *n* is large. This method is similar to bootstrapping involving random sampling and averaging over a large sample to account for the normal distribution of radiosensitivity parameter in the calculated TCP.

   Thus, per method 1 radiosensitivity 'x' is sampled from the normal distribution (with α_x mean and σ_α standard deviation) n times and TCP is calculated as per equation 4-1.

$$TCP = \frac{[\sum_1^n TCP(x)_i]}{n} \qquad \textbf{Eqn. 4-1}$$

2. The second method of accounting normally distributed radiosensitivity in the TCP model would be to integrate and normalize the TCP(x) [i.e. dP(x) in figure 4-2] function over the normal distribution where α_x is the mean radiosensitivity and σ_α is the standard deviation of the normal distribution as shown in equation 4-2.

$$TCP = \frac{\left[\int_{\alpha x-3\sigma_x}^{\alpha x+3\sigma_x} \mathrm{TCP(x)dx}\right] * e^{\left[-(\alpha-\tilde{\alpha})^2/2{\sigma_\alpha}^2\right]} d\alpha}{\sigma_x\sqrt{(2\pi)}}$$

where TCP(x) is given by

$$TCP = \prod_i e^{\left[-\rho_{cl}V_i * e^{\left\{-\left(\alpha D_i\left(1+\frac{\beta}{\alpha}d_i\right)-(ln_2(T-T_k)/\alpha T_d)\right)\right\}}\right]} \qquad \textbf{Eqn. 4-2}$$

A Matlab® based simulation was conducted to verify that method one and two described above yielded the same TCP for a given DVH. A secondary aim of the simulation was to determine the number of random samples required to equate the TCP calculation of equation 4-1 and 4-2 to form an equivalence between both the methods.

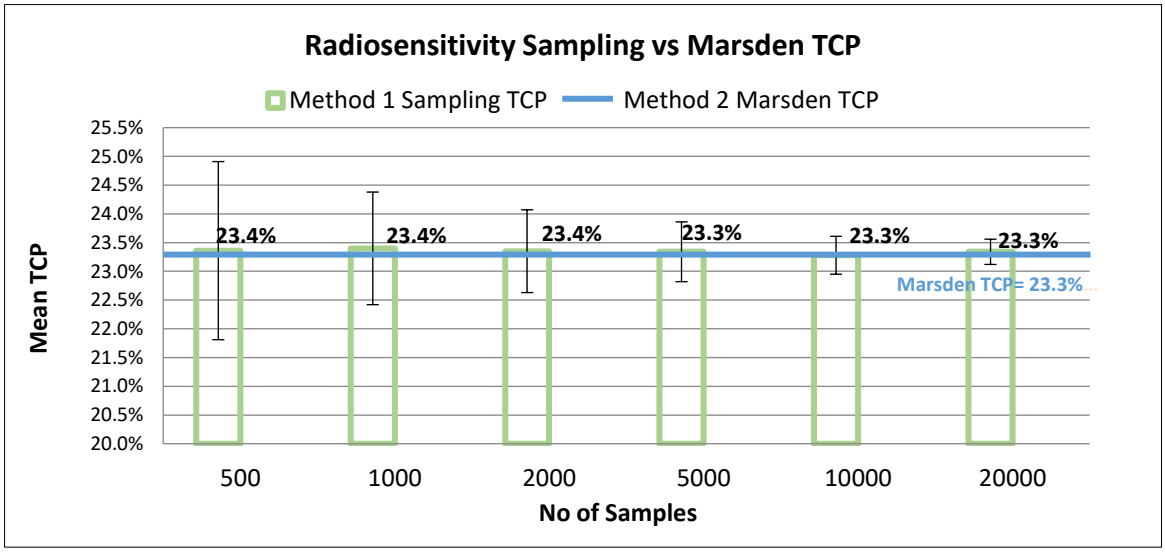

Figure 4-3 The figure shows the change in standard deviation in TCP calculation using method 1 for different number of samples. The calculation of TCP by method 2 is shown by the blue line for comparison with method 1.

A single DVH was used for calculating TCP for both the methods. Based on calculations undertaken $TCP_{Eqn\ 1} = TCP_{Eqn\ 2}$ when n= ~1000 (i.e. $TCP_{method\ 1}$ requires 1000 samples with randomly generated radiosensitivity values to be less than or

equal to $TCP_{method\ 2}$ by 0.1 (absolute value with a standard deviation of 0.01) with a maximum absolute error of 1%. A graph showing the variation in TCP through the sampling method (i.e. dependence on no. of samples for a low standard deviation) versus method 2 based Marsden model calculation is shown in fig 4-3. TCP calculation of a stratified subgroup of patients based on radiosensitivity can be achieved if radiosensitivity is sampled from different parts of the normal distributions as indicated by yellow, green and blue zones of the distribution shown in figure 4-1.

Using method 1, radiosensitivity(x) is sampled from a given region (yellow/green/blue region in fig 4-2) *n* times (minimum sample size 1000 to give a standard deviation of 1% as seen in fig 4-3). Then the TCP(x) is calculated and the average of TCP ($x_{1....n}$) is taken to get the TCP of the patient accounting for the radiosensitivity spread over the subpopulation of the cohort applying equation 4-1. On the other hand, the TCP of patients belonging to a given subgroup can be calculated using the Marsden Model by integrating the radiosensitivity 'x' over the selected region of radiosensitivity of the normal distribution with altered limits of the integral (relevant to the chosen subgroup – e.g. for green subgroup - α_x-σ_α to α_x-$3\sigma_\alpha$). Thus, TCP_{green}, TCP_{yellow} and TCP_{blue} (with reference to fig 4-2) would be calculated that would be the population averaged TCP of the subgroups of the patients which are part of the whole population (with radiosensitivity in the range α_x+$3\sigma_\alpha$ to α_x-$3\sigma_\alpha$). Theoretically, a weighted averaged TCP of the subpopulation should equate to the TCP calculated for the population as a whole using the Marsden TCP model as shown in equation 4-3.

$$0.16*TCP_{green}+0.68*TCP_{yellow}+ 0.16*TCP_{blue}= TCP_{(Eqn4\text{-}2\ldots Marsden\ TCP)} = TCP_{(Eqn4\text{-}1\ for\ n=1000)} \quad \textbf{.....Eqn. 4-3}$$

The cohorts represented by the green/yellow/blue regions in fig 4.2 are part of the whole population represented by the normal distribution (α_x, σ_α) and we do not sample the radiosensitivity of each patient (as part of the subpopulation green/yellow/blue) rather integrate over the region of the normal distribution. Thus, σ_α remains unchanged for the subgroup TCP calculation as the subgroups'

cohort is not individually sampled. Further, statistically σ of a subpopulation (with mean α) drawn out of a population will be lower by a factor √n (n=number of samples of the subpopulation) but here is no clinical data to validate that assumption. Thus, σ_α is used for the TCP calculation of subgroups to account for radiosensitivity spread within the cohort.

Table 4-3 Stratification of patients with normally distributed radio-sensitivity into subgroups

3-group stratification			
Radiosensitivity Level	Lower limit	Upper limit	AUC %
Low	x-3σ	x-σ	15.7%
Medium	x-σ	x+σ	68.3%
High	x+σ	x+3σ	15.7%
Full range	x-3σ	x+3σ	99.7%

If that were not the case, equation 4-3 would not hold true. This assumption is verified in the results section [e.g. table 4-4 Box (8,5) compared to Box (11,5)]. Also, the complexity of optimization algorithms used in this chapter mandated maximization of computing efficiency and compared to method 1, method 2 was significantly faster. As the difference between TCP calculation by either method was minimal, method 2 was implemented. Next, the methodology employed to demonstrate the effect of radiosensitivity data on treatment optimization achievable for different clinical scenarios is explained. These are described in detail in subsection 4.2.3 of the methodology section.

It is aimed to optimize treatment prescription dose and fractionation in an Iso-toxic (aka Iso-NTCP) manner as applied in chapter 3 (level 1 & 2). In order to make the analysis computationally viable, the computation is restricted to data for the tumour and a *single* primary OAR endpoint. For the lung tumour cohort, the RTOG grade 2 radiation pneumonitis risk, and for the prostate tumour cohort the RTOG grade 2 rectal bleeding endpoints are considered as the principal dose-limiting toxicity endpoint. The TCP and NTCP model parameters used are available in table 4-1 and table 4-2. The Marsden-model Lung tumour parameters (table 4-1) used are shown under the column with title Lung (α_x=0.307 Gy^{-1}, $\boldsymbol{\sigma}_\alpha$=0.037) and similarly for

prostate tumours the parameters under column with title Prostate4 (α/β=1.5 Gy) are used for TCP calculations of this chapter.

The above-mentioned optimizations (Level 1 and 2) are undertaken for two situations

1) Optimizations 'without' the availability of radiosensitivity information at the treatment planning stage
2) Optimizations 'with' the availability of radiosensitivity information at treatment planning stage (which allows stratification of patients on the basis of subgroups)

Iso-toxic dose individualization (level 1) and optimum dose & fraction number individualization (level 2) is performed over the entire cohort (for each patient DVH dataset in turn) and the results are reported as population-averaged TCP, NTCP, and optimal fraction number for each cohort for both the clinical scenarios listed above. The **percentage patient dropout** for each of the cohorts is also reported which is the number of patients having TCP<10% (post level 1 or level 2 optimization **$TCP_{threshold}$**) divided by the total number of patients in the cohort. This parameter helps in estimating the number of patients that are not likely to benefit from radical radiotherapy treatment. The interpretation of data generated for this analysis is notably dependent on the choice of $TCP_{threshold}$ value which should be clinically relevant. The different levels of dose individualization are explained in the next section which are applied to the clinical scenarios mentioned above (detailed in section 4.2.3).

4.2.2 Individualization and Optimization

4.2.2.1 Level 0 TCP Calculations – 'without' radiosensitivity stratification and 'with' stratification

The level 0 is a TCP calculation at the standard prescribed dose (55Gy20# for lung cohort and 60Gy20# for the prostate cohort). Firstly, level 0 TCP-NTCP analysis is performed where the TCP and NTCP of the patient is calculated for the standard prescription using the Marsden TCP Model (also explained in section 2.3, Chapter 2). The results provide the population-averaged TCP, forming the level 0 results without radiosensitivity stratification information. These TCP calculations would be

similar to those observed in Chapter 3 for Level 0 calculations with a dose scaling factor of 1 (if the same TCP model parameters and DVH is used). Now the patients are stratified into radiosensitivity subgroups and a level 0 TCP-NTCP calculation is performed for each patient considered in each radiosensitivity group and the variation in the TCP and NTCP of the patient is then compared to the standard prescription based TCP & NTCP calculations (55Gy20# for lung tumours and 60Gy20# for prostate tumours).

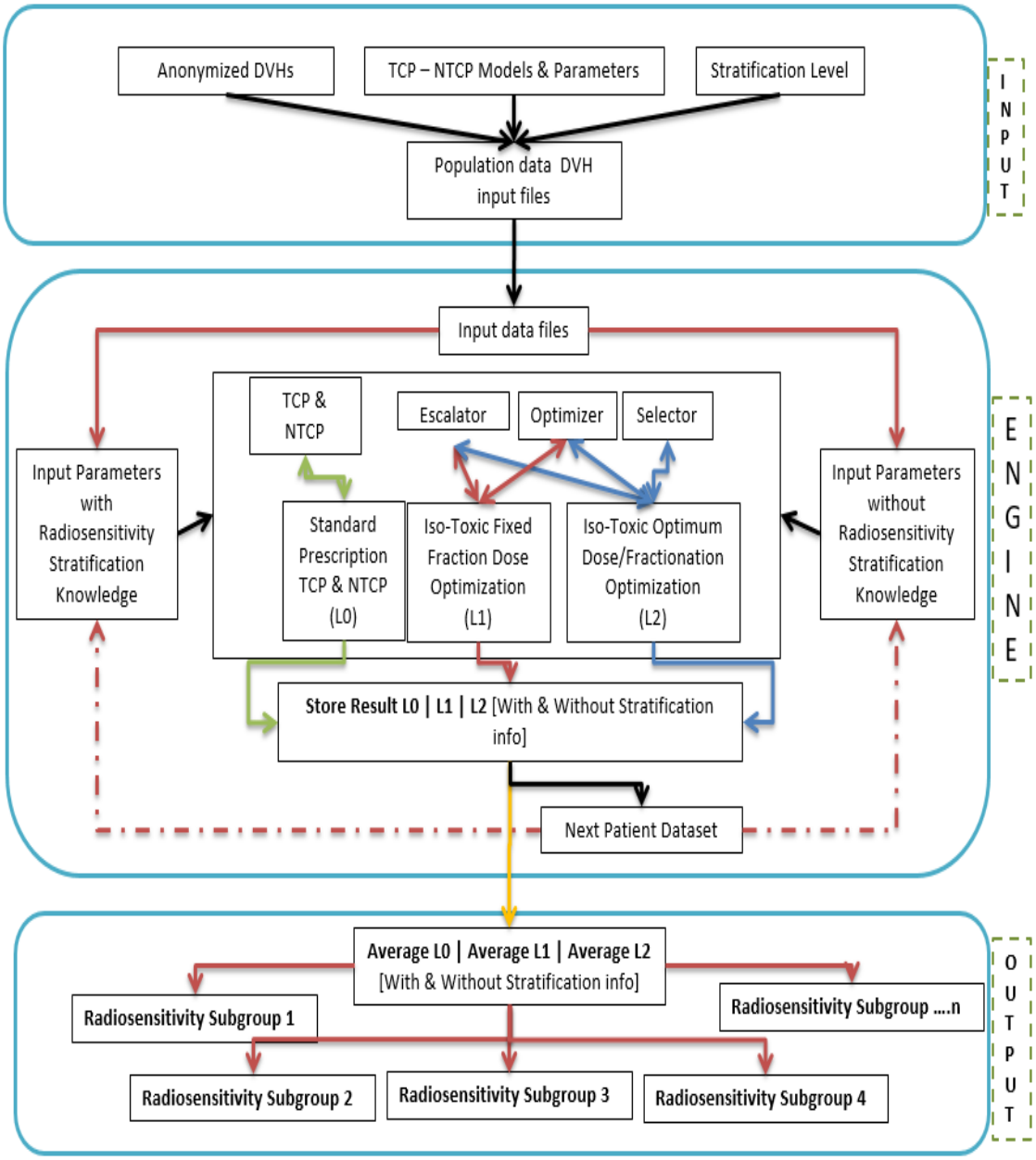

Figure 4-4 The flow diagram of the program that performs all the calculations is shown here. The program can be divided into 3 sections (Input, engine, output) and we use the escalator, optimizer and selector modules (refer Chapter 3, section 3.2.2-3.2.4) to perform the optimization.

4.2.2.2 *Level 1 & 2 Optimization -- 'without' radiosensitivity stratification and 'with' stratification*

The Level 1 optimization is a radiobiological model based Iso-toxic dose escalation at fixed fraction number wherein dose to the tumour is escalated until a given NTCP OAR dose tolerance limit is reached. Level 2 optimization refers to radiobiological model based Iso-toxic dose escalation where the tumour dose is Iso-toxically escalated (like level 1), but with an additional search criteria of finding the *minimum* number of fractions (yielding the highest TCP at an Iso-toxic NTCP). The dose-response curve of a tumour is sigmoidal in shape and plateaus beyond a given prescription dose (i.e. the slope of the curve becomes very small as dose increases) as shown in figure 4-5. A limit on dose escalation at this point is placed (called TCP_{cap} – 95% is selected here). This is done as the increase in therapeutic gain from further dose escalation is very low. An upper limit on TCP is thus actioned (i.e. **TCP_{cap}**) to limit dose escalation for level 1 and level 2 optimizations. An observation of the dose-response curve in Nahum & Uzan (2012) demonstrates this as shown in figure 4-5.

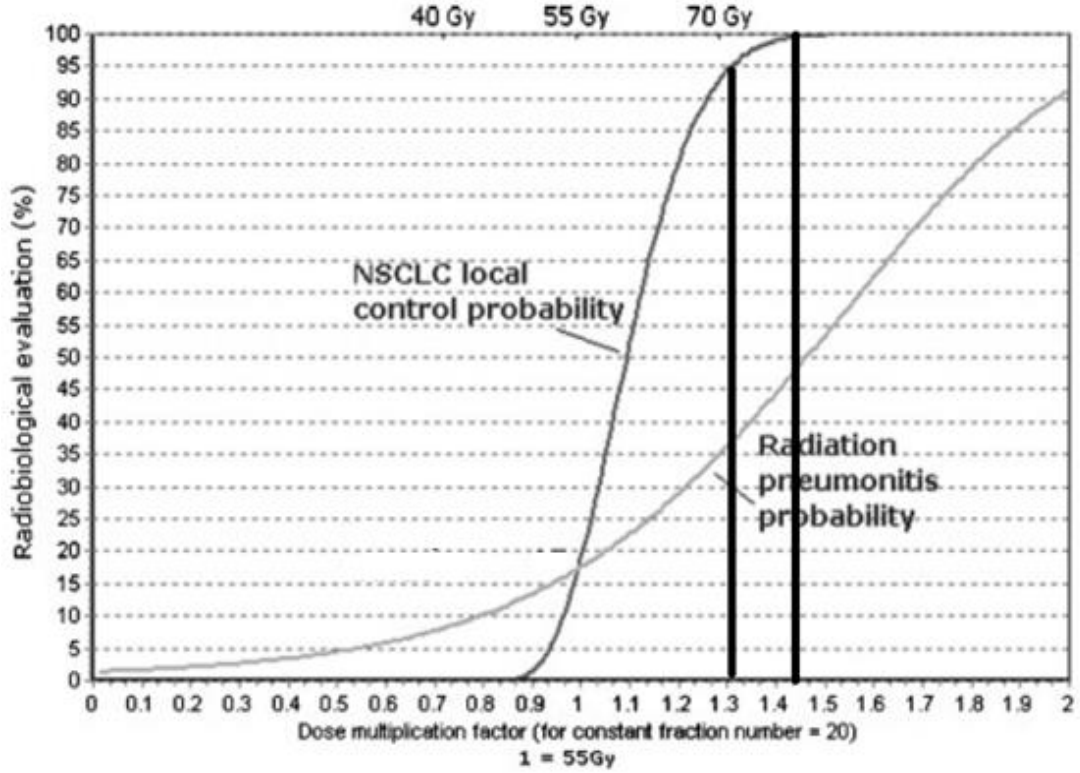

Figure 4-5 A NSCLC patient DVH based dose escalation is shown above. The slope of the NSCLC control probability curve reduces significantly from radiobiological evaluation 95% - 100% with dose rising by ~7 Gy on the x-axis as shown by the black bars. For the same change in the prescribed dose NTCP of radiation pneumonitis increases by ~3%. Thus, the relative therapeutic benefit of increasing prescribed dose after achieving a 95% TCP is very low. Courtesy: Nahum and Uzan (2012)

The optimizations are Iso-toxic whereby the algorithm is set to increase the dose and hence the TCP until a fixed NTCP constraint is reached. The dose multiplication factor that allows the optimizer to escalate dose to the tumour DVH to achieve 95% TCP is of course applied to the OAR DVH to obtain the patient's OAR toxicity probability (*i.e. as long as the set* NTCP limit is not crossed). For some patients, 95% TCP is achieved at a lower dose scaling factor than that yielding the current NTCP limit. This results in a lowering of the mean population NTCP ($NTCP_{population}$ | $NTCP_{pop}$) for a cohort/subgroup. For example, if the NTCP limit is set to 7%, the $NTCP_{pop}$ might be around 6.5% as some of the patients hit the TCP_{cap} and the optimizer/selector then reduces the dose scaling factor (and hence the NTCP). The comparison between different clinical scenarios may become problematic if the NTCPs are not equal.

To mitigate that, a NTCP-aim limit is set that allows dose escalation for individual patients such that the $NTCP_{pop}$ achieved is equal to the pre-set value making results comparable across the cohorts. The NTCP limit for Lung Radiation pneumonitis risk of 17% corresponds to a V20 of 30% for healthy lung tissue. Similarly, the rectal bleeding risk of 10% corresponds to V50<50% for rectum. These values were derived from a V_x – NTCP correlation exercise that is described in detail in chapter 6 and are the absolute individual NTCP limits used in the optimizations for the conventional fractionation scheme. L-K-B NTCP model used here accounts for the effect of fractions through the EQD_2 based DVH correction method introduced by Fowler (2001). Thus, the change in NTCP limit (based on Vx-NTCP co-relation) for a change in fractionation is not required.

Assuming that patients can be stratified into radiosensitivity subgroups; the computations now correspond to tumour radiosensitivity over a smaller area of the normal curve (yellow, green or blue zone – Fig 4-2). All the patients in the cohort are placed in the different subgroups, one at a time, and treatment individualization is performed. The flow chart explaining the process is shown in Figure 4-4. The TCP & NTCP model parameters, patient specific radiosensitivity subgroup information, tumour DVH and OAR DVH are passed to the program modules as inputs.

For level 1 dose individualization, the number of fractions is kept constant at 20 for both lung and prostate cohorts. The patients are now considered to belong to a given radiosensitivity subgroup (thus, the TCP calculations will only account for the radiosensitivity spread for that subgroup, e.g. $\alpha_{mean}+\sigma_\alpha$ to $\alpha_{mean}+2\sigma_\alpha$ for high radiosensitivity group fig 4-1).

The level 1 dose optimization is performed over the entire cohort to determine the average maximum prescription dose at 20 fractions not exceeding an average NTCP limit of 5%, 7%, 10%, 13% and 17% for radiation pneumonitis in the Lung cohort and 1%-10% for rectal bleeding in the prostate cancer cohort. Thus, a level 1 prescription dose and the optimized TCP for each patient of the cohort in the given tumour radiosensitivity subgroup will be available. This process is then performed considering the cohort to belong to each radiosensitivity subgroup, one at a time. The mean of these TCPs and NTCPs yields the optimum level 1 population response for each subgroup.

For level 2 dose fractionation individualization, the same procedure as above is performed along with optimization of the number of fractions for each patient DVH dataset, considering all patients in the same tumour radiosensitivity subgroup (i.e. all the patients are considered to belong to one sub group at a time). So, for level 2 individualization, an optimized TCP, NTCP, prescription dose and fraction number for each patient is calculated. After that the optimised prescription doses and fraction numbers of all the patients are then averaged to yield the level 2 optimised population dose and fractionation. This exercise is performed for average Iso-toxic NTCP limits (5%, 7%, 10%, 13% & 17% for the lung cohort) one at a time to produce an optimum TCP_{pop} versus Iso-$NTCP_{pop}$ curve.

4.2.3 Clinical Scenarios

For both types of optimizations (Level 1 & 2), calculations are performed for the following clinical scenarios and in the order below for all the cohorts. Depending on the clinical scenario the calculation of TCP changes as explained below. The change in the calculation is in the value of α and range of σ_α supplied as parameters to the model.

For any scenario described below, the output of Level 1 optimization is a Dose scaling factor (DSF), TCP (calculated using DSF, prescription dose, α, σ_α), and the NTCP limit. The output of Level 2 optimization is a dose scaling factor (DSF), optimal fraction number, TCP (calculated using DSF, prescription dose, α, σ_α), and the Iso-toxic NTCP limit.

Case 1) "Standard Optimization" No radiosensitivity information about the patient is available before or after individual treatment optimization.

During the optimizations for this scenario, the TCP is calculated for each tumour DVH with a mean radiosensitivity α and standard deviation +/-3 σ_α. The Marsden TCP model assumes normally distributed radiosensitivity across a population.

Thus, the output of level 1 & 2 optimization will be
Level 1 optimization output = (TCP $_{(\alpha+3\sigma,\ \alpha-3\sigma)}$, Iso-toxic NTCP, DSF $_{std}$ at 20 fractions)
Level 2 optimization output = (TCP $_{(\alpha+3\sigma,\ \alpha-3\sigma)}$, Iso-toxic NTCP, DSF $_{std}$ at Optimized fraction #)

The results of case 1 (levels 1 & 2) optimization will be equal to results of the optimization methodology used in chapter 3 (as long as input files and parameters are unchanged)

Case 2) "Without" – Patient-specific radiosensitivity information is only available *post* treatment and the TCPs for the Iso-toxic Prescription doses (of case 1) are re-calculated using the updated radiosensitivity information about the patient's tumour.

Range of radiosensitivity: Low Radiosensitivity - (α-3σ, α-σ)

Medium Radiosensitivity - (α-σ, α+σ)

High Radiosensitivity - (α+σ, α+3σ)

The TCP is now recalculated for the same patients per group:

Level 1 optimization output = ($TCP_{(\alpha\ Range)}$,Iso-toxic NTCP, DSF_{std} at 20 fractions)
Level 2 optimization output = ($TCP_{(\alpha\ Range)}$,Iso-toxic NTCP, DSF_{std} at optimized fraction #)

Use of the "α range" to correct the case-1 optimized TCP allows inclusion of radiosensitivity information about the patient retrospectively. This facilitates a subgroup-wise comparison of case 2 and case 3 results (in a retrospective vs prospective type comparison)

Case 3) "With" – Here, patient specific radiosensitivity information is made use of *before* individual treatment optimization and is used in the optimization.

In this case, TCP calculations are undertaken in the optimizations using the "α range". This results in optimizations that have accounted for patient-specific radiosensitivity. The output of the optimizations is shown below
Level 1 optimization output = ($TCP_{(\alpha\ Range)}$,Iso-toxic NTCP, $DSF_{\text{Radiosensitivity optimized}}$ at 20 fractions)
Level 2 optimization output = ($TCP_{(\alpha\ Range)}$,Iso-toxic NTCP, $DSF_{\text{Radiosensitivity optimized}}$ at optimized fraction #)

The optimizations have two limiting factors:

1) Iso-toxicity in terms of absolute NTCP and

2) TCP upper-bound limit.

The absolute Iso-toxicity NTCP limit is set to ensure that the optimization does not result in prescription doses that would cause clinically unacceptable damage in any

patient. The TCP upper bound limit is set as 95% as an increase in TCP beyond 95% would require a very large increase in prescription dose for a negligible clinical gain. This was explained in detail in section 4.2.2.2

The result of this entire analysis is a table of TCP & NTCP of radiosensitivity groups versus optimization levels with & without radiosensitivity information (e.g. table 4-4). This analysis is then repeated for average Iso-toxicity limits of 5%, 7%, 10%, 13% and 17% for the lung cohort and 1%, 3%,5%.7% and 10% for the prostate cohort. The final result is a TCP-NTCP graph for level 1 optimization and one for level 2 optimization comparing the 'without stratification' case 2 to the 'with stratification' case 3 over a range of NTCP limits (e.g. figure 4-9). The above analysis is also undertaken for a 5-group radiosensitivity classification to assess if there is any benefit of finer patient radiosensitivity segregation. The patient dropout for each of the cohorts in each subgroup is also calculated and compared to the patient dropout for the non-stratified optimization analysis (Patient dropout is defined at the end of section 4.2.1).

The exercise is performed using the DVH datasets for two anonymised cohorts, one of 59 lung patients (originally prescribed 55Gy20#) and the other of 56 prostate patients (originally prescribed 60Gy20#).

4.3 Results

4.3.1 Lung Cohort Results

Table 4.4 shows level 0 calculations plus optimization results for level 1 and level 2 strategies performed over a lung cancer cohort. All the results in this section are population averages and display the cumulative effect of having/not having radiosensitivity information on Iso-toxic radiotherapy treatment optimization.

4.3.1.1 Level 0 – TCP NTCP calculations (3 Group)

Level 0 analysis is shown in figure 4-6 where TCP_{pop} & $NTCP_{pop}$ calculations for a lung cohort belonging to the low / medium / high radiosensitivity group are compared to generic population radiosensitivity based $TCP_{population}$ & $NTCP_{population}$ estimates. It can be seen that TCP calculated using generic population radiosensitivity (assumed to be normally distributed over the whole population) overestimates individual TCPs for the radio-resistant group of patients (Level 0 Case 3-Low, table 4-4) and underestimates it for the highly radio-sensitive group of patients (Level 0 Case 3-High, table 4-4).

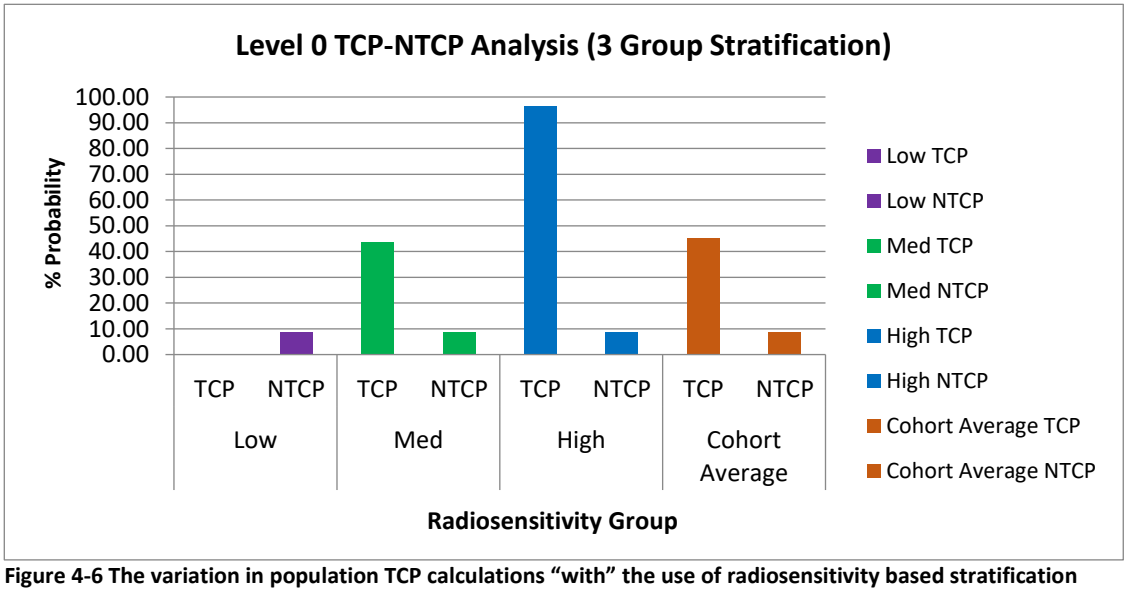

Figure 4-6 The variation in population TCP calculations "with" the use of radiosensitivity based stratification shown for cohorts falling in "low", medium - "med" and "high" radiosensitivity subgroups compared to TCP calculations "without" patient radiosensitivity information (Cohort Average TCP). NTCP remains unaffected as normal tissue radiosensitivity is assumed to be constant across the population.

Also, a weighted average TCP of the population in the stratified group yields the same TCP as in the case of 'without' scenario which validates the subgroup TCP calculations. This can be observed from table 4-4 comparing box (8,2) & (8,4). As the

normal tissue radiosensitivity variation is not accounted for, $NTCP_{population}$ for 'with' & 'without' stratification case is the same.

4.3.1.1 Level 1 Optimization (3 Group)

To see the effect of having the ability to stratify patients (on the basis of radiosensitivity) on level 1 Iso-toxic optimization look at figure 4-7 (row 5 & 6 of table 4-4). It is observed in Figure 4-7 that when Iso--toxic conditions are maintained (7% NTCP here) TCP would be higher 'with' radiosensitivity knowledge compared to 'without' it (in all subgroups). To compare the overall gain in both the scenarios the weighted average TCP and NTCP is calculated [Table 4-4 box (8,5) & box (8,6) shows a definite therapeutic gain]. The use of stratification leads to a 2.2% improvement in the stratification based TCP_{pop} compared to the case 2 based TCP optimization at same average Iso-toxic NTCP. TCP_{pop} of 'low' group is higher than the 'without' scenario TCP_{pop} – this unexpected finding is due to TCP saturation observed in some of the patients driving the average TCP_{pop} higher for 'with' category compared to 'without' category. This is critically analysed in the lung cohort results discussion section (refer section 4.4.1).

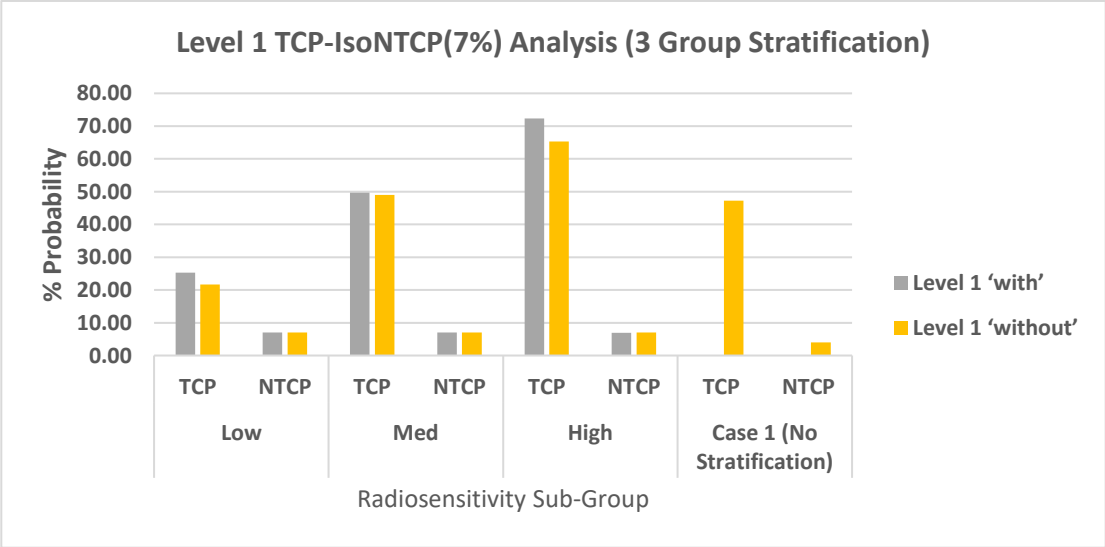

Figure 4-7 shows level 1 lung treatment optimization results for 'without' case 2 and 'with' case 3 scenarios with respect to radiosensitivity stratification. Also, the result of level 1 case 1 - no stratification scenario is shown for comparison.

Comparing row 5a and 6a in table 4-4, it is seen that 66% patients may have dropped out of radiotherapy treatment if information about their tumour radiosensitivity had been available compared to a 37% drop-out rate for the

'without' stratification scenario. Also, for patients in the high radiosensitivity group, only 12% would have dropped out compared to 37% patients as per 'no stratification' / 'without' case optimization. The dropout of patients (TCP post optimization < 10%) observed is high as the NTCP is limited to average 7% which restricts dose escalation in many cases. The effect of this in the low radiosensitivity group is most noticeable. A low tumour radiosensitivity requires higher doses to achieve a high TCP but this also raises NTCP faster and as the radiosensitivity of OARs is assumed to be constant, a low optimized DSF (i.e. with low TCP resulting in higher dropout) results. However, if this NTCP limit is increased to 17%, the dropout for the level 1 no-stratification scenario (case 2) is found to be zero, versus 22% in the level 1 case 3 ('with') optimized low radiosensitivity subgroup and 1.7% in medium radiosensitivity subgroups (0% dropout in high radiosensitivity subgroup for both the cases). In summary, the dropout rate is affected by the choice of Iso-NTCP limit which drives the dose escalation (that drives the TCP up). Further, it is important to note that these results are based on limited amount of retrospective datasets and need to be further validated by data from larger and varied population datasets and along with radiosensitivity data to be clinically useful.

4.3.1.2 Level 2 Optimization (3 Group)

Figure 4-8 (Rows 7 & 8 of table 4-4) shows the results of employing level 2 radiotherapy optimization 'with' (case 3) or 'without' (case 2) patient-specific

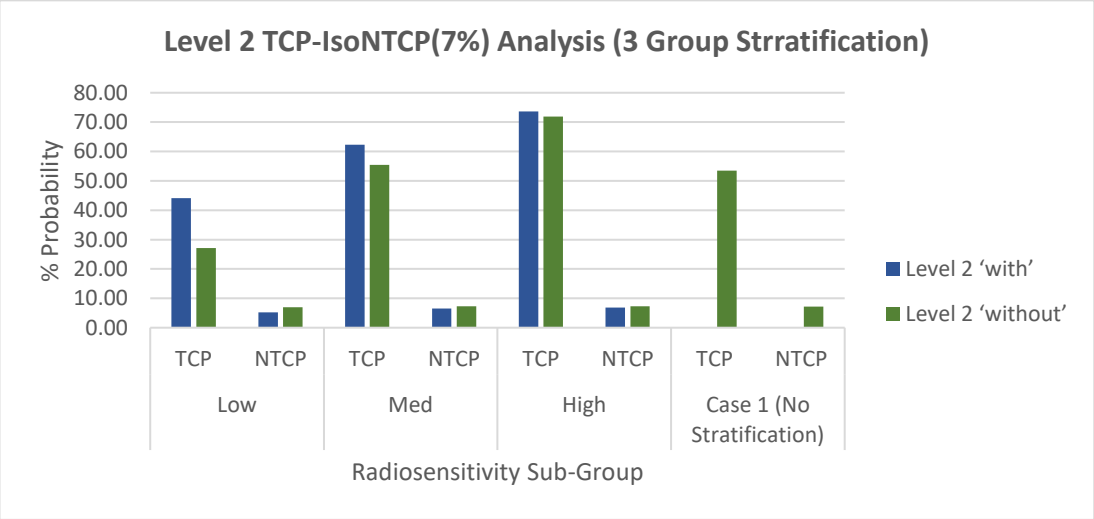

Figure 4-8 A level 2 optimization to compare 'with' and 'without' radiosensitivity information scenario with respect to radiosensitivity stratification. The results of level 2 case 1 - no stratification scenario is shown for comparison.

tumour radiosensitivity information. At ~7% average NTCP, the weighted-average population TCP [box (8,8) in table 4-4], i.e. combining all subgroups, shows a 8.35% improvement over the population TCP achieved without using the radiosensitivity information [box (8,7) table 4-4]. The percentage patient dropout for level 2, case 3 for the low radiosensitivity subgroup was 19% higher than that for level 2, case 2 result. Also, for the high radiosensitivity group, the patient dropout was lower by

Table 4-4 Radiosensitivity (3 group) based Radiotherapy Individualization - Lung Tumour (7% NTCP limit)												
No	1	2	3	4	5	6	7	8	9	10	11	12
1		TCP	NTCP	TCP	NTCP	TCP	NTCP	TCP	NTCP	Fraction No with highest Frequency	Case 1 TCP	Case 1 NTCP
2	Level 0 Case 1	45.07	8.63	45.07	8.63	45.1	8.63	45.06	8.63	20 (100%)		
3	Groups	Low		Med		High		All (weighted average)			No Stratification Optimization Case 1	
4	Level 0 Case 3	0.27	8.63	43.51	8.63	96.6	8.63	45.07	8.63	20 (100%)		
5	Level 1 Case 2	21.63	7.00	48.96	7.00	65.3	7.00	47.21	7.00	20 (100%)	47.2	7.00
5a	Drop out	37%		37%		37%						
6	Level 1 Case 3	25.30	7.00	49.68	7.00	72.3	6.88	49.40	6.98	20 (100%)		
6a	Drop out	66%		39%		13%						
7	Level 2 Case 2	27.07	7.26	55.39	7.26	71.9	7.26	53.51	7.26	15 (80%)	53.5	7.22
7a	Drop out	25%		25%		25%						
8	Level 2 Case 3	44.08	5.27	62.26	6.58	73.6	6.85	61.15	6.41	[Lo Med Hi] 15 (56% 80% 90%)		
8a	Drop out	44%		24%		12%						

13%. This shows that many patients maybe be considered for a different treatment option or strategy had the tumour specific radiosensitivity been known. Furthermore, the percentage of patients showing the highest TCP at 15 fractions is considerably different in the case 3 based results (Low-56%, Medium-80%, High-90%) compared to the standard 'no' stratification scenario case 2 based results (80%) shown in box (10,8) & box (10,7) in table 4-4.

Columns 8 and 9 (table 4-4) are weighted averages of TCPs and NTCPs of various subgroups. The difference between level 1, case 2 weighted average TCP & NTCP

[Table 4.4 box (8,5), (9,5)] and level 1 case 1 [Table 4.4 box (11,5), (12,5) calculated using the program used for chapter 3] is negligible. These calculations are performed using independent programs and quality check the TCP, NTCP and Level 1 optimization results obtained for this chapter. The same is true for calculations of level 2 optimization. The programming is thus observed to be consistent across algorithms used for chapter 3 & 4 of this thesis. The uncertainty in model parameters and their contribution to error in absolute predictions by the models is acknowledged but here the model predictions are used in relative terms to compare scenarios in the current analysis which suggests that uncertainty in the results is mostly contributed by the tolerance limit of the optimizer module cost function (set to 0.001 – systematic error).

The results for 3-group stratification for both Level 1 and Level 2 indicate that using radiosensitivity information for treatment individualization significantly impacts the highly radiosensitive or radio-resistant subgroup treatment optimization. The 'medium' subgroup is minimally affected by the application of radiosensitivity information for optimization.

4.3.1.3 Lung Cohort Result - 5 Groups Stratification

A similar analysis was performed with the patients stratified into 5 subgroups (radiosensitivity level – very low, low, medium, high, very high) instead of 3 (Low, Medium, High) and the results are reported in table 4-5.

Use of radiosensitivity based stratification improves overall population TCP_{pop} estimates by 2.29% for level 1 [Box (12,6) – Box (12,5), table 4-5] and by 7.95% [Box (12,8) – Box (12,7), table 4-5] for level 2 optimization compared to the scenario where patient specific radiosensitivity information is not used in optimization. Further, in the case of 5 subgroups, the number of fractions required by different subgroups for achieving optimal TCP varies considerably, but most of the patients achieve optimized results at 15 fractions. Comparing rows 7a and 8b in table 4-5, it is seen that if the patients were in the very low radiosensitivity group, an extra 34% patients could have dropped out of the treatment if the tumour radiosensitivity information had been available to optimize treatment regimens and in the very high radiosensitivity cohort 26% of patients could have been prescribed curative

optimized treatments compared to level 2, case 2 optimization where they would have dropped out of treatment. It is important to mention again that the % drop-out would decrease if the Iso-toxic NTCP limit were increased, as the increase in dose escalation would increase the TCP. For level 2 optimization (case 3), 15 fractions remain the ideal regimen for the majority of the patients in all the subgroups but there is a notable variation in the percentage of patients for whom 15 fractions are ideal, when sequentially observing results for very low to very high radiosensitivity subgroups. Also, if the radiosensitivity information had not been available 15 fractions would have been the optimum fraction schedule for 80% of the patients. This is shown in row 7 of table 4-5, Box (14,7).

Table 4-5 Radiosensitivity (5 group) based Radiotherapy Individualization - Lung Tumour (7% NTCP limit)

No	1	2	3	4	5	6	7	8	9	10	11	12	13	14	15	16
1		TCP	NTCP	TCP	NTCP	TCP	NTCP	TCP	NTCP	TCP	NTCP	TCP	NTCP	No of Fraction	TCP	NTCP
2	Level 0 Case 1	45.0	8.63	45.0	8.63	45.0	8.63	45.07	8.63	45.0	8.63	44.95	8.61	20.00		
3	Group	VLow		Low		Med		High		Vhigh		All (weighted average)			No Stratification Optimization Case 1	
4	Level 0 Case 3	0.00	8.63	0.31	8.63	43.5	8.63	96.14	8.63	99.6	8.63	44.95	8.61	20		
5	Level 1 Case 2	2.47	7.00	24.7	7.00	48.9	7.00	64.00	7.00	73.5	7.00	47.10	6.98	20	47.2	7.00
5a	Drop out	37%		37%		37%		37%		37%						
6	Level 1 Case 3	17.9	7.00	26.8	7.00	49.6	7.00	70.99	6.89	83.4	6.55	49.39	6.96	20		
6a	Drop out	80%		64%		39%		22%		3%						
7	Level 2 Case 2	3.40	7.26	30.8	7.26	55.3	7.26	70.92	7.26	78.1	7.26	53.38	7.24	15 (80%)	54.0	8.00
7a	Drop out	29%		29%		29%		29%		29%						
8	Level 2 Case 3	29.5	4.45	46.1	5.12	62.2	6.58	74.40	6.70	84.5	6.50	61.33	6.33			
8a	Optimum fraction (Frequency)	15 (47%)		15 (56%)		15 (69%)		15 (80%)		15 (81%)						
8b	Level 1 Case 2	63%		46%		24%		20%		3%						

Comparing table 4-5 Box (14,7) to table 4-5 row (8a), it is observed that for most of the patients belonging to the very low or low radiosensitivity groups, 15 fractions would not be an optimum fractionation schedule.

4.3.1.4 3 - Group Stratification versus 5 - Group Stratification

For the lung cohort, level 1 and 2 optimizations are performed next at various Iso-toxic $NTCP_{population}$ limits in the 5%-17% NTCP limit range for 3- and 5-group stratification scenarios. The TCP-NTCP graphs below compare the 'with' and 'without' cases over the NTCP range at different Iso-toxic limits.

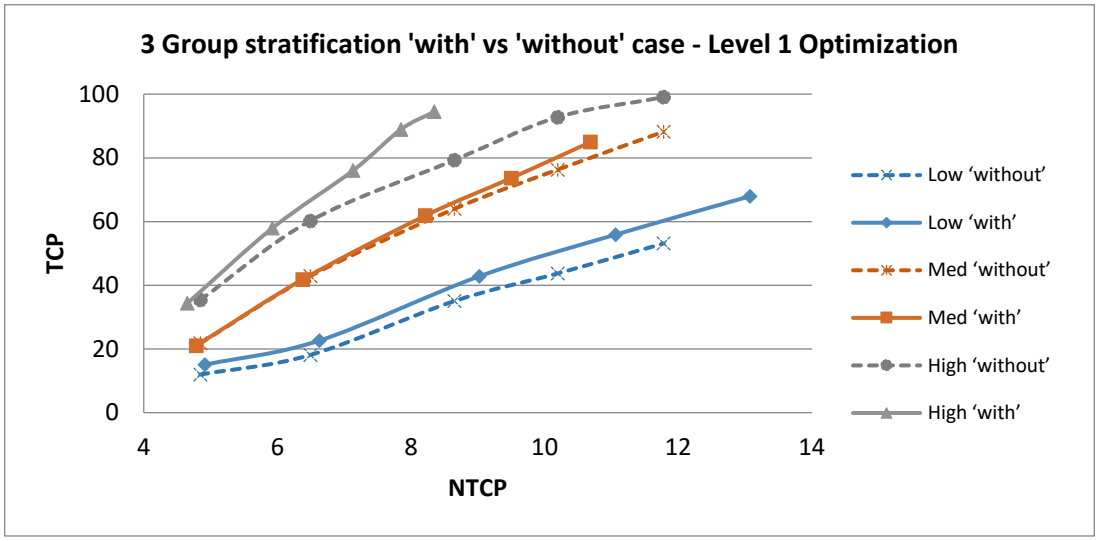

Figure 4-9 TCP-NTCP graph for comparing Level 1 optimization for 'with' and 'without' radiosensitivity information scenarios for various Iso-toxicity limits for 3 radiosensitivity subgroup (High, Medium "med", Low) stratification – Lung Cohort

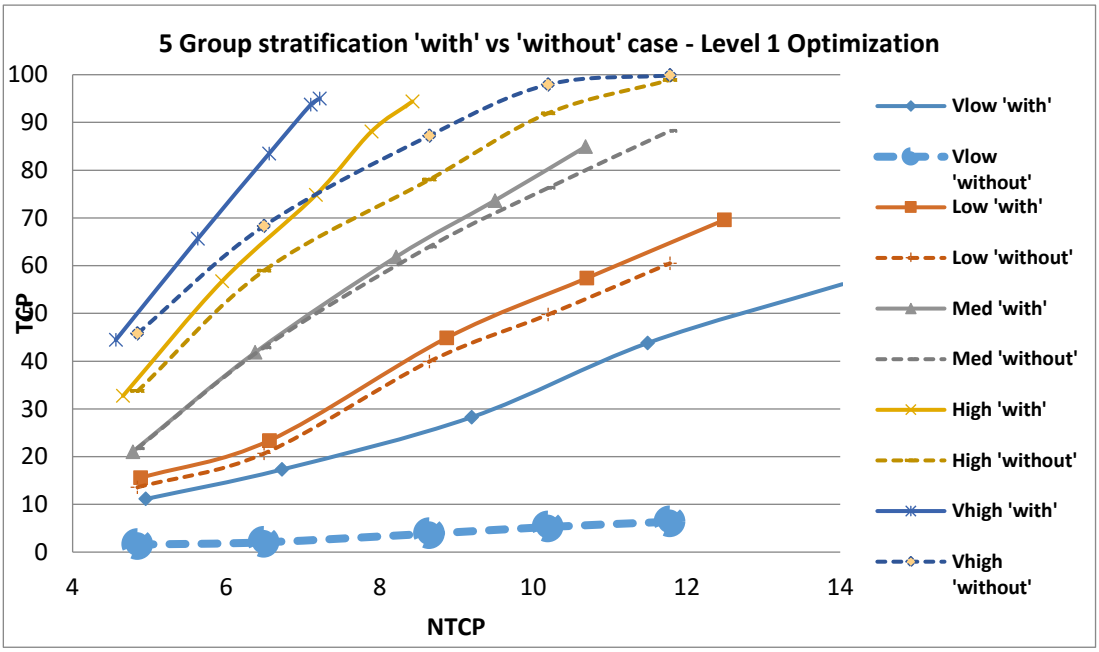

Figure 4-10 TCP-NTCP graph for comparing Level 1 optimization for 'with' and 'without' radiosensitivity information scenarios for various Iso-toxicity limits for the 5 radiosensitivity subgroup (Very High "Vhigh", High, Medium "Med", Low, Very Low "Vlow") stratification – Lung Cohort.

It can be seen that the group of patients furthest from the mean population radiosensitivity are the ones experiencing the highest variation in TCP values. The Figure 4-9 & Figure 4-10 show that the improvement in TCP estimates for highly radiosensitive and highly radio-resistant groups compared to the medium radiosensitivity group from case 2 'without' to case 3 'with' is relatively large.

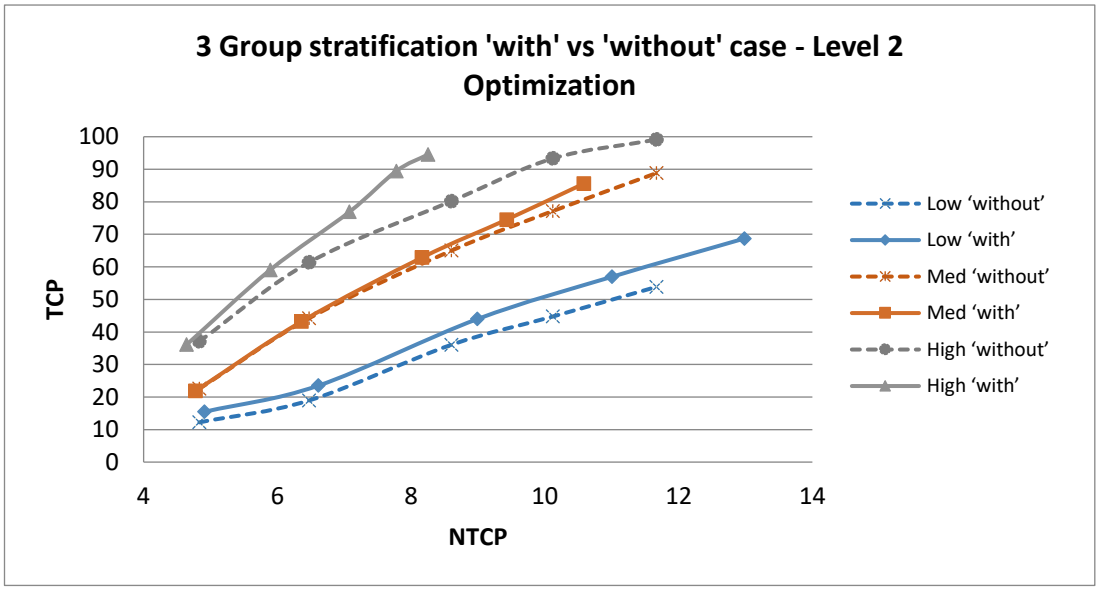

Figure 4-11 TCP-NTCP graph for comparing Level 2 optimization for 'with' and 'without' radiosensitivity information scenarios for various Iso-toxicity limits for 3 radiosensitivity subgroup (High, Medium "Med", Low) stratification – Lung Cohort.

This can be observed by comparing the increasing gap (indicative of therapeutic gain) between 'with' and 'without' cases for different radiosensitivity subgroups as the Iso-toxic limit is increased. A similar trend can be seen for level 2 optimization over a range of NTCP limits in fig. 4-11 & fig. 4-12.

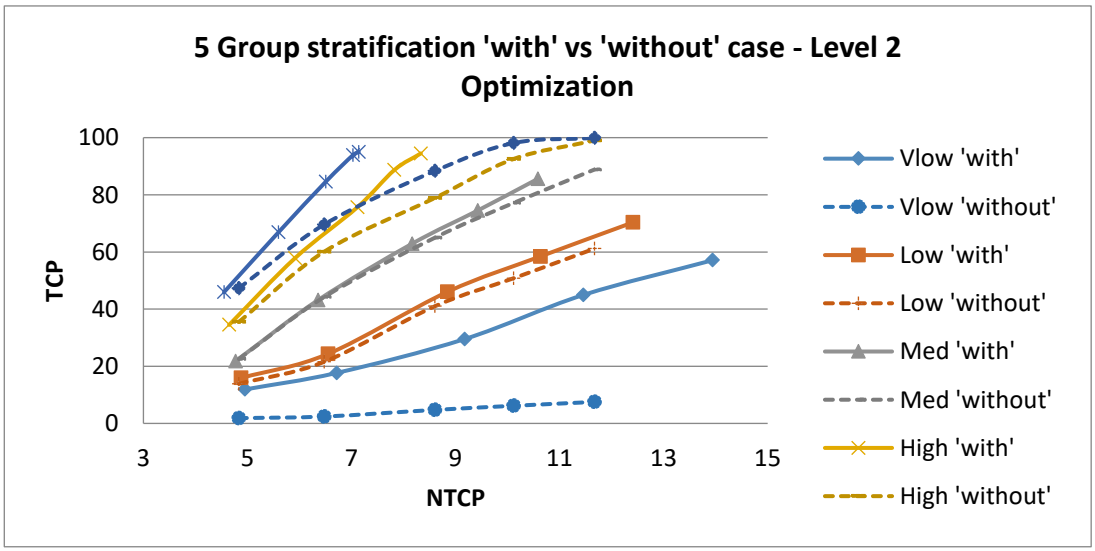

Figure 4-12 TCP-NTCP graph for comparing Level 2 optimization for 'with' and 'without' radiosensitivity information scenarios for various Iso-toxicity limits for 5 radiosensitivity subgroup (Very High "Vhigh", High, Medium "Med", Low, Very Low "Vlow") stratification – Lung Cohort

A comparison of the overall weighted average population TCP & NTCP of the 3-group and 5-group stratification (fig. 4-13) reveals that as the resolution of stratification increases the therapeutic gain improves slightly. Quantification of this therapeutic gain can be done at a fixed Iso-toxic level for patients in a given radiosensitivity subgroup. The highest difference in TCP_{pop} is ~5% as seen in the low radiosensitivity group at 12.5% Iso-toxic NTCP, where 5 levels is superior to 3 levels.

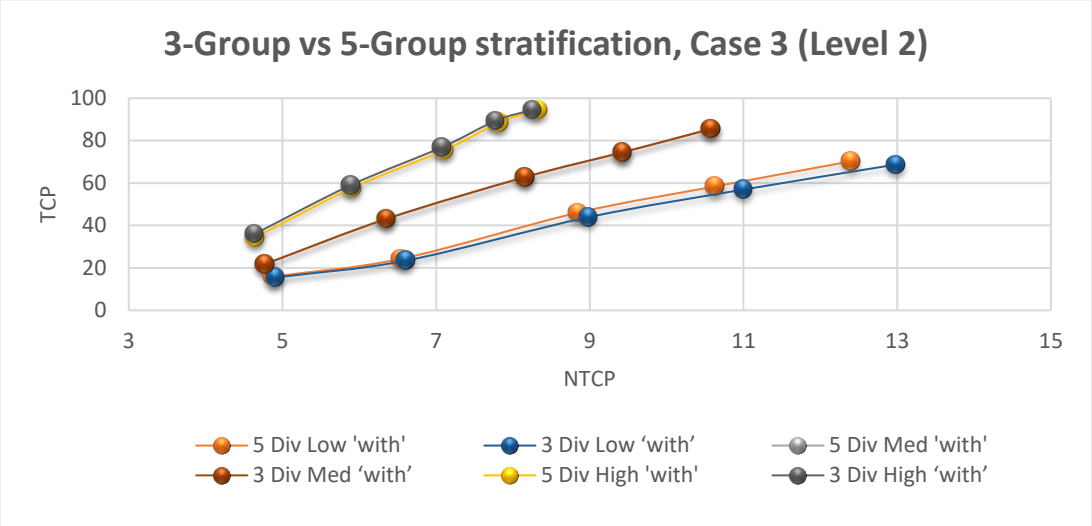

Figure 4-13 The comparison between 3 group (High, Medium "Med", Low radiosensitivity) versus 5 group (Very High "Vhigh", High, Medium "Med", Low, Very Low "Vlow" radiosensitivity) stratification for lung patient cohorts after level 2 optimization.

The high radiosensitivity group shows the same trend but the improvement in TCP at any given NTCP is very small (~1%). The medium radiosensitivity group does not show any improvement.

Another important finding reported here is that radiosensitivity stratification would notably affect extremely radio-resistant patients, who could be considered for palliative treatment / alternative treatment. On the other hand, highly radiosensitive patients might be prescribed a less 'aggressive' treatment (i.e. individualized treatment in terms of total dose and or a number of fractions) to achieve a cure. It is arguable that the above results depend on the categorization of patients solely based on a statistically chosen range of radiosensitivity that is not validated clinically. However, such stratification tests if they were available could aid in categorising patients who could be considered for a different treatment pathway (possibly a clinical trial/research regimen) after gathering further clinical evidence (further tests that help ascertain if the patient may benefit from alternative treatment).

4.3.2 Prostate Cohort Results

In this section, the results of applying level 0, 1 and 2 optimizations to prostate patient datasets are presented considering a tumour α/β=1.5 Gy and 5% Iso-toxic NTCP limit. Also, TCP was calculated with parameters labelled "prostate4" in table 4.1. The 3-subgroup stratification results are shown in table 4-6 and 5-subgroup stratification based results in table 4-7. Looking at Level 0 (case 2 vs case 3) in table 4-6 for the standard prescription (60Gy20#), TCP-NTCP calculations show that TCP is severely underestimated for the radiosensitive subgroup patients (high) and severely overestimated for the radio-resistant (low) subgroup patients if the radiosensitivity based stratification is unavailable or is not used in the TCP calculations. The 5-subgroup tumour radiosensitivity stratification shown in table 4-7 shows similar results.

Table 4-6 Radiosensitivity (3 group) based Radiotherapy Individualization 5% Iso-toxicity- Prostate Tumour (α/β=1.5 Gy)

No	1	2	3	4	5	6	7	8	9	10	11	12
1		TCP	NTCP	TCP	NTCP	TCP	NTCP	TCP	NTCP	No of Fractions	Case 1 TCP	Case 1 NTCP
2	Level 0 Case2	62.5	1.6	62.5	1.6	62.5	1.6	62.5	1.6	20		
3	Group	Low		Med		High		All (weighted average)			No stratification Optimization Case 1	
4	Level 0 Case3	0.0	1.6	68.0	1.6	95.0	1.6	61.5	1.6	20		
5	Level 1 Case2	0.0	5.0	80.1	5.0	95.0	5.0	69.8	5.0	20	70.8	5.0
6	Level 1 Case3	0.0	5.0	80.1	5.0	95.0	0.01	69.8	4.2	20		
7	Level 2 Case2	0.5	5.0	90.7	5.0	95.0	5.0	77.1	5.0	5	78.1	5.0
8	Level 2 Case3	0.5	2.5	90.5	4.8	95.0	0.0	76.9	3.7	[3 5 5]		

Comparing Level 1 optimization result shown in case 3 [Table 4-6, Box (8,6) (9,6)] scenario, the weighted average TCP & NTCP of the entire population is marginally better (same TCP at a lower NTCP) than for the case 2 scenario [Box (8,5) (9,5)]. The case 3 weighted average TCP is similar to that of the case 2 weighted average TCP

but is achieved at a lower average NTCP (in case 3). The result for the level 2 optimization comparison between the case-2 and case-3 weighted average results is similar. The lowering of NTCP occurs as the TCP hits the 95% cap (explained previously) and thus the optimizer module of the program tries to reduce the NTCP in order to keep the TCP at 95%. The % dropout of patients in each of the subgroup remains the same and knowledge of tumour radiosensitivity before or after the treatment seems to confer no significant benefit except for the high and very high radiosensitivity subgroups.

Table 4-7 Radiosensitivity (5 group) based Radiotherapy Individualization 5% Isotoxicity- Prostate Tumour (α/β=150 cGy)																
No	1	2	3	4	5	6	7	8	9	10	11	12	13	14	15	16
1		TCP	NTCP	TCP	NTCP	TCP	NTCP	TCP	NTCP	TCP	NTCP	TCP	NTCP	No of Fraction	Case 1 TCP	Case 1 NTCP
2	Level 0 Case 2	62.5	1.6	62.5	1.6	62.5	1.6	62.5	1.6	62.5	1.6	62.3	1.6	20.0		
3	Group	VLow		Low		Med		High		Vhigh		All (weighted average)		No Stratification Optimization		
4	Level 0 Case 3	0.0	1.6	0.0	1.6	68.0	1.6	95.0	1.6	95.0	1.6	61.4	1.6	20.0		
5	Level 1 Case 2	0.0	5.0	0.0	5.0	80.1	5.0	95.0	5.0	95.0	5.0	69.7	5.0	20.0	70.8	5.0
6	Level 1 Case 3	0.0	5.0	0.0	5.0	80.1	5.0	95.0	0.0	95.0	0.0	69.7	4.2	20.0		
7	Level 2 Case 2	0.0	5.0	0.5	5.0	90.7	5.0	95.0	5.0	95.0	5.0	77.0	5.0	5.0	78.1	5.0
8	Level 2 Case 3	0.0	0.0	0.5	2.5	90.5	4.8	95.0	0.0	95.0	0.0	76.8	3.6	[1 3 5 5 5]		

The population-averaged optimization and individualization results of the 5 sub-group classification of patients is given in table 4-7 where level 1 & 2 optimization results were obtained at 5% Iso-toxic limit for rectal bleeding complication for the prostate cohort. The use of 5-subgroup radiosensitivity stratification instead of 3 subgroups does not appear to improve the population TCP at 5% Iso-toxic NTCP [compare table 4-7 box (12,8) to table 4-6 box (8,8)]. The results of performing similar analysis over a range of Iso-toxic limits (1-10% NTCP) are shown next in fig. 4-14 & 4-15 below. There is no significant benefit of level 1 or 2 optimizations with use of radiosensitivity information except for the high radiosensitivity group.

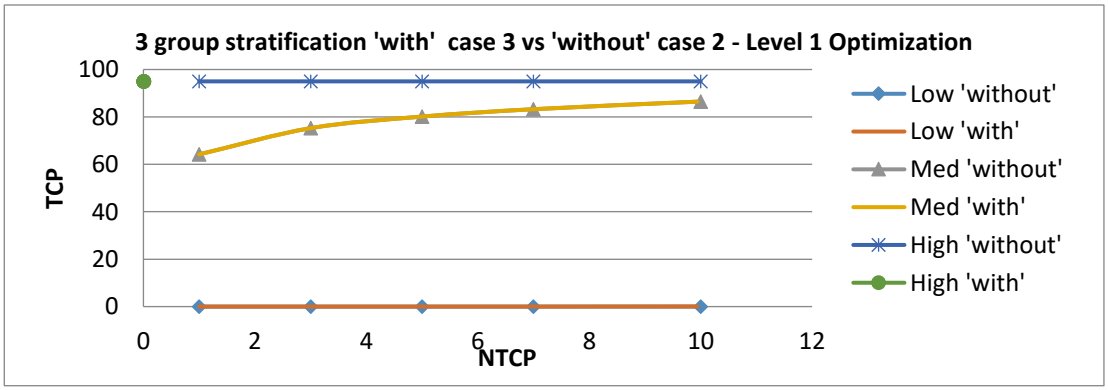

Figure 4-14 TCP-NTCP graph for comparing Level 1 optimization for 'with' and 'without' radiosensitivity information scenarios for various Iso-toxicity limits for 3 radiosensitivity subgroup (High, Medium "Med", Low radiosensitivity) stratification – Prostate Cohort

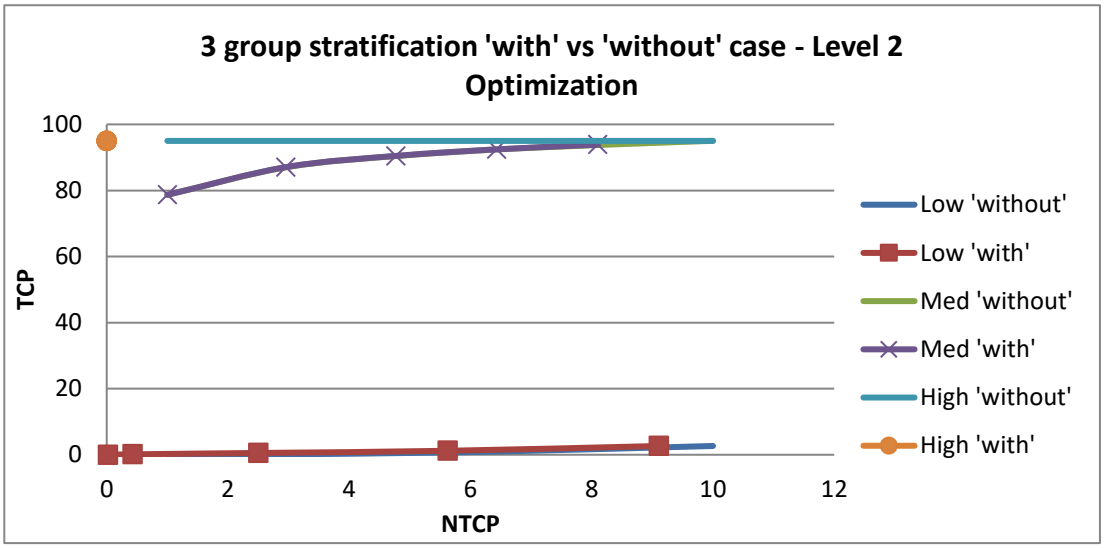

Figure 4-15 TCP-NTCP graph for comparing Level 2 optimization for 'with' and 'without' radiosensitivity information scenarios for various Iso-toxicity limits for 3 radiosensitivity subgroup (High, Medium "Med", Low radiosensitivity) stratification – Prostate Cohort

Looking at Figure 4.14-4.15, it can be seen that the low and high radiosensitivity groups seem to have either very high TCP or very low TCP across the range of Iso-toxic optimization conditions. This suggests that the effect of a change in the value of α has a significant effect on the TCP; however, the difference between the 'with' and 'without' scenarios on level 1 & 2 optimizations over a range of NTCP values is negligible. Nevertheless, as the TCP is affected significantly by a change in α, the patients that are highly radio-resistant or radiosensitive should be evaluated further to be considered for alternative treatment. Only level 2 optimization yields a significant advantage, achieving a high TCP for a low NTCP for the cohort. Although the variation in TCP & NTCP across the subgroups is high, the variation in optimization results between case 2 and case 3 scenarios is very low which invites discussion on possible reasons behind such results (see section 4.4.2).

4.4 Discussion

The aim of this investigation was to assess the potential effect of tumour radiosensitivity based stratification of patients on radiotherapy individualization. Level 1 and level 2 individualizations would yield individual patient-specific prescription doses and fraction numbers that are expected to improve therapeutic gain (in terms of TCP & NTCP) for a given patient. The use of stratification (assessed through a clinically valid method) firstly will aid the clinician in deciding if palliative or curative treatment is preferable for a given patient and level 1 & 2 optimizations on top of that for curative cases will give an indication of the improvement in the tumour control that can be achieved for each patient (by means of increased dose at a set toxicity level). It is emphasized, however, that this exercise utilizes a single OAR (the principal toxicity-governing OAR) per tumour type and has a dependence on the radiobiological models used; absolute predictions from which are susceptible to large uncertainties especially in the case of prostate tumour model predictions. Analysis of a large heterogenous set of patient tumour cells for radiosensitivity quantification through a clinically validated study is warranted to validate the above set of results obtained for this model based retrospective study.

The above optimizations are performed for each patient dataset in the order of scenarios explained in 4.2.2. A population-average (TCP_{pop} & $NTCP_{pop}$) is formed to compare the 'with' case 3 and 'without' case 2 stratification scenarios for each subgroup. The Case 2 calculation allows comparison with the Case 3 calculation thereby enabling an assessment of the benefit to patients of using this radiosensitivity knowledge pre-treatment. This assessment in the form of a prospective vs retrospective comparison at a subgroup level.

The TCP_{pop} & the $NTCP_{pop}$ for a subgroup (with 'n' patients) is formed by averaging the $TCP_{1..n}$ and $NTCP_{1..n}$ obtained for each level of optimization. The average based results give an idea about the overall variation across the cohort, but when considering individual patients, the TCP/NTCP optimization may be different than the trend indicated by the averaged TCP_{pop} and $NTCP_{pop}$. This is because 'mean'/'average' as a metric is statistically susceptible to bias due low sample size

of an experiment and particularly affected by outliers. Although, for the current analysis the "median" metric would not be a representative central tendency assessment statistic as the median fails to account for all the samples when there is a duplication of numbers in a sample. Therefore, the mean of optimized TCP was chosen to assess the population response (i.e. the central tendency).

4.4.1 Discussion: Lung Cohort Result

Results of this analysis as seen in Figure 4-7 & Figure 4-8 for Level 1 &2 optimization for the Lung patient cohort are unexpected [Figure 4-7 TCP 'low' column 'with' subgroup is higher compared to TCP 'low' column 'without' – The expectation was exactly the opposite for the low radiosensitivity subgroup]. The low radiosensitivity group 'with' stratification has a higher population TCP at Iso-toxic 7% NTCP compared to the radiosensitivity corrected 'without' case. This can be attributed to the proportion of highly favourable patients in the dataset and its effect on the $TCP_{population}$. The term 'highly favourable patient' is explained below.

The Iso-toxic escalation of tumour dose is likely to be affected by the location of the tumour in relation to the OARs (with respect to level 1 & 2 optimizations). Further, if the patient is highly 'favourable' (i.e. has a small tumour, tumour is isolated-located away from OARs, high tumour radiosensitivity), a high TCP can be achieved at a lower than standard NTCP limit through level 1 & 2 optimization as all of these factors improve control probability by either allowing improved dose escalation or more efficacious cell kill due to radiation exposure (per the Marsden TCP model based optimization).

Ideally, if a patient is radio-resistant the average TCP of level 1 optimization for 'with' stratification case 3 will be lower than 'without' case 2. The above remains true as far as TCP calculation alone is concerned but not for L1 or L2 optimization (where TCP is a complex function of the Iso-NTCP based dose scaling factor) of individual patient datasets. From the optimization algorithm point of view, if this same patient is very favourable (i.e. let us say; has a very small anatomically isolated tumour) then the optimized prescription dose (level 1) that will achieve a 95% TCP will be very low irrespective of the radiosensitivity subgroup he/she

belongs to. Now if in a radio-resistant cohort of patients, there are many favourable patients then the average TCP of the population is still going to be high. The effect of variance in radiosensitivity is minimal on the TCP as the patient is favourable.

Also, for favourable patients assumed to belong to the low radiosensitivity sub-group, a somewhat higher dose will be required to raise the TCP to the upper-bound limit compared to those in the other radiosensitivity sub-groups. Therefore, the dose-scaling factor (DSF) set by the L1 or L2 optimizer will be higher in this case than for the same patient in any of the other radiosensitivity groups, as a higher DSF will be required to 'hit' the TCP_{cap}. This will not be the situation in the 'standard' optimization (case 1). The DSF used to calculate the case 2 'without' TCP will be lower resulting in a lower TCP as compared to the optimized L1 or L2 case 3 'with' TCP.

Thus, for 'favourable' patients in the low radiosensitivity group, the $TCP_{(\alpha \text{ low range, case } 3)}$ can be higher compared to $TCP_{(case\ 2)}$ as L1 optimization requires a lower dose to reach the upper bound TCP limit. A few extremely favourable patients can drive the population $TCP_{(\alpha \text{ low range})}$ higher for the low radiosensitivity group compared to the population $TCP_{(radiosensitivity\ corrected)}$ group. Please refer section 4.2.3 for details of the cases [1-3] referred above.

Also, the TCP_{pop} of the low subgroup (table 4-4, Box (2,6) & Box (2,8)) are lower than 'standard' case 1 L1 & L2 optimization results (table 4-4 Box (11,5) & Box (11,7)); which is as expected. The improvement in TCP_{pop} observed in the low radiosensitivity group for case 3 (L1 & L2 optimization) compared to case 2 (L1 & L2 optimization) is most likely to be a result of a bias created in the TCP_{pop} due to TCP saturation (i.e. TCP=95%) for highly favourable patient datasets. If the cohort has many favourable patients and is also highly radio-sensitive on the average, a high population TCP will be achieved at a reduced NTCP (i.e. reduced total dose). This is because the optimizer module is programmed to reduce the NTCP if at a given dose scaling factor the optimizer achieves 95% TCP.

Another important aspect that adds to uncertainty in the observed results is the prediction accuracy of the models used. Although the parameters used for the Marsden Model and L-K-B NTCP model are derived from clinical outcomes, the parameters used are fits to data and thus add to the uncertainty of absolute calculations (addressed in section 3.4.3 of Chapter 3). However, the current analysis uses model predictions to form a relative comparison between 'with' and 'without' clinical scenarios and thus as long as model parameters used currently are not changed significantly (unlike prostate tumour α/β changing from 10 Gy to 1.5 Gy) the results will be acceptable (with low precision but not misleading). It is important to note that these results are based on limited amount of retrospective datasets and need to be further validated to make them truly comparable to what is observed in clinical practice.

In summary, it was shown that radiosensitivity information makes the most impact for patients at the extreme ends of the radiosensitivity normal distribution. Possessing patient specific radiosensitivity information can have significant implications in treatment optimization as the number of fractions that yield the best TCP at fixed NTCP level exhibits a large variation when one goes from the most radio-resistant to the most radiosensitive group in both the 3- and 5-subgroup stratification analysis (especially for lung patients). This is also demonstrated in table 4.5 row 8a where the percentage of patients with 15 as optimum fraction number varies considerably for different subgroups. The point made here is that having access to patient-specific radiosensitivity information for individualization and optimization of treatments could have a notable effect on the treatment selection and resource management - this is demonstrated for the lung cohort in table 4-4 & table 4-5 by comparing the percentage patient dropout and optimum fractions for patients in case 2 and case 3 (level 2 optimization). It is also important to note that the interpretation of the above results for the highly radiosensitive group lies on the chosen value of TCP_{cap} variable and for the radio-resistant group lies on the chosen $TCP_{threshold}$ value which for the purpose of this analysis is based on mathematical/statistical considerations.

4.4.2 Discussion: Prostate Cohort Results

The Level 0 calculation of TCP for the prostate patient datasets (table 4-6) showed that radiosensitivity of the patients when divided into sub groups, notably affects TCP calculations and optimization results; except for the medium radiosensitivity group. However, it was also observed that availability of information pre- or post-treatment was not very effective in improving the optimization results (comparing level 1 case 2 versus level 1 case 3, table 4-6). The purpose of comparing case 1 and case 2 analysis was to retrospectively assess the improvement on the TCP that could have been attained in the optimization (using radiosensitivity information), which was not the case for the prostate cohort. The limited gain observed was for the high or very high radiosensitivity group of cohorts where TCP=95% was achieved at a relatively lower NTCP for case 3 scenario. Investigating case 1 and case 2 NTCP values of all the patients it was found that the average NTCP across the cohort was 1.4% and average TCP was 62.4% without any optimization for the 60 Gy in 20 fraction regimen (prostate tumour α/β=1.5 Gy).

Further, the prostate tumour TCP parameters employed were α/β=1.5 Gy, α=0.155 and σ_α=0.058 which suggests that the possible change in the value of α is almost a third of the mean value. This is likely to affect TCP calculations significantly as one moves from a low radiosensitivity (resulting in almost zero TCP at Iso-NTCP limit - table 4-6 [Box (2,6), Box (3,6) | Box (2,8), Box (3,8)] sub group cohort to a high radiosensitivity sub cohort (resulting in 95% TCP at really low NTCP table 4-6 [Box(6,6) -Box(7,6)]. Further, for level 2 optimization (optimization of the number of fractions) it is observed that a low prostate tumour α/β=1.5 Gy leads to higher TCP at lower numbers of fraction [table 4-6 Box (6,8), Box (7,8)].

Thus, due to the large effect of σ_α on TCP calculation the optimizer finds a solution of achieving 95% TCP_{pop} at 5 fractions for <1% $NTCP_{pop}$ for the highly radiosensitive group which seems unrealistic especially considering the fact that variation in normal tissue radiosensitivity is not accounted for in the current analysis. The algorithm is heavily reliant on the response of two separate models and uncertainties in prediction by these models affect the results of the optimizer which

can result in false positives/negatives. Refitting of both TCP and NTCP parameters over larger datasets is likely to yield more accurate model predictions reducing uncertainty in the results of the optimization algorithm. Another factor possibly contributing to such results for the prostate cohort is the lack of use of multiple OAR based optimization.

4.5 Summary and Conclusions

In this chapter, the availability of patient-specific tumour radiosensitivity information has been assumed and its effect analysed in a hypothetical clinical scenario. The cohort was divided into 3 and 5 radiosensitivity subgroups and the TCP & NTCP 'with' and 'without' radiosensitivity information for each subgroup was calculated. Further, level 1 and level 2 individualization & optimization of the treatment DVH datasets was carried out and the effect of having patient specific radiosensitivity information on optimized TCP and NTCP was analysed. For the lung cohort dataset, at 7% Iso-toxic NTCP, individualization of treatment would result in an average TCP increase of 17% (but with a very high dropout rate 44%) for the low tumour radiosensitivity subgroup but only 2% for the highly radiosensitive tumour cohort (with a 12% absolute reduction in dropout rate) when comparing clinical scenarios of case 3 'with' to case 2 'without' (using level 2 optimization). Dropout rate as discussed previously is directly affected by the choice of a threshold value of TCP (categorising a patient to not qualify for a given treatment strategy) and indirectly affected by the specified dose limiting Iso-NTCP. A higher threshold value of TCP will increase the dropout rate (as fewer patients will cross the TCP threshold) and setting a higher Iso-NTCP value will reduce the dropout rate (as more patients will be able to achieve the threshold TCP). Stratification of patients into 5 radiosensitivity subgroups, as opposed to 3, results in slightly improved (1-2%) individualized level 2 TCP for lung tumour treatment but not for prostate.

HYPRO/CHHiP trials quote a relatively high control probability (nearly 90% average tumour control with 9-10% average grade 2 GI toxicity – Dearnaley & Hall, 2017) without the use of stratification and it is likely that in the distant future dose escalation may reach a plateau. Robustness of the results especially for the prostate

tumour dataset is likely to increase with use of model parameters ascertained based on the latest clinical outcome data.

Further work would include assessing the effect of patient-specific normal-tissue radiosensitivity variation on treatment individualization. Having patient-specific information on OAR radiosensitivity is likely to improve the current NTCP estimates and this would certainly affect (Iso-NTCP) individualization and optimization of radiotherapy treatments.

As a part of the future work for this research chapter, the following updates and development to the software are planned to be undertaken.

- Output results of this program to RadOpt software GUI interface allowing users to interact with the graphs in an improved manner forming a better user interface.
- Program 'handles' in the code that allow interaction with other software systems like treatment planning systems.
- I would also like to accommodate TCP and NTCP models implementing proton radiobiology in the current program and assess the effects of optimization on patients' TCP and NTCP for proton treatment datasets.

Another line of thought is exploring the relationship of OAR radiosensitivity to tumour radiosensitivity. How would a relation between OAR radiosensitivity and tumour radiosensitivity affect Iso-toxic treatment optimization and what would be the benefit of having this information? Also, accounting for other dose-limiting OARs whilst performing "level 1 & 2 optimizations" is recommended as that may improve the robustness of optimization results, as shown in the results of chapter 3.

Chapter 5 Radiobiological Inverse-Planned Treatment Individualization and Optimization

5.1 Introduction

Current treatment planning best practice involves the use of dose-volume based criteria. Dose deposition in the target volume is generally aimed to be uniform accounting for the microscopic spread, geometric setup errors and motion artifacts. At the same time, sparing of OAR from radiation dose is emphasized. A clinically acceptable plan requires the prescription dose to be deposited in the tumour whilst not exceeding the OAR's dose tolerance limit. The prescription dose (the total dose to be delivered in a fixed number of fractions) for a given type of tumour (non-small-cell lung and prostate here) is continually evolving as clinical outcomes evolve.

Radiobiological models are occasionally used to retrospectively assess treatment plans. Radiobiological modelling applied to radiotherapy data allows assessment of a treatment plan or aids comparison of two or more competing plans accounting for the behaviour of tumour/OAR in response to radiation exposure. The use of radiobiological models in the treatment planning process was advocated in AAPM report 166. Also, ICRU report 83 recommended that NTCP be reported in research studies (AAPM Task Group 166, 2012; ICRU, 2010).

5.1.1 Treatment planning

Treatment planning is performed with the active participation of a planner who defines the beam characteristics and the beam direction using a CT scan of the patient to conform a high dose of radiation to a specific target volume. In 'forward treatment planning', the planner has absolute control of the system and decides on all the parameters of the geometric plan; the calculation of the total planned dose is then performed by the software. '3D-CRT' treatment plans are usually forward planned.

The introduction of IMRT and VMAT technologies has enabled treatment planners to better spare the normal tissues for a given target dose (De La Fuente Herman *et*

al., 2010; Deb & Fielding, 2009). The complexity of treatment planning has increased with the advent of IMRT/VMAT that allow better OAR sparing and thus forward planning is becoming less feasible. Further, automation in treatment planning (Inverse treatment planning) provided by current treatment planning systems (TPS) allows the development of complex plans in a relatively short time. In inverse treatment planning, the planner starts by loading the TPS system with a 3D-CT image dataset. The OARs and target volumes containing the tumour are then 'contoured' on the CT 'slices' as per the protocol followed at the centre using the TPS. Further, the planner inputs a list of *objectives* to be maximized and *constraints* not to be violated in relation to the target volume in the TPS. Inverse treatment planning is now undertaken which is an iterative process whereby the planning system, using an optimization algorithm, searches for the optimal solution to achieve set objectives and satisfy constraints.

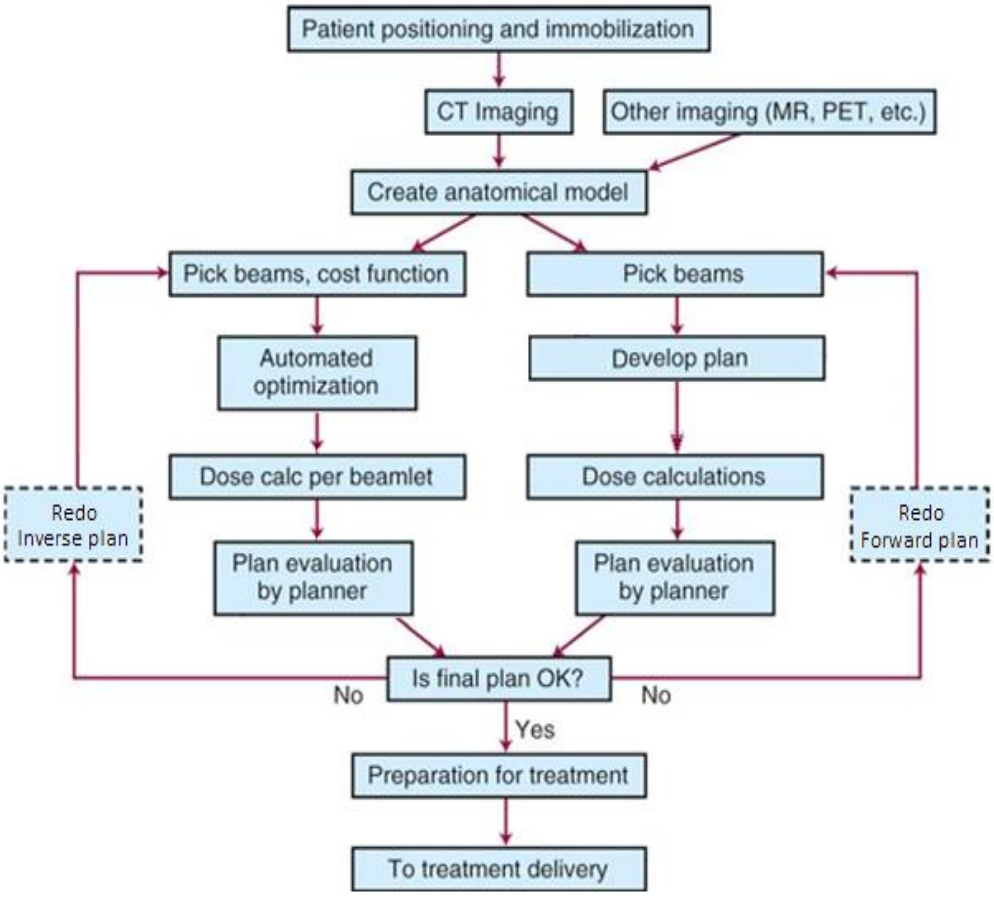

Figure 5-1 Flowchart showing the forward and inverse treatment planning processes.

Once the planner inputs the patient dataset, beam information (e.g. beam energy and beam angles) and the plan criteria, the inverse planning algorithm searches for the optimal solution, i.e. the treatment plan yielding a dose distribution with optimal objective value and satisfied constraints. The diagram in Figure 5-1 indicates how forward and inverse treatment planning approaches work.

The iterative inverse treatment planning algorithm aims to minimize the difference between the target dose distribution and the achievable dose distribution in terms of improving the objectives as much as possible while satisfying the constraints. The difference between the desired dose and the dose at each iteration is a score used to drive the optimization.

$$\boldsymbol{Cost\ function = f(D_d - D_i)} \qquad \textbf{Eqn. 5-1}$$

Where Dose D = $\sum C_{i,j} * W_j$ for j=1-n with D_d= $Dose_{Desired}$, D_i=$Dose_{iteration}$;
W_j is the weight of bixel *j*
C_{ij} determines the dose contribution of bixel *j* to voxel *i*

This score assigned to every plan used for comparison is also known as a cost function calculated as shown in equation 5-1 (Webb, 2003). The algorithm adjusts the beam characteristics, e.g. the MU and the leaf positions of each control point (or segment) from which the bixel weights are computed in every iteration to reduce the cost function to its minimum value. As per communication with Raysearch Labs, the RayStation system algorithm optimizes segment MU (aka segment weights) and leaf positions, from which the fluence map (bixel weights) are computed, from which the dose distribution is computed. Different objectives and constraints can be given different weighting and sophisticated optimization algorithms can be built to improve the solutions; minimizing the time a system takes to converge to an optimal solution (Bokrantz, 2013). The idea of using biologically based functions to optimize treatment plans was initially presented by Wu *et al.* (2002). The first implementation of radiobiologically based planning was in the Monaco treatment planning system which made use of the EUD function to optimize treatment plans (Alber et al., 1999; Pyshniak et al., 2014; Semenenko et al., 2008). Since then, RayStation and the Pinnacle *research* planning systems have developed alternatives which allow scripting of custom functions or use of the TCP

and NTCP models as objectives or constraints (Uzan *et al.*, 2016). Further, the research version of RayStation TPS (RaySearch Laboratories®) used in this work was customised with the Marsden model-based TCP cost function. In the next section, the RayStation treatment planning system is introduced.

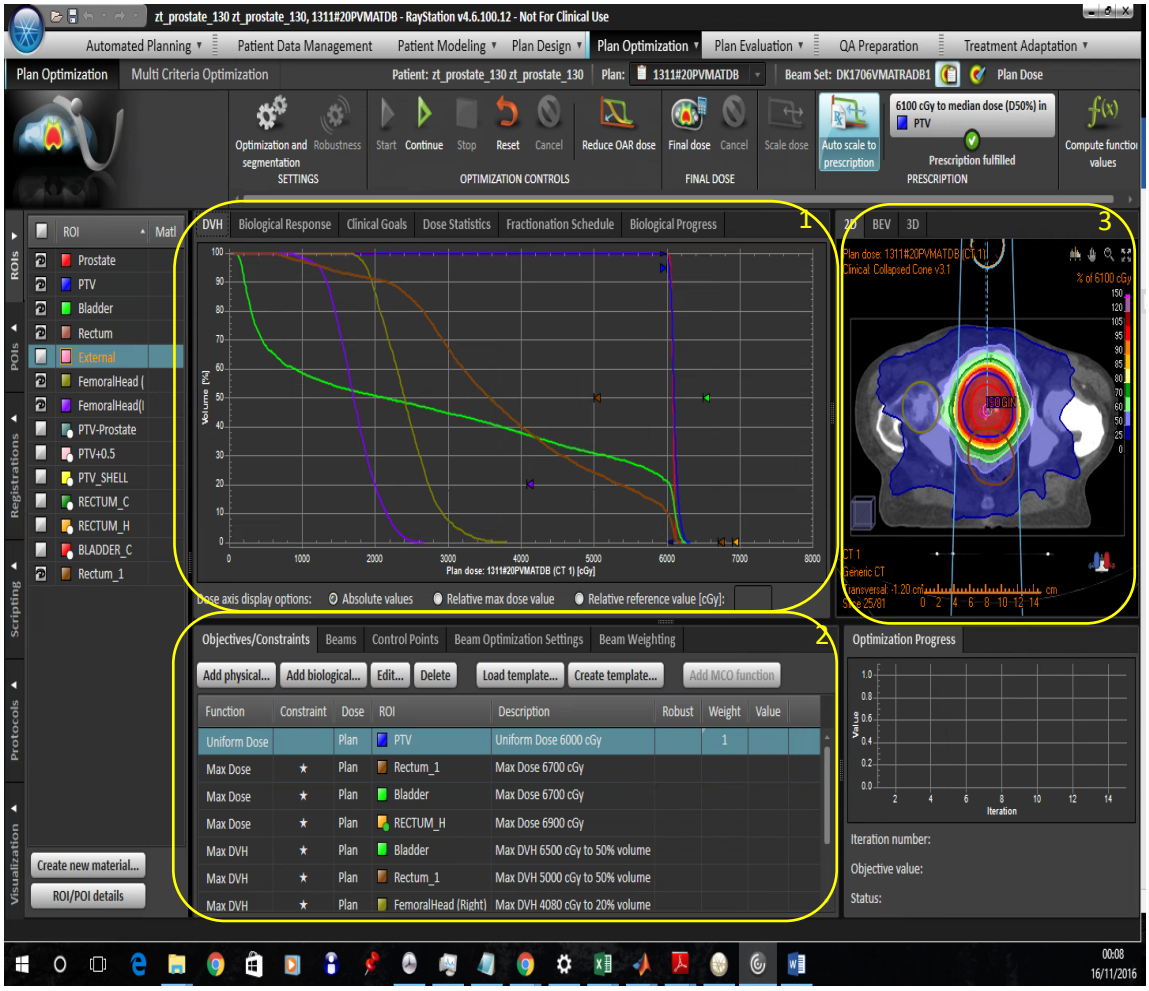

Figure 5-2 RaySearch Laboratories' Raystation Treatment planning system user-interface

5.1.2 The RaySearch Treatment Planning System

RaySearch Laboratories, Sweden provided a 'research' version of their treatment planning software RayStation to pursue the research described in this chapter. The workflow of the planning system is of tab-based navigation format and the interface is very user friendly. The system allows import of data in the DICOM format from multiple radiotherapy and imaging archival systems. The most important tabs of the system for this study are shown and described in the sections below.

5.1.2.1 Patient Data Management

This module of the user interface enables the user to import/export patient CT datasets and generate plan reports. Further, it enables editing of patient identification data if necessary.

5.1.2.2 Patient Modelling

This 'tab' allows the user to create and modify structures on the CT dataset. The software has tools that enable addition and subtraction of structures to form new structures (i.e. lung-GTV). Also, there are features for manual and automatic contouring, 3D editing, region-of-interest statistics and many others.

5.1.2.3 Plan design

This 'tab' enables the user to create a treatment plan for a given patient. The system requires the user to input plan identification information, prescription information, radiotherapy treatment technique and clinical delivery system model specification (e.g. Elekta Synergy 10 MV Photon Beam). The beam specification (Gantry rotation, Energy, Iso-centre) is also fed to the system in this tab. This is necessary information to initiate the treatment planning process. There are options to add, copy and edit available treatment plans as well.

5.1.2.4 Plan Optimization

The plan optimization tab of the user interface is divided into three sections. On the top are the plan evaluation tools, at the bottom is the optimization criteria specification section and, on the right, is the 3D CT based plan visualization tool. This is highlighted in Figure 5-2 with yellow boxes marked 1, 2 and 3.

5.1.2.5 Optimization section

This section has multiple tabs that allow the user to input optimization objectives and constraints, beam weighting and beam optimization settings for the inverse planning algorithm. The objective/constraints section is mostly used in this work. The planning criteria listed in tables 5.1 and 5.2 are input in this section. The objectives can be either physical-dose based or radiobiological-model based. The constraints can however be any combination of physical and radio-biological metrics. There is also an interlinked-library (separate module to the treatment

planning system) of radiobiological models pertaining to specific OARs and tumours. They also provide a reference to find a given publication where the model was originally cited and allow customization of organ-specific parameters as required by the user. For this analysis, LKB NTCP and Marsden TCP models have been used. The parameters used for the models are the same as those used in chapters 3 & 4 (See table 3.1 and table 3.2 in Chapter 3 for details).

5.1.3 Goals

The aim of this chapter is to use radiobiological models to create inverse radiotherapy treatment plans and compare them to standard dose-volume (objective/constraint) based plans.

For each radiotherapy patient dataset, a standard inverse treatment plan [DB-plan] is initially formed (Plan 1- clinically acceptable in terms of standard dose-based objectives & constraints) using dose-based metrics as cost functions (uniformity of dose, total dose, minimum dose, maximum dose). Next, a plan is created on the same patient with the same fractionation schedule using radiobiological constraints and objectives (RB-Plan). These two plans are ranked using TCP & NTCP models and the DVH based metrics used clinically. The DVHs are also used to compare plans. The question to be answered is "Between the DB-plan and the RB-plan which is better therapeutically?"

A secondary aspect to this chapter was to question the current clinical norm of "uniform target dose". "Uniform dose to target (PTV)" is a standard dose-volume based objective used in clinical treatment planning; it regulates dose variation across the target structure (ICRU report 50 requires the dose in the target to be between the range defined by -5% to +7% of the prescription). The introduction of VMAT & IMRT and the improvement in treatment delivery technology (IGRT, OAR Motion tracking/gating) has resulted in better sparing of normal tissues for a given tumour dose. In line with the above considerations, extra DB- plans were created after removing the uniformity in PTV requirement to assess the effect of this objective in relation to finding an optimal plan for a patient (for both lung and prostate patient datasets).

Our DVH based retrospective optimization of Lung Patient data in Chapter 3 suggests that 15 fractions was the optimal number of fractions for NSCLC patients (based on retrospective level 2 optimization of DVH datasets).Thus, as a tertiary aim, a second set of plans at 15 fractions were created for the lung patient datasets to evaluate if radiobiology based individualized hypo-fractionation at 15 fractions resulted in therapeutically better or worse lung treatment plans. The radiobiological metrics TCP and NTCP of the generated plans are used to compare the plans along with dose-based metrics & DVHs of the OARs.

5.2 Methodology

5.2.1 RayStation System Quality Assurance

Initially, the radiobiological model calculations of RayStation were checked against those of 'Biosuite' (C++ based) and 'RadOpt' (MATLAB based), both independent radiobiological modelling software developed at Clatterbridge Cancer Center. Two plans were created; one each for a lung and a prostate patient CT dataset and TCP was calculated for the 'PTV' & 'GTV' structures and NTCP for the 'total lung' or 'rectum' structures using RayStation, Biosuite & RadOpt software. The calculations were checked for different fractionation schedules to ascertain if repopulation in tumours was accounted for by RayStation in the same way as in BioSuite and RadOpt (& vice versa). This relative TCP calculation check over independent systems ensured the consistency of application of the Marsden TCP & LKB NTCP models across all systems.

5.2.2 Inverse Treatment Planning Methodology

The current analysis was performed on 4 anonymised patient datasets (radiotherapy treatment plans with structures) with all the structures delineated by a clinician. There are two lung cancer and two prostate cancer patient datasets. The objectives and constraints to be used in forming the treatment plans have been established with the help of current planning recommendations in the literature and from current/past protocols used at Clatterbridge Cancer centre (ISTART & CHHiP Protocols).

For the purpose of this chapter, the following abbreviations for structure names in the plans, figures and tables apply/appear.

- Total – Healthy Lung / Lung-GTV
- BPlexus – Brachial Plexus
- CordPRV – Spinal Cord
- Rectum1 – Rectum
- Rectum_H – Rectum overlapping Tumour

For each of the patients, 3 plans have been created using the VMAT technique (full rotation single arc) (Bhide & Nutting, 2010; Haslett *et al.*, 2016, 2014). The criteria for ranking the plans is based on the (ICRU, 2010) report 83 parameters of homogeneity index, TCP and NTCP of the target volume and the OARs respectively along with dose volume parameters like $V_{20\,Gy}$ for healthy lung, $V_{50\,Gy}$ for rectum, & D_{max} for the spinal cord. Qualitative comparison of the plans is performed by assessing DVH data and the dose distributions overlaid on the CT scan 'slice' of the patient at the iso-centre.

The RayStation treatment planning system (described in section 5.1.2) has been used to create all the treatment plans. All the plans require an external ROI (Region-of-Interest) encompassing the patient body surface to be delineated; this ROI defines the area of dose deposition and includes the selection of a dose-specification point (set as the centre of GTV in this work for all the plans). The plans were made with the beam specification of the Elekta Synergy® 6 MV (Lung Treatment Plans) and 10 MV (Prostate Treatment Plans) radiotherapy unit - this was selected from a list of available options in the RayStation System. The TCP, NTCP, homogeneity index and dose-volume based metrics (for OARs) are reported for all plans. For this analysis, LKB NTCP and Marsden TCP models have been used. The parameters used for the models are the same as those used in chapters 3 & 4 (See Table 3.1 and 3.2 in Chapter 3 for details).

5.2.2.1 Lung Cancer Treatment Plans

The analysis is divided into two phases for each lung patient dataset. Phase 1 (plan 1 & 2) compares a dosimetric constraint/objective based inverse treatment plan

(DB-plan) to a radiobiological constraint/objective based inverse treatment plan (RB-plan) for a conventional fractionation schedule (20 fractions for lung tumours). Phase 2 (plan 3) makes the same comparison but the plans are generated with 15 fractions and only for the lung patient CT datasets. Plan 4 (55Gy 20#) is an additional DB-plan created to assess the effect of removing 'uniformity' requirement of a plan. Plans 1-4 are explained in detail below. The structures were delineated by a clinician and thus the naming convention was left unaltered.

The aim of this exercise is to generate an isotoxic RB-plan and rank it against a conventional DB-plan.

- **Plan 1**

The first plan has been made using only DV constraints for a 20-fraction schedule. The objectives & constraints for the NSCLC treatment plan are given in Table 5-1. The tumour is delineated as the GTV and PTV. The objective of the planning exercise is to create a plan imparting a quasi-uniform 55 Gy dose to the tumour (PTV). If objectives and constraints are in conflict, the optimizer always prioritizes the constraints since they are not allowed to be violated for an optimal solution. A dose-scaling function is available and was used to ensure the DB-plans were within 95% to 107% of the prescription dose (for the DB-plan). The OARs are healthy lung, oesophagus, heart, spinal cord and the brachial plexus that could receive maximum dose / maximum V_{xx} as per the clinical OAR dose limits shown below.

Function	Constraint	Dose	ROI	Description
Uniform Dose		Plan	PTV	Uniform Dose 5500 cGy
Max DVH	★	Plan	Heart	Max DVH 5700 cGy to 33% volume
Max Dose	★	Plan	CordPRV	Max Dose 4800 cGy
Max DVH	★	Plan	total	Max DVH 2000 cGy to 30% volume
Max Dose	★	Plan	Oesophagus	Max Dose 5800 cGy
Max DVH	★	Plan	BPlexus	Max DVH 5500 cGy to 1% volume
Min DVH	★	Plan	PTV	Min DVH 5500 cGy to 95% volume

Table 5-1 The objectives & constraints for the NSCLC treatment DB-plan

- **Plan 2**

The second plan is an isotoxic inverse plan formed using radiobiological model-based objectives and constraints (where possible) for the same patient's CT dataset for a 20-fraction schedule. The objective is to maximize TCP over the PTV with NTCP of healthy lung & oesophagus not exceeding that of plan 1 (i.e. isotoxic to DB-plan). Further, none of the OARs should exceed the clinically recommended OAR tolerance doses. The constraints are shown in Table 5-2. The constraints are marked with an "asterisk" in the constraint column and the rows without an asterisk indicate objectives.

Function	Constraint	Dose	ROI	Description
TCP COMP				
TCP Marsden, Repopulation		Plan	PTV	TCP Marsden: NSC Lung, MarsdenDefault, Whole, User defined
Max DVH	★	Plan	Heart	Max DVH 5700 cGy to 33% volume
Max Dose	★	Plan	CordPRV	Max Dose 2200 cGy
Max Dose	★	Plan	Oesophagus	Max Dose 5800 cGy
Max DVH	★	Plan	BPlexus	Max DVH 5500 cGy to 1% volume
Max Dose	★	Plan	External	Max Dose 8500 cGy
NTCP LKB	★	Plan	Oesophagus	NTCP LKB < 0.01: Esophagus, Esophagitis, grade >= 2 , From the
NTCP LKB	★	Plan	total	NTCP LKB < 0.03: Lung_LKB_CCC, Pneumonitis (1), Grade >= 2, ,

Table 5-2 The objectives & constraints for the lung treatment RB-plan

- **Plan 3**

Plan 3 is similar to Plan 2 in terms of planning objectives/constraints but is developed for a 15-fraction schedule. The NTCP constraints for the OARs from a 15 fraction DB-plan (adjusted for fractionation for each OAR using the EQD_2 correction) were used as radiobiological constraints for the same OARs in Plan 3. The formation of plan 3 is undertaken only for the lung patient datasets.

- **Plan 4**

Plan 4 is similar to the DB-plan created for each patient but the uniformity objective is replaced with a minimum D_{95}>=prescription dose and a Dmax=107*prescription dose. This is referred to as DB-plan$_{(non\text{-}uniform)}$. This is undertaken to assess the effect of a 'uniformity' objective on the optimizer's ability to find an optimal plan for the patient.

5.2.2.2 *Prostate Cancer Treatment Plan*

➢ **Plan 1 & 2**

For prostate patient datasets, 3 plans for each patient were created to compare standard dose-volume-based treatment planning to a radiobiological model-based approach. The reference prescription for the dose-based plans was 60 Gy in 20 fractions. The list of objectives used for creating the DB-plans is given in Table 5-3.

Function	Constraint	Dose	ROI	Description	Robust	Weight
Physical Composite Objective						
Min DVH		Plan	PTV	Min DVH 6000 cGy to 95% volume		1
Uniform Dose		Plan	PTV	Uniform Dose 6000 cGy		0.6
Max DVH	★	Plan	Bladder	Max DVH 4000 cGy to 50% volume		
Max DVH	★	Plan	Rectum_1	Max DVH 4000 cGy to 60% volume		
Max DVH	★	Plan	FemoralHead (Right)	Max DVH 4000 cGy to 50% volume		
Max DVH	★	Plan	FemoralHead(Left)	Max DVH 4000 cGy to 50% volume		
Max DVH	★	Plan	Rectum_1	Max DVH 6000 cGy to 3% volume		
Max DVH	★	Plan	Bladder	Max DVH 6000 cGy to 5% volume		
Max DVH	★	Plan	RECTUM_H	Max DVH 5900 cGy to 50% volume		

Table 5-3 The objectives & constraints for the prostate treatment DB-plan

The objective functions used to make the RB-plans are given in Table 5-4. The uniform dose to PTV objective function (of the DB-plans) is replaced by maximizing the TCP (using PTV structure) for the RB-plan. The use of Min DVH D_{95}>=60 Gy is to make the system search for a clinically acceptable plan or converge on a close to clinically acceptable plan, i.e. the optimizer is pushed to achieve a minimum dose in the PTV. The physical dose to the rectum is replaced by the NTCP of the rectum in terms of rectal bleeding NTCP and faecal incontinence NTCP for the RB-plans. The NTCP limits for both of these complications are derived from the NTCP analysis of the DB-plan structures' DVHs. The clinical goals used for assessing a prostate treatment plan for validity are given in Table 5-5

Function	Constraint	Dose	ROI	Description
TCP COMP				
TCP Marsden		Plan	PTV	TCP Marsden: Prostate, MarsdenDefault, Whole, User defined
Max DVH	★	Plan	Bladder	Max DVH 6000 cGy to 5% volume
Max DVH	★	Plan	Bladder	Max DVH 4000 cGy to 50% volume
Max DVH	★	Plan	FemoralHead (Right)	Max DVH 4000 cGy to 50% volume
Max DVH	★	Plan	FemoralHead(Left)	Max DVH 4000 cGy to 50% volume
Min DVH	★	Plan	PTV	Min DVH 6000 cGy to 95% volume
NTCP LKB	★	Plan	Rectum	NTCP LKB < 0.04: Rectum, Feacal Incontinence, grade >= 2, The rectum (solid
Max DVH	★	Plan	Rectum	Max DVH 6000 cGy to 3% volume
NTCP LKB	★	Plan	Rectum	NTCP LKB < 0.05: Rectum, Late rectal bleeding, grade >= 2, The rectum (solid

Table 5-4 The objectives & constraints for the prostate treatment RB-plan

➢ **Plan 3**

For prostate treatment datasets, an extra dose-based plan was also formed without the uniformity objective but achieving a "D_{95}>=Prescription dose" objective. Other applicable constraints and objectives were similar to those used for plan 1. As mentioned earlier, this was undertaken to assess the effect of "uniformity" on the planning system's ability to form an optimal treatment plan.

5.2.3 Plan Ranking and Analysis

Qualitative and quantitative methods were employed to rank plans that were generated by the dosimetric parameter and radiobiological parameter approach. The plans were compared qualitatively by assessing the plan colour wash in transverse, sagittal and coronal planes of the patients' CT scans. The DVHs were also examined & compared and finally the radiobiological (TCP, NTCP) and dosimetric parameters (V_{xx}, D_{yy}) for each OAR and PTV were compared. The prescription dose for the purpose of assessment and comparison of plans was defined as the average dose in the PTV.

ROI/POI	Clinical goal	Value	Result
Bladder	At most 10.00 % volume at 6000 cGy dose	5.25 %	✓
Bladder	At most 50.00 % volume at 4080 cGy dose	22.59 %	✓
FemoralHead (Right)	At most 20.00 % volume at 4080 cGy dose	0.91 %	✓
FemoralHead(Left)	At most 20.00 % volume at 4080 cGy dose	1.31 %	✓
PTV	At least 0.70 TCP Marsden, Prostate, MarsdenDefault, Whol	0.73	✓
PTV	At least 95.00 % volume at 6000 cGy dose	96.15 %	✓
PTV	At least 6000 cGy dose at 95.00 % volume	6043 cGy	✓
PTV	At least a homogeneity index of 0.50 at 100.00 % volume	0.71	✓
Rectum	At most 5.00 % volume at 6000 cGy dose	4.37 %	✓
Rectum	At most 60.00 % volume at 4080 cGy dose	26.35 %	✓
Rectum_1	At most 0.10 NTCP LKB, Rectum_1, Late rectal bleeding, gra	0.04	✓
Rectum_1	At most 0.10 NTCP LKB, Rectum_1, Late rectal bleeding, gra	0.05	✓

Table 5-5 Clinical goals to assess Prostate treatment plans

The RayStation interface allows setting of clinical goals that function as plan assessment metrics along with the DVHs and ROI dose statistics. As an example, the values of clinical goals for the lung treatment plans (as shown in table 5-6) are recorded for all the plans for ranking purposes. The 'value' column provides the absolute value of the clinical goal extracted from a given plan and the results

column provides a very quick visual check to assess if the objective and constraints have been met (green tick mark icon) or not (orange exclamation mark icon). The clinical goals used for plan ranking and assessment can differ from the planning objectives & constraints used by the inverse plan algorithm. This functionality allows the user to assess multiple clinical parameters for a given plan at the same time.

For example, the user can check the value of V_{20Gy} for the healthy lung (ROI 'total' in Table 5-6) and also see the associated LKB NTCP prediction if required. Similarly, D_{95} and the TCP (Marsden model based) of the ROI 'PTV' can be simultaneously assessed. The system can also report the homogeneity index of the plan. Further, the clinical goals table is fully customisable as per user requirement.

There is a plan evaluation tab provided in the system that allows comparison of up to 3 treatment plans simultaneously. It offers both qualitative and quantitative assessment metrics as described in the section above.

ROI/POI	Clinical goal	Value	Result
BPlexus	At most 5500 cGy dose at 0.1 cm³ volume	69 cGy	✓
CordPRV	At most 4800 cGy dose at 0.1 cm³ volume	1771 cGy	✓
GTV	At least 0.90 TCP Marsden, Repopulation, NSC Lung, Marsde	0.78	!
Heart	At most 33.00 % volume at 5700 cGy dose	0.00 %	✓
Oesophagus	At most 0.10 NTCP LKB, Esophagus, Esophagitis, grade >= 2 ,	0.00	✓
Oesophagus	At most 5800 cGy dose at 0.1 cm³ volume	1565 cGy	✓
PTV	At least 0.90 TCP Marsden, Repopulation, NSC Lung, Marsde	0.69	!
PTV	At least 95.00 % volume at 5500 cGy dose	95.40 %	✓
PTV	At least a homogeneity index of 0.50 at 100.00 % volume	0.86	✓
total	At most 0.20 NTCP LKB, Lung_LKB_CCC, Pneumonitis (1), Gr	0.04	✓
total	At most 20.00 % volume at 2000 cGy dose	12.76 %	✓

Table 5-6 Treatment plans assessment metrics - NSCLC treatment plan

5.3 Results & Analysis

The results of the QC exercise are shown below in Tables 5-7, 5-8, and 5-9. The TCP values (Marsden model) for various target-volume DVHs as calculated by RayStation (RS), BioSuite and RadOpt agree closely with a variation of less than 1%. Further, this variation is the same irrespective of 'repopulation' (ON/OFF) criteria.

Target volume	File	PTV (cc)	Fractions	Repopulation	RS (TCP)	RadOpt (TCP)	Biosuite (TCP)
Lung-PTV	Pat1Plan1	239.7	20	On	81.0%	80.5%	80.5%
Lung-PTV	Pat1Plan2	239.7	20	On	45.0%	44.3%	44.3%
Lung-GTV	Pat1Plan1	79.7	20	On	98.0%	98.0%	98.0%
Lung-GTV	Pat1Plan2	79.7	20	On	66.0%	65.9%	66.0%
Prostate-PTV	Pat1Plan1	279.1	32	Off	76.0%	75.7%	75.7%
Lung-PTV	Pat1Plan1	239.7	20	Off	55.0%	55.2%	55.1%

Table 5-7 TCP computed by RayStation, Biosuite & RadOpt

In order to check the implementation of repopulation in the TCP model in RayStation, the values of the parameters T_{pot} & T_{delay} were varied and the RS and BioSuite TCP values were compared for a single-bin DVH (65 Gy dose, 133.5 cc volume, 30 fractions).

Tpot (days)	Tdelay (days)	RS (TCP)	BioSuite (TCP)	Difference
3	20	42.4%	41.3%	1.1%
5	30	58.7%	57.9%	0.8%
7	20	55.4%	54.9%	0.5%

Table 5-8 TCP comparison of RayStation vs Biosuite for variations in T_{pot} & T_{delay}

The results show that the agreement between the two systems is acceptable. Next, the NTCP calculations for prostate and lung-tumour OAR structures across the three systems are compared:

Dataset	RayStation (NTCP)	RadOpt (NTCP)	Biosuite (NTCP)
Pt1Plan1_Lung	10%	9.3%	9.3%
Pt2Plan1_Lung	7%	7.5%	7.5%
Pt1Plan1_Rectum	4%	3.8%	3.8%
Pt2Plan1_ Rectum	1%	1.6%	1.6%

Table 5-9 LKB NTCP comparisons between RayStation, BioSuite & RadOpt

It is seen that the error in the calculation is again less than 1% and is probably largely attributable to the way all the three systems are programmed to calculate the NTCP based on the LKB model (i.e. different programming languages implementing the same model). The 3 systems are therefore deemed comparable in

terms of radiobiological model calculations. Next, dose-volume-based inverse planning is compared to radiobiological-model-based inverse planning.

5.3.1 Lung Cancer Treatment Plan Comparison

A library of lung DVH datasets (59 patients) with PTV and healthy lung DVHs was used for this comparison. Using these DVHs, a TCP library plot (from PTV DVHs) and a NTCP library plot (from Healthy Lung DVHs) was created as shown in figure 5.3.

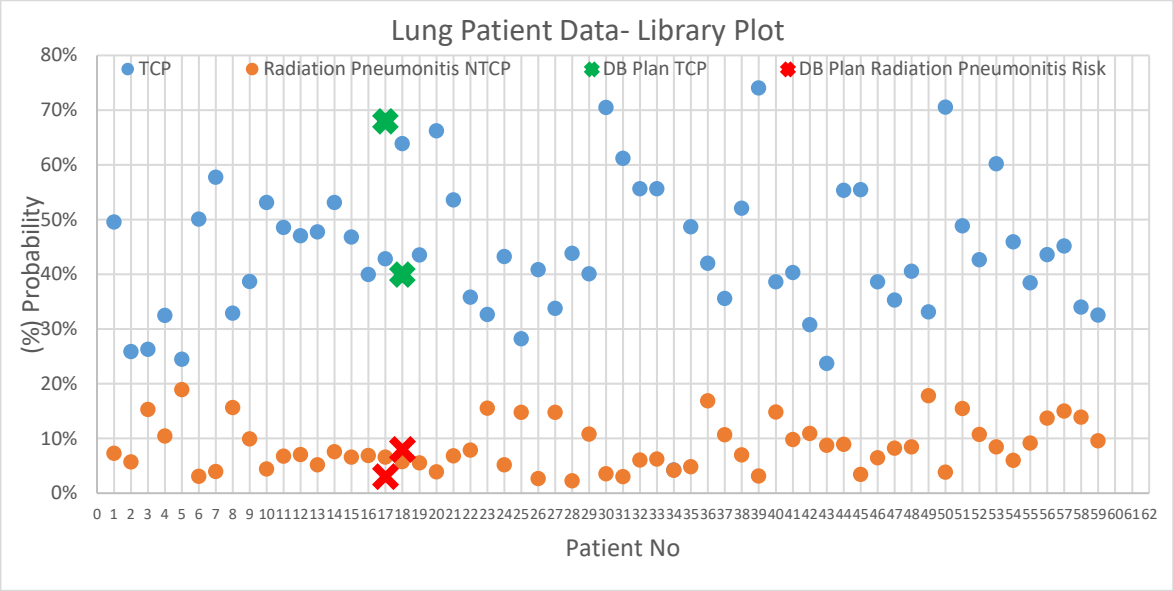

Figure 5-3 TCP and NTCP Library plot for the lung cohort data

This allowed visualization of the range of the TCPs & NTCPs and their spread across a small population. Further, in the same figure, the TCP and the NTCP of the DB-plans of patient 1 and 2 are plotted to check if the DB-plans were similar to the TCP and the NTCP of clinical plan data. As depicted in the figure 5-3, TCP and NTCP of both the patients shown by the green and red crosses are within the same TCP and NTCP ranges as of the patients in the DVH library indicating that DB-plans formed for this chapter are clinically representative.

Next, the DB-plan and the Isotoxic RB-plan are compared for both lung cancer patients for the 20-fraction schedule. For the creation of the RB-plans the objective was to maximize TCP (Marsden model) of the PTV at an isotoxic NTCP (Radiation Pneumonitis NTCP as observed for the DB-plan of the respective patients for a given fractionation schedule). To achieve this, the optimization algorithm tries to increase the dose in the PTV of the RB-plans which thus increases the average dose

(viz. Prescription Dose) associated with them, however, it is emphasized that RB-planning is not based on the aim to have a specific prescription dose.

Table 5-10 Quantitative comparison of DB-plan and RB-plans for Lung cancer patients

Parameter	Patient 1				Patient 2			
Plan	DB-plan	DB-plan (Non-Uniform)	RB-plan	RB-plan	DB-plan	DB-plan (Non-Uniform)	RB-plan	RB-plan
Plan Dose (cGy)	5700	5774	7429	7055	5650	5819	6894	6497
No of Fractions	20	20	20	15	20	20	20	15
Tumour TCP (PTV)	68%	71%	97%	99.9%	40%	51%	78%	85%
Radiation Pneumonitis NTCP	3%	4%	3%	4%	8%	7%	7%	8%
Total Lung (V20)	10.1%	10.6%	6.8%	8.8%	18.8%	18.2%	15.6%	15%
Esophagitis NTCP	0%	0%	0%	0%	2%	2%	1%	0%
Spinal Cord (Dmax cGy)	1671	1518	1662	1011	3028	2942	2108	2289
Heart (V57 cGy)	0	55	0	0	71	69	68	63
Homogeneity Index (100% Vol)	0.87	0.86	0.61	0.73	0.89	0.86	0.60	0.63

Similarly, the oesophagitis risk for all the plans is 1% different for compared plans for each patient and lower for the RB-plans$_{20\#}$ compared to DB-plans$_{20\#}$. From the dosimetric perspective, the DVHs (Figure 5-4) of the DB-plan$_{20\#}$ and RB-plan$_{20\#}$ for patient 1 demonstrate that RB-plan achieves superior sparing of oesophagus and healthy lung ('total' – in Figure 5-4) in the mid and low dose ranges. However, the maximum dose observed is higher for the RB-plan$_{20\#}$ compared to the DB-plan for the healthy lung and oesophagus OARs. Considering healthy lung OARs' parallel organ architecture (n=1), the higher max dose is unlikely to increase the risk of radiation pneumonitis. The increase in the max dose for oesophagus in the RB-plan$_{20\#}$ compared to the DB-plan is marginal (table 5-10). The max dose to the spinal cord OAR of the RB-plan$_{20\#}$ is marginally lower than that for the DB-plan. The dose to heart in all the plans for patient 1 was zero except in the DB-plan$_{(Non\text{-}Uniform)}$.

Comparing the DVHs of DB-plan and RB-plan$_{20\#}$ for patient 2 in figure 5-5, it is observed that RB-plans significantly spare all the OARs. The max dose of the healthy lung OAR is higher in the RB-plan compared to the DB-plan but dose sparing in the low-mid dose range is far superior in the RB-plan. The radiation pneumonitis risk for

all the plans for respective patients as measured by LKB NTCP model is the same (i.e. about 1% difference at the most- table 5-10).

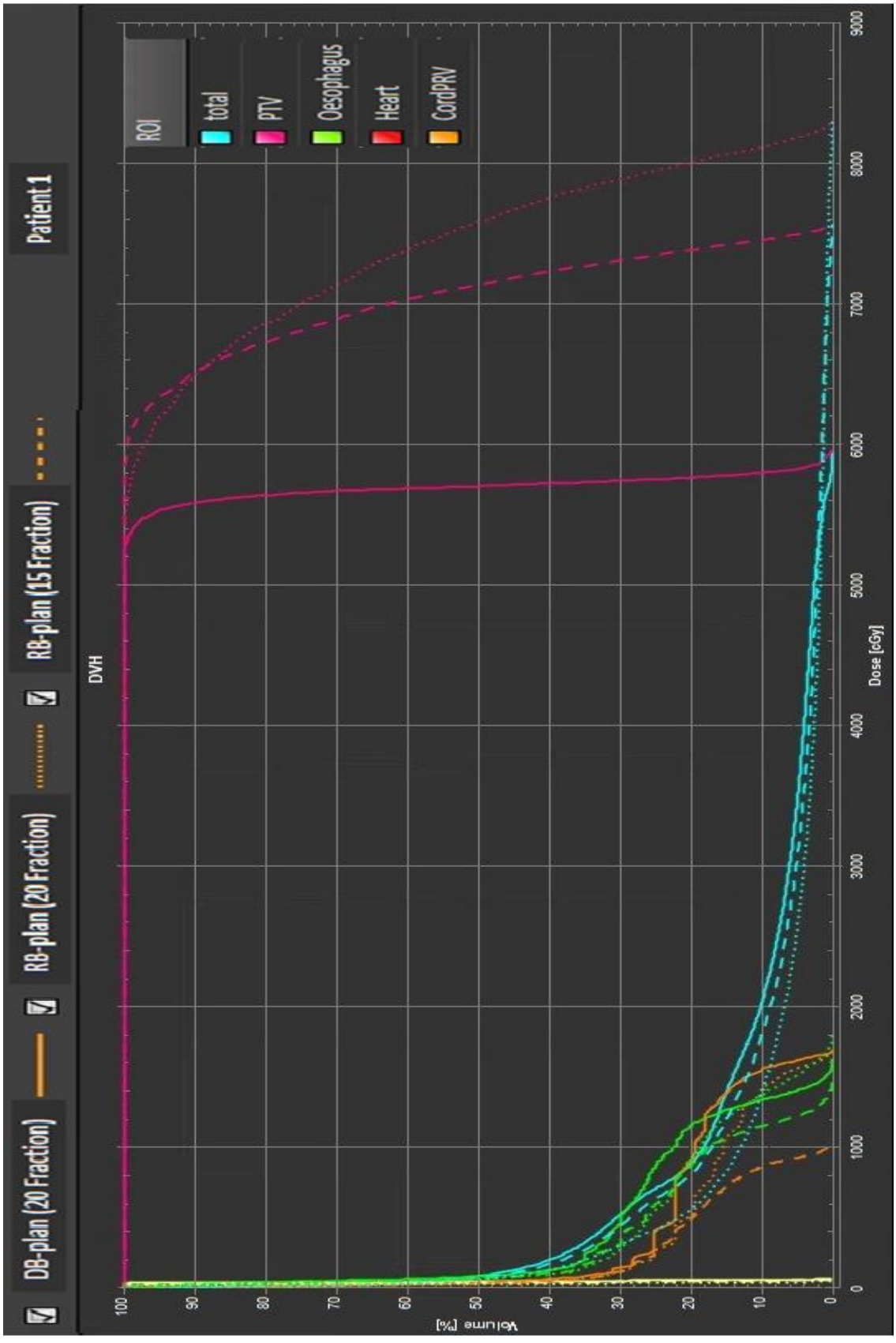

Figure 5-4 Comparison of DVHs of DB-plan (20#), RB-plan (20#) and RB-plan (15#) for lung patient 1

Figure 5-5 Comparison of DVHs of the DB-plan (20 frac.), RB-plan (20 frac.) and RB-plan (15 frac.) for lung patient 2

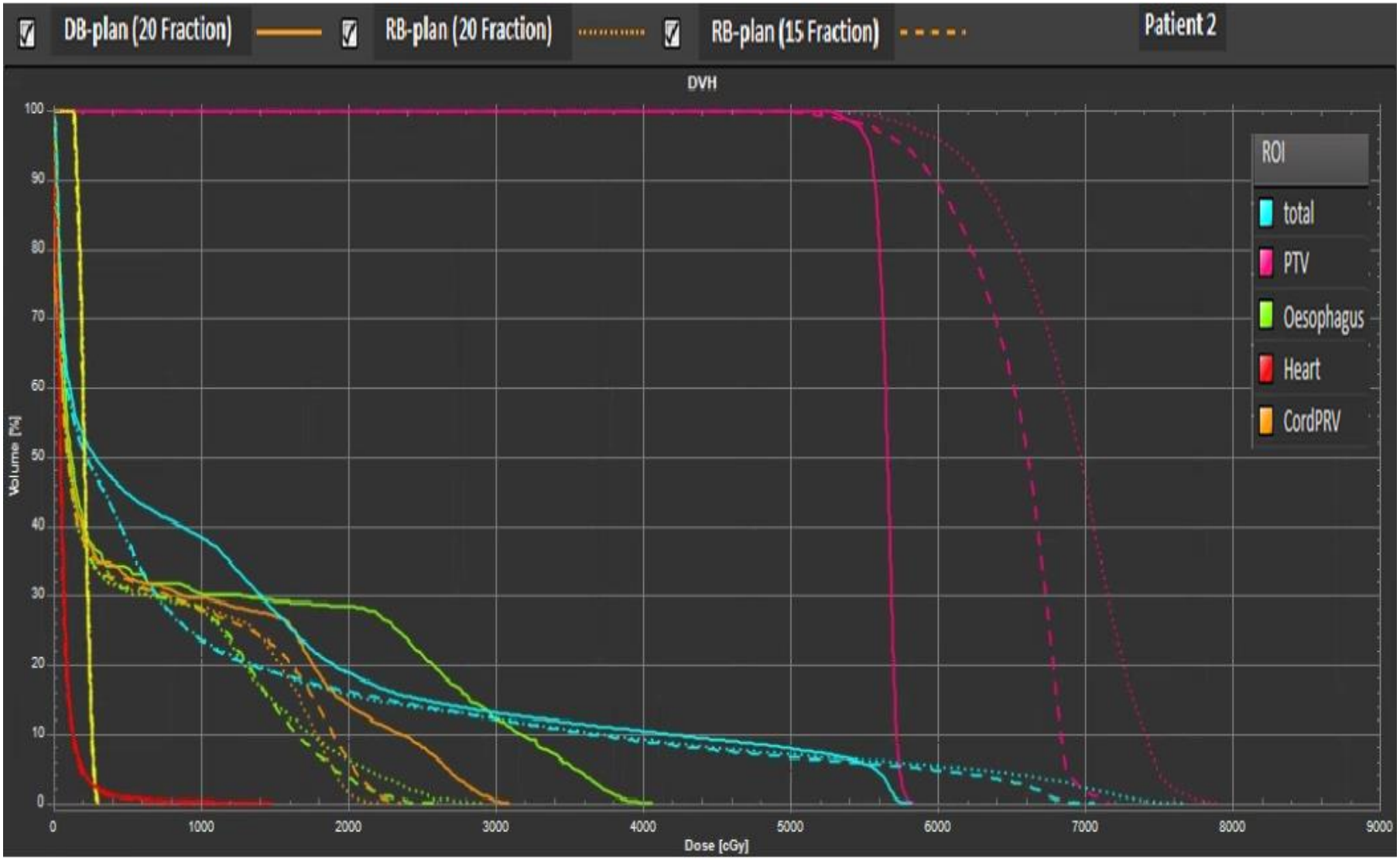

The set dosimetric constraint for spinal cord is D_{max} = 48Gy (based on ISTART trial protocol) and it is seen that all the plans for patient 2 are well below this limit for spinal cord myelopathy. Also, the V_{20Gy} of healthy lung for the RB-plans is ~2-3% lower than for the DB-plans for both patients. It is pointed out that healthy lung and oesophagus were the only organs for which radiobiological constraints were used (as reliable LKB model parameters for other OARs were not available). The dose to heart in all the plans for patient 2 was similar and very low (measured using V_{57Gy}). Thus, it is established that RB-plans created here are Iso-toxic or better (relatively safer) in terms of dosimetric and radiobiological model based metrics.

The next important aspect of this exercise was to compare the dose deposition and TCP for the PTV. A higher planned dose is observed in the PTV with a significant increase in TCP for RB-plans of both patients (planned dose is a metric calculated by the system although the objective was to maximize TCP). It can be observed that the TCP of the RB-plans (for both patients) is higher than the TCP of the DB-plans by ~30-40% (Table 5-10). Analysis of the DVHs in fig. 5-4 and fig. 5-5 shows that the RB-plans deposit more dose in the target structure. The homogeneity of dose deposition (across 100% of the PTV) of the DB-plan is higher compared to the RB-plan in both the patients (table 5-10). Also, 100% of the PTV receives more than 55 Gy dose in the RB-plan (fig. 5-4 and fig. 5-5). This was expected as the goal of the planning exercise was to increase the therapeutic ratio for the RB-plans whereas the DB-planning explicitly requires a quasi-uniform dose to the tumour PTV.

The DB-plan$_{(non\text{-}uniform)}$ (plan 4) created for both patient 1 and patient 2 are isotoxic as far as OAR toxicity constraints are concerned (table 5-10). The relaxation in the 'uniformity' objective in the DB-plan$_{(non\text{-}uniform)}$ has resulted in a gain in the overall dose deposition in the target. The improvement in the target TCP for patient 1 was 3% and for patient 2 it was 11% (table 5-10). It is interesting to note that the gain in the TCP is achieved for a nominal (3%) reduction in the homogeneity index for both the patients.

Next, the 15-fraction RB-plan (plan 3) is compared to the 20-fraction DB & RB-plans. For patient 1, the RB-plan (15 fractions) is comparable to the RB-plan (20 fractions)

in terms of Iso-toxicity and in terms of TCP (with a slight improvement in the 15 fractions RB-plan TCP). The max dose to the spinal cord for the 15 fractions RB-plan is lower for patient 1 and comparable to the max dose in the RB-plan (20 fractions) which is still lower than the standard DB-plan. For patient 2 the TCP of the RB-plan (15 fraction) is 7% higher than that of the RB-plan (20 fractions) with a slight increase in dose to OARs. Overall, it is observed that RB-plans are superior compared to the DB-plan for all the lung patients. The 15-fraction RB-plan achieves the highest TCP for a similar NTCP (lung-GTV, i.e. healthy lung & Oesophagus toxicity) and a reduced maximum dose to the spinal cord (patient 1). The DVHs of principal OARs of all the plans for both the patients are shown in fig. 5-4 and fig. 5-5.

Visual qualitative comparisons of plans 1-3 of each patient are presented in Figure 5-6 and Figure 5-7. Transverse, coronal and sagittal CT slices are overlaid with colourwash doses (aligned at the isocentre). The scale in the colour wash is in % of 55 Gy to make the comparison consistent across all the plans. For patient 1 in Figure 5-6, in the transverse section of the DB-plan, it is seen that the right lung is comprehensively covered by the 25-50% Iso-doses for the anterior to posterior walls; however, the RB-plan$_{20\#}$ spares the anterior right lung (covered by the 10% Iso-dose area). Further, the 15 fraction RB-plan spares the oesophagus and spinal cord distinctly as seen in the transverse slice compared to both the other plans. Similarly, dose in the sternum in the coronal slice is quite high for the DB-plan compared to the RB-plan as seen in the coronal section.

For patient 2 (Figure 5-7), a hot region of dose deposition can be observed in the left lung in the transverse section of the DB-plan which is reduced in the RB-plan$_{20\#}$ and non-existent in the 15-fraction RB-plan. The sparing of the healthy lung in the RB-plan$_{15\#}$ for patient 2 is considerably better than that in the 20-fraction RB-plan. Furthermore, both the RB-plans are better at sparing healthy lung than the DB-plan for both the patients.

Figure 5-6 Qualitative comparison (Lung Patient 1) of the DB-plan and RB-plans using colour-wash doses at the iso-centre CT slice in transverse, coronal and sagittal planes

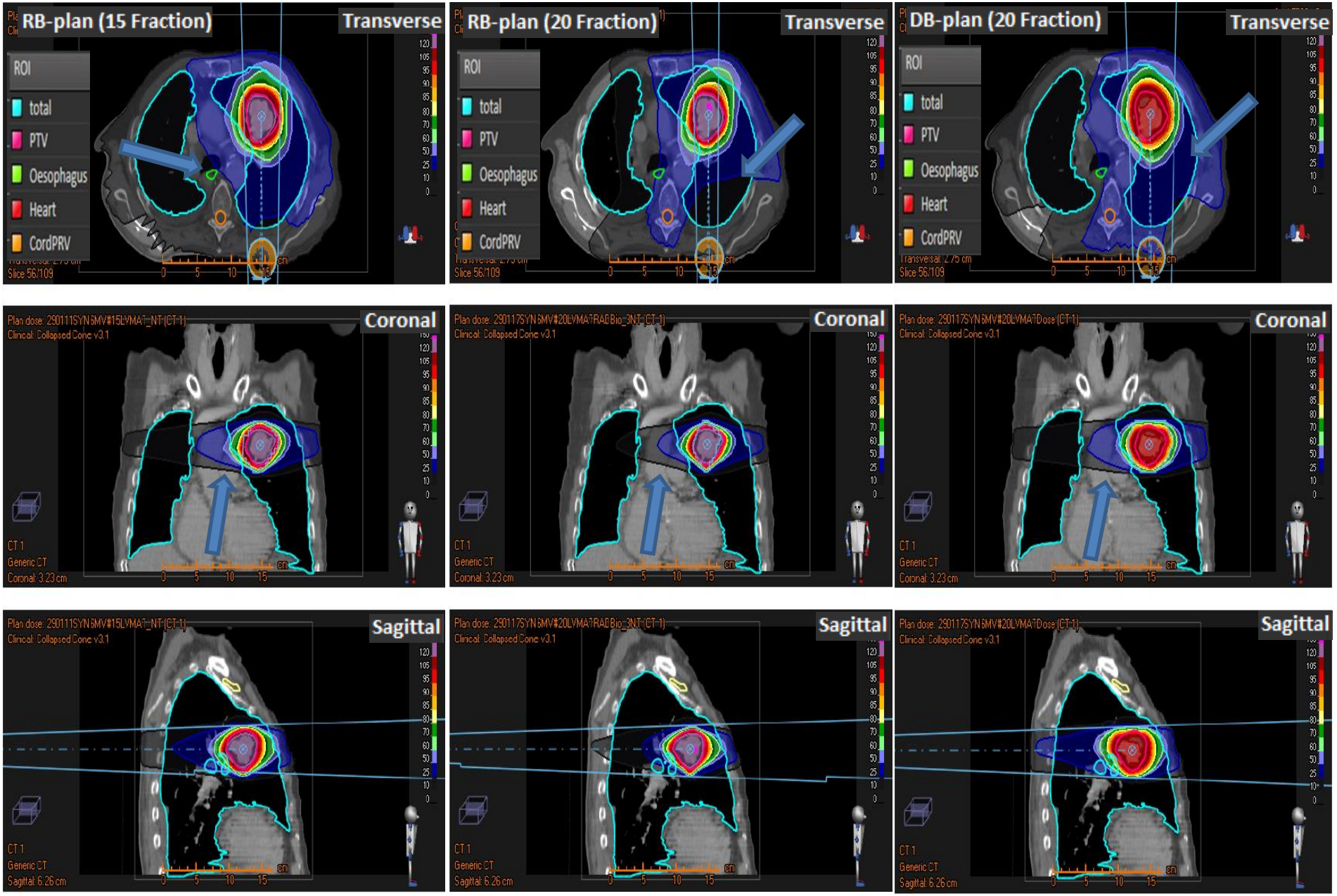

Figure 5-7 Qualitative comparison (NSCLC Patient 2) of the DB-and RB-plans using colour-wash doses at the Isocentre CT slices in transverse, coronal and sagittal planes.

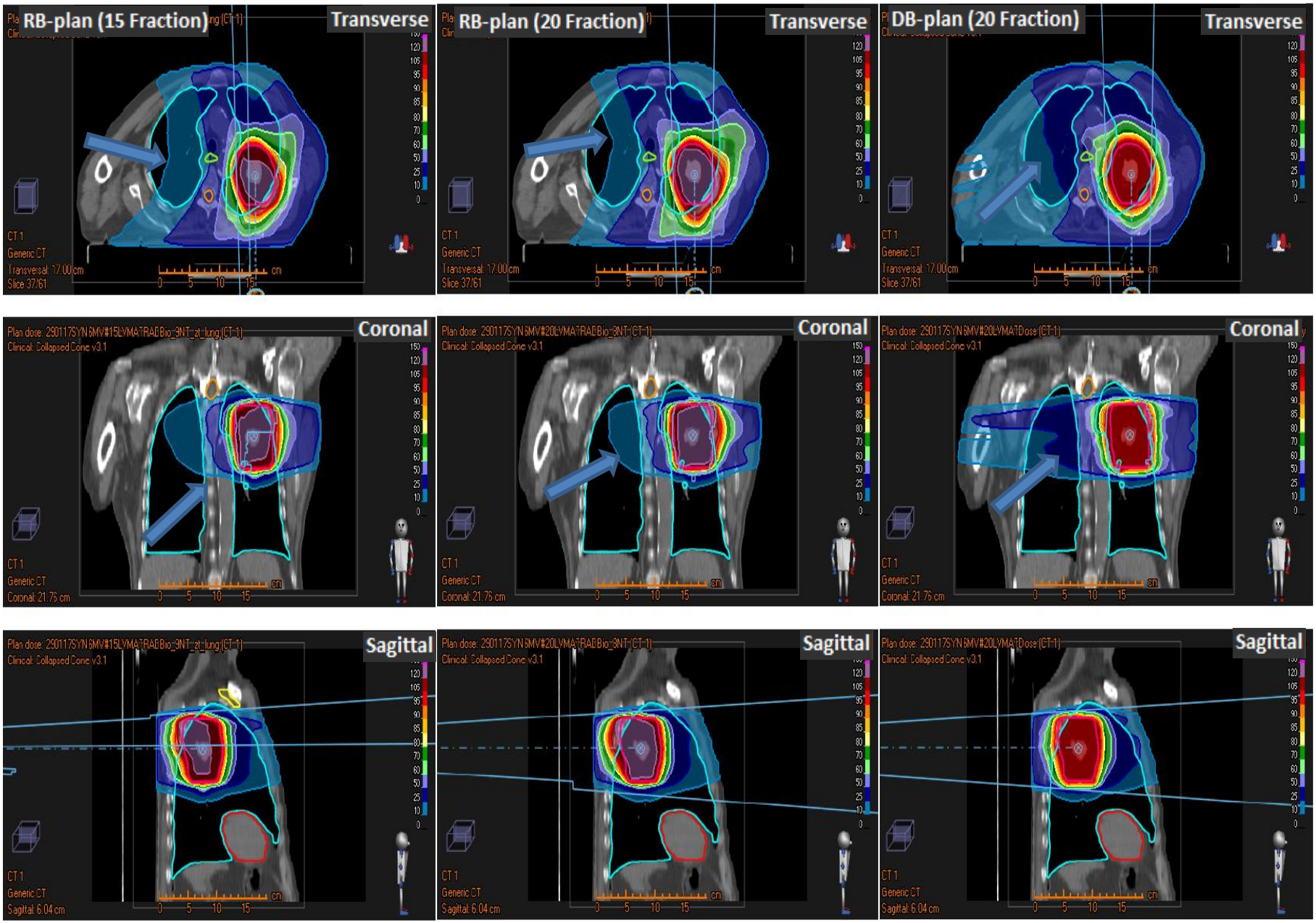

5.3.2 Prostate Cancer Treatment Plan Comparison

Having access to a library of about 56 prostate patient DVH datasets (60Gy 20 fraction schedule), a TCP and a NTCP (rectal bleeding risk) library plot was created. The observed TCP and NTCP of the DB-plans (Patient 1 and 2) were added to the same plot to assess the clinical equivalence of DB-plans created for this chapter. It is observed in figure 5-8 that the DB-plan NTCPs (yellow Dots) are very close to the normally observed NTCPs of clinical plans. The TCP of the DB-plan (Grey Dots) DVHs are found to be slightly higher than the TCP_{max} observed in the cohort (figure 5-8). However, the TCPs of the DB-plans are slightly higher than the highest TCP for any tumour DVH in the library but with a very small difference indicating that the patients were most likely favourable and certainly do not invalidate the plans formed here.

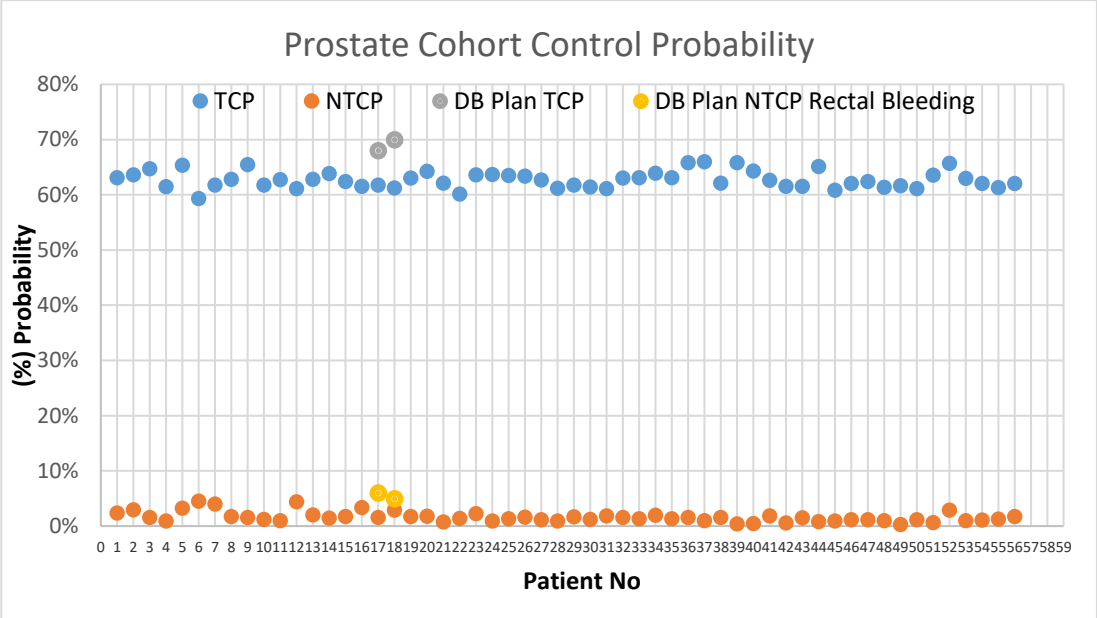

Figure 5-8 TCP and NTCP Library plot for the prostate cohort data

Table 5-11 compares the DB-plans and RB-plans for the two prostate cancer cases**.** Firstly, iso-toxicity between DB-plans and the RB-plan (for each patient) is assessed by evaluating the NTCP of various endpoints (principal dose limiting side-effects) followed by a comparison of the dosimetric parameters that are currently used to assess the risk of OAR toxicity. Then, the tumour dose and TCP of the plans are compared.

Table 5-11 Quantitative comparison of DB- and RB-plans for the prostate cancer cases

Parameter	Patient 1			Patient 2		
Plan	DB-plan	DB-Plan Non-Uniform	**RB-plan**	DB-plan	DB-Plan Non-Uniform	**RB-plan**
Plan Dose (cGy)	6100	6400	6862	6105	6300	6670
Fractions	20	20	20	20	20	20
PTV (TCP)	68%	71%	73%	70%	72%	74%
Rectal Bleeding NTCP	6%	4%	4%	5%	4%	3%
Faecal Incontinence NTCP	9%	7%	5%	7%	6%	5%
Bladder ($V_{40.8Gy}$)	23.5%	18.7%	22.6%	41%	36.9%	40.1%
Rectum ($V_{40.8Gy}$)	57.8%	45.8%	26.3%	42.4%	34.6%	27.2%
Rectum (V_{60Gy})	3.6%	3.6%	4.4%	4.8%	4.2%	2.9%
PTV Homogeneity (100% Vol)	0.92	0.78	0.71	0.93	0.79	0.71
Femoral Head (Right) $V_{40.8Gy}$	0%	0%	0.9%	0%	0%	0%
Femoral Head (Left) $V_{40.8Gy}$	0%	0%	1.3%	0%	0%	0%

It can be seen in Table 5-11 that the NTCP for rectal bleeding for all the plans is below 6%. The risk of faecal incontinence is also below 9% for all the plans. Further, the risk of rectal bleeding and faecal incontinence in the RB-plans is lower by about 2-4% than for the DB-plans for both patients. It can also be seen that the TCP of the RB-plan for both the patients is higher than that of the DB-plans. The RB-plan of patient 1 was achieved by the optimizer after about 100 iterations and it is not Isotoxic compared to the DB-plan (as Rectal Bleeding NTCP is only 4% which is better than the DB-plan).

To ensure Isotoxicity, the dose in the RB-plan of patient 1 was subjected to scaling such that the NTCP would be 7% and the gain in the TCP would be comparable. But it was not possible to do so as it was found that other constraints were being violated if the plan dose was to be scaled or the intensity of radiation from a given beamlet could not be increased. The comparison of dosimetric parameters of Rectum ($V_{40.8\ Gy}$) suggests that RB-plans are very effective at sparing the rectum OAR (8-19% volume) at the cost of a slight increase in V_{60Gy} of the rectum (~2% volume). The rectum being a serial-parallel OAR (n=0.09 for rectal bleeding) / (n=1 for faecal incontinence), the effect of higher doses in RB-plans should be carefully considered. $V_{40.8\ Gy}$ for the bladder OAR is same (<1% difference) for the DB-plans and the RB-plan of both the patients.

The comparisons of the DVHs of important structures of the DB-plans and the RB-plan for prostate patient 1 and prostate patient 2 are shown in fig. 5-9 and fig. 5-10. The solid lines represent the DB-plan structures and dotted lines represent the RB-plan structures. For both patients, it can be observed that the PTV DVH of the DB-plans show a sharp drop in %volume at 60 Gy indicating uniform dose across the tumour. For the RB-plan the minimum dose to 100% target volume is ~57 Gy with the maximum at about 76 Gy. It can be seen that the RB-plans for both the patients achieve superior rectal sparing even when the average dose to the tumour is significantly higher than that in the DB-plan.

A visual comparison of therapeutic gain is shown by the yellow and blue bi-directional arrows; these show the relative sparing of the rectum and the increase in tumour dose for the RB- vs DB-plans for patients 1 &2 (fig. 5-11 & fig. 5-12). The distance between the PTV DVH and the rectum DVH which expresses the therapeutic gain is higher for the RB-plan compared to the DB-plan.

Plan 3 DB-Plan$_{(non\text{-}uniform)}$

From table 5-11, it is observed that DB-Plan$_{(non\text{-}uniform)}$ that does not have 'PTV dose uniformity' as an objective, spares the rectum greatly compared to the standard DB-plan (assessment of $V_{40.8\ Gy}$ or $V_{60\ Gy)}$ in both the patients. It is also observed that the DB-plan$_{(non\text{-}uniform)}$ spares the bladder better (~4% volume) in both the patients. From a radiobiological perspective, the NTCP of the principal OAR is lower and the TCP is higher for the DB-Plan$_{(non\text{-}uniform)}$ than that of the standard uniform PTV objective based DB-plan.

Thus, the DB-plan$_{(non\text{-}uniform)}$ has a higher therapeutic ratio than the standard uniform DB-plan which is a critical finding from this work and this is attributed to improvement in treatment delivery technique (IMRT/VMAT). Schwarz *et al.* (2005) compared 3D CRT and IMRT planning techniques to assess the potential of dose escalation in 10 selected NSCLC patient plans (2.25 Gy/fraction schedule in the control arm). They also showed that dose in the tumour could be escalated by up to 35% by allowing heterogeneity of dose deposition in the tumour. Nielsen *et al.* (2014a, 2014b) published their findings based on a study of 20 NSCLC stage I-III

plans (66Gy/33fraction control arm vs dose escalated arm) where they performed dose escalation allowing inhomogeneous dose distribution in the PTV. They compared the plans using two TCP models (Martel TCP model and Marsden TCP model) and showed that mean dose in the tumour can be escalated without increasing lung toxicity compared to the standard homogeneous tumour dose approach used for the control arm.

Further, the RB-plan is found to be therapeutically better than the DB-Plan$_{(non\text{-}uniform)}$ (table 5-11) except for sparing for the bladder which is better in the DB-Plan$_{(non\text{-}uniform)}$ for both the patients. This finding should be validated over a larger cohort. The CT slices in transverse planes aligned at the iso-centre are compared for patient 1 and 2 in Figure 5-11 and Figure 5-13. It can be seen in the transverse section for both patients that the RB-plans spare the dose to rectum much better than the DB-plans. Another observation is that in the DB-plans, if the rectum were to be spared further, additional structures like (RECTUM_H Figure 5-11 & figure 5-12) would need to be built to instruct the optimizer to spare this volume whereas with RB-plans just one single constraint on NTCP achieves superior sparing. This suggests that radiobiological-model-based inverse planning helps improve optimizer efficiency. This deserves further study.

Figure 5-9 Comparison of DVHs of the DB-plan (20 fractions) and the RB-plan (20 fractions) for prostate patient 1

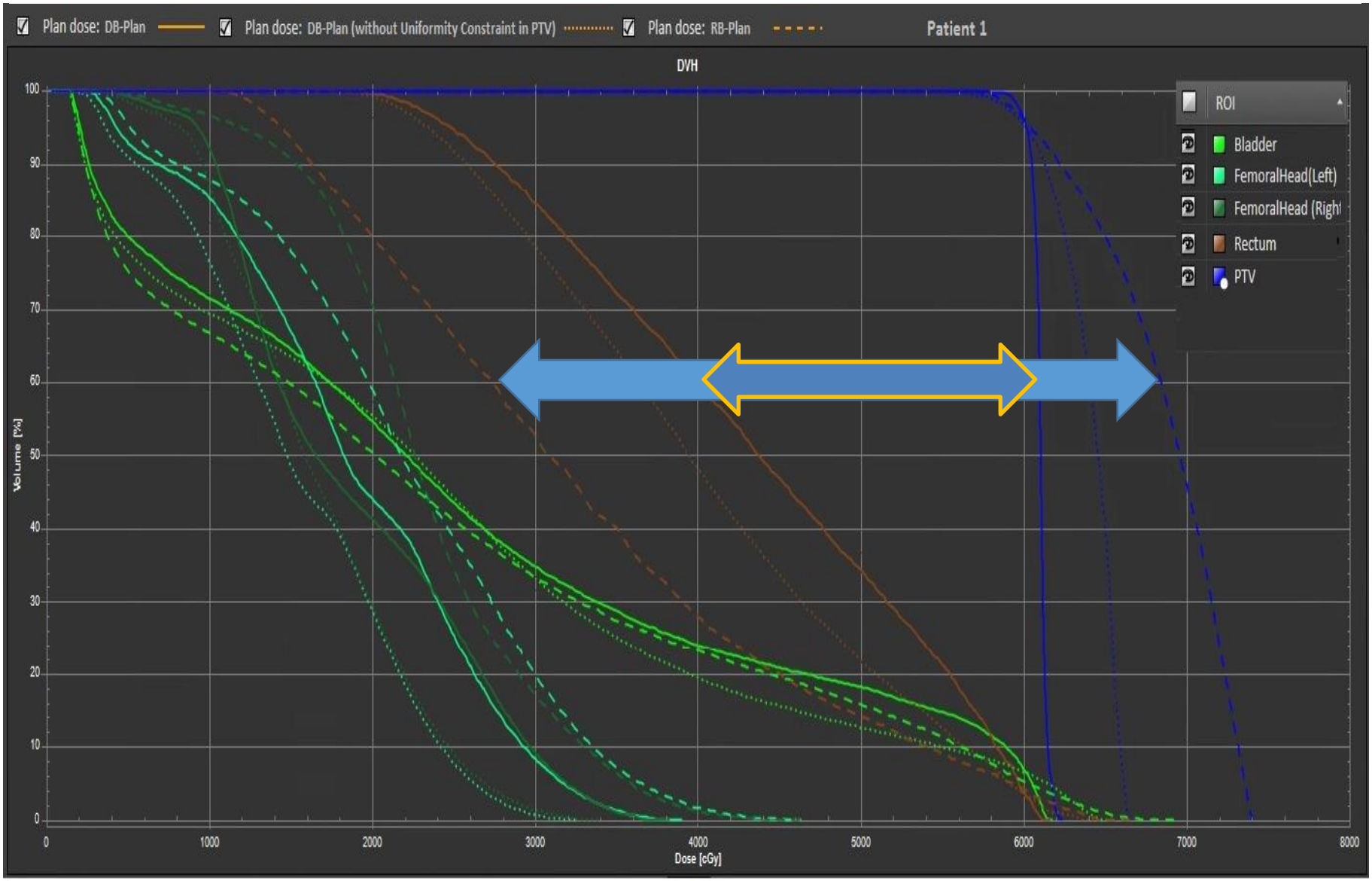

Figure 5-10 Comparison of DVHs of the DB-plan (20 fractions) and RB-plan (20 fractions) for prostate patient 2

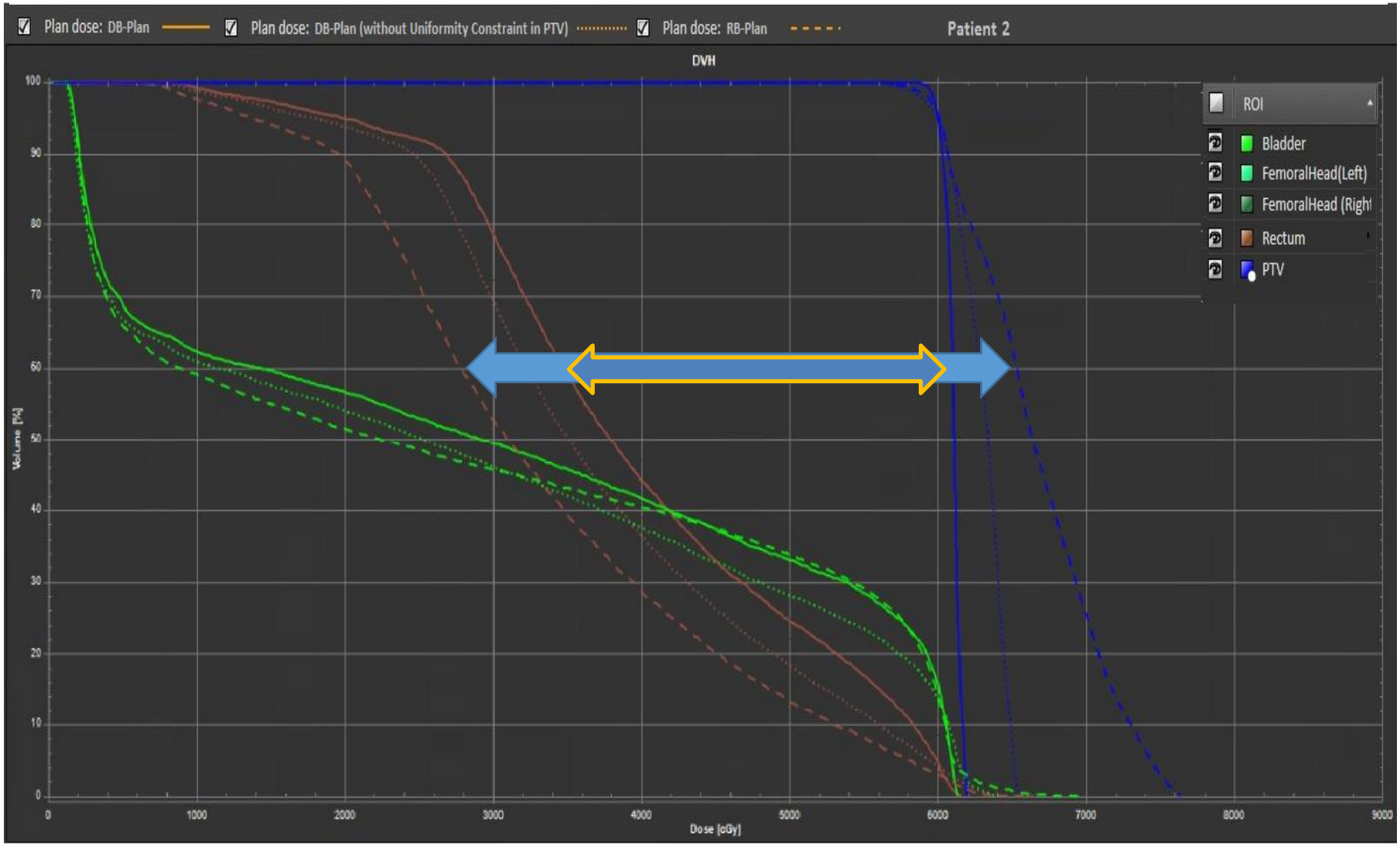

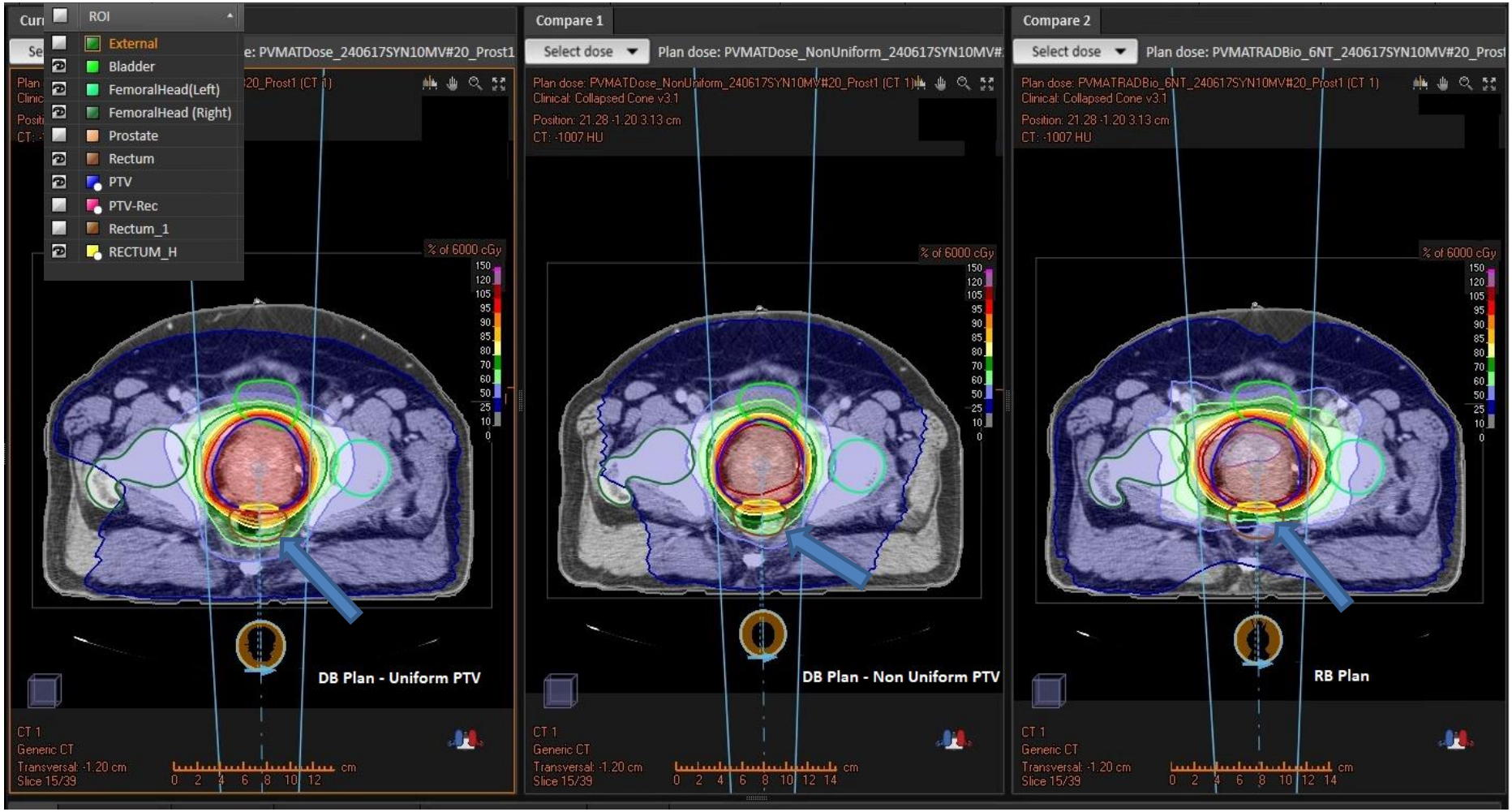

Figure 5-11 The figure compares the transverse sections of the DB-plan (for with standard PTV uniformity objective), DB-Plan (without the uniformity objective in the target) and RB-Plan for patient 1. The relative sparing of dose to rectum is shown by the blue arrows. The aspect ratio of the images is altered to fit the images on the same page to ease comparison.

Figure 5-12 Qualitative comparison of DB-plan and RB-plans using Dose colour wash at Iso-centre in CT slices in transverse, coronal and sagittal plane for patient 1

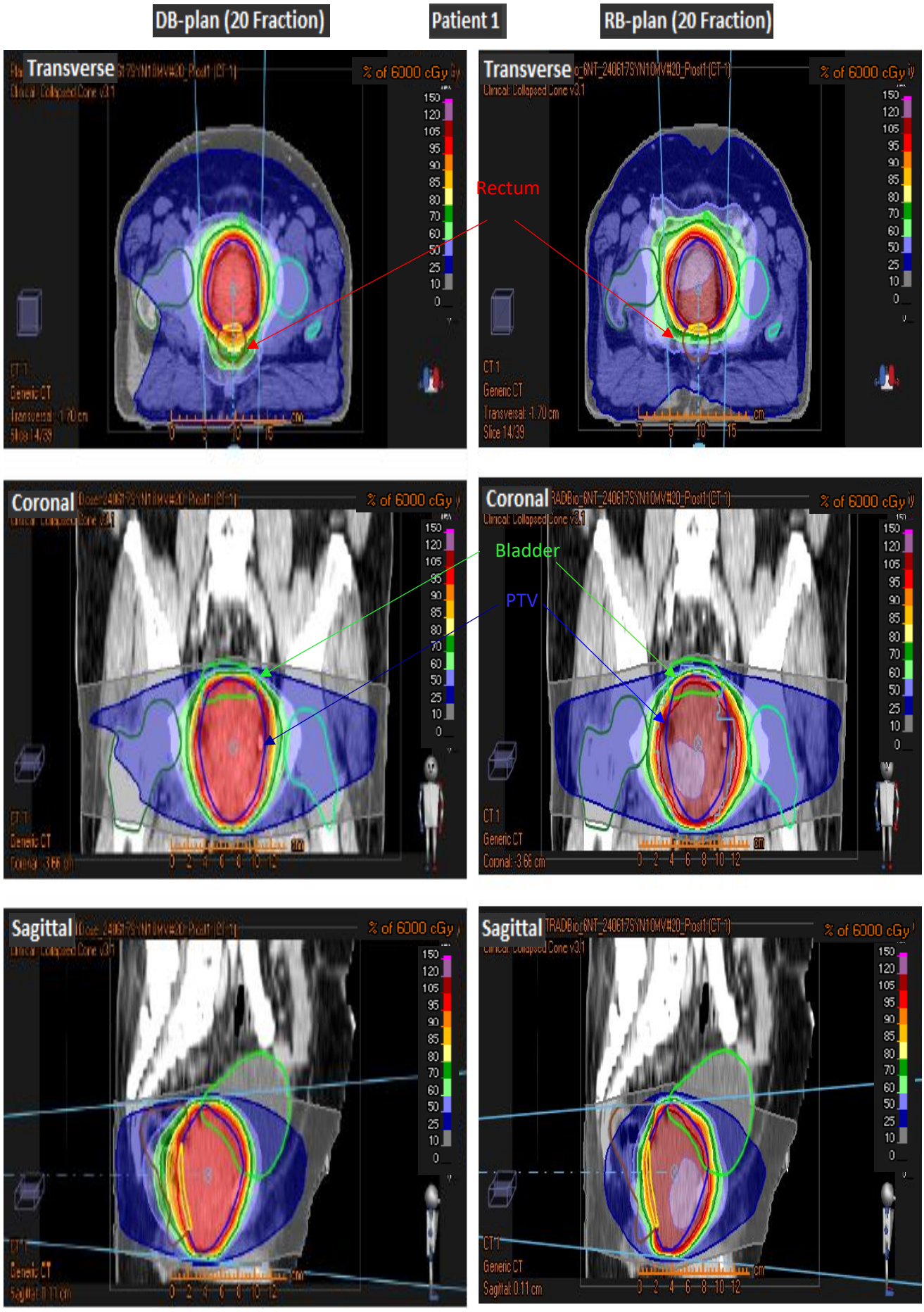

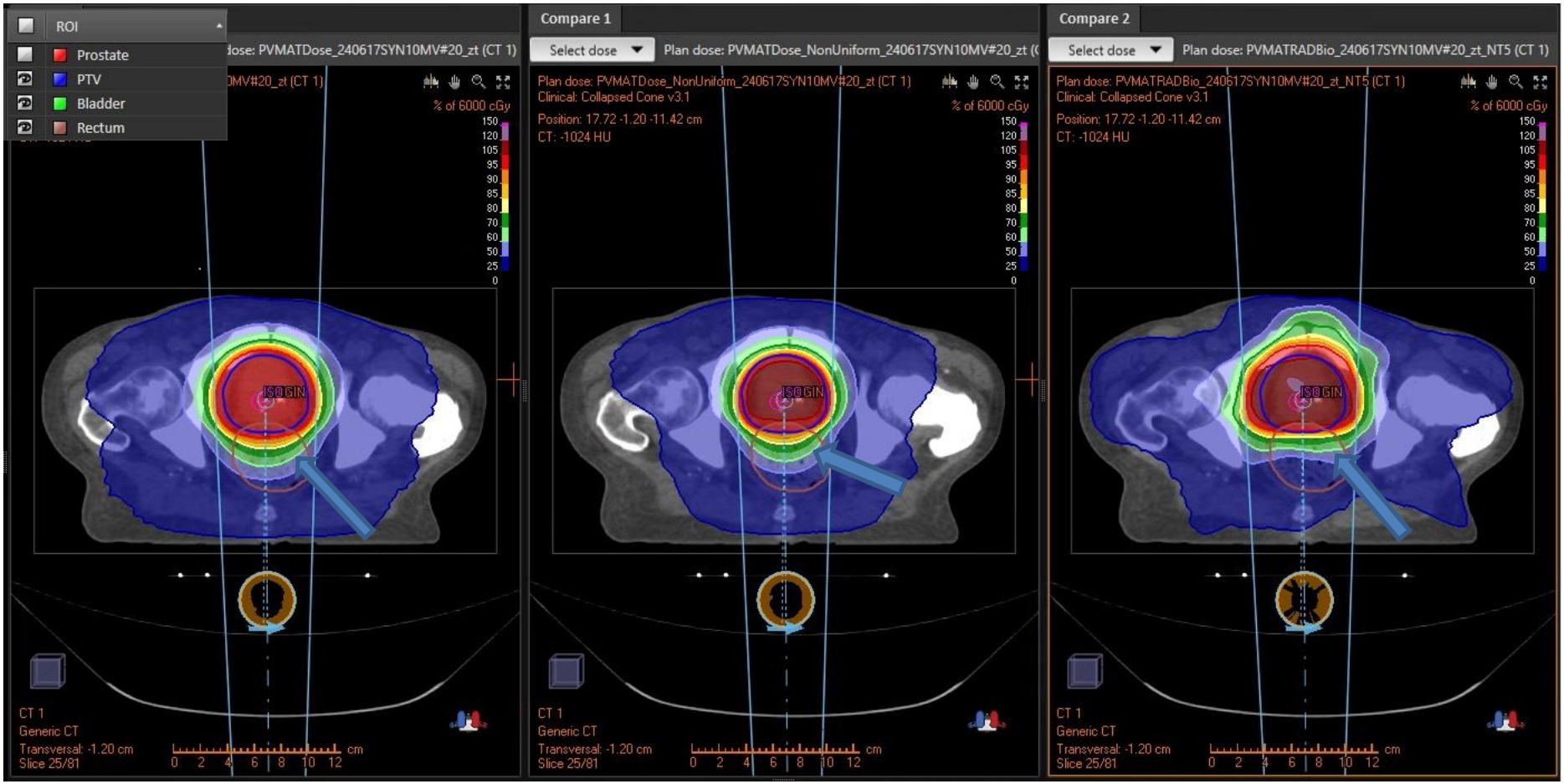

Figure 5-13 below compares the transverse sections of the DB-plan (for with standard PTV uniformity objective), DB-Plan (without the uniformity objective in the target) and RB-Plan for patient 2. The relative sparing of dose to rectum is shown by the blue arrows.

Figure 5-14 Qualitative comparison of DB-plan and RB-plans using Dose colour wash at Iso-centre in CT slices in transverse, coronal and sagittal plane for patient 2

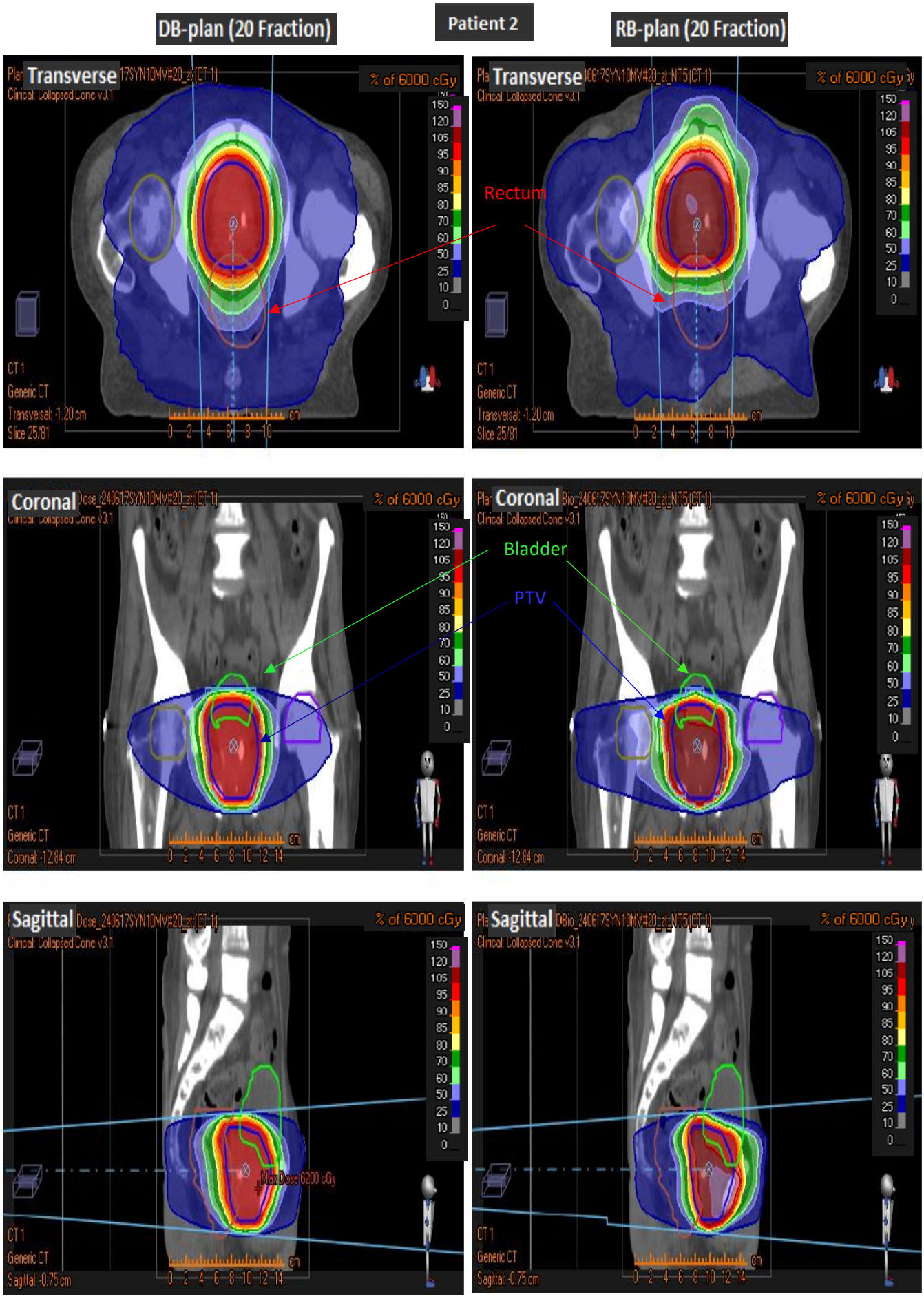

5.3.3 Dose Escalation (Standard versus Radiobiologically Based)

5.3.3.1 Lung Cohort Isotoxic Dose Escalation

To assess the change in TCP over a range of Iso-toxic NTCP, treatment plans at different Iso-toxic limits were created for a lung patient dataset. The TCP values of all the RB-plans created for the lung patient were extracted and plotted against the NTCP of the principal OAR. This resulted in TCP vs NTCP plots that allowed an overall comparison of dose escalation in radiobiologically inverse planned treatment plan versus dose-volume based treatment plan (Figure 5-15).

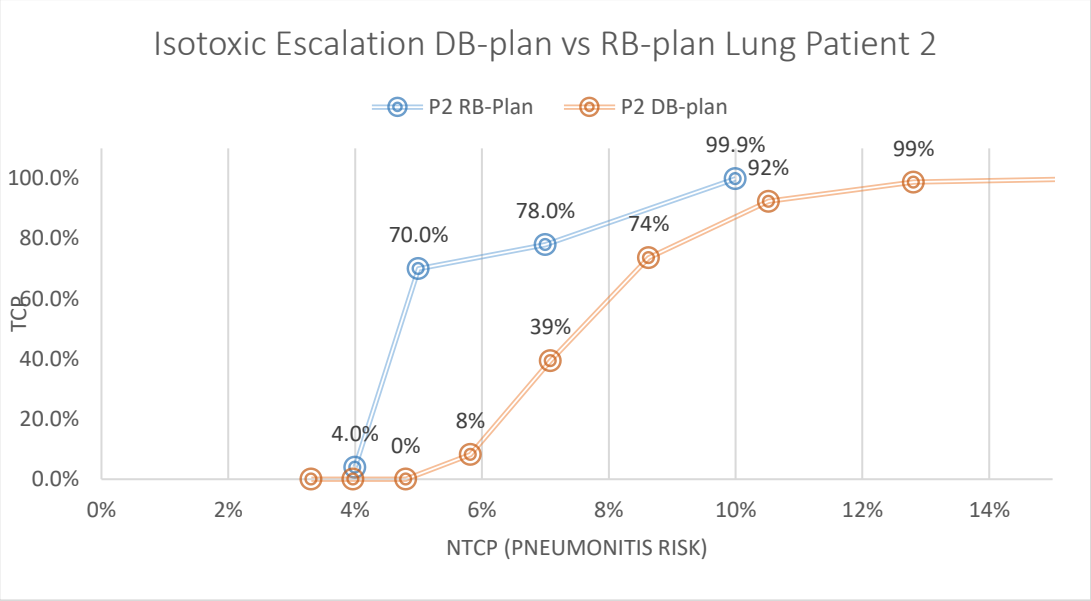

Figure 5-15 TCP-NTCP plots comparing Isotoxic dose escalation between radiobiological inverse treatment planning to dose-volume inverse planning for an NSCLC patient.

To create the TCP vs NTCP plots of the DB-plan, the dose of the DVHs was scaled until the dose tolerance limit of any of the OARs was not exceeded and then the TCP and NTCP were calculated from the respective DVHs. DB-plan constraints are dose-volume limits that do not account for the biological response of the OAR. Using EUD based constraints, one of the behavioural aspects of the tissue biology (serial or parallel behaviour) can be taken into account. It is seen for lung-tumour patient 2 in figure 5.15 that isotoxic radiobiological optimization is superior to dose-volume based inverse planning over a range of NTCP values (NTCP relates to radiation pneumonitis risk). The same Isotoxic dose escalation for Patient 1 was not undertaken as it was a very favourable case, with a small tumour volume in a relatively 'isolated' anatomical location in the lung. Overall, it can be observed that

radiobiological inverse treatment planning is superior to dose-based optimization for lung patient 2 (blue vs red curve, fig. 5-15).

5.3.3.2 Prostate Cohort Isotoxic Dose Escalation

Isotoxic dose escalation for the prostate plans was not successful as the optimizer could not escalate the dose to PTV without increasing the dose to 'Rectum' which resulted in a breach of rectal bleeding or faecal incontinence toxicity endpoint. The results for prostate patient dose escalation are somewhat different (compared to the lung cohort) as multiple toxicity endpoints limit escalation of dose for both the patients. The rectum is associated with rectal bleeding (LKB model n=0.09) and faecal incontinence (LKB model n=1) endpoints. The LKB model parameter 'n' is suggestive of the serial or parallel architecture of the OAR and rectum has associated endpoints that are attributed to both the extremes making dose escalation particularly challenging. However, radiobiological isotoxic dose optimization does not allow escalation of dose if either endpoint toxicity limit is breached for a given OAR. This is a unique feature associated with radiobiological inverse planning. Also, for some of the DB-plans of all the patients, dose scaling could not be performed as the intensity of radiation could not be scaled up for a given set of beamlets of the beam from some angles. This observed restriction is believed to be related to maximum fluence that can be physically delivered through a given beam segment.

5.4 Clinical Relevance, Conclusion and Future Work

In this chapter, radiobiological inverse treatment planning was compared to dose-volume-based (i.e. conventional) inverse treatment planning using an advanced commercially available treatment planning system that offers radiobiological cost-function based inverse treatment planning.

For the two-lung cancer patient CT datasets, two 55Gy in 20 fractions inverse VMAT treatment plan (DB-plan$_{standard}$ and DB-plan$_{(non\text{-}uniform)}$) and two isotoxic inverse plans (with a 20-fractions and a 15-fractions schedule) using radiobiological model-based constraints/objectives (RB-plan) were created.

The TCP of the RB-plans for both NSCLC cases was higher by ~30% compared to the DB-plans. It was also observed that sparing of healthy lung volume was about 2-4% (V_{20}) better for the RB-plans compared to the DB-plan. Thus, in terms of therapeutic ratio and principal OAR volume sparing it is reported that radiobiologically based inverse treatment plans are superior to standard dose-volume-based inverse plans for both lung patients in this study. It is demonstrated that the RB-plans without uniform dose objectives yield increased TCP, lower or isotoxic NTCP and increased dose sparing of principal OARs compared to the DB-plans. It was also demonstrated that 15-fraction schedule plans were better for both NSCLC patients in line with the results observed in Chapter 3 that suggested that individualized isotoxic treatment plans at 15 fractions were better than the 20-fraction schedule based plans for lung patients. It should be noted that the difference in the TCP for 20 versus 15 fractions depends on the value assumed for the potential tumour doubling time (t_{pot}).

For the two prostate cancer CT datasets, a standard 60 Gy 20 fractions plan and a radiobiologically based inverse treatment plan were created. Further, an additional DB-plan (without the target-dose uniformity objective) was created to assess the effect of uniformity objective on the treatment plan quality. All the plans were assessed using a combination of clinical dosimetric parameters and radiobiological metrics. It was found that RB-plan had a higher TCP than the DB-plan by 4-5%. The RB-plans were superior as far as OAR sparing was concerned in both dosimetric and radiobiological terms. The NTCP of rectal toxicities for the RB-plans was lower than

that of the DB-plans by about 2-4%. The $V_{40.8\,Gy}$ for the bladder was the same for both the set of plans or slightly lower for the RB-plans.

Inverse treatment plans with NTCP constraints of 5%, 7%, 10% and 13% for radiation pneumonitis for the NSCLC patient 2 were also created. The inverse DB-plans were re-scaled using 5 dose-scaling factors to obtain the corresponding TCP and NTCP values to make an overall comparison of the dose-escalation strategy versus an isotoxic radiobiological optimization strategy. Overall, the radiobiologically isotoxic dose escalation strategy comparison plot (TCP vs NTCP plot - figure 5-15) for the NSCLC patient 2 showed that isotoxic radiobiological dose optimization could be very beneficial yielding very favourable therapeutic gains. Due to multiple complications (with opposing response architecture, i.e. rectal bleeding LKB parameter n=0.09 and faecal incontinence n=1) associated with the rectum OAR, isotoxic dose escalation could not be successfully carried on the prostate patient set. Clinically, this is a very important finding as dose-based optimization would not have accounted for multiple toxicity endpoints for a given inverse treatment plan optimization.

Another observation from this analysis is that the use of radiobiological-model-based OAR NTCP as constraints in treatment planning is likely to result in a notable reduction in planning complexity as additional artificial structures required to increase the sparing of organs like rectum may not be necessary (as per the observation of both the RB-plans created for the prostate patient datasets). The probable explanation is that the radiobiological characteristics of the organs concerned are embedded in the NTCP model 'mathematics'. With dosimetric constraints, the solution finding process becomes rather linear (of binary nature) however with the involvement of model-based cost functions a degree of flexibility is available. The correctness of the absolute prediction by models considering the uncertainty associated with model parameters can be questioned. It has been demonstrated that radiobiological model-based plans that are therapeutically better compared to the standard plans, (in terms of TCP, NTCP and dose-based metrics) can be formed using the currently available TCP & NTCP model parameters. Evidence of the effectiveness of this should be sought in clinical trials.

In this work, the effect of not using the orthodox uniform target dose as an objective in the treatment plan of lung and prostate patient datasets was also assessed. Based on the findings of this chapter, treatment plans (DB-plans) without uniform target dose constraints (replaced by a minimum dose to the target and or a D_{95}>Prescription dose) can result in therapeutically better treatment plans that spare OARs and deposit a higher dose into the tumours. None of the plans generated for this analysis exceeded clinically recommended dose tolerance limits and attained the target dose deposition limits set as per the defined clinical trial protocols.

It was observed that for lung patient datasets, RB-plans are superior both in standard dosimetric terms and radiobiological terms. Further, hypofractionated 15-fraction RB-plans are observed to be better than the 20 fraction DB-plans and RB-plans. This provides evidence supporting the results of level-2 iso-toxic dose escalation for the lung cohort in chapter 3 of this thesis where it was found that 15 fractions regimen was superior to 20 fraction regimen for most lung cancer patient datasets. For the prostate patient datasets, it was shown that the RB-plans are therapeutically better than the DB-plans and it was also demonstrated that with the currently available state of art technology, the “uniform target dose” objective should be reassessed clinically. It is acknowledged that for the safety of the patient, the plans formed using any of the methods described (i.e. constraints used for planning) in this chapter should always be vetted in terms of both dosimetric and radiobiological parameters.

Although the RB-plans generated were therapeutically better than the DB-plans (for both lung and prostate cancer patient CT datasets), it is to be noted that delivery of the high dose PTV distribution should be undertaken carefully. A “target miss” due to inter fraction tumour motion or change in the size of the tumour is a practical reality that can result in ineffective treatment causing tumour relapse or high unexpected toxicity due to unnecessary irradiation of OARs. It is recommended that such events be avoided by making use of advance imaging techniques like MRI and or online adaptive radiotherapy. The results of the pilot BIOPROP study reported by Onjukka *et al.* (2017), where the safety of quasi-radiobiologically optimized

treatment plans to boost dose to the PTV (by boosting dose to dominant intra-prostatic lesions in 28 patients) was established, are encouraging.

The absolute value of TCP & NTCP calculations are prone to statistical uncertainties due to uncertainties/robustness of radiobiological model parameters. Current methodology uses absolute values of TCP & NTCP to guide the treatment plan optimizer to find a dose distribution that satisfies set constraints & objectives. It is thus likely that the plan reported here may be sub-optimal. A cautious approach to the implementation of this methodology with critical analysis of such RB-plans in line with routine clinical methodology is recommended. Efforts have been made to ensure that the DB-plans are clinically acceptable, and the RB-plans are analysed in line with constraints and objectives of the DB-plans to ensure that the RB-plans are iso-toxic and efficacious (compared to DB-plans in dosimetric terms as well as radiobiological terms).

Looking to the future, it is strongly advocated that a study with a larger number of patients be conducted to reinforce the findings of this chapter. Further, I envision working on assessing the effects of using different modelling parameters in radiobiological inverse treatment planning to explore the sensitivity of the results in relation to the values of the model parameters.

Chapter 6 Iso-toxic Dose Constraint Conversion

6.1 Introduction

The aim of radiotherapy treatment planning is to create a plan that will deliver the prescribed dose of radiation to the tumour without exceeding the tolerance limits of adjacent OARs. The most up-to-date guidance on the use of OAR tolerance metrics are set out in ICRU Report 83 Section 3.4 (2010); these are based on dose-based metrics such as V_{xx} (%OAR volume receiving at the least dose xx Gy), D_{mean} and D_{max}. ICRU Report 83 also suggests reporting NTCP values in research studies.

In the current chapter, a methodology that converts a physical dose-based metric for one regimen to the corresponding metric for a different regimen is developed. This conversion methodology uses the LKB NTCP model that is well established in the literature in relation to OAR toxicity risk prediction using the OAR DVH. The currently used method to convert constraints across different regimens uses the EQD_2 Wither's formula and is susceptible errors that are discussed in the next section.

The Iso-effect relationship initially developed and proposed by Withers *et al.* (1983) enabled an alternative fractionation regimen to be derived that would generate an equivalent risk of biological damage to the reference regimen. The Withers' formula is as follows:

$$\frac{\boldsymbol{D_{new}}}{\boldsymbol{D_{ref}}} = \frac{\{\mathbf{1}+(\frac{\boldsymbol{\beta}}{\boldsymbol{\alpha}})\boldsymbol{d_{ref}}\}}{\{\mathbf{1}+(\frac{\boldsymbol{\beta}}{\boldsymbol{\alpha}})\boldsymbol{d}_{\mathbf{new}}\}} \qquad \textbf{Eqn. 6-1}$$

The above formula is based on the LQ expression for cell killing and its two key coefficients are α and β. The values for these parameters in the case of tumour clonogens are derived from in-vitro techniques that vary and need standardization as per Chapman (2003,2014). For normal tissues, the α/β ratio has been deduced from fitting observed toxicity data from large trial datasets. The latter method was used by Fowler (1990) and Van Dyk, Mah, & Keane (1989) to estimate the normal

lung α/β ratio. Further, the α/β ratio was assumed to be low (α/β = 3 Gy) for all late responding tissues and high (α/β = 10Gy) for early responding tissues (Mayles, Nahum & Rosenwald, 2007). This is a highly questionable generalization for a number of tissues (e.g. α/β = 1.3-1.8 Gy for the prostate tumour as per a recent publication by Dearnaley & Hall (2017), analysing recently reported prostate cancer clinical trial results).

The α/β-ratio-based BED formula fails to consider the volume effect associated with normal tissue toxicity. Marks *et al.* (2010) suggest that a normal lung tissue α/β ratio = 3 Gy and Michalski *et al.* (2010) suggests α/β=3 Gy for rectal tissue; however, the radiotherapy related toxicity for these tissues are quite different based on 2 Gy/fraction doses. Assume $V_{50\ Gy}$<50% in 2 Gy fraction is used as a constraint in radiotherapy for limiting radiation pneumonitis in lung and rectal incontinence in prostate therapy. Using the LQ based BED formula, an equivalent toxicity-limiting constraint for 3Gy/fraction treatment for both normal lung and rectal tissue will be $V_{42\ Gy}$<50%. Normal lung tissue has been shown to have a parallel architecture [n = 1, Marks (2010)] and the rectum, on the other hand, has a serial architecture [n = 0.09, Michalski (2010)] and thus the radiation based toxicity associated with both these tissues at different doses is likely to be quite different. Thus, the new $V_{42\ Gy}$<50% constraint derived for 3Gy/fraction regimen may not be optimal for the rectum and or the lung tissue. Further, the current BED based V_{xx} conversion method is based on a single point on the DVH and does not account for the range of dose (in a DVH) that contribute to tissue toxicity.

Michalski (2010) suggests that keeping $V_{50\ Gy}$<50% or $V_{60\ Gy}$<35% is likely to minimize rectal bleeding risk to less than 15% in conventional 2 Gy/fraction treatments up to 79 Gy. However, if the $V_{50\ Gy}$<50% in 2 Gy/fraction regimen is converted to a 3 Gy/fraction regimen using the BED formulation, the new constraint would be $V_{41.7\ Gy}$<50%. There is no validation available that shows if using $V_{41.7\ Gy}$<50% considering 3 Gy/fraction plan is iso-toxic to $V_{50\ Gy}$<50% used for 2 Gy/fraction plan in terms of assessing rectal bleeding risk. One may certainly argue that based on the results of CHIPP trial, the observed average rectal bleeding toxicity in 2Gy/fraction arm (using $V_{50\ Gy}$<60% constraint) was the same as average toxicity of 3Gy/fraction regimen

(using the $V_{40\,Gy}$<60%) whereas for the HYPRO trial regimen the difference in average GI toxicity between the 2 regimens was 6% (and 8% in the case of the Fox Chase regimens) (Dearnaley & Hall, 2017).

A validity of EQD_2 based conversion is questioned as it fails to account for the considerable variation in dose range observed in a DVH (i.e. lowest to highest dose in the DVH) and relies on a single point on the DVH to form an iso-toxic equivalent constraint. High uncertainty around these calculations is suspected as the biological behaviour of the OAR is not accounted for in the Wither formula based conversion method. LKB NTCP models allow one to address the above concerns and thus is employed in the development of a new Iso-toxic parameter conversion method. The next section describes the methodology employed.

6.2 Methodology

In this chapter, a method is developed to convert a V_{xx} 'dose-limiting' normal-tissue DVH parameter from one ('standard') dose-fractionation regimen to an alternative regimen. The principle followed here is that the fractional volume for a fixed dose level can be modified to account for changed fractionation. This differs from the standard approach in which the fractional volume is fixed and the dose level is modified according to the BED expression. A comparison between both the methods to convert constraints across different regimens is presented in the discussion section. The lung cancer patient database (or cohort) consists of around 59 DVH datasets, with dose prescriptions in the range 52.5-55 Gy with fraction sizes around 2.6-2.75Gy. For prostate cancer, there are approximately 56 patients in the database/cohort and these were prescribed 60-62 Gy in 20 fractions. The prescription dose range quoted was estimated by calculating the mean dose to the PTV DVH for each of the patient DVH datasets as I was provided only with anonymised DVH datasets and no other information about the DVHs. The DVHs for normal lung, oesophagus, spinal cord and / or heart (OARs) were available for the lung cohort. For the prostate cohort, the DVHs of bladder, rectum and femoral heads were available.

The LKB NTCP model was used for the purpose of this analysis. The parameters used for the LKB NTCP model are shown in Table 6-1.

Table of L-K-B NTCP model parameters						
	>= Grade 2 complications	TD50 (cGy)	n	m	a/b (Gy)	Reference
Lung Cancer	Radiation Pnuemonitis	31.40 (29-34.7)	1	0.45(0.39-0.51)	3	Marks et al. (2010)
	Oesophagitis	51 (29–82)	0.44 (0.11–1.41)	0.32 (0.19–0.57)	3	Chapet et al. (2005)
Prostate Cancer	Rectal Bleeding	76.9 (73.7–80.1)	0.09 (0.04–0.14)	0.13 (0.10–0.17)	3	Michalski et al.(2010)
	Faecal Incontinence	105 (90–138)	1	0.43 (0.38–0.49)	3	Peeters et al. (2006)

Table 6-1 The table of NTCP model parameters used for the purpose of the calculations in this chapter

The Marks *et al.* (2010) paper recommends V_{20}<30% as an acceptable planning constraint in relation to lung radiation pneumonitis. Similarly, for spinal cord and heart, D_{max} and $V_{25\text{-}40}$ have been shown to correlate with spinal cord complications and pericarditis incidence respectively. The corresponding parameters for rectal complications and bladder complications are V_{35} & V_{50} respectively [V_{20}, V_{35}, V_{50} correspond to % volume of OAR receiving at least 20, 30 or 50 Gy respectively].

All patient DVHs for a given OAR are loaded into an in-house algorithm that calculates the specified V_{xx} and the NTCP of the DVH for a given dose-fractionation schedule and model parameters. As an example, consider the standard lung cancer cohort prescribed 55 Gy in 20 fractions. The normal lung DVH (Total lung-GTV) was analysed to assess the risk of radiation pneumonitis, i.e. the NTCP. The program is supplied with the 55 Gy prescription dose (D_{pres}), 20 fractions and the DVH as input. The V_{20} from the DVH and the corresponding NTCP (LKB model) are then calculated. A plot of V_{20} versus the NTCP for all the patients in the database receiving 55 Gy in 20 fractions was produced. Using this plot, the NTCP value corresponding to the V_{20}≈30% for lung radiation pneumonitis is found. Each point on the plot represents a patient DVH dataset whose V_{xxGy} and NTCP is calculated to form the plot.

Now it is assumed that there is a change in treatment schedule and a new prescription dose (D_{pnew}) fraction scheme is proposed (say 40 Gy in 15 fractions). The mean dose of the OAR is changed by multiplying all the doses in the DVH by the factor ($D_{pnew/}$ D_{pres}). For the NTCP calculations corresponding to these converted DVHs, the standard correction for fraction size is made to the DVH doses using the EQD_2 correction, exactly as for the NTCP calculations belonging to the standard fractionation regimen. A second plot of V_{20} versus NTCP is thus created.

NTCP vs V_{xx} datasets are then plotted for both regimens on a single graph. Further, Matlab's linear regression graphical-user interface was used to fit a polynomial, exponential or power law expression to the datasets to yield a function forming best co-relation between V_{xx} and NTCP of the given regimen. The regression uses robust fitting and the fitting procedure explores the best fit of the models based on R-squared, Adjusted R-squared and root mean squared error goodness-of-fit model parameters. Thus, a function is derived as below

$$\mathbf{NTCP = f(V_{xx}) \text{ for each regimen}}$$

Now, V_{xxA} of regimen A gives a corresponding $NTCP_A$ which is used to calculate V_{xxB} in regimen B using the function derived above. The best model fit over the given data is accepted (per the criterion in section 6.2.1).

$$\mathbf{V_{xxB} = f^{-1}(NTCP_B) \text{ such that } NTCP_A = NTCP_B} \qquad \textbf{Eqn. 6-2}$$

For model fitting, exponential and polynomial (2nd Order) models were used. The equations for the respective models are given below.

For the exponential model, the equation was

$$\mathbf{f(x) = a*e^{(b*x)}} \qquad \textbf{Eqn. 6-3}$$

For the polynomial model the equations were

$$\mathbf{f(x) = p_1*x + p_2 \ (1^{st} \text{ Order})} \qquad \textbf{Eqn. 6-4}$$

$$\mathbf{f(x) = p_1*x^2 + p_2*x + p_3 \ (2^{nd} \text{ Order})} \qquad \textbf{Eqn. 6-5}$$

To find the V_{xx} for a given NTCP value, the $f^{-1}(x)$ of the above functions were calculated. Graphically, similar results can be achieved by dropping horizontal and vertical lines from both the curve-fit trend lines. Going back to the example, V_{20} for the D_{pres}-based regimen was 27% corresponding to 17% NTCP, then the same NTCP on the (V_{20} v NTCP) plot for D_{pnew} would yield the equivalent value of $V_{20\,Gy}$ for the new scheme (e.g. as shown in fig 6-3).

$V_{20\,Gy}$ vs NTCP plots were created for various treatment schedules: 55Gy20#, 60Gy30#, 70Gy30# and 40Gy15#. A similar analysis was performed on the prostate tumour DVH dataset to find iso-toxically equivalent $V_{50\,Gy}$ for 62Gy20#, 80Gy40#

(Arcangeli *et al.*, 2012) and 70Gy28# (Kim *et al.*, 2014; Kupelian*et al.*, 2007) as used in some of the recent clinical trials. These regimens were selected randomly to assess the utility of this method over a broad range of schedules. This procedure enables conversion between various regimens iso-toxically (Iso-NTCP). The results section shows the data and the line fits along with the trend lines for Grade 2 or > radiation pneumonitis & oesophagitis for lung cancer data, and Grade 2 or > rectal bleeding & faecal incontinence for prostate cancer cohort data.

6.2.1 Goodness-of-fit

The adjusted R^2 and RMSE value were used to assess the goodness-of-fit of the regression line forming the V_{xx}-NTCP co-relation. Adjusted R^2 accounts for the number of independent variables forming the model fit. Thus, if the fitting exercise makes use of excess variables to form better fits the adjusted R^2 value decreases. This helps ensure the model is simple yet a good fit to the data. Adjusted R^2 is expected to be in a range of 0 to 1 whilst RMSE (root mean squared error) is expected to be as small as possible.

The criterion used to reject a curve-fitting is based on R-Squared, Adjusted R-Squared and RMSE values for each fitting parameter. R-Squared & Adjusted R-Squared are expected to be closer to 1 and fitting is rejected for R-Squared or Adjusted R-Squared less than 60% with RMSE higher than 15. There are no set guidelines for rejecting a model except for R-Squared & Adjusted R-Squared equal 0 and RMSE equal to infinity. For a perfect fit, RMSE will be zero; however, there is no upper bound / recommended absolute limit suggested for it. The choice of these parameters reflect the accuracy that is aimed to be achieved out of the fitting exercise.

6.3 Results

6.3.1 Lung Cohort

As stated in the methodology section, the V_{xx} vs NTCP plot for various regimens used in lung cancer radiotherapy for radiation pneumonitis risk is presented.

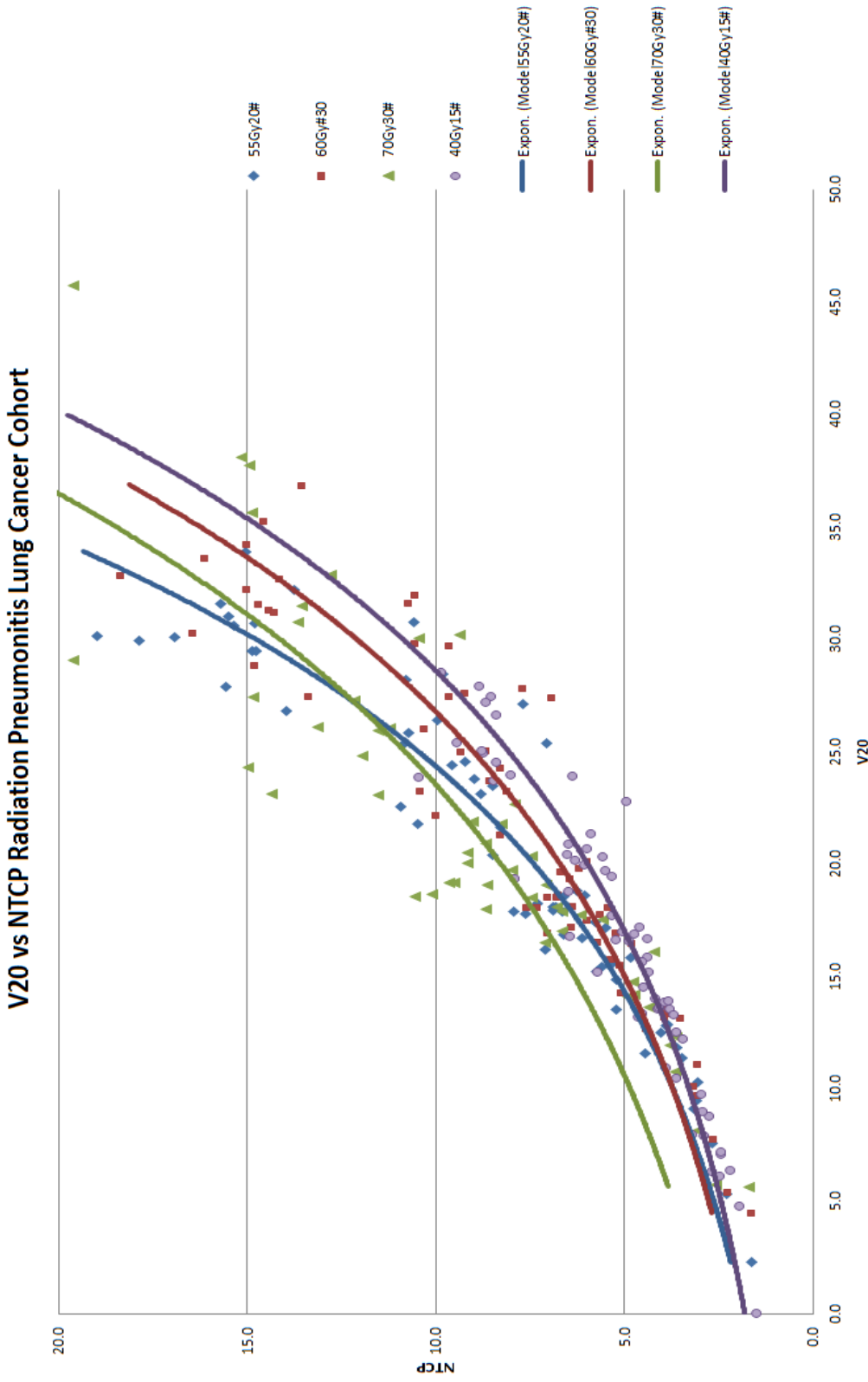

Figure 6-1 The figure shows the V_{20} vs NTCP data for Radiation Pnuemonitis complication. The figure also shows fitted line curves that model the relationship between V_{20} and NTCP for 55Gy in 20#, 60Gy in 30#, 70Gy in 30# and 40Gy in 15#.

Figure 6-2 (a, b, c, d) show the line fitting of V_{20} vs NTCP dataset for 55Gy20#, 60Gy30#, 70Gy30# & 40Gy15# shown in figure 6-1 above.

Table 6-2: The goodness of fit parameters of R-Squared, Adjusted R-Squared and RMSE are shown in the table for the line fits of figures 6.2(a-d)

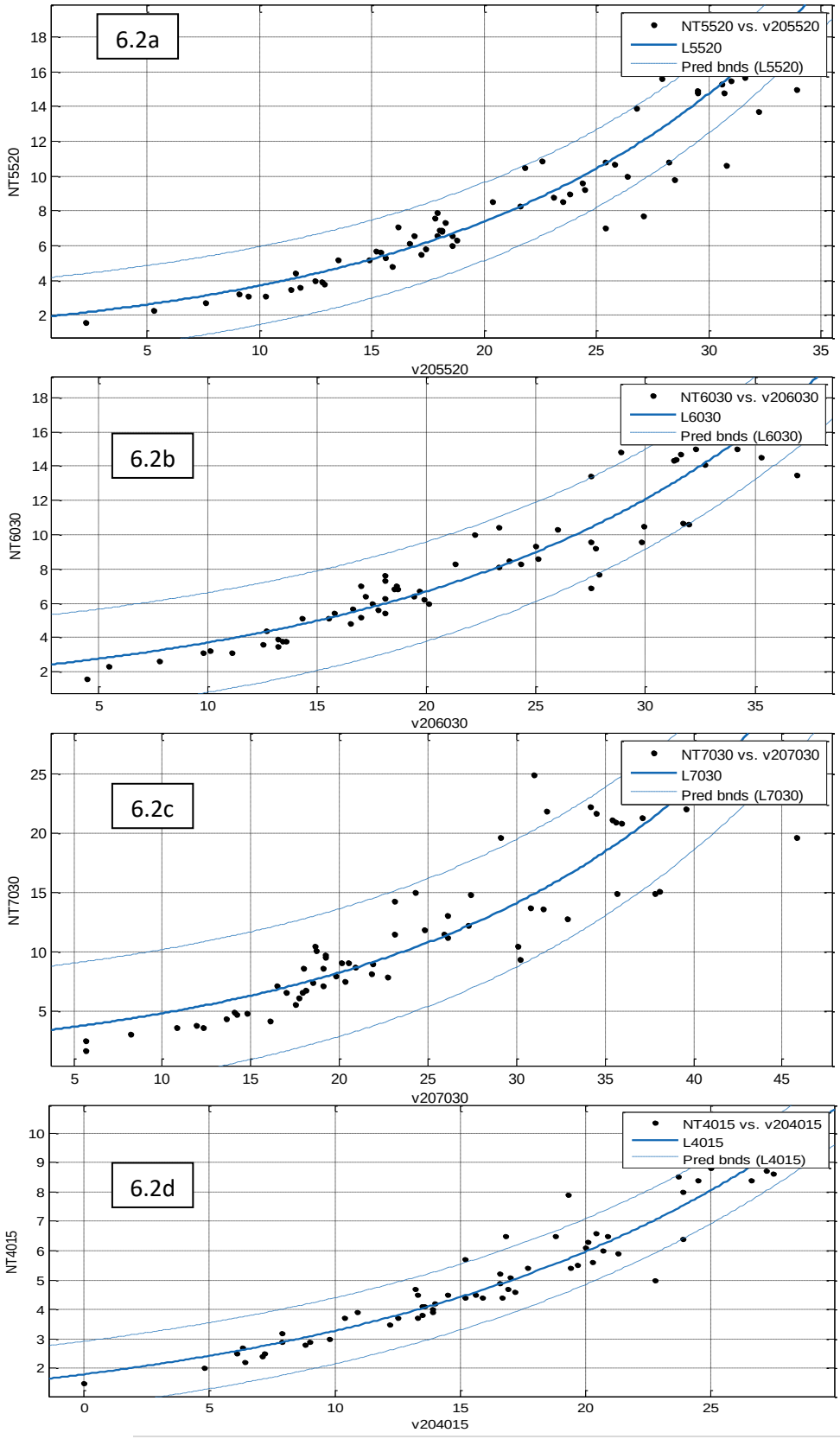

Table 6-2

Model												
Exponential (a*e^bx)												
s with 95% Confidence Bounds												
	Model	SSE	R-Squared	Adjusted R-Squared	RMSE	a	Lower bound	Upper bound	b	Lower bound	Upper bound	
55Gy20#	exp1	75.080	0.936	0.935	1.109	1.857	1.597	2.116	0.069	0.064	0.074	
60Gy#30	exp1	125.900	0.881	0.879	1.437	2.056	1.692	2.421	0.059	0.053	0.065	
70Gy30#	exp1	432.300	0.831	0.829	2.662	2.832	2.256	3.408	0.054	0.048	0.059	
40Gy15#	exp1	18.730	0.938	0.937	0.554	1.803	1.629	1.977	0.060	0.055	0.064	

Figure 6-3 shows a graphical method of Iso-NTCP conversion of V_{20} from 55Gy in 20# regimen (using NSCLC cohort data) to 60Gy in 30#, 70Gy in 30# and 40Gy in 15#.

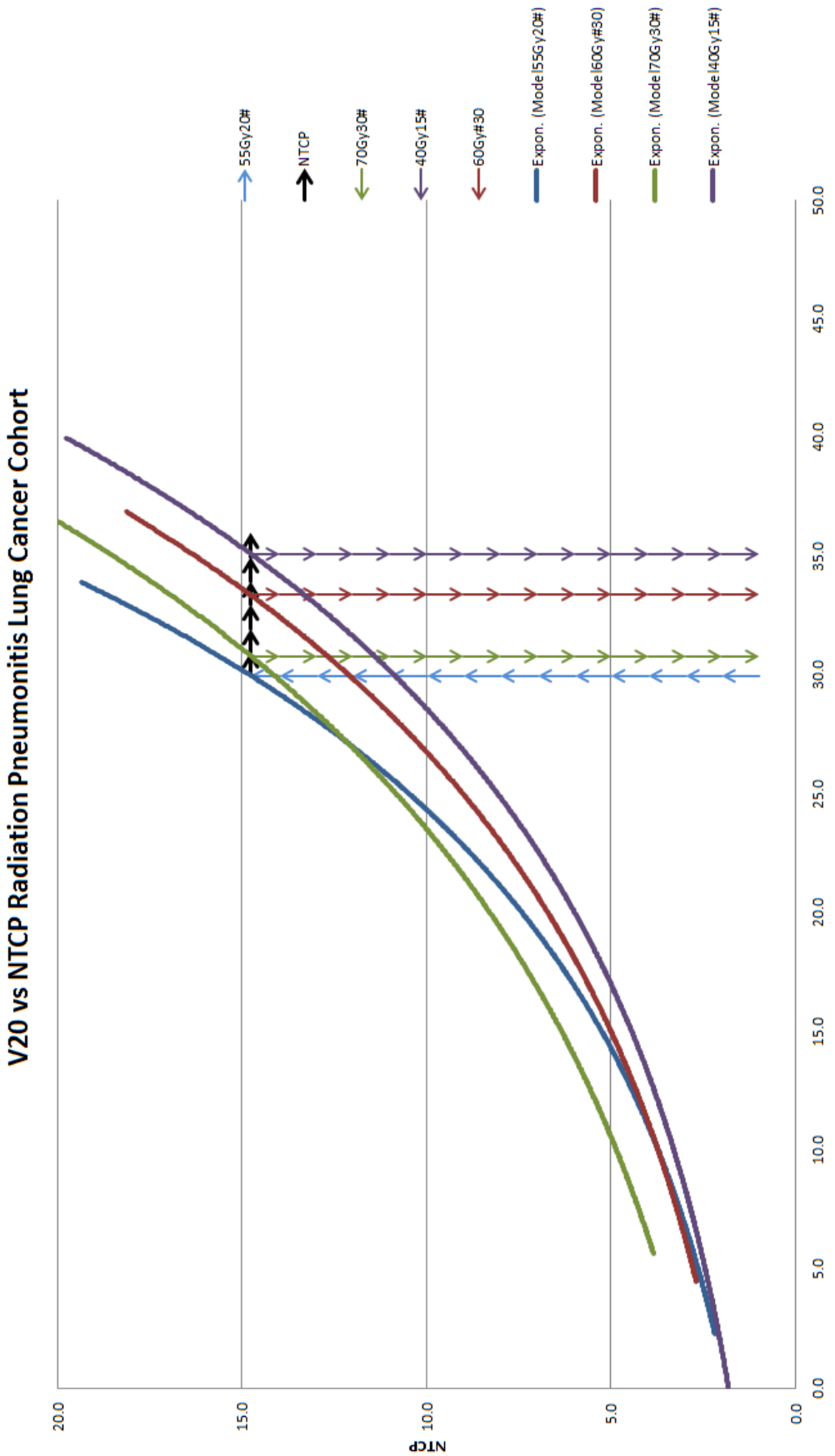

Fig 6-3 The figure shows the Iso-NTCP conversion method for converting V_{20} among four different regimens. We take 55Gy in 20# as the reference regimen and use the blue arrowed line (representing V_{20} for 55Gy20# regimen) to find the Iso-toxic NTCP. Drawing a horizontal line at that Iso-NTCP value gives the relevant Iso-NTCP intersection points for other regimens. Dropping a perpendicular from these intersections provides with the equivalent V_{20} in those regimens. This is the graphical method that can be used to quickly assess the equivalence with less accuracy. The mathematical version is explained in methodology section which can give precise answers. Here V_{20} 30% for 55Gy in 20# corresponds to Iso-NTCP V_{20} of 33.4%, 30.8% and 35.1% for 60Gy in 30#, 70Gy in 30# and 40Gy in 15# regimens.

Figure 6-4 shows the V_{35} – NTCP Analysis for the oesophagitis complication. This is represented in a similar way as for the radiation pneumonitis complication.

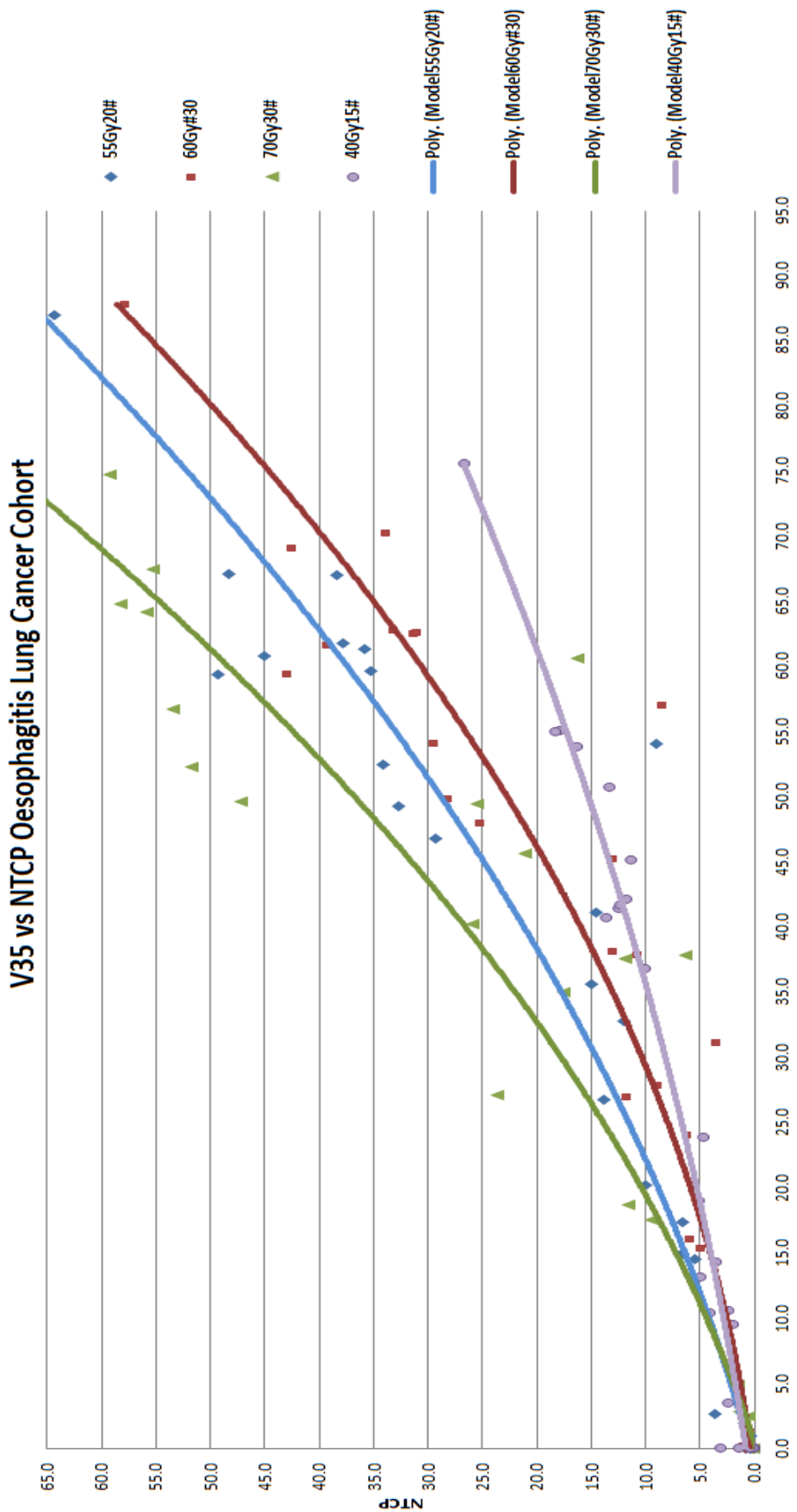

Figure 6-4 shows the V_{35} vs NTCP data for Oesophagitis complication >= grade 2. The figure also shows fitted line curves that model the relationship between V_{35} and NTCP. Further, a sample Iso-Toxic NTCP based conversion of V_{35}=30% for 55Gy20# to 60Gy30#, 70Gy30# and 40Gy15# regimens is shown. A V_{35} of 30% in 55Gy20# equals to V_{35} of 37.6, 25.9 & 48.5 for 60Gy30#, 70Gy30# and 40Gy15# regimens.

Figure 6-5 The linear regression based line fits of V35-NTCP data for each regimen are shown in Figures 6-5 (a, b, c, d) below. Table 6-3 provides fitting co-efficient and goodness-of-fit information for each of the line fits shown in Figure 6-5.

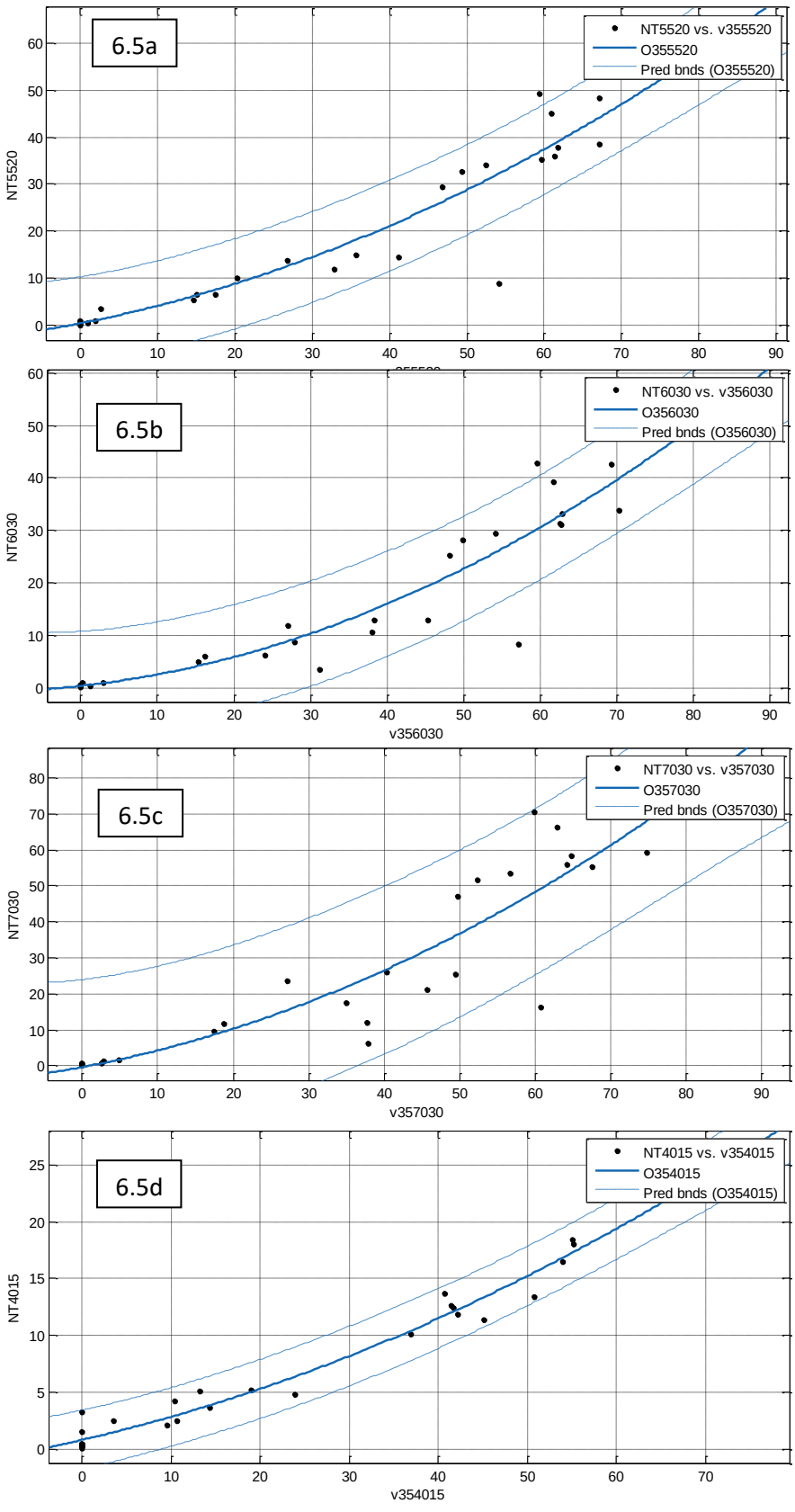

MATLAB FIT	Parameters	Model	SSE	R-Squared	Degree of Freedom	Adjusted R-Squared	RMSE	No of Coef	p1	Lower bound	Upper bound	p3	Lower bound	Upper boun
O354015	NT4015 vs. v354015	poly2	35.392	0.973	24.000	0.971	1.214	3.000	0.002	0.001	0.003	0.813	0.029	1.597
O355520	NT5520 vs. v355520	poly2	482.487	0.948	24.000	0.944	4.484	3.000	0.005	0.002	0.008	0.456	-2.936	3.849
O356030	NT6030 vs. v356030	poly2	525.424	0.927	24.000	0.921	4.679	3.000	0.006	0.003	0.009	0.363	-3.474	4.200
O357030	NT7030 vs. v357030	poly2	2839.411	0.850	24.000	0.838	10.877	3.000	0.007	0.000	0.014	-0.354	-9.692	8.983

Table 6-3

Figure 6-6 below shows the Iso-NTCP based graphical method of converting V_{35} from 55Gy in 20# reference regimen to 60Gy in 30#, 70Gy in 30# and 40Gy in 15# schedules for oesophagitis complication >= grade 2 in lung cancer radiotherapy

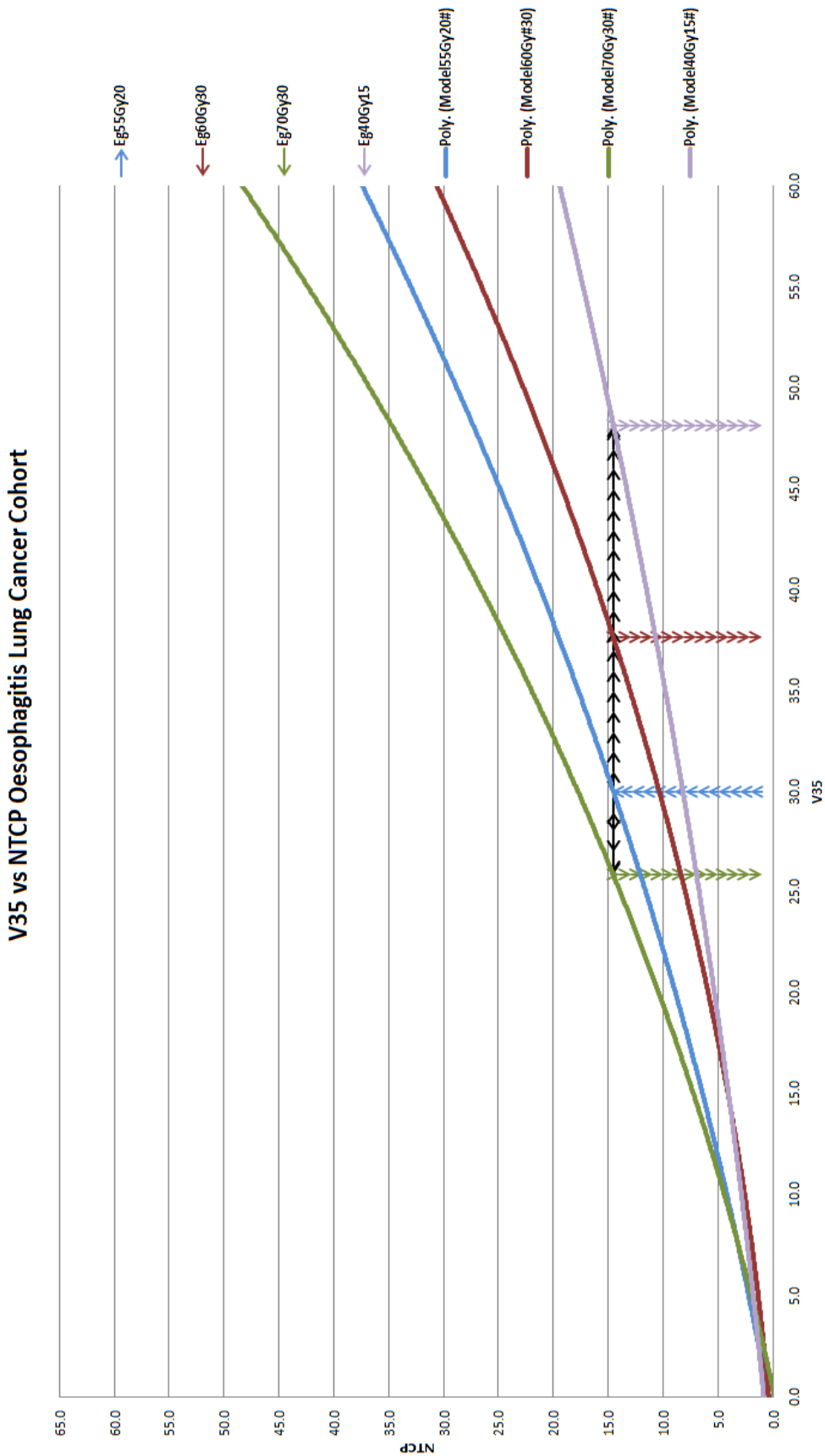

Fig 6-6 The figure also shows the fitted line curves that model the relationship between V_{35} and NTCP. Further, a sample Iso-Toxic NTCP based conversion of V_{35}=30% for 55Gy20# to 60Gy30#, 70Gy30# and 40Gy15# regimens is shown. A V_{35} of 30% in 55Gy20# equals to V_{35} of 37.6%, 25.9% & 48.5% for 60Gy30#, 70Gy30# and 40Gy15# regimens.

6.3.2 Prostate Cohort

In this section, the result of the V_{xx}- NTCP conversion for the toxicity endpoints rectal bleeding (Fig. 6.7a) and faecal incontinence (Fig. 6.7b) encountered after prostate radiotherapy are displayed. The analysis is performed in the same manner as for the lung tumour cohort.

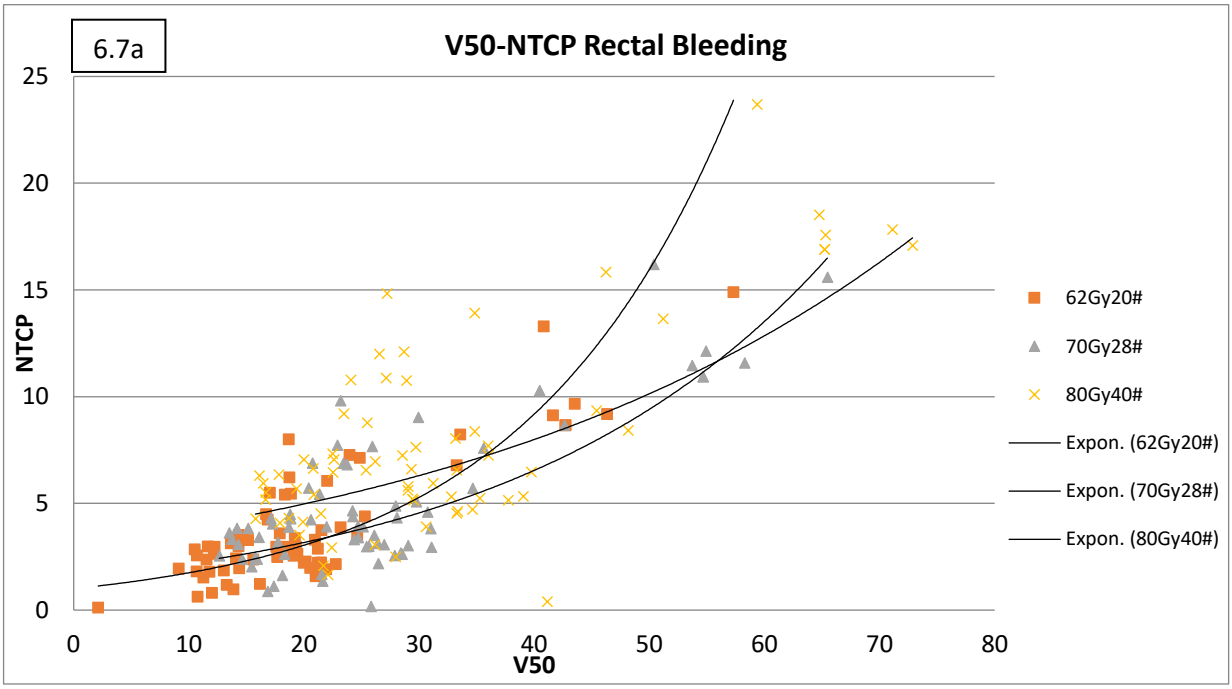

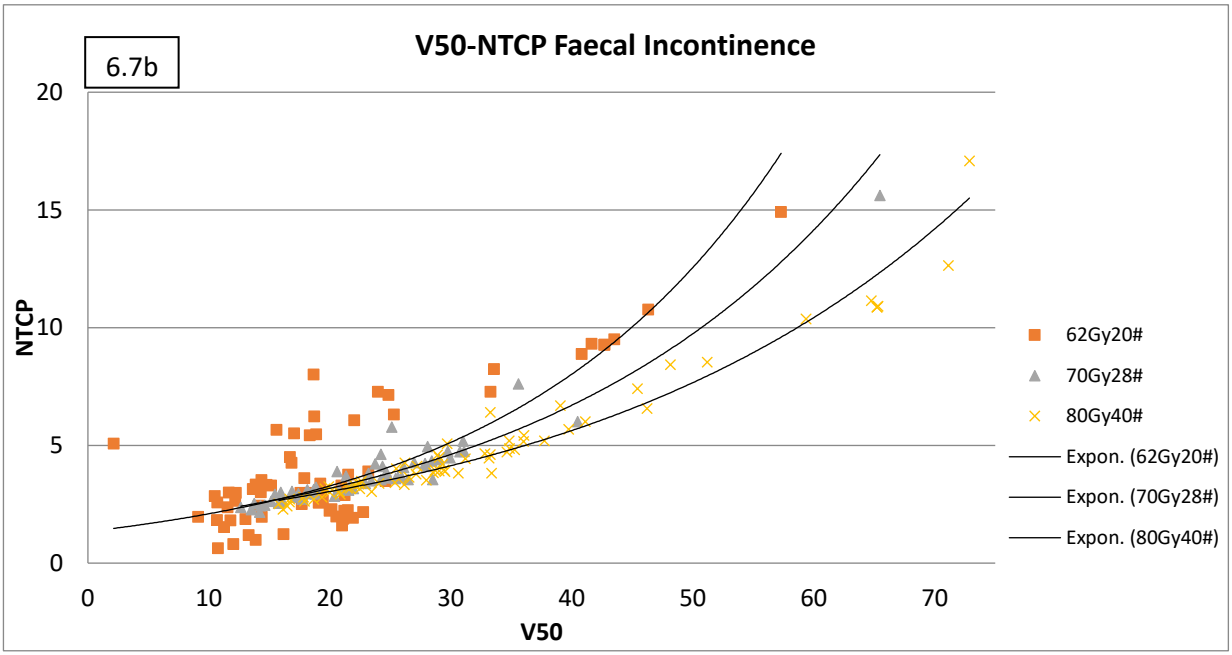

Figure 6-7 The V_{xx}-NTCP conversion for prostate cancer related OAR toxicities. The regimens considered are 62Gy20#, 70Gy28# and 80Gy40# a) V_{xx}-NTCP conversion for the rectal bleeding endpoint b) Vxx-NTCP conversion for the faecal incontinence endpoint.

The fits to the data correlating V_{50} and NTCP (rectal bleeding & faecal incontinence) are assessed using the Adjusted R-Squared and RMSE values associated with the fits. These are shown in table 6.4.

Regimen	Rectal Bleeding		Faecal Incontinence	
	Adjusted R-Squared	RMSE	Adjusted R-Squared	RMSE
62Gy20# (Arcangeli *et al.*, 2012)	0.778	1.374	0.691	1.560
70Gy28# (W. R. Lee et al., 2016)	0.730	1.759	0.981	0.350
80Gy40# (Arcangeli *et al.*, 2012)	0.643	2.812	0.981	0.384

Table 6-4 The line fitting goodness-of-fit parameters for different regimens for line fits in figure 6.7 (a,b).

The adjusted-R squared values and RMSE values indicate a good fit of the exponential model to the data as per the criteria defined in section 6.2.1 in the methodology section. Using the fitted models, it was calculated that for the rectal bleeding toxicity endpoint $V_{50\,Gy}$=50% for a 70Gy in 28# regimen is equivalent to $V_{50\,Gy}$=41.2% for 62Gy in 20# and $V_{50\,Gy}$=44% for 80Gy in 40#.

Faecal incontinence is another endpoint associated with the rectum with respect to prostate radiotherapy side effects. The Isotoxic V_{50}=50% for the 70Gy in 28# regimen which is equivalent to V_{50} = 41.70% for 62Gy in 20# and to V_{50}=56.34% for 80Gy in 40#.

It can be seen that for the same OAR, two endpoints with different biological responses to radiation exposure can be accounted for using this conversion method (figure 6.7a & b). If purely dose-based metrics had been used, the clinicians would have used the $V_{50\,Gy}$<50% as the dose constraint for limiting dose to the rectum. This constraint gives the recommended dose tolerance to avoid rectal bleeding only and does not account for faecal incontinence (which is also a side effect of radiotherapy related to the rectum).

6.4 Discussion

In this section, a critical view of the methodology employed is discussed. The results are then discussed and analysed including a justification of the use of radiobiological modelling to estimate equivalent V_{xx} for different regimens.

The absolute error in LKB NTCP model predictions is dependent on the robustness of fitted model parameters. The more robust the parameters, the better are the predictions. Two important aspects define the robustness of a given model. One is the statistical uncertainty surrounding the parameters used to fit a given model to clinical outcomes and the second is the quantity and quality of the data used to produce the parameters for fitting the model. When using NTCP models with a given set of parameters, the accuracy of prediction improves if the cohort for whom predictions are made is similar (possibly the same prescribed treatment, tumour type and staging) to the original cohort whose data were used to derive estimates of current parameters. The parameters used for each of the models along with their references are shown in Table 6-1.

The technological changes in treatment planning and delivery has improved OAR dose sparing and improved dose uniformity in the target. As NTCP models are empirical, a periodic review and update of model parameters based on the latest clinical outcome data is important to reduce the absolute error in model predictions. The latest LKB NTCP model parameters for radiation pneumonitis were available from Marks *et al.* (2010) in the Quantec set of review papers recommending dosimetric and radiobiological model parameters related to OAR complications.

For oesophagitis NTCP models, Chapet *et al.* (2005) and Belderbos *et al.* (2005) each published parameters that were broadly within each other's confidence intervals. Chapet *et al.* (2005) parameters were selected as their 'power of study' was the higher of the two.

NTCP model parameters for the late rectal bleeding endpoint were published in the Quantec review by Michalski *et al.* (2010), Gulliford *et al.* (2012) and D'Avino *et al.* (2015). The reported parameters (at least one of TD_{50}, n, m) differed from one

publication to the other. The Quantec NTCP model parameter set was selected for the current analysis as the Quantec papers were comprehensively peer-reviewed.

For faecal incontinence, Defraene *et al.* (2012) and Peeters *et al.* (2005) published LKB NTCP model parameters. However, the Peeters *et al.* (2005) parameter set was selected as the 95% confidence interval limits for TD_{50}, *n* and *m* were significantly narrower compared to the other publication by Defraene *et al.* (2012), indicating a better fit.

It is to be noted that the choice of model parameters is likely to affect the overall results of this method but if the data used for analysis is representative (in terms of similar planning technique & OAR position at the least) of the datasets used to form model parameters, the errors are likely to be small. Thus, validation of the model parameter set selected for analysis is crucial in order to minimize errors associated with this technique. An analysis on these lines using a larger set of data should allow quantification of the variation in results of this method if different representative model parameter sets are used for analysis.

Figure 6-1 shows the plots of V_{20}-NTCP for four radiotherapy lung cancer prescription regimens. The solid lines (blue, red, green and purple) represent the exponential-model fits to the data points in the graph for the respective regimens. Figure 6-2 shows the individual regression-line fits with the 95% confidence interval limits indicated. Table 6-1 gives parameters that help assess the goodness-of-fit of the line fitting.

For the V_{20}-NTCP Lung cohort analysis of radiation pneumonitis toxicity, the minimum 'Adjusted R-squared' value is 0.829 which indicates an acceptable fit (combined with an RMSE of 2.66 & relatively wider 95% confidence interval prediction bounds). The highest value of 'Adjusted R-squared' is 0.937 (with RMSE 0.56 and relatively narrow 95% confidence interval prediction bounds) indicating a robust fit. A V_{20} of 30% corresponds to 16+/-1% probability of radiation pneumonitis occurrence (1% error is formed by rounding the 0.56% RMSE value of the model fitting). Based on a dataset of 100 patients Wang *et al.* (2013) showed that MLD was highly correlated with radiation pneumonitis risk whereas V_{20Gy} was not. This

contradicts Marks *et al.* (2010) who provide a stronger, critically evaluated evidence to support a correlation between V_{20} and radiation pneumonitis risk.

Similarly, for oesophagitis, the V_{35Gy}-NTCP correlation raw data points along with the fitted regression-based models are shown in Figure 6-3**.** The individual regression line fits with 95% confidence intervals and goodness-of-fit data are shown in Figure 6-3 and the associated Table 6-2. The lowest adjusted R-squared value is 0.838 (along with RMSE of 10.87 and relatively wide 95% confidence interval bounds) for the 70 Gy in 30 fractions regimen. The RMSE of this line fit is relatively large which indicates high variance but not necessarily a poor fit. This can be caused by outliers that affect the model fits and represents one of the pitfalls associated with this method.

The iso-BED based method and iso-NTCP based method use the concept of iso-effectiveness to convert the constraint but these methods convert the constraint in different ways making direct comparison difficult but challenging. As an example, V_{20}<30% paired lung volume is taken here. As per table 6-5, it can be seen that the iso-BED method changes the dose part of the constraint ('xx' of V_{xx} is affected and percentage volume remains constant).

Table 6-5 BED based Iso-effective constraints of V_{20}<30% radiation pneumonitis constraint for different regimens.

Regimen	BED Dose	Effective Constraint (BED based)
60Gy30#	20	V_{20}<30%
55Gy20#	17.4	$V_{17.4}$<30%
40Gy8#	12.5	$V_{12.5}$<30%
48Gy4#	6.7	$V_{6.7}$<30%
60Gy3#	4.3	$V_{4.3}$<30%

Figure 6-8 Iso-BED based constraint conversion and relative error on NTCP calculations. V_{20}<30% constraint for radiation pneumonitis prediction and its Iso-BED equivalent in other regimens compared using NTCP modelling

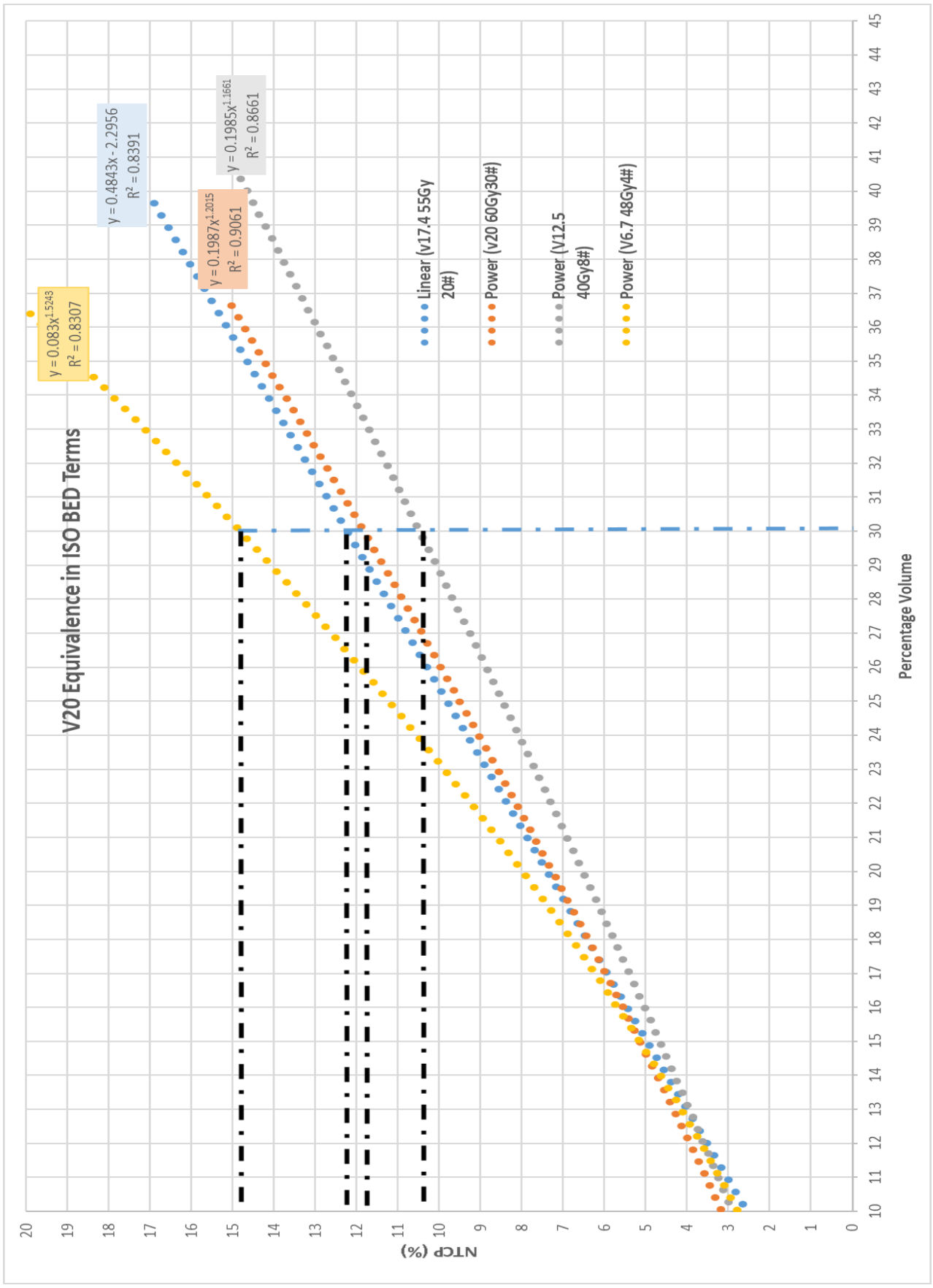

If the Iso-NTCP technique is used the percentage volume part of the constraint changes. Thus, direct comparison of these methods against each other is problematic. However, the aim was to show how the iso- effective BED-based method brings variations in overall NTCP and that the conversion method is not iso-toxic. The BED-based conversion of parameters between regimens simply converts the DVH dose scale using the EQD_2 formulae which is a linear correction and does not account for the volume effect contributing to the complication in the OAR. Table 6-5 shows the BED based equivalent constraint derived for various regimens (3D CRT, VMAT & SABR regimens) for the 2 Gy equivalent dose constraint used to limit radiation pneumonitis ($V_{20\,Gy}$<30%). If the Iso-BED based constraints were iso-toxic, plotting curves of V_{xx} versus NTCP for all the DVHs (after scaling the total dose and correcting for the fractionation effect) would be aligned for different regimens. It is also expected that iso-effective constraints for different regimens should yield a constant NTCP. However, plotting the graph of NTCP and V_{20} (for 60Gy20#), $V_{17.4}$ (for 55Gy20#), $V_{12.5}$ (for 40Gy8#), and $V_{6.7}$ (for 48Gy4#) it was seen that the line fits were not aligned indicating that Iso-BED based conversion is not isotoxic. Examining figure 6.8, it can be observed that NTCP does not remain constant, varying by an average of 4-5% when effective constraints (calculated using the BED method) are assessed for different regimens. The variation increases for an increase in %volume associated with the constraint. However, it is also noted that for smaller changes in total dose or dose/fraction, the difference in NTCP is minimal (i.e. if the OAR was parallel in nature).

The NTCP models are organ-specific and moderately well established. Increase in dose affects the complication probability in the OAR in a sigmoid fashion governed by the serial/parallel architecture of the organ. The NTCP-based method proposed here accounts for different types of side effects (acute / late / grade 1/2/3) the organ is likely to suffer due to an increase in dose and fraction number or fraction size. Using the proposed method, the V_{xx} conversion between various regimens can be performed as long as robust NTCP parameters and representative datasets are available for a given complication. It is also important to note that one of the pitfalls

of this method is the requirement of data to fit models well to be able to undertake this analysis.

It is acknowledged that there is still room for improvement in the predictive power of the models. However, when comparing two different regimens the relative error contributed due to use of the same NTCP model is minimal. The absolute error in this method is attributable to the robustness of line fits indicated by the RMS value which for radiation pneumonitis (V_{20} constraint conversion fitting for four regimens in Table 6.2) was average 1.44 and 1.9 for the rectal bleeding fitting (shown in Table 6.4). This method of fitting, encompassing a larger set of data points (DVH datasets), over varying tumour sizes is likely to yield a representative output allowing one to form a chart for converting standard V_{xx} constraints. Also, undertaking this analysis over DVH datasets generated by techniques like IGRT/IMRT are likely to yield different results compared to the results formed using data from DVHs generated from 3D-CRT plans. This is because complication rates observed in IMRT/IGRT are lower than 3D-CRT; which is attributable to improved OAR sparing achieved by IMRT/IGRT plans. This is observed when studying outcomes of the recent & past reported prostate cancer trials (Dearnaley & Hall, 2017).

The aim of this chapter is to provide a method for radiotherapy professionals to quickly and efficiently determine the change in V_{xx} corresponding to a change in treatment regimen. As discussed in the methodology section and showcased in the results section, there are two slightly different but complementary techniques for converting $V_{xx\,Gy}$ from one regimen to another on an iso-NTCP basis. The first method uses the $f^{-1}(x)$ of the regression model functions. However, this requires some calculation effort (e.g. software for efficient calculation). The second method is graphical and requires only a pencil and a scale to convert $V_{xx\,Gy}$ from one regimen to another. It is emphasised that this conversion method should be used to find estimates rather than absolute equivalents of V_{xx} in different regimens.

6.5 Clinical Relevance, Conclusion & Future Work

In this chapter, a new method of converting dosimetric OAR planning constraints, of the form $V_{xx\,Gy}$, from one fractionation regimen to the other has been presented. A critical analysis of the currently used BED formula-based method was done initially.

It is accepted that the BED method is simpler. The method introduced here (iso-NTCP) accounts for the radiobiology of the OAR as expressed through the LKB NTCP model with parameters specific to the complication endpoint. The graphical method employed is also relatively simple and efficient. It is acknowledged that the formation of V_{xx} – NTCP plots and relative fitting is likely to be affected by the treatment modality of the derived data. However, if the data used to form the plots is representative of the treatments under analysis, the currently proposed method can provide an efficient way for clinicians to iso-toxically convert $V_{xx\,Gy}$ across different regimens.

It is recommended that studies involving larger pools of data that are homogeneous (in terms of treatment modality) be used to form robust, endpoint- and regimen-specific $V_{xx\,Gy}$ NTCP conversion tables/charts.

Chapter 7 Conclusions

'Individualization and optimization of radiotherapy treatments using radiobiological models' is the core theme of this research. The focus has been on three different methods to individualize and optimize radiotherapy; additionally, a new method to Iso-toxically convert dose-volume-based metrics from one fractionation regimen to another is presented. The Marsden TCP model and the Lyman-Kutcher-Burman NTCP model were used to perform all the analyses. Multiple OAR complications (for both lung and prostate tumour treatments) were accounted for to make the analysis as clinically relevant as possible. Anonymised DVH datasets of previously treated cancer patients were obtained from the Pinnacle and Eclipse treatment planning systems. The algorithms used for the analysis in each chapter were developed in-house and programmed in the MATLAB environment version 2015B. The TCP & NTCP computations by the in-house software were quality checked against the published Biosuite software and against the *Raystation* TPS.

In chapter 3, Iso-toxic treatment individualization has been further developed through the creation of a software that analyses large sets of patient cohort data. For the lung-tumour cohort, an average improvement in TCP of 16% (level 1 at 20 fractions) and 19% (level 2 at 15-17 fractions) compared to the current 55Gy in 20 fractions regimen was obtained at the same 8.6% NTCP. It was found that 15-17 fractions yielded the highest therapeutic gain for the lung cohort. For the prostate tumour cohort, assuming α/β=10 Gy, and at 10% $NTCP_{pop}$, level 1 (20 fractions) & level 2 (50 fractions) dose individualization yielded TCP gains of 0.72% and 12.6% respectively compared to standard dose escalation (level 0). Assuming α/β=1.5 Gy, it was found that, also at 10% NTCP, level 2 optimization yielded a 9.7% increase in TCP_{pop} over level 1 (20 fractions) optimization and nearly average 10% increase in TCP_{pop} compared to level 0 optimization. At α/β=10 Gy and at α/β=5 Gy, 50 fractions (the maximum number investigated) yielded the highest therapeutic ratio, (TR) whereas for α/β=1.5 Gy the highest TR was for one single fraction. In either case, level-2 individualization significantly improved the TCP compared to level 1 and level 0. Analysis based on varying the parameters for the same tumour type

showed a large variation in the optimization results (e.g. fig 3-15 – level 2 optimized TCP for two sets of lung tumour parameters shows 8-10% variation at 8.6% NTCP) and this emphasizes the vulnerability of models to the quality of input parameters. In all cases, the use of radiobiological-model-based level 2 individualization yielded superior outcomes compared to current regimens for lung and prostate cancer radiotherapy treatments.

Selector & optimizer programming modules (chapter 3) and the 'RadOpt' software were built to perform the analyses. These modules optimize tumour control probability at each (Iso-toxic) complication limit in turn (reducing the NTCP if the TCP_{cap} is reached). The results are presented in the form of population TCP-NTCP plots that allow user-friendly evaluation of the various treatment strategies & parameter variation for a given cohort of patients via the 'RadOpt' user interface.

In chapter 4 the effect of incorporating patient-specific tumour radiosensitivity information was explored. It was found that radiosensitivity information would be most useful for patients whose radiosensitivity was far from the population mean value. This was true for both lung and prostate cancer patients. It was also found that a finer stratification (5 groups vs 3 groups) of patient radiosensitivity would yield improvements for the lung cohort but not for the prostate cohort. The above analyses involved only a single dose-limiting OAR.

Radiobiological-model based inverse treatment planning is explored in chapter 5. Dose-volume based inverse treatment plans (DB-plans) developed for a standard regimen (55Gy20# for lung tumours, 60Gy20# for prostate tumours) were compared to the TCP-NTCP-based inverse treatment plans (RB-plans) created on the Raystation TPS. For the lung cancer treatments (n=2 patients), RB-plans (of 20- and 15-fractions) yielded superior tumour control with the same or less toxicity for the principal OAR. It was also demonstrated for both the patients that RB-plans at 15 fractions were superior to those at 20 fractions and were superior to all the DB-plans. A similar analysis for two prostate cancer datasets showed that RB-plans were superior to DB-plans in terms of TCP (by 4-5%) and dose sparing of the principal OAR (NTCP 2% lower, rectum $V_{40.8Gy}$ – 15 to 30% lower for RB-plans). A key

finding was a significant reduction in planning complexity (no additional structures needed to be drawn) for the RB-plans to reduce dose to OARs like rectum. Further, it was also demonstrated that prostate DB-plans without the homogeneity objective yield a therapeutically better dose distribution (NTCP 2% lower, TCP 2-3% higher, rectum $V_{40.8Gy}$ – 7 to 12% reduction) at a 14% lower homogeneity index compared to the conventional DB-plans. The DB-plan$_{(non\ uniform)}$ for lung patients were similarly superior to the conventional homogeneous PTV dose plans.

Chapter 6 describes a novel NTCP-based method to convert dose-volume based OAR tolerance limits (V_{xx}) from one fractionation regimen (say 55 Gy in 20 fractions for lung tumours) to the other. The limitations associated with the current BED formula-based method were presented and it was shown how the new method overcomes these limitations (e.g. accounting for the volume effect that plays a vital role in causing tissue toxicity, in the conversion). Compared to the Iso-NTCP method proposed here, the Iso-BED method showed an overall variation of 4-5% NTCP on conversion of V_{20Gy}<30% for lung cancer data for various regimens. The Iso-NTCP method was shown to be able to account for multiple endpoints related to the same OAR whilst forming V_{xx} conversion estimates from one regimen to another. The technique would be straightforward to implement in the clinic.

This research has presented strong ‘macroscopic’ (i.e. patient-cohort based) evidence and techniques to support moving away from orthodox methods (fixed prescription dose, fixed number of fractions) of dose prescribing in radiotherapy in favour of individualized prescribing that takes into account the radiobiology of the normal tissues and tumours via NTCP and TCP models.

Bibliography

AAPM Task Group 166, T. P. C. (2012). *The Use and QA of Biologically Related Models for Treatment Planning Report of AAPM Task Group 166*. *New York*. https://doi.org/10.1118/1.3685447

Ahunbay, E. E., Peng, C., Holmes, S., Godley, A., Lawton, C., & Li, X. A. (2010). Online adaptive replanning method for prostate radiotherapy. *International Journal of Radiation Oncology, Biology, Physics*, *77*(5), 1561–72. https://doi.org/10.1016/j.ijrobp.2009.10.013

Alber, M., Nüsslin, F., Boersma L J, (1999). An objective function for radiation treatment optimization based on local biological measures. *Physics in Medicine and Biology*, *44*(2), 479–493. https://doi.org/10.1088/0031-9155/44/2/014

Allen Li, X., Alber, M., Deasy, J. O., Jackson, A., Ken Jee, K.-W., Marks, L. B., … Yorke, E. D. (2012). The use and QA of biologically related models for treatment planning: short report of the TG-166 of the therapy physics committee of the AAPM. *Medical Physics*, *39*(3), 1386–409. https://doi.org/10.1118/1.3685447

Alonzi, R. (2015). Functional Radiotherapy Targeting using Focused Dose Escalation. *Clinical Oncology*, *27*(10), 601–617. https://doi.org/10.1016/j.clon.2015.06.015

Arabloo, J., Hamouzadeh, P., Mousavinezhad, S. M., Mobinizadeh, M., Olyaeemanesh, A., & Pooyandjoo, M. (2016). Health technology assessment of image-guided radiotherapy (IGRT): A systematic review of current evidence. *Medical Journal of the Islamic Republic of Iran, 30, 318. Retrieved from http://www.ncbi.nlm.nih.gov/pubmed/27390688*

Arcangeli, S., Strigari, L., Gomellini, S., Saracino, B., Petrongari, M. G., Pinnarò, P., … Arcangeli, G. (2012). Updated Results and Patterns of Failure in a Randomized Hypofractionation Trial for High-risk Prostate Cancer. *International Journal of Radiation Oncology*Biology*Physics, 84(5), 1172–1178. https://doi.org/10.1016/j.ijrobp.2012.02.049*

Azria, D., Ozsahin, M., Kramar, A., Peters, S., Atencio, D. P., Crompton, N. E. A., … Rosenstein, B. S. (2008). Single nucleotide polymorphisms, apoptosis, and the development of severe late adverse effects after radiotherapy. *Clinical Cancer Research : An Official Journal of the American Association for Cancer Research*, *14*(19), 6284–8. https://doi.org/10.1158/1078-0432.CCR-08-0700

Azzeroni, R., Maggio, A., Fiorino, C., Mangili, P., Cozzarini, C., De Cobelli, F., … Calandrino, R. (2013). Biological optimization of simultaneous boost on intra-prostatic lesions (DILs): Sensitivity to TCP parameters. *Physica Medica*, *29*(6), 592–598. https://doi.org/10.1016/j.ejmp.2012.10.002

Baker, C., Carver, A., & Nahum, A. (2015). PO-0910: Local control prediction for NSCLC using a common LQbased TCP model for both SABR and 3D-CRT fractionation. Radiotherapy and Oncology, 115, S471. https://doi.org/10.1016/S0167-8140(15)40902-8

Barrett, J. (2008). The timely delivery of radical radiotherapy : standards and guidelines for the management of unscheduled treatment interruptions , Third edition.

Barnett, G. C., Coles, C. E., Elliott, R. M., Baynes, C., Luccarini, C., Conroy, D., … West, C. M. L. (2012). Independent validation of genes and polymorphisms reported to be associated with radiation toxicity: a prospective analysis study. *The Lancet. Oncology*, *13*(1), 65–77. https://doi.org/10.1016/S1470-2045(11)70302-3

Barnett, G. C., Kerns, S. L., Noble, D. J., Dunning, A. M., West, C. M. L., & Burnet, N. G. (2015). Incorporating Genetic Biomarkers into Predictive Models of Normal Tissue Toxicity. *Clinical Oncology (Royal College of Radiologists (Great Britain))*, *27*(10), 579–87. https://doi.org/10.1016/j.clon.2015.06.013

Barnett, G. C., Thompson, D., Fachal, L., Kerns, S., Talbot, C., Elliott, R. M., … West, C. M. L. (2014). A genome wide association study (GWAS) providing evidence of an association between common genetic variants and late radiotherapy toxicity. *Radiotherapy and Oncology*, *111*(2), 178–185. https://doi.org/10.1016/j.radonc.2014.02.012

Belderbos, J., Heemsbergen, W., Hoogeman, M., Pengel, K., Rossi, M., & Lebesque, J. (2005). Acute esophageal toxicity in non-small cell lung cancer patients after high dose conformal radiotherapy. *Radiotherapy and Oncology : Journal of the European Society for Therapeutic Radiology and Oncology*, *75*(2), 157–64. https://doi.org/10.1016/j.radonc.2005.03.021

Bentzen, S. M., Saunders, M. I., & Dische, S. (2002). From CHART to CHARTWEL in non-small cell lung cancer: clinical radiobiological modelling of the expected change in outcome. *Clinical Oncology (Royal College of Radiologists (Great Britain)), 14(5), 372–81. Retrieved from http://www.ncbi.nlm.nih.gov/pubmed/12555876*

Bentzen, S. M., & Ritter, M. a. (2005). The α/β ratio for prostate cancer: What is it, really? *Radiotherapy and Oncology*, *76*(1), 1–3. https://doi.org/10.1016/j.radonc.2005.06.009

Bezjak, A., Rumble, R. B., Rodrigues, G., Hope, A., & Warde, P. (2012). *Intensity-modulated Radiotherapy in the Treatment of Lung Cancer*. *Clinical Oncology* (Vol. 24). https://doi.org/10.1016/j.clon.2012.05.007

Bhide, S. A., & Nutting, C. M. (2010). Recent advances in radiotherapy. *BMC Medicine*, *8*(1), 25. https://doi.org/10.1186/1741-7015-8-25

Bishop, W. J. (1960). *The early history of surgery*. *British Journal of Surgery* (Vol. 48). London: John Wiley & Sons, Ltd. https://doi.org/10.1002/bjs.18004820858

Bokrantz, R. (2013). *Multicriteria optimization for managing tradeoffs in radiation therapy treatment planning*. *Retrieved from https://www.raysearchlabs.com/globalassets/about-overview/media-center/wp-re-ev-n-pdfs/publications/doctoral-thesis-multicriteria-optimization_rasmus_bokrantz_2013.pdf*

Bondar, M. L., Hoogeman, M. S., Mens, J. W., Quint, S., Ahmad, R., Dhawtal, G., & Heijmen, B. J. (2012). Individualized nonadaptive and online-adaptive intensity-modulated radiotherapy treatment strategies for cervical cancer patients based on pretreatment acquired variable bladder filling computed tomography scans. *International Journal of Radiation Oncology, Biology, Physics*, *83*(5), 1617–23. https://doi.org/10.1016/j.ijrobp.2011.10.011

Bortfeld, T., Schlegel, W., Dykstra, C., Levegrün, S., & Preiser, K. (1996). Physical vs. biological objectives for treatment plan optimization. *Radiotherapy and Oncology : Journal of the European Society for Therapeutic Radiology and Oncology, 40(2), 185–7. https://doi.org/10.1016/0167-8140(96)01772-0*

Bostrom, P. J., & Soloway, M. S. (2007). Secondary cancer after radiotherapy for prostate cancer: should we be more aware of the risk? *European Urology*, *52*(4), 973–82. https://doi.org/10.1016/j.eururo.2007.07.002

Bradley, J., Graham, M. V., Winter, K., Purdy, J. A., Komaki, R., Roa, W. H., … Emami, B. (2005). Toxicity and outcome results of RTOG 9311: A phase I–II dose-escalation study using three-dimensional conformal radiotherapy in patients with inoperable non–small-cell lung carcinoma. *International Journal of Radiation Oncology*Biology*Physics, 61(2), 318–328.* *https://doi.org/10.1016/j.ijrobp.2004.06.260*

Brown, J. M. (2007). Tumor hypoxia in cancer therapy. *Methods in Enzymology*, *435*, 297–321. https://doi.org/10.1016/S0076-6879(07)35015-5

Burman, C., Kutcher, G. J., Emami, B., & Goitein, M. (1991). Fitting of normal tissue tolerance data to an analytic function. *International Journal of Radiation Oncology, Biology, Physics*, *21*(1), 123–35. Retrieved from http://www.ncbi.nlm.nih.gov/pubmed/2032883

Burnet, N. G. (2004). Defining the tumour and target volumes for radiotherapy. *Cancer Imaging*, *4*(2), 153–161. https://doi.org/10.1102/1470-7330.2004.0054

Calais, J., Cao, M., & Nickols, N. G. (2018). The Utility of PET/CT in the Planning of External Radiation Therapy for Prostate Cancer. Journal of Nuclear Medicine, 59(4), 557–567. https://doi.org/10.2967/jnumed.117.196444

Cao, F., Ramaseshan, R., Cooper, N., Elith, C. A., Nuraney, N., Steiner, P., … Karvat, A. (2015). Template-based Intensity-Modulated Radiation Therapy: A Cost-effective Intensity-Modulated Radiation Therapy Planning Procedure for Prostate Cancer. Journal of Medical Imaging and Radiation Sciences, 46(3), 325–330. https://doi.org/10.1016/j.jmir.2015.04.013

Carlone, M. C., Warkentin, B., Stavrev, P., & Fallone, B. G. (2006). Fundamental form of a population TCP model in the limit of large heterogeneity. *Medical Physics*, *33*(6), 1634–42. Retrieved from http://www.ncbi.nlm.nih.gov/pubmed/16872071

Carver, A., Uzan, J., Baker, C., & Nahum, A. (2015). PD-0450: A more exact approach to uncertainties in radiobiological parameter estimation. *Radiotherapy and Oncology, 115, S219–S220.* *https://doi.org/10.1016/S0167-8140(15)40446-3*

Chadwick, K. H., Leenhouts, H. P., W, B. G., J, B., J, D. E., J, H. E., … W, T. R. and T. P. (1973). A molecular theory of cell survival. *Physics in Medicine and Biology*, *18*(1), 7. https://doi.org/10.1088/0031-9155/18/1/007

Chadwick, K., & Leenhouts, H. (1981). *The molecular theory of radiation biology*. Berlin Heidelberg: Springer.

Chanyavanich, V., Das, S. K., Lee, W. R., & Lo, J. Y. (2011). Knowledge-based IMRT treatment planning for prostate cancer. *Medical Physics*, *38*(5), 2515. https://doi.org/10.1118/1.3574874

Chao, K. S., Deasy, J. O., Markman, J., Haynie, J., Perez, C. A., Purdy, J. A., & Low, D. A. (2001). A prospective study of salivary function sparing in patients with head-and-neck cancers receiving intensity-modulated or three-dimensional radiation therapy: initial results. *International Journal of Radiation Oncology, Biology, Physics*, *49*(4), 907–16. Retrieved from http://www.ncbi.nlm.nih.gov/pubmed/11240231

Chapet, O., Kong, F.-M., Lee, J. S., Hayman, J. A., & Ten Haken, R. K. (2005). Normal tissue complication probability modeling for acute esophagitis in patients treated with conformal radiation therapy for non-small cell lung cancer. *Radiotherapy and Oncology : Journal of the European Society for Therapeutic Radiology and Oncology*, *77*(2), 176–81. https://doi.org/10.1016/j.radonc.2005.10.001

Chapman, J.D., Nahum, A. E. (2015). *Radiotherapy treatment planning : Linear-quadratic radiobiology* (CRC Press). London.

Chapman, J. D. (2003). Single-hit mechanism of tumour cell killing by radiation. *International Journal of Radiation Biology*, *79*(2), 71–81. Retrieved from http://www.ncbi.nlm.nih.gov/pubmed/12569011

Chapman, J. D. (2014). Can the two mechanisms of tumor cell killing by radiation be exploited for therapeutic gain? *Journal of Radiation Research*, *55*(1), 2–9. https://doi.org/10.1093/jrr/rrt111

Charras, G. T. (2008). A short history of blebbing. *Journal of Microscopy*, *231*(3), 466–478. https://doi.org/10.1111/j.1365-2818.2008.02059.x

Chatterjee, S., Willis, N., Locks, S. M., Mott, J. H., & Kelly, C. G. (2011). Dosimetric and radiobiological comparison of helical tomotherapy, forward-planned intensity-modulated radiotherapy and two-phase conformal plans for radical radiotherapy treatment of head and neck squamous cell carcinomas. *The British Journal of Radiology, 84(1008), 1083–1090. https://doi.org/10.1259/bjr/53812025*

Cheng, C.-W., & Das, I. J. (1999). Treatment plan evaluation using dose–volume histogram (DVH) and spatial dose–volume histogram (zDVH). *International Journal of Radiation Oncology*Biology*Physics*, *43*(5), 1143–1150. https://doi.org/10.1016/S0360-3016(98)00492-1

Christakis, P. (2011). The birth of chemotherapy at Yale. Bicentennial lecture series: Surgery Grand Round. *The Yale Journal of Biology and Medicine*, *84*(2), 169–72. Retrieved from http://www.pubmedcentral.nih.gov/articlerender.fcgi?artid=3117414&tool=pmcentrez&rendertype=abstract

Christodoulou, M., Bayman, N., McCloskey, P., Rowbottom, C., & Faivre-Finn, C. (2014). New radiotherapy approaches in locally advanced non-small cell lung cancer. *European Journal of Cancer (Oxford, England : 1990)*, *50*(3), 525–34. https://doi.org/10.1016/j.ejca.2013.11.027

Clenton, S. J., Fisher, P. M., Conway, J., Kirkbride, P., & Hatton, M. Q. (2005). The use of lung dose-volume histograms in predicting post-radiation pneumonitis after non-conventionally fractionated radiotherapy for thoracic carcinoma. *Clinical Oncology (Royal College of Radiologists (Great Britain))*, *17*(8), 599–603. Retrieved from http://www.ncbi.nlm.nih.gov/pubmed/16372484

Coco Martin, J. M., Mooren, E., Ottenheim, C., Burrill, W., Nunez, M. I., Sprong, D., … Begg, A. C. (1999). Potential of radiation-induced chromosome aberrations to predict radiosensitivity in human tumour cells. *International Journal of Radiation Biology*, *75*(9), 1161–8. Retrieved from http://www.ncbi.nlm.nih.gov/pubmed/10528924

Cox, J. D., Azarnia, N., Byhardt, R. W., Shin, K. H., Emami, B., & Perez, C. A. (1991). N2 (clinical) non-small cell carcinoma of the lung: prospective trials of radiation therapy with total doses 60 Gy by the Radiation Therapy Oncology Group. *International Journal of Radiation Oncology, Biology, Physics*, *20*(1), 7–12.

Crompton, N. E., & Ozsahin, M. (1997). A versatile and rapid assay of radiosensitivity of peripheral blood leukocytes based on DNA and surface-marker assessment of cytotoxicity. Radiation Research, 147(1), 55–60. Retrieved from http://www.ncbi.nlm.nih.gov/pubmed/8989370

CTCA. (2015). Lung cancer treatment statistics and results. Retrieved July 28, 2016, from http://www.cancercenter.com/lung-cancer/statistics/tab/lung-cancer-NSCLC-survival-statistics/#statisticalmethodologynonsmallcelllung

Curran, W. J., Paulus, R., Langer, C. J., Komaki, R., Lee, J. S., Hauser, S., … Cox, J. D. (2011). Sequential vs. concurrent chemoradiation for stage III non-small cell lung cancer: randomized phase III trial RTOG 9410. *Journal of the National Cancer Institute*, *103*(19), 1452–60. https://doi.org/10.1093/jnci/djr325

D'Avino, V., Palma, G., Liuzzi, R., Conson, M., Doria, F., Salvatore, M., … Cella, L. (2015). Prediction of gastrointestinal toxicity after external beam radiotherapy for localized prostate cancer. *Radiation Oncology (London, England)*, *10*(1), 80. https://doi.org/10.1186/s13014-015-0389-5

Dale, R. G., Hendry, J. H., Jones, B., Robertson, A. G., Deehan, C., & Sinclair, J. A. (2002). Practical methods for compensating for missed treatment days in radiotherapy, with particular reference to head and neck schedules. Clinical Oncology (Royal College of Radiologists (Great Britain)), 14(5), 382–393.

Dale, R., & Jones, B. (2007). *Radiobiological Modelling in Radiation Oncology* (1st ed.). London: British Institute of Radiology. Retrieved from http://www.amazon.co.uk/Radiobiological-Modelling-Radiation-Oncology-Roger/dp/090574960X

Das, S. (2009). A role for biological optimization within the current treatment planning paradigm. *Medical Physics, 36(10), 4672–82. https://doi.org/10.1118/1.3220211*

Dawson, A., & Hillen, T. (2006). Derivation of the Tumour Control Probability (TCP) from a Cell Cycle Model. *Computational and Mathematical Methods in Medicine*, *7*(2–3), 121–141. https://doi.org/10.1080/10273660600968937

De La Fuente Herman, T., Ahmad And, S., & Vlachaki, M. T. (2010). Intensity modulated radiation therapy versus three dimensional conformal radiation therapy for treatment of high grade glioma: a radiobiological modeling study. *Journal of X-Ray Science and Technology, 18(4), 393–402. https://doi.org/10.3233/XST-2010-0270*

Dearnaley, D. P., Hall, E., Lawrence, D., Huddart, R. A., Eeles, R., Nutting, C. M., … Horwich, A. (2005). Phase III pilot study of dose escalation using conformal radiotherapy in prostate cancer: PSA control and side effects. *British Journal of Cancer*, *92*(3), 488–498.

Dearnaley, D., & Hall, E. (2017). Prostate cancer and hypofractionation: reflections on recent randomised phase III clinical trial results*. Translational Andrology and Urology, 6(1), 134–136. Retrieved from* http://tau.amegroups.com/article/view/13466/13824

Dearnaley, D. P., Jovic, G., Syndikus, I., Khoo, V., Cowan, R. A., Graham, J. D., … Sydes, M. R. (2014). Escalated-dose versus control-dose conformal radiotherapy for prostate cancer: long-term results from the MRC RT01 randomised controlled trial. *The Lancet. Oncology, 15(4), 464–73. https://doi.org/10.1016/S1470-2045(14)70040-3*

Dearnaley, D., Syndikus, I., Mossop, H., Khoo, V., Birtle, A., Bloomfield, D., … al., et. (2016a, 2016b). Conventional versus hypofractionated high-dose intensity-modulated radiotherapy for prostate cancer: 5-year outcomes of the randomised, non-inferiority, phase 3 CHHiP trial. *The Lancet Oncology*, *17*(8), 1047–1060. https://doi.org/10.1016/S1470-2045(16)30102-4

Deb, P., & Fielding, A. (2009). Radiobiological model comparison of 3D conformal radiotherapy and IMRT plans for the treatment of prostate cancer. *Australasian Physical & Engineering Sciences in Medicine, 32(2), 51–61. Retrieved from http://www.ncbi.nlm.nih.gov/pubmed/19623855*

Defraene, G., Van den Bergh, L., Al-Mamgani, A., Haustermans, K., Heemsbergen, W., Van den Heuvel, F., & Lebesque, J. V. (2012). The benefits of including clinical factors in rectal normal tissue complication probability modeling after radiotherapy for prostate cancer. *International Journal of Radiation Oncology, Biology, Physics*, *82*(3), 1233–42. https://doi.org/10.1016/j.ijrobp.2011.03.056

Denker, J. (2012). Uncertainty as Applied to Measurements and Calculations. Retrieved from https://www.av8n.com/physics/uncertainty.htm#bib-probability-intro

Din, O. S., Harden, S. V., Hudson, E., Mohammed, N., Pemberton, L. S., Lester, J. F., … Hatton, M. Q. F. (2013). Accelerated hypo-fractionated radiotherapy for non small cell lung cancer: Results from 4 UK centres. Radiotherapy and Oncology, 109(1), 8–12. https://doi.org/10.1016/j.radonc.2013.07.014

Drzymala, R. E., Mohan, R., Brewster, L., Chu, J., Goitein, M., Harms, W., & Urie, M. (1991). Dose-volume histograms. *International Journal of Radiation Oncology*Biology*Physics*, *21*(1), 71–78. https://doi.org/10.1016/0360-3016(91)90168-4

Dubois, L. J., Lieuwes, N. G., Janssen, M. H. M., Peeters, W. J. M., Windhorst, A. D., Walsh, J. C., … Lambin, P. (2011). Preclinical evaluation and validation of [18F]HX4, a promising hypoxia marker for PET imaging. *Proceedings of the National Academy of Sciences of the United States of America*, *108*(35), 14620–5. https://doi.org/10.1073/pnas.1102526108

Dunne, A. L., Price, M. E., Mothersill, C., McKeown, S. R., Robson, T., & Hirst, D. G. (2003). Relationship between clonogenic radiosensitivity, radiation-induced apoptosis and DNA damage/repair in human colon cancer cells. British Journal of Cancer, 89(12), 2277–83. https://doi.org/10.1038/sj.bjc.6601427

Emami, B., Lyman, J., Brown, A., Coia, L., Goitein, M., Munzenrider, J. E., … Wesson, M. (1991). Tolerance of normal tissue to therapeutic irradiation. *International Journal of Radiation Oncology, Biology, Physics*, *21*(1), 109–22. Retrieved from http://www.ncbi.nlm.nih.gov/pubmed/2032882

Faria, S. L., Souhami, L., Portelance, L., Duclos, M., Vuong, T., Small, D., & Freeman, C. R. (2006). Absence of toxicity with hypofractionated 3-dimensional radiation therapy for inoperable, early stage non-small cell lung cancer. *Radiation Oncology*, *1*(1), 42. https://doi.org/10.1186/1748-717X-1-42

Feng, F. Y., Kim, H. M., Lyden, T. H., Haxer, M. J., Feng, M., Worden, F. P., … Eisbruch, A. (2007). Intensity-modulated radiotherapy of head and neck cancer aiming to reduce dysphagia: early dose-effect relationships for the swallowing structures. *International Journal of Radiation Oncology, Biology, Physics*, *68*(5), 1289–98. https://doi.org/10.1016/j.ijrobp.2007.02.049

Fenwick, J. D., Nahum, A. E., Malik, Z. I., Eswar, C. V, Hatton, M. Q., Laurence, V. M., … Landau, D. B. (2009). Escalation and intensification of radiotherapy for stage III non-small cell lung cancer: opportunities for treatment improvement. *Clinical Oncology (Royal College of Radiologists (Great Britain))*, *21*(4), 343–60. https://doi.org/10.1016/j.clon.2008.12.011

Ferreira, B. C., do Carmo Lopes, M., Mateus, J., Capela, M., & Mavroidis, P. (2010). Radiobiological evaluation of forward and inverse IMRT using different fractionations for head and neck tumours. *Radiation Oncology, 5(1), 57. https://doi.org/10.1186/1748-717X-5-57*

Fertil, B., & Malaise, E. P. (1985). Intrinsic radiosensitivity of human cell lines is correlated with radioresponsiveness of human tumors: analysis of 101 published survival curves. *International Journal of Radiation Oncology, Biology, Physics*, *11*(9), 1699–707. Retrieved from http://www.ncbi.nlm.nih.gov/pubmed/4030437

Fletcher, G. H. (1973). *Textbook of Radiotherapy* (2nd ed.). Philadelphia: Lea & Febiger.

Forman, J. D., Duclos, M., Shamsa, F., Porter, A. T., & Orton, C. (1996). Hyperfractionated conformal radiotherapy in locally advanced prostate cancer: results of a dose escalation study. *International Journal of Radiation Oncology, Biology, Physics*, *34*(3), 655–662.

Fournel, P. (2011). RTOG 94-10: Keenly Awaited Results Validating the Best Therapeutic Strategy for Locally Advanced Non-Small Cell Lung Cancer. *JNCI Journal of the National Cancer Institute*, *103*(19), 1425–1427. https://doi.org/10.1093/jnci/djr348

Fowler, J. (1989). The linear-quadratic formula and progress in fractionated radiotherapy. *Br J Radiol*, *62*(740), 679–694. https://doi.org/10.1259/0007-1285-62-740-679

Fowler, J. (2010). 21 years of Biologically Effective Dose. *The British Journal of Radiology*, *83*(991), 554–568. https://doi.org/10.1259/bjr/31372149

Fowler, J. F. (2001). Normal tissue complication probabilities: How well do the models work? *Physica Medica*, *17*(Suppl. 2), 24–35.

Gagliardi, G., Constine, L. S., Moiseenko, V., Correa, C., Pierce, L. J., Allen, A. M., & Marks, L. (2010). Radiation Dose–Volume Effects in the Heart. *International Journal of Radiation Oncology*Biology*Physics*, *76*(3), S77–S85. https://doi.org/10.1016/j.ijrobp.2009.04.093

Geng, C., Paganetti, H., & Grassberger, C. (2017). Prediction of Treatment Response for Combined Chemo- and Radiation Therapy for Non-Small Cell Lung Cancer Patients Using a Bio-Mathematical Model. Scientific Reports, 7(1), 13542. https://doi.org/10.1038/s41598-017-13646-z

Gerstner, N., Wachter, S., Knocke, T. H., Fellner, C., Wambersie, A., & Pötter, R. (1999). The benefit of Beam's eye view based 3D treatment planning for cervical cancer. *Radiotherapy and Oncology : Journal of the European Society for Therapeutic Radiology and Oncology*, *51*(1), 71–8. Retrieved from http://www.ncbi.nlm.nih.gov/pubmed/10386719

Gerweck, L. E., Vijayappa, S., Kurimasa, A., Ogawa, K., & Chen, D. J. (2006). Tumor cell radiosensitivity is a major determinant of tumor response to radiation. *Cancer Research*, *66*(17), 8352–5. https://doi.org/10.1158/0008-5472.CAN-06-0533

Ghilezan, M., Yan, D., & Martinez, A. (2010). Adaptive radiation therapy for prostate cancer. *Seminars in Radiation Oncology*, *20*(2), 130–7. https://doi.org/10.1016/j.semradonc.2009.11.007

Girinsky, T., Bernheim, A., Lubin, R., Tavakoli-Razavi, T., Baker, F., Janot, F., … Duverger, A. (1994). In vitro parameters and treatment outcome in head and neck cancers treated with surgery and/or radiation: cell characterization and correlations with local control and overall survival. *International Journal of Radiation Oncology, Biology, Physics*, *30*(4), 789–94. Retrieved from http://www.ncbi.nlm.nih.gov/pubmed/7960980

Good, D., Lo, J., Lee, W. R., Wu, Q. J., Yin, F.-F., & Das, S. K. (2013). A Knowledge-Based Approach to Improving and Homogenizing Intensity Modulated Radiation Therapy Planning Quality Among Treatment Centers: An Example Application to Prostate Cancer Planning. *International Journal of Radiation Oncology*Biology*Physics*, *87*(1), 176–181. https://doi.org/10.1016/j.ijrobp.2013.03.015

Grutters, J. P. C., Kessels, A. G. H., Pijls-Johannesma, M., De Ruysscher, D., Joore, M. A., & Lambin, P. (2010). Comparison of the effectiveness of radiotherapy with photons, protons and carbon-ions for non-small cell lung cancer: a meta-analysis. *Radiotherapy and Oncology : Journal of the European Society for Therapeutic Radiology and Oncology*, *95*(1), 32–40. https://doi.org/10.1016/j.radonc.2009.08.003

Guckenberger, M., Wulf, J., Mueller, G., Krieger, T., Baier, K., Gabor, M., … Flentje, M. (2009). Dose–Response Relationship for Image-Guided Stereotactic Body Radiotherapy of Pulmonary Tumors: Relevance of 4D Dose Calculation. *International Journal of Radiation Oncology*Biology*Physics, 74(1), 47–54. https://doi.org/10.1016/j.ijrobp.2008.06.1939*

Gulliford, S. L., Partridge, M., Sydes, M. R., Webb, S., Evans, P. M., & Dearnaley, D. P. (2012). Parameters for the Lyman Kutcher Burman (LKB) model of Normal Tissue Complication Probability (NTCP) for specific rectal complications observed in clinical practise. *Radiotherapy and Oncology : Journal of the European Society for Therapeutic Radiology and Oncology*, *102*(3), 347–51. https://doi.org/10.1016/j.radonc.2011.10.022

Gupta, T., & Narayan, C. A. (2012). Image-guided radiation therapy: Physician's perspectives. *Journal of Medical Physics / Association of Medical Physicists of India*, *37*(4), 174–82. https://doi.org/10.4103/0971-6203.103602

Haimovitz-Friedman, A., Kolesnick, R., & Fuks, Z. (1996). Modulation of the Apoptotic Response: Potential for Improving the Outcome in Clinical Radiotherapy. *Seminars in Radiation Oncology*, *6*(4), 273–283. https://doi.org/10.1053/SRAO00600273

Hall, J. S., Iype, R., Senra, J., Taylor, J., Armenoult, L., Oguejiofor, K., … West, C. M. L. (2014). Investigation of radiosensitivity gene signatures in cancer cell lines. *PloS One*, *9*(1), e86329. https://doi.org/10.1371/journal.pone.0086329

Haslett, K., Franks, K., Hanna, G. G., Harden, S., Hatton, M., Harrow, S., … Faivre-Finn, C. (2016). Protocol for the isotoxic intensity modulated radiotherapy (IMRT) in stage III non-small cell lung cancer (NSCLC): a feasibility study. *BMJ Open*, *6*(4), e010457. https://doi.org/10.1136/bmjopen-2015-010457

Haslett, K., Pöttgen, C., Stuschke, M., & Faivre-Finn, C. (2014). Hyperfractionated and accelerated radiotherapy in non-small cell lung cancer. *Journal of Thoracic Disease*, *6*(4), 328–35. https://doi.org/10.3978/j.issn.2072-1439.2013.11.06

Hirsch, J. S., & Holzknecht, G. (1926). The Principles and Practice of Roentgen Therapy. *British Journal of Radiology: BIR Section*, *31*(308), 114–115. https://doi.org/10.1259/bir.1926.0028

Hoffmann, A. L., Huizenga, H., & Kaanders, J. H. A. M. (2013). Employing the therapeutic operating characteristic (TOC) graph for individualised dose prescription. *Radiation Oncology (London, England)*, *8*(1), 55. https://doi.org/10.1186/1748-717X-8-55

Huang, B.-T., Lu, J.-Y., Lin, P.-X., Chen, J.-Z., Li, D.-R., & Chen, C.-Z. (2015). Radiobiological modeling analysis of the optimal fraction scheme in patients with peripheral non-small cell lung cancer undergoing stereotactic body radiotherapy. *Scientific Reports*, *5*, 18010. https://doi.org/10.1038/srep18010

Hunter, R. (2006). The Royal College of Radiologists Radiotherapy and oncology. *The British Journal of Radiology*. https://doi.org/10.1259/0007-1285-48-575-960-a

Hussein, M., Aldridge, S., Guerrero Urbano, T., & Nisbet, A. (2012). The effect of 6 and 15 MV on intensity-modulated radiation therapy prostate cancer treatment: plan evaluation, tumour control probability and normal tissue complication probability analysis, and the theoretical risk of secondary induced malignancies. *The British Journal of Radiology, 85(1012), 423–432. https://doi.org/10.1259/bjr/24514638*

IAEA. (2010). *Radiation Biology: A Handbook for Teachers and Students*. Vienna: IAEA. Retrieved from http://www-pub.iaea.org/books/IAEABooks/8219/Radiation-Biology-A-Handbook-for-Teachers-and-Students

ICRU. (1993a). *Prescribing, Recording, and Reporting Photon Beam Therapy Report 50*. *Journal of the ICRU*.

ICRU. (1993b). *Prescribing, recording and reporting photon beam therapy (ICRU report 50)*. *ICRU report*. https://doi.org/10.2307/3578862

ICRU. (1999). ICRU Report 62. Prescribing, Recording, and Reporting Photon Beam Therapy (Supplement to ICRU Report 50). *Journal of ICRU*, Ix +52. https://doi.org/10.1259/bjr.74.879.740294

ICRU. (2010). Report 83 The International Commission on Radiation Units and Measurements. *Journal of the ICRU*, *10*(1), 27–38. https://doi.org/10.1093/jicru/ndq001

Jackson, A., Marks, L. B., Bentzen, S. M., Eisbruch, A., Yorke, E. D., Ten Haken, R. K., … Deasy, J. O. (2010). The Lessons of QUANTEC: Recommendations for Reporting and Gathering Data on Dose-Volume Dependencies of Treatment Outcome. *International Journal of Radiation Oncology Biology Physics*, *76*(3 SUPPL.), 155–160. https://doi.org/10.1016/j.ijrobp.2009.08.074

Jeremić, B., Milicić, B., Acimović, L., & Milisavljević, S. (2005). Concurrent hyperfractionated radiotherapy and low-dose daily carboplatin/paclitaxel in patients with early-stage (I/II) non-small-cell lung cancer: long-term results of a phase II study. *Journal of Clinical Oncology : Official Journal of the American Society of Clinical Oncology*, *23*(28), 6873–80. https://doi.org/10.1200/JCO.2005.22.319

Jiang, X., Li, T., Liu, Y., Zhou, L., Xu, Y., Zhou, X., & Gong, Y. (2011). Planning analysis for locally advanced lung cancer: dosimetric and efficiency comparisons between intensity-modulated radiotherapy (IMRT), single-arc/partial-arc volumetric modulated arc therapy (SA/PA-VMAT). *Radiation Oncology (London, England)*, *6*(1), 140. https://doi.org/10.1186/1748-717X-6-140

Joiner, M. C., & van der Kogel, A. (2009). Basic clinical radiobiology (Fourth). CRC Press.

Jones, B., & Dale, R. G. (2000). Radiobiological modeling and clinical trials. *International Journal of Radiation Oncology*Biology*Physics*, *48*(1), 259–265. https://doi.org/10.1016/S0360-3016(00)00542-3

Källman, P., Agren, A., & Brahme, A. (1992). Tumour and normal tissue responses to fractionated non-uniform dose delivery. *International Journal of Radiation Biology*, *62*(2), 249–62. Retrieved from http://www.ncbi.nlm.nih.gov/pubmed/1355519

Kaster, T. S., Yaremko, B., Palma, D. A., & Rodrigues, G. B. (2015). Radical-intent hypofractionated radiotherapy for locally advanced non-small-cell lung cancer: a systematic review of the literature. *Clin Lung Cancer*, *16*(2), 71–79. https://doi.org/10.1016/j.cllc.2014.08.002

Kerns, S. L., Dorling, L., Fachal, L., Bentzen, S., Pharoah, P. D. P., Barnes, D. R., … West, C. M. L. (2016). Meta-analysis of Genome Wide Association Studies Identifies Genetic Markers of Late Toxicity Following Radiotherapy for Prostate Cancer. *EBioMedicine*, *10*, 150–163. https://doi.org/10.1016/j.ebiom.2016.07.022

Kerns, S. L., West, C. M. L., Andreassen, C. N., Barnett, G. C., Bentzen, S. M., Burnet, N. G., … Rosenstein, B. S. (2014). Radiogenomics: the search for genetic predictors of radiotherapy response. *Future Oncology (London, England)*, *10*(15), 2391–406. https://doi.org/10.2217/fon.14.173

Kibrom, A. Z., & Knight, K. A. (2015). Adaptive radiation therapy for bladder cancer: a review of adaptive techniques used in clinical practice. *Journal of Medical Radiation Sciences, 62(4), 277–85.* https://doi.org/10.1002/jmrs.129

Kim, H., Kim, J. W., Hong, S. J., Rha, K. H., Lee, C.-G., Yang, S. C., … Cho, J. (2014). Treatment outcome of localized prostate cancer by 70 Gy hypofractionated intensity-modulated radiotherapy with a customized rectal balloon. *Radiation Oncology Journal, 32(3), 187–97. https://doi.org/10.3857/roj.2014.32.3.187*

King, C. R. (2002). LDR vs. HDR brachytherapy for localized prostate cancer. *Brachytherapy, 1(4), 219–226. https://doi.org/10.1016/S1538-4721(02)00101-0*

Ko, E. C., Forsythe, K., Buckstein, M., Kao, J., & Rosenstein, B. S. (2011). Radiobiological rationale and clinical implications of hypofractionated radiation therapy. *Cancer Radiothérapie : Journal de La Société Française de Radiothérapie Oncologique*, *15*(3), 221–9. https://doi.org/10.1016/j.canrad.2010.12.007

Komatsu, S., Fukumoto, T., Demizu, Y., Miyawaki, D., Terashima, K., Sasaki, R., … Murakami, M. (2011). Clinical results and risk factors of proton and carbon ion therapy for hepatocellular carcinoma. *Cancer*, *117*(21), 4890–904. https://doi.org/10.1002/cncr.26134

Kong, F.-M., Ten Haken, R. K., Schipper, M. J., Sullivan, M. A., Chen, M., Lopez, C., … Hayman, J. A. (2005). High-dose radiation improved local tumor control and overall survival in patients with inoperable/unresectable non–small-cell lung cancer: Long-term results of a radiation dose escalation study. *International Journal of Radiation Oncology*Biology*Physics, 63(2), 324–333. https://doi.org/10.1016/j.ijrobp.2005.02.010*

Koontz, B. F., Das, S., Temple, K., Bynum, S., Catalano, S., Koontz, J. I., … Oleson, J. R. (2009). Dosimetric and Radiobiologic Comparison of 3D Conformal Versus Intensity Modulated Planning Techniques for Prostate Bed Radiotherapy. *Medical Dosimetry, 34(3), 256–260. https://doi.org/10.1016/j.meddos.2008.10.005*

Krause, B. J., Beck, R., Souvatzoglou, M., & Piert, M. (2006). PET and PET/CT studies of tumor tissue oxygenation. *The Quarterly Journal of Nuclear Medicine and Molecular Imaging : Official Publication of the Italian Association of Nuclear Medicine (AIMN) [and] the International Association of Radiopharmacology (IAR), [and] Section of the Society of Radiopharmaceutica*, *50*(1), 28–43. Retrieved from http://www.ncbi.nlm.nih.gov/pubmed/16557202

Kupelian, P. A., Reddy, C. A., Carlson, T. P., Altsman, K. A., & Willoughby, T. R. (2002). Preliminary observations on biochemical relapse-free survival rates after short-course intensity-modulated radiotherapy (70 Gy at 2.5 Gy/fraction) for localized prostate cancer. *International Journal of Radiation Oncology, Biology, Physics*, *53*(4), 904–12. Retrieved from http://www.ncbi.nlm.nih.gov/pubmed/12095556

Kupelian, P. A., Thakkar, V. V, Khuntia, D., Reddy, C. A., Klein, E. A., & Mahadevan, A. (2005). Hypofractionated intensity-modulated radiotherapy (70 gy at 2.5 Gy per fraction) for localized prostate cancer: long-term outcomes. *International Journal of Radiation Oncology, Biology, Physics*, *63*(5), 1463–8. https://doi.org/10.1016/j.ijrobp.2005.05.054

*Kupelian, P. A., Willoughby, T. R., Reddy, C. A., Klein, E. A., & Mahadevan, A. (2007). Hypofractionated Intensity-Modulated Radiotherapy (70 Gy at 2.5 Gy Per Fraction) for Localized Prostate Cancer: Cleveland Clinic Experience. International Journal of Radiation Oncology*Biology*Physics, 68(5), 1424–1430. https://doi.org/10.1016/j.ijrobp.2007.01.067*

Kutcher, G. J., Burman, C., Cohen, L., Dritschilo, A., Chaffer, J. T., Bloomer, W. D., … Casarett, G. (1989). Calculation of complication probability factors for non-uniform normal tissue irradiation: the effective volume method. *International Journal of Radiation Oncology, Biology, Physics*, *16*(6), 1623–30. https://doi.org/10.1016/0360-3016(89)90972-3

Lambert, B. (2001). *Chapter 3 Radiation : early warnings ; late effects in Late lessons from early warnings: the precautionary principle 1896-2000*. *EEA*. Retrieved from http://www.eea.europa.eu/publications/environmental_issue_report_2001_22

Lambin, P., Petit, S. F., Aerts, H. J. W. L., van Elmpt, W. J. C., Oberije, C. J. G., Starmans, M. H. W., … De Ruysscher, D. (2010). The ESTRO Breur Lecture 2009. From population to voxel-based radiotherapy: exploiting intra-tumour and intra-organ heterogeneity for advanced treatment of non-small cell lung cancer. *Radiotherapy and Oncology : Journal of the European Society for Therapeutic Radiology and Oncology*, *96*(2), 145–52. https://doi.org/10.1016/j.radonc.2010.07.001

Landau, D. B., Hughes, L., Baker, A., Bates, A. T., Bayne, M. C., Counsell, N., … Fenwick, J. D. (2016). IDEAL-CRT: A Phase 1/2 Trial of Isotoxic Dose-Escalated Radiation Therapy and Concurrent Chemotherapy in Patients With Stage II/III Non-Small Cell Lung Cancer. *International Journal of Radiation Oncology, Biology, Physics, 95(5), 1367–1377. https://doi.org/10.1016/j.ijrobp.2016.03.031*

Le, Q.-T., Sutphin, P. D., Raychaudhuri, S., Yu, S. C. T., Terris, D. J., Lin, H. S., … Giaccia, A. J. (2003). Identification of osteopontin as a prognostic plasma marker for head and neck squamous cell carcinomas. *Clinical Cancer Research : An Official Journal of the American Association for Cancer Research, 9(1), 59–67. Retrieved from http://www.ncbi.nlm.nih.gov/pubmed/12538452*

Lee, S., Cao, Y. J., & Kim, C. Y. (2015). Physical and Radiobiological Evaluation of Radiotherapy Treatment Plan. *In Evolution of Ionizing Radiation Research. InTech. https://doi.org/10.5772/60846*

Lee, W. R., Dignam, J. J., Amin, M. B., Bruner, D. W., Low, D., Swanson, G. P., … Sandler, H. M. (2016). Randomized Phase III Noninferiority Study Comparing Two Radiotherapy Fractionation Schedules in Patients With Low-Risk Prostate Cancer. *Journal of Clinical Oncology, 34(20), 2325–2332. https://doi.org/10.1200/JCO.2016.67.0448*

Lester, J. F., Macbeth, F. R., Brewster, A. E., Court, J. B., & Iqbal, N. (2004). CT-planned accelerated hypofractionated radiotherapy in the radical treatment of non-small cell lung cancer. Lung Cancer, 45(2), 237–242. https://doi.org/10.1016/j.lungcan.2004.01.018

Li, X., Quan, E. M., Li, Y., Pan, X., Zhou, Y., Wang, X., … Zhang, X. (2013). A fully automated method for CT-on-rails-guided online adaptive planning for prostate cancer intensity modulated radiation therapy. *International Journal of Radiation Oncology, Biology, Physics*, *86*(5), 835–41. https://doi.org/10.1016/j.ijrobp.2013.04.014

Liang, X., Penagaricano, J., Zheng, D., Morrill, S., Zhang, X., Corry, P., … Brahme, A. (2016). Radiobiological impact of dose calculation algorithms on biologically optimized IMRT lung stereotactic body radiation therapy plans. *Radiation Oncology*, *11*(1), 10. https://doi.org/10.1186/s13014-015-0578-2

Lievens, Y., Nulens, A., Gaber, M. A., Defraene, G., De Wever, W., Stroobants, S., & Van den Heuvel, F. (2011). Intensity-modulated radiotherapy for locally advanced non-small-cell lung cancer: a dose-escalation planning study. *International Journal of Radiation Oncology, Biology, Physics*, *80*(1), 306–13. https://doi.org/10.1016/j.ijrobp.2010.06.025

Liu, Q., Wang, M., Kern, A. M., Khaled, S., Han, J., Yeap, B. Y., … Willers, H. (2015). Adapting a drug screening platform to discover associations of molecular targeted radiosensitizers with genomic biomarkers. *Molecular Cancer Research : MCR*, *13*(4), 713–20. https://doi.org/10.1158/1541-7786.MCR-14-0570

Livsey, J. E., Cowan, R. A., Wylie, J. P., Swindell, R., Read, G., Khoo, V. S., & Logue, J. P. (2003). Hypofractionated conformal radiotherapy in carcinoma of the prostate: five-year outcome analysis. *International Journal of Radiation Oncology, Biology, Physics*, *57*(5), 1254–1259.

Luijk, P. van, Delvigne, T. C., Schilstra, C., & Schippers, J. M. (2003). Estimation of parameters of dose–volume models and their confidence limits. *Physics in Medicine and Biology, 48(13), 1863–1884. https://doi.org/10.1088/0031-9155/48/13/301*

Lukka, H., Hayter, C., Julian, J. A., Warde, P., Morris, W. J., Gospodarowicz, M., … Kwan, W. (2005). Randomized trial comparing two fractionation schedules for patients with localized prostate cancer. *Journal of Clinical Oncology : Official Journal of the American Society of Clinical Oncology*, *23*(25), 6132–6138.

Luxton, G., Hancock, S. L., & Boyer, A. L. (2004). Dosimetry and radiobiologic model comparison of IMRT and 3D conformal radiotherapy in treatment of carcinoma of the prostate. *International Journal of Radiation Oncology*Biology*Physics, 59(1), 267–284. https://doi.org/10.1016/j.ijrobp.2004.01.024*

Lyman, J. T. (1985). Complication probability as assessed from dose-volume histograms. *Radiation Research. Supplement, 8, S13-9. Retrieved from http://www.ncbi.nlm.nih.gov/pubmed/3867079*

Machtay, M., Bae, K., Movsas, B., Paulus, R., Gore, E. M., Komaki, R., … Curran, W. J. (2012). Higher biologically effective dose of radiotherapy is associated with improved outcomes for locally advanced non-small cell lung carcinoma treated with chemoradiation: an analysis of the Radiation Therapy Oncology Group. *International Journal of Radiation Oncology, Biology, Physics*, *82*(1), 425–34. https://doi.org/10.1016/j.ijrobp.2010.09.004

Mackay, R. I., & Hendry, J. H. (1999). The modelled benefits of individualizing radiotherapy patients' dose using cellular radiosensitivity assays with inherent variability. *Radiotherapy and Oncology*, *50*(1), 67–75. https://doi.org/10.1016/S0167-8140(98)00132-7

Maguire, J., Khan, I., McMenemin, R., O'Rourke, N., McNee, S., Kelly, V., … Snee, M. (2014). SOCCAR: A randomised phase II trial comparing sequential versus concurrent chemotherapy and radical hypofractionated radiotherapy in patients with inoperable stage III Non-Small Cell Lung Cancer and good performance status. *European Journal of Cancer (Oxford, England : 1990), 50(17), 2939–49. https://doi.org/10.1016/j.ejca.2014.07.009*

Mariano Ruiz de Almodóvar, J., Guirado, D., Isabel Núñez, M., López, E., Guerrero, R., Teresa Valenzuela, M., … del Moral, R. (2002). Individualisation of radiotherapy in breast cancer patients: possible usefulness of a DNA damage assay to measure normal cell radiosensitivity. *Radiotherapy and Oncology*, *62*(3), 327–333. https://doi.org/10.1016/S0167-8140(01)00490-X

Marks, L. B., Bentzen, S. M., Deasy, J. O., Kong, F.-M. S., Bradley, J. D., Vogelius, I. S., … Jackson, A. (2010). Radiation dose-volume effects in the lung. *International Journal of Radiation Oncology, Biology, Physics*, *76*(3 Suppl), S70-6. https://doi.org/10.1016/j.ijrobp.2009.06.091

Marks, L. B., Yorke, E. D., Jackson, A., Ten Haken, R. K., Constine, L. S., Eisbruch, A., … Deasy, J. O. (2010). Use of normal tissue complication probability models in the clinic. *International Journal of Radiation Oncology, Biology, Physics*, *76*(3 Suppl), S10-9. https://doi.org/10.1016/j.ijrobp.2009.07.1754

Marshall, A., Sun, A., Yap, M., Higgins, J., Vines, D., Clarke, K., … Bissonnette, J.-P. (2016). Dose Escalation in Radiotherapy for Locally Advanced Non-small Cell Lung Cancer Using 4D FDG PET/CT: A Planning Study. *Journal of Medical Imaging and Radiation Sciences*, *47*(1), S18–S19. https://doi.org/10.1016/j.jmir.2015.12.057

Martel, M. K., Ten Haken, R. K., Hazuka, M. B., Kessler, M. L., Strawderman, M., Turrisi, A. T., … Lichter, A. S. (1999). Estimation of tumor control probability model parameters from 3-D dose distributions of non-small cell lung cancer patients. *Lung Cancer (Amsterdam, Netherlands), 24(1), 31–7. Retrieved from http://www.ncbi.nlm.nih.gov/pubmed/10403692*

Mavroidis, P. (2013). Clinical implementation of radiobiological measures in treatment planning. Why has it taken so long? *International Journal of Cancer Therapy and Oncology. https://doi.org/10.14319/ijcto.0101.9*

Mavroidis, P., Lind, B. K., & Brahme, A. (2001). Physics in Medicine & Biology Biologically effective uniform dose (¯ ¯ D) for specification, report and comparison of dose response relations and treatment plans. *Phys. Med. Biol, 46, 2607–2630. Retrieved from http://iopscience.iop.org.liverpool.idm.oclc.org/article/10.1088/0031-9155/46/10/307/pdf*

Mayles, P., Nahum, A., & Rosenwald, J. C. (2007). *HANDBOOK OF RADIOTHERAPY*. *Taylor & Francis Group, LLC* (Vol. 1). https://doi.org/10.1136/bmj.1.4813.770

Mayo, C., Martel, M. K., Marks, L. B., Flickinger, J., Nam, J., & Kirkpatrick, J. (2010). Radiation Dose-Volume Effects of Optic Nerves and Chiasm. *International Journal of Radiation Oncology Biology Physics*, *76*(3 SUPPL.), 28–35. https://doi.org/10.1016/j.ijrobp.2009.07.1753

Menegakis, A., Yaromina, A., Eicheler, W., Dörfler, A., Beuthien-Baumann, B., Thames, H. D., … Krause, M. (2009). Prediction of clonogenic cell survival curves based on the number of residual DNA double strand breaks measured by gammaH2AX staining. *International Journal of Radiation Biology*, *85*(11), 1032–41. https://doi.org/10.3109/09553000903242149

Méry, B., Guy, J.-B., Swalduz, A., Vallard, A., Guibert, C., Almokhles, H., … Magné, N. (2015). The evolving locally-advanced non-small cell lung cancer landscape: Building on past evidence and experience. *Critical Reviews in Oncology/hematology*, *96*(2), 319–27. https://doi.org/10.1016/j.critrevonc.2015.05.020

Michalski, J. M., Gay, H., Jackson, A., Tucker, S. L., & Deasy, J. O. (2010). Radiation Dose-Volume Effects in Radiation-Induced Rectal Injury. *International Journal of Radiation Oncology Biology Physics*, *76*(3 SUPPL.), 123–129. https://doi.org/10.1016/j.ijrobp.2009.03.078

Miller, J., Fuller, M., Vinod, S., Suchowerska, N., & Holloway, L. (2009). The significance of the choice of Radiobiological (NTCP) models in treatment plan objective functions. Australasian Physics & Engineering Sciences in Medicine*, 32(2), 81–87.* https://doi.org/10.1007/BF03178632

Nahum, A. E., & Sanchez-Nieto, B. (2001, August 10). Tumour control probability modelling: Basic principles and applications in treatment planning. *PHYSICA MEDICA*. Retrieved from http://publications.icr.ac.uk/295/

Nahum, A. E., Chapman, J. D., Coutard, H., Steel, G. G., Santos, J. D. L., Popple, R., … al., et. (2015). The radiobiology of hypofractionation. *Clinical Oncology (Royal College of Radiologists (Great Britain)), 27(5), 260–9.* https://doi.org/10.1016/j.clon.2015.02.001

Nahum, A., Uzan, J., Jain, P., Malik, Z., Fenwick, J., & Baker, C. (2011). SU-E-T-657: Quantitative Tumour Control Predictions for the Radiotherapy of Non-Small-Cell Lung Tumours. *Medical Physics, 38(6), 3641–3641.* https://doi.org/10.1118/1.3612620

Nahum, A. E., & Tait, D. M. (1992). Maximizing Local Control by Customized Dose Prescription for Pelvic Tumours. In *Tumor Response Monitoring and Treatment Planning* (pp. 425–431). Berlin, Heidelberg: Springer Berlin Heidelberg. https://doi.org/10.1007/978-3-642-48681-4_71

Nahum, A. E., & Uzan, J. (2012). (Radio)Biological Optimization of External-Beam Radiotherapy. *Computational and Mathematical Methods in Medicine*, *2012*, 1–13. https://doi.org/10.1155/2012/329214

National Institute of Health. (2010). Common Terminology Criteria for Adverse Events v4.0 (CTCAE). *(Vol. 2009). Retrieved from* http://evs.nci.nih.gov/ftp1/CTCAE/CTCAE_4.03_2010-06-14_QuickReference_5x7.pdf

Nenoi M (2015). "*Evolution of Ionizing Radiation Research*". ISBN 978-953-51-2167-1

NHS England. (2016). NHS England Evidence review: Hypofractionated radiotherapy compared with conventional fractionated radiotherapy to treat prostate cancer. *Retrieved from* https://www.engage.england.nhs.uk/consultation/clinical-commissioning-policy-for-hypofractionated/user_uploads/hypofractionated-evidence-review.pdf

NICE. (2014). National Institute for Health and Care Excellence. National Institute for Health and Care Excellence (NICE) clinical guideline: prostate cancer: diagnosis and treatment (CG175*). NICE.*

NICE Guideline Lung cancer: diagnosis and management. (2011). NICE Guideline Lung cancer: diagnosis and management. Retrieved from https://www.nice.org.uk/guidance/cg121/chapter/1-Guidance#treatment

Nielsen, T. B., Hansen, O., Schytte, T., & Brink, C. (2014a). Four-dimensional dose evaluation of inhomogeneous dose distributions planned for non-small cell lung cancer patients with lymph node involvement. *Acta Oncologica*, *53*(5), 707–712. https://doi.org/10.3109/0284186X.2013.835492

Nielsen, T. B., Hansen, O., Schytte, T., & Brink, C. (2014b). Inhomogeneous dose escalation increases expected local control for NSCLC patients with lymph node involvement without increased mean lung dose. *Acta Oncologica*, *53*(1), 119–125. https://doi.org/10.3109/0284186X.2013.790560

Niemierko, A., & Goitein, M. (1993a). Implementation of a model for estimating tumor control probability for an inhomogeneously irradiated tumor. *Radiotherapy and Oncology : Journal of the European Society for Therapeutic Radiology and Oncology, 29(2), 140–7. Retrieved from http://www.ncbi.nlm.nih.gov/pubmed/8310139*

Niemierko, A., & Goitein, M. (1993b). Modeling of normal tissue response to radiation: the critical volume model. *International Journal of Radiation Oncology, Biology, Physics, 25(1), 135–145 https://www.ncbi.nlm.nih.gov/pubmed/8416870*

Niemierko, A. (1997). Reporting and analyzing dose distributions: a concept of equivalent uniform dose. Medical Physics, *24(1), 103–110. https://doi.org/10.1118/1.598154*

Nordsmark, M., Eriksen, J. G., Gebski, V., Alsner, J., Horsman, M. R., & Overgaard, J. (2007). Differential risk assessments from five hypoxia specific assays: The basis for biologically adapted individualized radiotherapy in advanced head and neck cancer patients. *Radiotherapy and Oncology : Journal of the European Society for Therapeutic Radiology and Oncology*, *83*(3), 389–97. https://doi.org/10.1016/j.radonc.2007.04.021

Norkus, D., Karklelyte, A., Engels, B., Versmessen, H., Griskevicius, R., De Ridder, M., … Valuckas, K. P. (2013). A randomized hypofractionation dose escalation trial for high risk prostate cancer patients: interim analysis of acute toxicity and quality of life in 124 patients. *Radiation Oncology (London, England)*, *8*(1), 206. https://doi.org/10.1186/1748-717X-8-206

Nwankwo, O., Mekdash, H., Sihono, D. S. K., Wenz, F., Glatting, G., Good, D., … Lo, J. (2015). Knowledge-based radiation therapy (KBRT) treatment planning versus planning by experts: validation of a KBRT algorithm for prostate cancer treatment planning. *Radiation Oncology*, *10*(1), 111. https://doi.org/10.1186/s13014-015-0416-6

Nutting, C. M., Morden, J. P., Harrington, K. J., Urbano, T. G., Bhide, S. A., Clark, C., … PARSPORT trial management group. (2011). Parotid-sparing intensity modulated versus conventional radiotherapy in head and neck cancer (PARSPORT): a phase 3 multicentre randomised controlled trial. The Lancet. Oncology, 12(2), 127–36. https://doi.org/10.1016/S1470-2045(10)70290-4

O'Rourke, N., Roqué I Figuls, M., Farré Bernadó, N., & Macbeth, F. (2010). Concurrent chemoradiotherapy in non-small cell lung cancer. *The Cochrane Database of Systematic Reviews*, (6), CD002140. https://doi.org/10.1002/14651858.CD002140.pub3

O'Rourke, S. F. C., McAneney, H., & Hillen, T. (2009). Linear quadratic and tumour control probability modelling in external beam radiotherapy. *Journal of Mathematical Biology*, *58*(4–5), 799–817. https://doi.org/10.1007/s00285-008-0222-y

Office of National Statistics. (2015). *Cancer Registration Statistics, England, 2013*. *Cancer Registration Statistics* (Vol. 44). Retrieved from http://www.ons.gov.uk/ons/rel/vsob1/cancer-statistics-registrations--england--series-mb1-/no--44--2013/stb-cancer-registration-2013.html#tab-Cancer-incidence-in-England-

Ohkura, H. (2015). Meiosis: an overview of key differences from mitosis. Cold Spring Harbor Perspectives in Biology, 7(5), a015859. https://doi.org/10.1101/cshperspect.a015859

Ohri, N., Werner-Wasik, M., Grills, I. S., Belderbos, J., Hope, A., Yan, D., … Xiao, Y. (2012). Modeling local control after hypofractionated stereotactic body radiation therapy for stage I non-small cell lung cancer: a report from the elekta collaborative lung research group. *International Journal of Radiation Oncology, Biology, Physics*, *84*(3), e379-84. https://doi.org/10.1016/j.ijrobp.2012.04.040

Olive, P. L., & Banáth, J. P. (2004). Phosphorylation of histone H2AX as a measure of radiosensitivity. *International Journal of Radiation Oncology, Biology, Physics*, *58*(2), 331–5. Retrieved from http://www.ncbi.nlm.nih.gov/pubmed/14751500

Onishi, H., Shirato, H., Nagata, Y., Hiraoka, M., Fujino, M., Gomi, K., … Araki, T. (2007). Hypofractionated stereotactic radiotherapy (HypoFXSRT) for stage I non-small cell lung cancer: updated results of 257 patients in a Japanese multi-institutional study. *Journal of Thoracic Oncology : Official Publication of the International Association for the Study of Lung Cancer*, *2*(7 Suppl 3), S94-100. https://doi.org/10.1097/JTO.0b013e318074de34

Ontario Cancer Care Practice Guidelines Initiative. (2000). Lung Cancer Disease Site Group and Cancer Care Ontario Practice Guidelines Initiative. Altered fractionation of radical radiation therapy in the management of unresectable nonsmall cell lung cance. *Ontario Cancer Care Practice Guidelines Initiative*, 7–12.

Onjukka, E., Uzan, J., Baker, C., Howard, L., Nahum, A., & Syndikus, I. (2017). Twenty Fraction Prostate Radiotherapy with Intra-prostatic Boost: Results of a Pilot Study. *Clinical Oncology, 29(1), 6–14.* https://doi.org/10.1016/j.clon.2016.09.009

Orth, M., Lauber, K., Niyazi, M., Friedl, A. A., Li, M., Maihöfer, C., … Belka, C. (2014). Current concepts in clinical radiation oncology. *Radiation and Environmental Biophysics, 53(1), 1–29.* *https://doi.org/10.1007/s00411-013-0497-2*

Partridge, M., Tree, A., Brock, J., McNair, H., Fernandez, E., Panakis, N., & Brada, M. (2009). Improvement in tumour control probability with active breathing control and dose escalation: A modelling study. *Radiotherapy and Oncology, 91(3), 325–329.* *https://doi.org/10.1016/j.radonc.2009.03.017*

Paterson, R. (1963). *The Treatment of Malignant Disease by Radiotherapy* (2nd ed.). London: Edward Arnold.

Peeters, S. T. H., Heemsbergen, W. D., van Putten, W. L. J., Slot, A., Tabak, H., Mens, J. W., … Koper, P. C. M. (2005). Acute and late complications after radiotherapy for prostate cancer: results of a multicenter randomized trial comparing 68 Gy to 78 Gy. *International Journal of Radiation Oncology, Biology, Physics*, *61*(4), 1019–1034.

Peeters, S. T. H., Hoogeman, M. S., Heemsbergen, W. D., Hart, A. A. M., Koper, P. C. M., & Lebesque, J. V. (2006). Rectal bleeding, fecal incontinence, and high stool frequency after conformal radiotherapy for prostate cancer: Normal tissue complication probability modeling. *International Journal of Radiation Oncology*Biology*Physics*, *66*(1), 11–19. https://doi.org/10.1016/j.ijrobp.2006.03.034

Pemberton, L. S., Din, O. S., Fisher, P. M., & Hatton, M. Q. (2009). Accelerated Radical Radiotherapy for Non-small Cell Lung Cancer using Two Common Regimens: a Single-centre Retrospective Study of Outcome. *Clinical Oncology*, *21*(3), 161–167. https://doi.org/10.1016/j.clon.2008.11.016

Perez, C. A., Pajak, T. F., Rubin, P., Simpson, J. R., Mohiuddin, M., Brady, L. W., … Rotman, M. (1987). Long-term observations of the patterns of failure in patients with unresectable non-oat cell carcinoma of the lung treated with definitive radiotherapy. Report by the Radiation Therapy Oncology Group. *Cancer*, *59*(11), 1874–1881.

Pfahlery, G. E., Spackman, E. W., Alberti, W., Alberti, W., Audan, Kuentz, … Williams, T. A. (1931). Roentgen Therapy in Pituitary Tumors. *American Journal of Ophthalmology*, *14*(8), 796–807. https://doi.org/10.1016/S0002-9394(31)91882-5

Podgorsak, E. B. (2005). *Radiation Oncology Physics: A Handbook for Teachers and Students*. International Atomic Energy Agency. Retrieved from http://www.amazon.com/Radiation-Oncology-Physics-Handbook-Teachers/dp/9201073046

Pollack, A., Zagars, G. K., Starkschall, G., Antolak, J. a, Lee, J. J., Huang, E., … Rosen, I. (2002). Prostate cancer radiation dose response: results of the M. D. Anderson phase III randomized trial. *International Journal of Radiation Oncology*Biology*Physics*, *53*(5), 1097–1105. https://doi.org/10.1016/S0360-3016(02)02829-8

Press, W. H., Teukolsky, S. A., Vetterling, W. T., & Flannery, B. P. (1992). *Numerical Recipes in Fortran 77: The Art of Scientific Computing*. Cambridge University Press. Retrieved from citeulike-article-id:3997504

Public Health England. (2013). *Human radiosensitivity*. Retrieved from https://www.gov.uk/government/publications/human-radiosensitivity

Pyshniak, V., Fotina, I., Zverava, A., Siamkouski, S., Zayats, E., Kopanitsa, G., & Okuntsau, D. (2014). Efficiency of biological versus physical optimization for single-arc VMAT for prostate and head and neck cases. *Journal of Applied Clinical Medical Physics, 15(4), 39–53.* https://doi.org/10.1120/jacmp.v15i4.4514

Qi, X. S., Semenenko, V. A., & Li, X. A. (2009). Improved critical structure sparing with biologically based IMRT optimization. *Medical Physics, 36(5), 1790–1799.* *https://doi.org/10.1118/1.3116775*

Ramaekers, B. L. T., Grutters, J. P. C., Pijls-Johannesma, M., Lambin, P., Joore, M. A., & Langendijk, J. A. (2013). Protons in head-and-neck cancer: Bridging the gap of evidence. *International Journal of Radiation Oncology Biology Physics*, *85*(5), 1282–1288. https://doi.org/10.1016/j.ijrobp.2012.11.006

Raphael, C., Brahme A, Wolbarst A B. (1992). Mathematical modelling of objectives in radiation therapy treatment planning. *Physics in Medicine and Biology*, *37*(6), 1293–1311. https://doi.org/10.1088/0031-9155/37/6/007

Reminick, G. (2001). *Nightmare in Bari: The World War II Liberty Ship Poison Gas Disaster and Coverup*. Glencannon Press. Retrieved from https://books.google.com.pk/books?id=jKUJAAAACAAJ

Reya, T., Morrison, S. J., Clarke, M. F., & Weissman, I. L. (2001). Stem cells, cancer, and cancer stem cells. *Nature*, *414*(6859), 105–11. https://doi.org/10.1038/35102167

Roland, T., Mavroidis, P., Gutierrez, A., Goytia, V., & Papanikolaou, N. (2009). A radiobiological analysis of the effect of 3D versus 4D image-based planning in lung cancer radiotherapy. Physics in Medicine and Biology, 54(18), 5509–5523. https://doi.org/10.1088/0031-9155/54/18/011

Rosenstein, B. S. (2011). Identification of SNPs associated with susceptibility for development of adverse reactions to radiotherapy. *Pharmacogenomics*, *12*(2), 267–75. https://doi.org/10.2217/pgs.10.186

Rowell, N. P., & Williams, C.J. (2001). Radical radiotherapy for stage I/II non-small cell lung cancer in patients not sufficiently fit for or declining surgery (medically inoperable). *The Cochrane Database of Systematic Reviews*, (2), CD002140. https://doi.org/10.1002/14651858.CD002935 also see https://doi.org/10.1002/14651858.CD002935.pub2

RTOG. (2015). RTOG/EORTC Late Radiation Morbidity Scoring Schema. Retrieved October 23, 2015, from https://www.rtog.org/ResearchAssociates/AdverseEventReporting/RTOGEORTCLateRadiationMorbidityScoringSchema.aspx

Royal College of Radiologists (RCR). (2008). The timely delivery of radical radiotherapy: standards and guidelines for the management of unscheduled treatment interruptions, *Third edition. Retrieved from http://www.sascro.co.za/downloads/BFCO_RT_Interruptions.pdf*

Rutkowska, E., Baker, C., & Nahum, A. (2010). Mechanistic simulation of normal-tissue damage in radiotherapy--implications for dose-volume analyses. *Physics in Medicine and Biology*, *55*(8), 2121–36. https://doi.org/10.1088/0031-9155/55/8/001

Sanchez-Nieto, B., & Nahum, A. . (1999). The delta-TCP concept: a clinically useful measure of tumor control probability. *International Journal of Radiation Oncology*Biology*Physics*, *44*(2), 369–380. https://doi.org/10.1016/S0360-3016(99)00029-2

Sanchez-Nieto, B., & Nahum, A. E. (2000). Bioplan: Software for the biological evaluation of radiotherapy treatment plans. *Medical Dosimetry*, *25*(2), 71–76. https://doi.org/10.1016/S0958-3947(00)00031-5

Saunders, M., Dische, S., Barrett, A., Harvey, A., Gibson, D., & Parmar, M. (1997). Continuous hyperfractionated accelerated radiotherapy (CHART) versus conventional radiotherapy in non-small-cell lung cancer: a randomised multicentre trial. CHART Steering Committee. *Lancet (London, England)*, *350*(9072), 161–165.

Saunders, M., Dische, S., Barrett, A., Harvey, A., Griffiths, G., & Palmar, M. (1999). Continuous, hyperfractionated, accelerated radiotherapy (CHART) versus conventional radiotherapy in non-small cell lung cancer: mature data from the randomised multicentre trial. CHART Steering committee. *Radiotherapy and Oncology : Journal of the European Society for Therapeutic Radiology and Oncology*, *52*(2), 137–148.

Schell, S., Wilkens, J. J., & Oelfke, U. (2010). Radiobiological effect based treatment plan optimization with the linear quadratic model. *Zeitschrift Für Medizinische Physik*, *20*(3), 188–196. https://doi.org/10.1016/j.zemedi.2010.02.003

Schilstra, C., & Meertens, H. (2001). Calculation of the uncertainty in complication probability for various dose–response models, applied to the parotid gland. *International Journal of Radiation Oncology*Biology*Physics, 50(1), 147–158. https://doi.org/10.1016/S0360-3016(00)01553-4*

Schuster-Uitterhoeve, A. L., van de Vaart, P. J., Schaake-Koning, C. C., Benraadt, J., Koolen, M. G., González González, D., & Bartelink, H. (1990). Feasibility of escalating daily doses of cisplatin in combination with accelerated radiotherapy in non-small cell lung cancer. *European Journal of Cancer*, *32A*(8), 1314–1319.

Schwarz, M., Alber, M., Lebesque, J. V., Mijnheer, B. J., & Damen, E. M. F. (2005). Dose heterogeneity in the target volume and intensity-modulated radiotherapy to escalate the dose in the treatment of non–small-cell lung cancer. *International Journal of Radiation Oncology*Biology*Physics*, *62*(2), 561–570. https://doi.org/10.1016/j.ijrobp.2005.02.011

Semenenko, V. A., Reitz, B., Day, E., Qi, X. S., Miften, M., & Li, X. A. (2008). Evaluation of a commercial biologically based IMRT treatment planning system. *Medical Physics*, *35*(12), 5851–5860. https://doi.org/10.1118/1.3013556

Seppenwoolde, Y., Lebesque, J. V., de Jaeger, K., Belderbos, J. S. a, Boersma, L. J., Schilstra, C., … Ten Haken, R. K. (2003). Comparing different NTCP models that predict the incidence of radiation pneumonitis. *International Journal of Radiation Oncology Biology Physics*, *55*(3), 724–35. https://doi.org/10.1016/S0360-3016(02)03986-X

Siochi, R. A., Kim, Y., & Bhatia, S. (2015). Tumor control probability reduction in gated radiotherapy of non-small cell lung cancers: a feasibility study. *Journal of Applied Clinical Medical Physics, 16(1), 8–21. https://doi.org/10.1120/jacmp.v16i1.4444*

Slevin, N., West, C., Wilson, G., & Hendry, J. (1999). Discussion. *Radiotherapy and Oncology*, *51*(2), 109–111. https://doi.org/10.1016/S0167-8140(99)00067-5

Słonina, D., & Gasińska, A. (1997). Intrinsic radiosensitivity of healthy donors and cancer patients as determined by the lymphocyte micronucleus assay. *International Journal of Radiation Biology*, *72*(6), 693–701. Retrieved from http://www.ncbi.nlm.nih.gov/pubmed/9416792

Sountoulides, P., Koletsas, N., Kikidakis, D., Paschalidis, K., & Sofikitis, N. (2010). Secondary malignancies following radiotherapy for prostate cancer. *Therapeutic Advances in Urology*, *2*(3), 119–25. https://doi.org/10.1177/1756287210374462

South, C. P., Barry, M. A., Hussein, M., Adams, E. J., Jordan, T. J., & Nisbet, A. (2015). PO-0877: Knowledge-based treatment planning of IMRT for prostate cancer. *Radiotherapy and Oncology*, *115*, S448–S449. https://doi.org/10.1016/S0167-8140(15)40869-2

Steel*, G. (1991). The ESTRO Breur lecture cellular sensitivity to low dose-rate irradiation focuses the problem of tumour radioresistance. Radiotherapy and Oncology, 20(2), 71–83. https://doi.org/10.1016/0167-8140(91)90140-C*

Stausbøl-Grøn, B., & Overgaard, J. (1999). Relationship between tumour cell in vitro radiosensitivity and clinical outcome after curative radiotherapy for squamous cell carcinoma of the head and neck. *Radiotherapy and Oncology : Journal of the European Society for Therapeutic Radiology and Oncology*, *50*(1), 47–55. Retrieved from http://www.ncbi.nlm.nih.gov/pubmed/10225557

Stirling, A., & Gee, D. (2002). Science, precaution, and practice. *Public Health Reports (Washington, D.C. : 1974)*, *117*(6), 521–33. Retrieved from http://www.pubmedcentral.nih.gov/articlerender.fcgi?artid=1497477&tool=pmcentrez&rendertype=abstract

Suriano, F., Altobelli, E., Sergi, F., & Buscarini, M. (2013). Bladder cancer after radiotherapy for prostate cancer. *Reviews in Urology*, *15*(3), 108–12. Retrieved from http://www.pubmedcentral.nih.gov/articlerender.fcgi?artid=3821989&tool=pmcentrez&rendertype=abstract

Syndikus, I., Uzan, J., Mayles, P., & Nahum, A. (2011). BioProp: a Proposed Three-arm Trial of Radiobiologically Optimised Prostate Dose Painting. *Clinical Oncology*, *23*(3), S25–S26. https://doi.org/10.1016/j.clon.2011.01.385

Tai, A., Erickson, B., Khater, K. A., & Li, X. A. (2008). Estimate of radiobiologic parameters from clinical data for biologically based treatment planning for liver irradiation. *International Journal of Radiation Oncology, Biology, Physics*, *70*(3), 900–907. https://doi.org/10.1016/j.ijrobp.2007.10.037

Teoh, M., Clark, C. H., Wood, K., Whitaker, S., & Nisbet, A. (2011). Volumetric modulated arc therapy: a review of current literature and clinical use in practice. *The British Journal of Radiology, 84(1007), 967–96. https://doi.org/10.1259/bjr/22373346*

Thames, H. D., Peters, L. J., & Ang, K. K. (1989). Time-dose considerations for normal-tissue tolerance. *Frontiers of Radiation Therapy and Oncology, 23, 113–30. Retrieved from http://www.ncbi.nlm.nih.gov/pubmed/2697649*

The Royal College of Radiologists. (2016). Radiotherapy Dose- Fractionation. Royal College of Radiologists, 48(December), 960–960. https://doi.org/10.1259/0007-1285-48-575-960-a

Tree, A. C., Alexander, E. J., Van As, N. J., Dearnaley, D. P., & Khoo, V. (2013). Biological Dose Escalation and Hypofractionation: What is There to be Gained and How Will it Best be Done? *Clinical Oncology, 25(8), 483–498. https://doi.org/10.1016/j.clon.2013.05.003*

Uzan, J., & Nahum, A. E. (2012). Radiobiologically guided optimisation of the prescription dose and fractionation scheme in radiotherapy using BioSuite. *The British Journal of Radiology*, *85*(1017), 1279–86. https://doi.org/10.1259/bjr/20476567

Uzan, J., Nahum, A. E., Syndikus, I., Dearnaley, D. P., Sydes, M. R., Graham, J. D., … al., et. (2016). Prostate Dose-painting Radiotherapy and Radiobiological Guided Optimisation Enhances the Therapeutic Ratio. *Clinical Oncology*, *28*(3), 165–170. https://doi.org/10.1016/j.clon.2015.09.006

Valdagni, R., Italia, C., Montanaro, P., Lanceni, A., Lattuada, P., Magnani, T., … Nahum, A. (2005). Is the alpha-beta ratio of prostate cancer really low? A prospective, non-randomized trial comparing standard and hyperfractionated conformal radiation therapy. *Radiotherapy and Oncology : Journal of the European Society for Therapeutic Radiology and Oncology*, *75*(1), 74–82. https://doi.org/10.1016/j.radonc.2004.12.019

Valero, R., Ko, Y. H., Chauhan, S., Schatloff, O., Sivaraman, A., Coelho, R. F., … Patel, V. R. (2011). [Robotic surgery: history and teaching impact]. *Actas Urologicas Españolas*, *35*(9), 540–5. https://doi.org/10.1016/j.acuro.2011.04.005

van Baardwijk, A.. (2011). Mature results of a Phase II trial on individualized radiation dose-escalation based on normal tissue constraints in concurrent chemo-radiation for stage III non-small cell lung cancer (NSCLC). *International Journal of Radiation Oncology Biology Physics*, *81*(2), S133–S134.

van Baardwijk, A., Bosmans, G., Boersma, L., Wanders, S., Dekker, A., Dingemans, A. M. C., … De Ruysscher, D. (2008). Individualized radical radiotherapy of non-small-cell lung cancer based on normal tissue dose constraints: a feasibility study. *International Journal of Radiation Oncology Biology Physics*, *71*(5), 1394–1401. https://doi.org/10.1016/j.ijrobp.2007.11.070

van Baardwijk, A., Reymen, B., Wanders, S., Borger, J., Ollers, M., Dingemans, A.-M. C., … De Ruysscher, D. (2012). Mature results of a phase II trial on individualised accelerated radiotherapy based on normal tissue constraints in concurrent chemo-radiation for stage III non-small cell lung cancer. *European Journal of Cancer (Oxford, England : 1990)*, *48*(15), 2339–46. https://doi.org/10.1016/j.ejca.2012.04.014

van Baardwijk, A., Wanders, S., Boersma, L., Borger, J., ??llers, M., Dingemans, A.-M. M. C., … De Ruysscher, D. (2010). Mature results of an individualized radiation dose prescription study based on normal tissue constraints in stages I to III non-small-cell lung cancer. *Journal of Clinical Oncology*, *28*(8), 1380–1386. https://doi.org/10.1200/JCO.2009.24.7221

van Herk, M. (2007). Different Styles of Image-Guided Radiotherapy. Seminars in Radiation Oncology, 17(4), 258–267. *https://doi.org/10.1016/j.semradonc.2007.07.003*

Vogelius, I. R., & Bentzen, S. M. (2013). Meta-analysis of the alpha/beta ratio for prostate cancer in the presence of an overall time factor: bad news, good news, or no news? *International Journal of Radiation Oncology, Biology, Physics*, *85*(1), 89–94. https://doi.org/10.1016/j.ijrobp.2012.03.004

Vral, A., Fenech, M., & Thierens, H. (2011). The micronucleus assay as a biological dosimeter of in vivo ionising radiation exposure. Mutagenesis, 26(1), 11–17. https://doi.org/10.1093/mutage/geq078

Walker, A. M., & Suit, H. D. (1981). Choosing between two formulations of a dose/cure function. *The British Journal of Radiology*, *54*(647), 1012–3. https://doi.org/10.1259/0007-1285-54-647-1012

Wallis, C. J. D., Mahar, A. L., Choo, R., Herschorn, S., Kodama, R. T., Shah, P. S., … Nam, R. K. (2016). Second malignancies after radiotherapy for prostate cancer: systematic review and meta-analysis. *BMJ*, *352*(mar02_7), i851. https://doi.org/10.1136/bmj.i851

Wang, C.-K. C. (2010). The progress of radiobiological models in modern radiotherapy with emphasis on the uncertainty issue. *Mutation Research*, *704*(1–3), 175–81. https://doi.org/10.1016/j.mrrev.2010.02.001

Wang, J. Z., Mayr, N. A., & C Yuh, W. T. (2008). Behind EUD. Acta Oncologica, 47(5), 971–972. https://doi.org/10.1080/02841860701885440

Wang, W., Xu, Y., Schipper, M., Matuszak, M. M., Ritter, T., Cao, Y., … Kong, F.-M. S. (2013). Effect of normal lung definition on lung dosimetry and lung toxicity prediction in radiation therapy treatment planning. *International Journal of Radiation Oncology, Biology, Physics*, *86*(5), 956–63. https://doi.org/10.1016/j.ijrobp.2013.05.003

Wang, Z.-Z., Li, W.-J., Zhang, H., Yang, J.-S., Qiu, R., & Wang, X. (2006). Comparison of clonogenic assay with premature chromosome condensation assay in prediction of human cell radiosensitivity. *World Journal of Gastroenterology*, *12*(16), 2601–5. Retrieved from http://www.pubmedcentral.nih.gov/articlerender.fcgi?artid=4087996&tool=pmcentrez&rendertype=abstract

Warren, M., Webster, G., Ryder, D., Rowbottom, C., & Faivre-Finn, C. (2014). An isotoxic planning comparison study for stage II-III non-small cell lung cancer: is intensity-modulated radiotherapy the answer? *Clinical Oncology (Royal College of Radiologists (Great Britain))*, *26*(8), 461–7. https://doi.org/10.1016/j.clon.2014.03.011

Webb, S. (2003). The physical basis of IMRT and inverse planning. The British Journal of Radiology, *76(910), 678–689. https://doi.org/10.1259/bjr/65676879*

Webb, S., & Nahum, A. E. (1993). A model for calculating tumour control probability in radiotherapy including the effects of inhomogeneous distributions of dose and clonogenic cell density. *Physics in Medicine and Biology*, *38*(6), 653. https://doi.org/10.1088/0031-9155/38/6/001

Werner-Wasik, M., Yorke, E., Deasy, J., Nam, J., & Marks, L. B. (2010). Radiation Dose-Volume Effects in the Esophagus. *International Journal of Radiation Oncology Biology Physics*, *76*(3 SUPPL.), 86–93. https://doi.org/10.1016/j.ijrobp.2009.05.070

West, C., Azria, D., Chang-Claude, J., Davidson, S., Lambin, P., Rosenstein, B., … Yuille, M. (2014). The REQUITE project: validating predictive models and biomarkers of radiotherapy toxicity to reduce side-effects and improve quality of life in cancer survivors. *Clinical Oncology (Royal College of Radiologists (Great Britain))*, *26*(12), 739–42. https://doi.org/10.1016/j.clon.2014.09.008

West, C. M., & Barnett, G. C. (2011). Genetics and genomics of radiotherapy toxicity: towards prediction. *Genome Medicine*, *3*(8), 52. https://doi.org/10.1186/gm268

West, C. M., Davidson, S. E., Roberts, S. A., & Hunter, R. D. (1997). The independence of intrinsic radiosensitivity as a prognostic factor for patient response to radiotherapy of carcinoma of the cervix. *British Journal of Cancer*, *76*(9), 1184–90. https://www.ncbi.nlm.nih.gov/pmc/articles/PMC2228123/

William and Wood. (1900). *Journal of Cutaneous Diseases Including Syphilis* (18th ed.). American Dermatological Association. Retrieved from https://books.google.com/books?id=EZPTAAAAIAAJ&pgis=1

Williams, J. R., Zhang, Y., Zhou, H., Gridley, D. S., Koch, C. J., Russell, J., … Little, J. B. (2008). A quantitative overview of radiosensitivity of human tumor cells across histological type and TP53 status. *International Journal of Radiation Biology*, *84*(4), 253–64. https://doi.org/10.1080/09553000801953342

Williams, M. V, James, N. D., Summers, E. T., Barrett, A., Ash, D. V, Audit Sub-Committe, F. of C. O., & Royal College of Radiologists. (2006). National survey of radiotherapy fractionation practice in 2003. *Clinical Oncology*, *18*(1), 3–14.

Willner, J., Baier, K., Caragiani, E., Tschammler, A., & Flentje, M. (2002). Dose, volume, and tumor control prediction in primary radiotherapy of non-small-cell lung cancer. International Journal of Radiation Oncology, Biology, Physics, 52(2), 382–9. *Retrieved from http://www.ncbi.nlm.nih.gov/pubmed/11872283*

Withers, H. R. (1975). The Four R's of Radiotherapy. In *Advances in Radiation Biology* (Vol. 5, pp. 241–271). https://doi.org/10.1016/B978-0-12-035405-4.50012-8

Withers, H. R., Taylor, J. M., & Maciejewski, B. (1988). Treatment volume and tissue tolerance. *International Journal of Radiation Oncology, Biology, Physics*, *14*(4), 751–9. Retrieved from http://www.ncbi.nlm.nih.gov/pubmed/3350731

Withers, H. R., Thames, H. D., & Peters, L. J. (1983). A new isoeffect curve for change in dose per fraction. *Radiotherapy and Oncology : Journal of the European Society for Therapeutic Radiology and Oncology*, *1*(2), 187–91. Retrieved from http://www.ncbi.nlm.nih.gov/pubmed/6680223

Wolff, R. F., Ryder, S., Bossi, A., Briganti, A., Crook, J., Henry, A., … Kleijnen, J. (2015). A systematic review of randomised controlled trials of radiotherapy for localised prostate cancer. *European Journal of Cancer*, *51*(16), 2345–2367. https://doi.org/10.1016/j.ejca.2015.07.019

Wu, Q., Mohan, R., Niemierko, A., & Schmidt-Ullrich, R. (2002). Optimization of intensity-modulated radiotherapy plans based on the equivalent uniform dose. International Journal of *Radiation Oncology, Biology, Physics, 52(1), 224–35. Retrieved from http://www.ncbi.nlm.nih.gov/pubmed/11777642*

Yaromina, A., Krause, M., & Baumann, M. (2012). Individualization of cancer treatment from radiotherapy perspective. *Molecular Oncology*, *6*(2), 211–21. https://doi.org/10.1016/j.molonc.2012.01.007

Yeoh, E. E. K., Fraser, R. J., McGowan, R. E., Botten, R. J., Di Matteo, A. C., Roos, D. E., … Borg, M. F. (2003). Evidence for efficacy without increased toxicity of hypofractionated radiotherapy for prostate carcinoma: early results of a Phase III randomized trial. *International Journal of Radiation Oncology, Biology, Physics*, *55*(4), 943–955.

Zaider, M., & Minerbo, G. N. (2000). Tumour control probability: a formulation applicable to any temporal protocol of dose delivery. *Physics in Medicine and Biology*, *45*(2), 279–293.

Zaider, M., Zelefsky, M. J., Cohen, G. N., Chui, C.-S., Yorke, E. D., Ben-Porat, L., & Happersett, L. (2005). Methodology for biologically-based treatment planning for combined low-dose-rate (permanent implant) and high-dose-rate (fractionated) treatment of prostate cancer. *International Journal of Radiation Oncology, Biology, Physics*, *61*(3), 702–713. https://doi.org/10.1016/j.ijrobp.2004.06.251

Zelefsky, M. J., Fuks, Z., Hunt, M., Lee, H. J., Lombardi, D., Ling, C. C., … Leibel, S. A. (2001). High dose radiation delivered by intensity modulated conformal radiotherapy improves the outcome of localized prostate cancer. *The Journal of Urology*, *166*(3), 876–81. Retrieved from http://www.ncbi.nlm.nih.gov/pubmed/11490237

Zhang, X., Li, Y., Pan, X., Xiaoqiang, L., Mohan, R., Komaki, R., … Chang, J. Y. (2010). Intensity-modulated proton therapy reduces the dose to normal tissue compared with intensity-modulated radiation therapy or passive scattering proton therapy and enables individualized radical radiotherapy for extensive stage IIIB non-small-cell lung canc. *International Journal of Radiation Oncology, Biology, Physics*, *77*(2), 357–66. https://doi.org/10.1016/j.ijrobp.2009.04.028

Zietman, A. L., DeSilvio, M. L., Slater, J. D., Rossi, C. J., Miller, D. W., Adams, J. A., & Shipley, W. U. (2005). Comparison of conventional-dose vs high-dose conformal radiation therapy in clinically localized adenocarcinoma of the prostate: a randomized controlled trial. *JAMA*, *294*(10), 1233–1239. https://doi.org/10.1001/jama.294.10.1233

Zindler, J. D., Thomas, C. R., Hahn, S. M., Hoffmann, A. L., Troost, E. G. C., & Lambin, P. (2016). Increasing the Therapeutic Ratio of Stereotactic Ablative Radiotherapy by Individualized Isotoxic Dose Prescription. *Journal of the National Cancer Institute*, *108*(2), djv305. https://doi.org/10.1093/jnci/djv305

Appendix A: List of Abbreviations

2-D / 2D	Two dimensional
3-D / 3D	Three dimensional
AAPM	American Association of Physicists in Medicine
AUC	Area under the curve
b.i.d	twice a day in latin "bis in die"
BED	Biological Effective Dose
bNED	Biochemical free survival
cGy	centi-Gray
CHART	Continuous Hyperfractionated Accelerated Radiotherapy
CHIPP	Conventional or Hypofractionated High Dose Intensity
CRT	Conformal Radiotherapy
CT	Computed Tomography
CTV	Clinical target volume
DIL	Dominant Intra prostatic lesion
Dpres	Prescription Dose
DSF	Dose Scaling Factor
DVB	Dose Volum Based
DVH	Dose Volume Histogram
external beam radiotherapy (EBRT)	
FSU	Functional Subunit
GTV	Gross tumour volume
GWAS	Gnenom-wide association study
Gy	Gray
ICRU	International Commission on Radiological Units and Measurements (ICRU)
IMRT	Intensity modulated radiotherapy
LKB / L-K-B	Lyman - Kutcher - Burman
LQ	Linear Quadratic
LQED	Linear Quadratic equivalent dose
MRI	Magnetic Resonance Imaging
NSCLC	Non-small cell lung cancer
NTCP	Normal Tissue Complication Probability
OAR / OR	Organ at risk
PET	Positron Emission Tomography
Pop	Population
PTV	Planning target volume
QUANTEC	Quantitative Analyses of Normal Tissue Effects in the Clinic
RB	Radiobiological model Based
RE	Relative Effectiveness
ROI	Region of Interest
RTOG	Radiation Therapy Oncology Group
SABR	Stereotactic abalative body radiotherapy
SBRT	Stereotactic body radiation therapy

SF	Surviving fraction
TCP	Tumour Control Probability
TD50	Dose causing 50% complication rate in a normal tissue
tot	Total
TPS	Treatment Planning System
TR	Therapeutic Ratio
VMAT	Volumetric Modulated Arc Therapy
Linac	Linear accelerator
MLC	Multi-leaf collimator

Appendix B: Additional Material

Figure A shows the optimum fraction numbers at which level 2 TCP was obtained for different α/β values of prostate tumour.

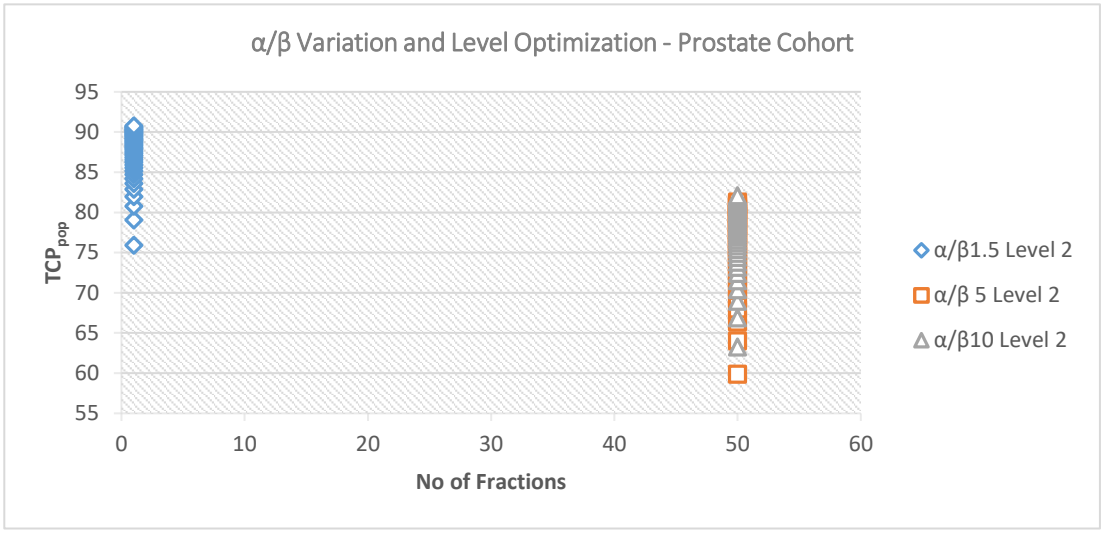

Figure B TCP-NTCP plots comparing Isotoxic dose escalation between radiobiological inverse treatment planning to dose-volume inverse planning for both NSCLC patient datasets. This figure is provided to show that dose escalation in patient 2 was successful but the data points for the RB-plan were limited as it was a very favourable patient (i.e. 100% TCP at 4% NTCP, P2 RB-plan). Patient 2 data points were thus excluded in the last submission – From old submission